

GENERALIZED FRAMEWORK FOR THE NAVIGATION
OF MULTI-VEHICLE SYSTEM BASED ON NONLINEAR
MODEL PREDICTIVE CONTROL

BY
BILAL AHMED SIDDIQUI

A Dissertation Presented to the
FACULTY OF THE COLLEGE OF GRADUATE STUDIES
KING FAHD UNIVERSITY OF PETROLEUM & MINERALS
DHAHRAN, SAUDI ARABIA

In Partial Fulfillment of the
Requirements for the Degree of

DOCTOR OF PHILOSOPHY
In
SYSTEMS ENGINEERING

DECEMBER, 2014


KING FAHD UNIVERSITY OF PETROLEUM & MINERALS
DHAHRAN 31261, SAUDI ARABIA

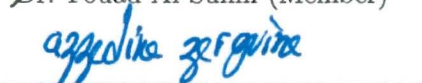
DEANSHIP OF GRADUATE STUDIES

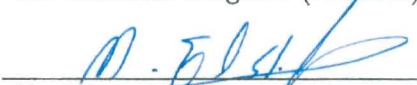
This thesis, written by **BILAL AHMED SIDDIQUI** under the direction of his thesis adviser and approved by his thesis committee, has been presented to and accepted by the Dean of Graduate Studies, in partial fulfillment of the requirements for the degree of **DOCTOR OF PHILOSOPHY IN SYSTEMS ENGINEERING**.

Dissertation Committee


Dr. Sami El-Ferik (Adviser)



Dr. Fouad Al-Sunni (Member)


Dr. Azzedine Zerguine (Member)


Dr. Mustafa El-Shafei (Member)


Dr. Muhammad Hawwa (Member)


Dr. Fouad Al-Sunni
Department Chairman


Dr. Salam A. Zummo
Dean of Graduate Studies

17/1/15
Date



©Bilal Ahmed Siddiqui
2014

This thesis is dedicated to my love Asma (A^2B) and children Maryam, Musa and Maria (M^3) who bore the brunt of my academic engagement. It is also dedicated to my Baba and Mama who made me who I am. To my wife's Daddy and Mumma for keeping faith in me and what I was doing. To my siblings who looked after my parents in my absence and believed I will reach the finish line. And last, but not the least, to the Muslim nation, the betterment of which remains my primary motivation.

TABLE OF CONTENTS

| | |
|--|--------------|
| LIST OF TABLES | ix |
| LIST OF FIGURES | x |
| ACKNOWLEDGMENTS | xii |
| ABSTRACT (ENGLISH) | xv |
| ABSTRACT (ARABIC) | xviii |
| CHAPTER 1 INTRODUCTION | 1 |
| 1.1 Prologue | 1 |
| 1.1.1 Nature Inspires Multi-Agent Systems | 2 |
| 1.1.2 Cooperative Control and Formation Keeping | 5 |
| 1.1.3 Uncertainty, Disturbances and Real World Effects | 7 |
| 1.2 Literature Review | 8 |
| 1.2.1 Formation Control and Conflict Resolution | 9 |
| 1.2.2 Robustness | 16 |
| 1.2.3 Gaps in Current Body of Work | 21 |
| 1.3 Problem Statement | 23 |
| 1.4 Research Contribution | 24 |
| 1.5 Thesis Organization | 27 |
| CHAPTER 2 NOTIONS OF STABILITY IN NONLINEAR SYS- TEMS | 30 |

| | | |
|---|---|------------|
| 2.1 | Introduction | 30 |
| 2.2 | Linear versus Nonlinear Systems | 32 |
| 2.3 | Discrete- versus Continuous-time models | 35 |
| 2.4 | Some Mathematical Theory Concepts | 36 |
| 2.4.1 | Set Theoretic Concepts | 36 |
| 2.4.2 | Functional Analysis Concepts | 41 |
| 2.5 | Notions of Stability | 45 |
| 2.5.1 | Stability of System with Feedback and no External Input | 45 |
| 2.5.2 | Stability of System with Feedback and External Input | 50 |
| 2.6 | Chapter Conclusion | 60 |
| CHAPTER 3 ROBUST NONLINEAR MPC CONTROL | | 61 |
| 3.1 | Introduction | 61 |
| 3.1.1 | Chapter Contributions | 63 |
| 3.2 | Nonlinear Model Predictive Control | 65 |
| 3.2.1 | Advantages and Disadvantages | 66 |
| 3.2.2 | Problem Formulation | 68 |
| 3.2.3 | Receding Horizon Strategy | 73 |
| 3.2.4 | Comparison with other Optimal Control Techniques | 77 |
| 3.2.5 | Robustness of NMPC Algorithm | 78 |
| 3.2.6 | Robust Recursive Feasibility of NMPC Algorithm | 92 |
| 3.2.7 | Robust Stability of NMPC Algorithm | 98 |
| 3.3 | Illustrative Examples: Quadratic Cost and Constraint Tightening | 112 |
| 3.4 | Conclusion | 118 |
| CHAPTER 4 OPTIMIZATION OF TERMINAL, CONTROL- | | |
| TABLE AND FEASIBLE SETS | | 119 |
| 4.1 | Introduction | 119 |
| 4.1.1 | Chapter Contributions | 120 |
| 4.2 | Introduction to Convex Analysis | 121 |
| 4.2.1 | Examples of Convex Sets | 122 |

| | | |
|-------|---|-----|
| 4.2.2 | Convex Optimization and LMIs | 124 |
| 4.3 | Terminal Control Design and Maximization of Terminal Constraint Set | 126 |
| 4.3.1 | Re-parametrization of Constraints | 126 |
| 4.3.2 | Terminal Control Design for Linearization around Vertex Points | 128 |
| 4.3.3 | Terminal Region Optimization | 131 |
| 4.3.4 | Description of Terminal Region Optimization Algorithms | 137 |
| 4.3.5 | Illustrative Example on Terminal Region Optimization | 139 |
| 4.4 | Determination of 1-Step Controllable Set to Terminal Constraint Set | 145 |
| 4.5 | Determination of Robust Output Feasible Set X_{MPC} | 151 |
| 4.6 | Illustrative Example of Overall Robust NMPC Scheme (Algorithm 1) | 156 |
| 4.7 | Conclusion | 161 |

CHAPTER 5 FORMATION CONTROL BASED ON ROBUST DISTRIBUTED NMPC 162

| | | |
|-------|--|-----|
| 5.1 | Introduction | 162 |
| 5.1.1 | Centralized versus Distributed Cooperative Control | 163 |
| 5.1.2 | Introduction to Graph Theory | 165 |
| 5.1.3 | Formation Control | 166 |
| 5.1.4 | Chapter Contributions | 170 |
| 5.2 | Problem Formulation | 171 |
| 5.2.1 | Neural Network based Trajectory Compression | 178 |
| 5.2.2 | Collision Avoidance | 183 |
| 5.3 | Robustness Analysis | 187 |
| 5.3.1 | Constraint Tightening | 188 |
| 5.4 | Robust Recursive Feasibility without Collision Avoidance | 195 |
| 5.5 | Stability Analysis | 196 |
| 5.5.1 | Stability of Individual Agents without Collision Avoidance | 197 |

| | | |
|---|---|------------|
| 5.5.2 | Stability of Team of Agents under NMPC, without Collision Avoidance | 204 |
| 5.5.3 | Stability of Individual Agents with Collision Avoidance . . | 210 |
| 5.5.4 | Stability of Multi-Agent Team with Collision Avoidance . | 216 |
| 5.5.5 | Terminal Region Optimization and Terminal Control Law Design | 217 |
| 5.6 | Illustrative Examples | 223 |
| 5.7 | Conclusion | 231 |
| CHAPTER 6 CONCLUSION AND FUTURE WORK | | 235 |
| 6.1 | Epilogue | 235 |
| 6.2 | Thesis Contributions | 236 |
| 6.2.1 | Robustness to Simultaneous Multiple Sources of Uncertainty | 236 |
| 6.2.2 | Results in Input-to-State Practical Stability | 238 |
| 6.2.3 | Results on Recursive Stability and Allowable Uncertainty . | 238 |
| 6.2.4 | Terminal Region Maximization and Terminal Control Optimization | 239 |
| 6.2.5 | Data Compression and Trajectory Reconstruction | 239 |
| 6.2.6 | Collision Avoidance | 240 |
| 6.2.7 | Stability of Different Network Topologies | 241 |
| 6.3 | Future Recommendations | 241 |
| 6.4 | Concluding Remarks | 242 |
| REFERENCES | | 244 |
| VITAE | | 261 |

LIST OF TABLES

| | | |
|-----|--|-----|
| 4.1 | Parameters of Constraint Set for Terminal Optimization | 140 |
| 4.2 | Vertex Matrices of Nonlinear Oscillator System | 141 |
| 4.3 | Solutions of Riccati Equations at Vertex Points | 142 |
| 4.4 | Computational Times of Algorithms 1-6 for Examples 3.3.2-4.6.1 . | 160 |
| 5.1 | Anatomy of a Typical Communication Packet. | 179 |

LIST OF FIGURES

| | | |
|------|---|-----|
| 1.1 | Inspirations of multi-agent systems from nature. | 5 |
| 1.2 | Examples of multi-agent systems inspired by nature. | 6 |
| 2.1 | Difference between ISS and ISpS stability. | 51 |
| 2.2 | Solution Sets for ISpS Stability. | 53 |
| 3.1 | Architecture of the NMPC controller for Single Vehicle | 74 |
| 3.2 | Basic concept of Nonlinear Model Predictive Control | 76 |
| 3.3 | Illustration of Sets in Theorem 3.2.2. | 102 |
| 3.4 | Growth of State Prediction Uncertainty along the Prediction Horizon | 117 |
| 3.5 | Constraint Tightening for the Nonlinear Oscillator | 118 |
| 4.1 | Convex Sets and Hulls | 122 |
| 4.2 | Warm Start Ellipsoids used in Algorithm 4 | 142 |
| 4.3 | Optimized Terminal Region using Algorithm 3 | 143 |
| 4.4 | Optimized Terminal Region in Tight-Constrained State Space . . | 144 |
| 4.5 | Relationship between Size of Controllable Set and Terminal Set . | 146 |
| 4.6 | Optimal Cost (4.44) for Example 4.4.1 for various Disturbance Levels | 148 |
| 4.7 | Boundary points of One Step Controllability Set calculated using Algorithm 5 for Example 4.4.1 | 149 |
| 4.8 | One Step Controllability Set shown in Constrained State Space . . | 150 |
| 4.9 | Recursive One-Step Controllable Sets in Example 4.5.1 | 155 |
| 4.10 | [Optimal Cost (4.44) for boundary points of 1-step Controllable Sets. | 156 |
| 4.11 | Robust Output Feasible Set X_{MPC} with Tightened Constraints . . | 157 |

| | | |
|------|---|-----|
| 4.12 | State Trajectory for Example 4.6.1, solved with Algorithm 1 | 158 |
| 4.13 | Time Evolution of States for Example 4.6.1 | 158 |
| 4.14 | Control History for Example 4.6.1 | 159 |
| 4.15 | Evolution of Optimization Cost Function for Example 4.6.1 | 160 |
| 5.1 | Depiction of Centralized, Decentralized and Distributed Control . | 164 |
| 5.2 | Compression of Trajectory and Data Transmission Process | 180 |
| 5.3 | Illustration of Collision Course | 184 |
| 5.4 | Illustration of Successful Collision Avoidance | 186 |
| 5.5 | Network Topology of Strongly Connected Team | 226 |
| 5.6 | Trajectory of Strongly Connected Team Example | 227 |
| 5.7 | State Evolution of Strongly Connected Team Example | 228 |
| 5.8 | Cost Evolution and Inter-Vehicle Distance of Strongly Connected Team Example | 228 |
| 5.9 | Propagation Delay Distribution in Strongly Connected Team . . . | 229 |
| 5.10 | Control Evolution in Strongly Connected Team Example | 229 |
| 5.11 | Network Topology of Weakly Connected Team | 230 |
| 5.12 | Trajectory of Weakly Connected Team Example | 231 |
| 5.13 | State Evolution of Weakly Connected Team Example | 232 |
| 5.14 | Minimum Inter-Vehicle Distance of Weakly Connected Team Example | 232 |
| 5.15 | Control Evolution in Weakly Connected Team Example | 233 |
| 5.16 | Small Gain Condition for Weakly Connected Team | 233 |

ACKNOWLEDGMENTS

Words can not do justice to the gratitude I owe to my mentor and teacher, Dr. Sami el-Ferik. He was the one who believed in me when I did not believe in myself. Who made me dream when I was only good at slumber. Were it not for his encouragement, patience (plenty), dedication and humour, this work would still have been a work in progress. It was not only his academic acumen and intellect from which I benefited, but his humane, compassionate and fatherly nature which kept me going. It would be unfair to call him a professor, for he is much more. I cherish his friendship, companionship and his astute world views more than his sharp engineering instincts. Dr. Al-Sunni's support was also always unflinching in all aspects of my stay here. I have been fortunate to take courses from all members of my thesis committee. I learned a lot from Dr. Hawwa, Dr. El-Shafei and Dr. Zerguine, both in terms of course material and other problem solving in general. It would also be unfair not to mention the support from graduate advisor Dr. Daffua, laboratory gurus Shawkat, Jose and Wududu, and department secretaries Hussain, Kassem and Mervin. Finally, no thanks can be enough to my ship mates Aminuddin, Sabih, Haris and Tariq for being valuable friends and peers.

LIST OF ABBREVIATIONS

| | | |
|-------|---|---|
| AUV | : | Autonomous Underwater Vehicle |
| DLQR | : | Discrete-time Linear Quadratic Regulator |
| DARE | : | Discrete-time Algebraic Riccati Equations |
| FH | : | Finite Horizon |
| FHOCP | : | Finite Horizon Optimal Control Problem |
| GPS | : | Global Positioning System |
| ISS | : | Input to State Stability/Stable |
| ISpS | : | Input to State practical Stability/Stable |
| LDI | : | Linear Differential Inclusion |
| LMI | : | Linear Matrix Inequality |
| LQR | : | Linear Quadratic Regulator |
| LTI | : | Linear Time Invariant |
| MEMS | : | Micro Electro-Mechanical Systems |
| MPC | : | Model Predictive Control |
| NMPC | : | Nonlinear Model Predictive Control |
| NN | : | Neural Network |
| OCP | : | Optimal Control Problem |
| PLDI | : | Polytopic Linear Differential Inclusion |
| RH | : | Receding Horizon |
| UAV | : | Unmanned Aerial Vehicle |

NOTATIONS

| | | |
|-------------------------|---|--|
| \mathbb{R} | : | Set of real numbers |
| $\mathbb{R}_{\geq 0}$ | : | Set of non-negative real numbers |
| \mathbb{Z} | : | Set of integers |
| $\mathbb{Z}_{\geq 0}$ | : | Set of non-negative integers |
| $ \cdot $ | : | Euclidean or 2-norm of a vector |
| $\ \cdot\ $ | : | Supremum of Euclidean norms of components of a time series |
| $\lambda_{\max}(\cdot)$ | : | Maximum eigenvalue of a square matrix |
| $\lambda_{\min}(\cdot)$ | : | Minimum eigenvalue of a square matrix |
| $P > 0$ | : | Indicates that the matrix P is positive-definite |
| $P \geq 0$ | : | definite (positive semi-definite) |
| I_m | : | Identity matrix of order m |
| 0_m | : | Square null matrix of order m |
| \mathcal{I} | : | Identity function |
| \mathcal{K} | : | Class \mathcal{K} comparison function |
| \mathcal{K}_{∞} | : | Class \mathcal{K}_{∞} comparison function |
| \mathcal{KL} | : | Class \mathcal{KL} comparison function |
| \mathcal{N} | : | Neural network |
| $\sup\{\cdot\}$ | : | Supremum of a set |
| $\inf\{\cdot\}$ | : | Infinimum of a set |

THESIS ABSTRACT

NAME: Bilal Ahmed Siddiqui

TITLE OF STUDY: Generalized Framework for the Navigation of Multi-Vehicle System based on Nonlinear Model Predictive Control

MAJOR FIELD: Systems Engineering

DATE OF DEGREE: 18th December, 2014

Recent advances in MEMS-based sensors, low consumption actuators, as well as affordable and high performance computing and communication equipment has allowed mobile robots to advance rapidly towards development of multi-agent systems. Control system of the robot, which consists of the sensors to quantify measurable variables affecting it, the software which takes this information to dictate the actuators to achieve prescribed goals. For multi-agent systems, the key ingredient is communication among the agents to coordinate decisions and control actions. Coordination efficiency is dictated by communication bandwidth and reliability, as well as computational power available. This thesis addresses the formation control of teams of mobile robot - or multi-agent system of autonomous

vehicles - by providing a rigorous generalized framework for distributed model predictive control of constrained nonlinear systems. We address leader-follower formation control of constrained autonomous vehicles operating in an environment where communication bandwidth is limited and transmission delays are present, along with other sources of uncertainty and disturbances. A number of sources of uncertainty are taken into account to provide robustness to the algorithms developed. In existing literature, usually only measurement / estimation errors or model mismatch are taken into account. We consider the simultaneous presence of six sources of uncertainty consisting of errors in estimation, modeling, prediction, data compression and loss of information due to delay. We provide detailed feasibility and stability analysis to derive closed form analytic expressions relating the growth of uncertainty along the prediction horizon, and its effect on recursive feasibility and robust stability. Nearly ten new algorithms are developed in this thesis for designing distributed robust NMPC controllers for multi-agent vehicle control based on a very general theoretical framework providing key insights in choosing design parameters for control design. The proposed algorithms can be divided into two main categories: offline and online algorithms. The offline algorithms are computationally intensive, but since they are executed offline, this is not a major concern. The online algorithms are fast processing and provide update to the receding horizon control strategy. We provide robustness by finding upper bounds on uncertainty growth and hence restricting the admissible states to tighter constraints. Recursive feasibility is shown to depend on controllability

characteristics of system dynamics, which restricts the maximum allowable uncertainty growth. Our approach is dual-mode NMPC, where stability is ensured by suitable selection of terminal weighting factor, terminal constraint set and a linear terminal control law. We provide a method of maximizing this terminal constraint set, which is a measure of stability. Similarly, output feasible set of NMPC algorithm is determined with proposed min-max optimization technique. We also propose a method for data compression and trajectory tail estimation.

We propose a practically stable (ultimately bounded) formulation of the distributed nonlinear model predictive controller (DNMPC), in which agents communicate compressed information to each other with propagation delays and collision avoidance is guaranteed, despite the presence of these delays and uncertainties. Data compression using neural networks approach is used ensuring a considerable reduction of the data packet size (as much as 75 %). Moreover, the approach allows the agents to be sampled locally at different rates as well as to have different dynamics, constraints and prediction horizons, while being robust to uncertainties and propagation delays. Collision avoidance is achieved by means of a novel spatial filter-based potential field. Analytical results proving Input to State Practical Stability (ISpS) and generalized small gain conditions are presented for both strongly connected and weakly connected networks. Extended analytical and simulation based examples are provided to show the efficacy of proposed algorithms.

THESIS ABSTRACT (ARABIC)

ملخص الرسالة

الاسم: بلال احمد صديقي

العنوان: الإطار العام للتنقل أسطول من المركبات بواسطة التحكم الموزعة التنبؤي غير خطي

التخصص: هندسة النظم

التاريخ: ديسمبر ٢٠١٤

نقوم في هذا البحث العلمي بمعالجة عملية تشكيل تركيبات ذات خاصية القائد والأتباع للتحكم في المركبات ذاتية الحركة المقيدة والتي تعمل في بيئة ذات عرض نطاق ترددي بالإضافة الى وجود تأخير وبطء في الاتصالات. نقترح تصميم نموذج تحكم تنبؤي غير خطي، بحيث لا تحتاج فيه الروبوتات إلى تقدير حركة الروبوتات المجاورة مع ضمان تجنب الاصطدام. لضمان تخفيض حجم حزمة البيانات المرسل، يتم ضغط البيانات باستخدام الشبكات العصبية. وعلاوة على ذلك، فإن اقتراحنا يتميز بتكيف الروبوتات مع قراءات لأجهزة الاستشعار بمعدلات مختلفة بالإضافة إلى التكيف مع ديناميات مختلفة وعوامل تنبؤ وتقيد مختلفة، مع كونها ذات قدرة على تحمل بطء في الاتصالات وعدم اليقين من مسارات الروبوتات المجاورة. نقترح في هذا البحث وسيلة مبتكرة في تحقيق تفادي الاصطدام. يتم عرض النتائج التحليلية التي تثبت رسوخ واستقرار نموذج التحكم المقترح أثناء تجربتها في أنماط شبكية مختلفة. توضح نتائج المحاكاة فعالية نموذج التحكم المقترح.

CHAPTER 1

INTRODUCTION

1.1 Prologue

Research in robotics until recently has focused on development of autonomous agents working as singular units to interact with the environment. It was soon realized, however, that in many cases it is far more advantageous - sometimes necessary - for robots to work together in teams to increase scope, efficiency and protect against single points of failure. The main impediment to such development were physical constraints in terms of lack of miniaturization and high power consumption of sensors and actuators, lack of high speed, high volume and reliable communication and low on-board computation power. Recent advances in MEMS-based sensors, low consumption actuators, as well as affordable and high performance computing and communication equipment has allowed robotics - especially mobile robots - to advance rapidly towards development of multi-agent systems. The core of any robotic system is its 'brain circuitry' or how it is pro-

grammed to interact with its environment to achieve its objectives. This is the control system of the robot, which consists of the sensors to quantify measurable variables affecting it, the software which takes this information to dictate the actuators to achieve prescribed goals. For multi-agent systems, the key ingredient is communication among the agents to coordinate decisions and control actions. Coordination efficiency is dictated by communication bandwidth and reliability, as well as computational power available. This thesis addresses the formation control of teams of mobile robot - or multi-agent system of autonomous vehicles - by providing a rigorous generalized framework for distributed model predictive control of constrained nonlinear systems, in the presence of propagation delays.

1.1.1 Nature Inspires Multi-Agent Systems

Many engineering solutions are inspired from nature. Attractive monikers like ‘biologically inspired engineering’, ‘biomimicry’, ‘bio-inspired design’, ‘bio-inspired robotics’, ‘artificial intelligence’ are of relatively recent origin, but the ideas of adopting ideas, processes and design from nature to solve human problems is as old as engineering itself. Over the time, engineers and scientists have realized that the most efficient artificial designs are those which mimic nature’s designs. For example, we see that the wire-and-strut bi-wings of the Wright Brothers in 1903 were probably less efficient than Leonardo da Vinci’s bat-inspired wings in 1503. Da Vinci’s design had one problem though: the lack of materials and technology to realize that design, which was probably why the Wright airplane resembled a

flying truss bridge more than a modern airplane. In the last couple of decades, emergent technologies have breached new frontiers in materials, communication, computation and miniaturization that has made it possible to re-engineer some of nature's solutions to meet new problems and needs in an affordable manner. This is especially true in the field of robotics and automation, which aims to mimic natural intelligence and physical implementation of intelligent decisions. From the beginnings of serious automation in 8th century Abbassid Baghdad with its peak in Al-Jazari's 12th century complex programmable humanoid automata [1] to the current state of the art in robotics, the main evolution has not been - as commonly thought - of the mechanical infrastructure. Instead, a careful study would show that medieval means of actuation have evolved only gradually, but the most startling improvements have been in sensors, artificial intelligence and computational resources. In other words, to imitate nature we need more brain than brawn, which ironically is a bit counterintuitive!

Hence, even though remote controlled vehicles started appearing in the 1870s, the first truly autonomous robots were only demonstrated in the 1950s, coinciding with the birth of digital computers and artificial intelligence (AI). Mobile robots and autonomous intelligent vehicles did not appear until the 1970s, owing to the time it took to miniaturize and customize sensors and computers. From that time to the late 1980s, research and development had concentrated on improving single mobile robots (autonomous vehicles). However, the robotics research community soon realized that organism and agents in nature seldom live or work alone. Even

simple organisms have structured leadership and/or team mechanisms which enable them to achieve complex tasks which can be performed much less efficiently by single agents, if at all. Many examples of collective behavior exist in nature, see Figure 1.1, where it can be seen that most obvious collaborations occur among members of a given species. However, one can have intra-species competition e.g. packs of wolves or dingos fighting over turf, and there might indeed be evolving cooperation and competition based on selfish interests. All of these interesting biological behaviors have been a source of inspiration in multi-agent robotic systems (MArS) [2]. Therefore, nature has inspired work on multi-agent systems with the ability to swarm/flock [3], forage/track while avoiding predators [4], prey herding [5], locomotion and climbing [6], traveling in formation [7], self organization/adaptation and reconfigurability [8] etc.

Recent advances in MEMS technology has resulted in plethora of affordable, customizable and embedded sensors capable of wireless communication. Coupled with progress in miniaturization of micro-controllers and actuators with low power consumption, now sensing, computation, communication and actuation resources can be embedded in miniature packaging [9]. This proved particularly useful for mobile robots (also known as autonomous vehicles) working in teams due to the need to maintain communication among team members at low power expenditure. Such multi-agent teams of autonomous vehicles have found both civilian and military applications on land [10] and sea [11], as well as in air [12], space [13] and underwater [14]. These teams do not have to consist of members of the same



Figure 1.1: Inspirations of multi-agent systems from nature. (Clockwise from top left): fire ants collaborating to form a bridge to let others cross with food; migratory birds flying in pattern to benefit from upwash of other agents; sharks cooperating to herd prey fish into a tight ball to close the surface; lions cooperate to isolate a prey from its herd, as the herd maintains strength in numbers from a distance.

species, and can even be heterogeneous [15]. Applications of these robotic vehicle teams include reconnaissance and surveillance [16], striking payload delivery [17], inspection ([18], [19]), exploration and mapping [20], search and rescue [21] etc. This thesis will focus on cooperative control of multi agent teams of heterogeneous autonomous vehicles.

1.1.2 Cooperative Control and Formation Keeping

Research in unmanned vehicle systems has gathered interest from academia and industry alike, particularly during the last couple of decades. Starting early as remote controlled vehicles, they have also experienced a considerable advance towards autonomy at all levels. Cooperation between autonomous vehicles (agents)



Figure 1.2: Examples of multi-agent systems inspired by nature. (Clockwise from top left): quadcopters cooperating to lift an object too heavy for single agent; UAVs flying in formation to refuel and benefit from upwash; microsubmarine team inspecting pipes for leaks (see author’s patent [19]); humanoid teams in soccer match.

working in teams extend these robots’ capabilities to a level beyond what can be achieved by a single vehicle. In addition, such cooperation has shown promising advantages in terms of robustness, adaptivity, reconfigurability, flexibility, and scalability. Cooperation has been defined as a close relationship among all agents in the team with information sharing playing an important role [22]. This includes cooperative tasks like formation control and flocking, collision avoidance, rendezvous at the control level, cooperative perception at the information level, and cooperative planning and decision making at the mission level [23]. As a subclass of cooperative control, formation control has three basic elements [24] in multi-agent formation control:

- a. Cohesion: attraction to distant neighbors up to a reachable distance.

- b. Separation: repulsion from neighbors within some minimum allowable distance.
- c. Alignment: velocity and average heading agreement with neighbors.

Formation control without collision avoidance is also called state synchronization. Additionally, the team of multiple agents may be required to avoid obstacles and predators, encircle or flock around targets, while maintaining team formation [5].

1.1.3 Uncertainty, Disturbances and Real World Effects

Besides computational and communication topologies, the real world environment in which the agents must operate is both uncertain and disturbed. In fact, uncertainty is a fact of life for us mortals (but the Immortal does not play dice, to quote Einstein). For example, the precision in knowing one quantity usually comes at the expense in being more uncertain of another related quantity (Heisenberg uncertainty principle), and measurements of a system cannot be made without disturbing the observed system itself (“observer effect”)! Then, there are other sources of uncertainty which cannot be reasonably ignored for a successful design of control algorithms. Despite tremendous advances in computational technologies, we can (and will) not be able compute control actions instantaneously, communication occurs over usually uncertain, undedicated channels with limited throughput and packet drops.

Hence, the formation control algorithm should also cater for disturbances, uncertainties, delays and asynchronicity. The environment is sensed by on-board sensors which may have different bandwidths, sampling rates and accuracy. Rely-

ing on inertial measurement unit (IMU) consisting of gyroscopes and accelerometers, alone for localization (known as dead reckoning) can lead to large errors due to integration. Position fixes can be provided by global positioning system (GPS) with high accuracy. GPS sensors have a much slower sampling rate but generally lower noise than gyroscopes and accelerometers. Hence, some sort of data fusion is required to locally estimate the position of individual agents [25]. However, GPS signal often suffers from lack of satellite coverage in built-up areas or under rain. GPS signals experience an attenuation of over 50 dB a meter below the sea surface [26]. Hence, for underwater autonomous vehicles (AUVs), novel localization means and algorithms have to be employed. Also, if agents in the team are trying to track or localize a target or predators, they may benefit from sharing and combining individual estimates cooperatively [5].

1.2 Literature Review

Cooperative control of systems with multiple autonomous vehicles to perform coordinated tasks has many civilian and military applications, such as autonomous search and rescue, exploration, targeting, surveillance etc. Formation control of such a team can be performed in either centralized or distributed fashion. However, centralized control is neither always feasible, nor desirable in most scenarios due to increased computational burden on the central hub, communication issues and single point of failure meaning failure of the entire system. This section will review primarily the work in distributed nonlinear multi-agent control and related

topics.

1.2.1 Formation Control and Conflict Resolution

Nonlinear cooperative control of a team of underactuated hovercraft with constrained inputs is achieved in [27] by stabilizing individual agents using cascade back-stepping and distributed potential function based control for formation control. Formation control without collision avoidance is also called state synchronization. Dynamic neural network based adaptive control scheme for distributed fleet state synchronization, without the need to know local or leader (nonlinear) dynamics is applied in [28]. Lyapunov analysis is used to derive tuning rules, with the implicit need for persistent excitation, for both strongly connected and weakly connected networks. However, delays, asynchronous measurements, collision avoidance and limits on control actuation forces are not considered. In a similar approach, synchronization of nonlinear Lagrangian systems with linear-in-parameter model uncertainties has been solved using distributed adaptive back-stepping and adaptive redesign [29]. But unlike [28], all agents are assumed to have access to group reference trajectory, which constitutes a further limitation. Synchronization of a fleet of nonlinear Euler-Lagrangian systems has also been achieved using distributed H_∞ controllers robust to model uncertainties and disturbances in fixed and switching network topologies guaranteeing input to state stability (ISS) [30].

One of the most promising techniques for formation control of both linear

and nonlinear systems is model predictive control (MPC), also known as receding horizon control (RHC) for its inherent ability to handle constraints, incorporation of non-local information and reconfigurability. The main disadvantage is the heavy computational load for solving constrained nonlinear optimization problem at each sampling time, which may not be feasible for very fast dynamics. Few attempts at centralized NMPC have been made (e.g. [31]-[32]), but computational complexity is major impediments towards its pursuit. Distributed implementation of NMPC for multi-agent systems is therefore an attractive alternative for real time applications.

Unlike multi-agent (also called large scale systems) chemical and electrical plants, unmanned autonomous vehicles are not dynamically coupled. They are coupled only in their constraints and cost functions. Work on multi-agent formation control of autonomous vehicles using MPC was pioneered by Dunbar at Caltech in 2001 [33]. He considered distributed NMPC for leader-less synchronization of agents with constrained, continuous dynamics. All agents had access to the dynamic model of every other agent as well as the virtual leader. Stability was ensured using terminal set and linear terminal control technique [34]. However, no delay was considered. This work has been extended later in [35] by requiring each agent to transmit its optimum control trajectory at every sampling instant to its neighbors. Each vehicle control is determined by solving an NMPC problem that minimizes a local cost function, which considers the received control trajectories and models of its neighbors. For stability, it is required that the actual trajec-

tory of each vehicle does not deviate too much from the one it transmitted to its neighbors. Hence, no account is taken of model uncertainties and delays. The need to know neighbors' dynamic models was removed in a recent work [36], by communicating state error trajectories to immediate neighbors, instead of vehicle trajectories. However, the results are conservative in that only a queue or string formation is considered.

A generalized framework for distributed NMPC for cooperative control of team of agents is proposed in [37], based on the terminal set approach in [38]. Asymptotic stability is ensured by means of invariance of a terminal set and terminal control law, such that all agents communicate their planned trajectories to all other agents. This last requirement was weakened to neighbor-to-neighbor communication in [39]. On a parallel course, a framework for NMPC without the restriction of terminal control and terminal set was introduced in [40]. Stability is guaranteed using "relaxed" dynamic programming arguments, instead of control Lyapunov function approach. This approach allows for shorter control and prediction horizons, as well as strategies for adapting the horizon [41]. This was extended to the multi-agent case recently in [42], where the individual agents solve their local optimization problem sequentially after receiving predicted states from their neighbors. However, the problem solved was non-cooperative distributed NMPC, such that the neighborhood information is used to design state constraints for collision avoidance, but the cost function in optimal control problem (OCP) of individual agents does not take into account this information. Also, the algorithm

is sequential, that is other agents have to wait for their turn till one agent finishes computing its control move. This may cause unacceptable delays in agents with fast dynamics or teams where the number of agents is large. Extending the work of [42], instead of sequential implementation, a quasi-parallel dispensation is shown to be asymptotically stable in [43]. Since agents impose state constraints on their neighbors, a covering algorithm assigns hierarchy to the agents to coordinate their actions. Agents at the same hierarchy level implement their control in parallel, even though the hierarchy itself is computed sequentially.

Moving a team of agents in close proximity to each other is challenging in the sense that performing relatively aggressive manoeuvres can cause collision among the agents. On the other hand obstacles between the team and the waypoint need to be avoided for safe conduct of the team. Similarly, a predator e.g. an enemy aircraft, has to be evaded. The ability to avoid collisions among team members and with external obstacles and evading predators will be called conflict resolution. Moreover, faults in individual agents can compromise both group cohesion and conflict resolution. Not only must predators, obstacles and neighbors be located using some sensors, but appropriate actions should be planned and executed for attaining mission objectives. Similarly, there should be a method for identifying faults, as well as measures for fault tolerance in the control architecture.

The pioneering work in distributed multi-agent MPC of [33] was extended using graph theory to specify distributed NMPC cost functions for agents, and ensuring collision avoidance by repelling potential field [44]. In a similar vein,

[45] considered collision and obstacle avoidance in a pursuit-evasion game among multiple vehicles by adding repulsive potential fields to local NMPC cost function and using current position and velocity of other vehicles to predict their future trajectories. However, the author did not provide stability proofs and ignored robustness issues. In [46], feedback linearization is used in the terminal set of NMPC, but only collision avoidance is considered in formation, without stability proofs. In contrast to this approach, in [47] the nonlinear dynamics is first linearized using feedback linearization in an inner loop and then MPC using the linearized model is employed to find collision free trajectories. It is assumed that the tracking error of predicted trajectories are exchanged among the vehicles without delay. Collision avoidance in a distributed NMPC setting for car-like robots is presented in [48] using potential-like functions to avoid collisions. Two communication strategies are considered. In one case, only the first element of the planned control action is transmitted and the receiving agent assumes this control would remain fixed during the entire prediction horizon. Using this assumption and a dynamic model of the neighbor, it predicts its neighbor's planned trajectory. In the other approach, the entire planned state trajectory is transmitted to all neighbors. It is shown through simulations that the latter approach is more successful in avoiding collisions. No stability proofs were provided. Centralized computation of NMPC is coupled with a finite state machine (FSM) in [49] for real time collision and obstacle avoidance. The FSM processes sensor information about obstacles and agents on collision course, and modifies the optimal control

problem (OCP) of NMPC by adding inequality constraints pertaining to the obstacle detected. Stability results provide are of a very preliminary nature. In [50], cost penalty is applied in OCP for obstacle avoidance and penalty combined with priority strategy for collision avoidance in the NMPC framework, using neighbors' randomly delayed information, which is assumed to be noise free. For collision avoidance, the vehicle with higher tracking error is given a higher priority and takes action to avoid collision, while the other vehicle continues on its course. No stability proofs were provided.

Distributed NMPC for simultaneous formation control and trajectory planning for multi-agent airport snow shoveling application in a partially known environment is considered in [51]. In this leader-follower approach, a virtual leader optimizes its trajectory with terminal set constraints (for stability), and the agents follow this trajectory at an offset. Both static and dynamic (including other team members) obstacles, which are not always known a priori, are avoided using a novel technique, which combines potential like functions with state constraints. It is also interesting that the overall objective is to maneuver the team to target in minimum time, and is achieved by splitting the prediction horizon into two parts. In the first segment, classical cost function penalizing distance from target and input energy is used, while in the second segment, the time to target is used in the cost function. However, no stability or convergence proof of this modification is offered. The only communication required is transmission of virtual leader's trajectory and sharing detected objects among agents.

A related development is non-cooperative distributed NMPC for multi-agent teams. In this approach, the information received from neighbors is processed as state constraints for the receiving agent, but their individual cost functions are not affected by this information. In other words there is no cooperation cost component in the distributed cost functions of the individual agents. The information received from other agents is used only for collision avoidance by applying state constraints, not potential-like functions in the distributed cost function. It is well known that in the non-cooperative setting the global minimum can no longer be reached, and the best result that can be hoped for is a Nash equilibrium. Non-cooperative distributed NMPC with terminal constrained set has been suggested in [52] for collision and obstacle-free trajectory planning for way-point tracking by unmanned fixed-wing aircraft (with identical dynamics and prediction horizons) sharing an airspace, but no common goals. In the event of failure to find feasible conflict-free trajectory, it is assumed that the aircraft are able to switch to safe loiter trajectory for an indefinite period of time. Hence, conflict resolution means avoiding intersection of aircraft trajectories and loiter patterns by incorporating predicted states received from other aircraft as state constraints (no-fly zones). NMPC, with linear dynamics but nonlinear constraints, is solved sequentially by the aircraft according to some ordering logic. In the distributed NMPC approach without terminal set taken in [42], predicted states trajectories received from the neighbors are treated as state constraints for collision avoidance for sequentially solving NMPC on individual agents. However, with or without terminal con-

straint set, sequential implementation can introduce unacceptably large delays if the number of agents are high, or agent dynamics is fast. A degree of parallelization of this approach was achieved recently in [43] using a sequential hierarchy assignment algorithm. In both of these works, asymptotic stability for nominal conditions was demonstrated using dynamic programming principles.

1.2.2 Robustness

Most research in distributed NMPC of autonomous vehicles is focused on finding solutions in ideal conditions, i.e. with fully known dynamics and no uncertainty, asynchronicity or delays. However, in many practical cases, there might be serious departure from these ideal conditions, which may lead to failure.

One of the chief reasons for collision among team members or with obstacles is development of sensor or physical faults in one or more team members. Since NMPC is a model based control technique, deviation of the vehicle dynamics or its measurement from that predicted by its internal model can lead to large errors or even instability and collisions. For a fleet of underwater vehicles [53], decentralized MPC was proposed, while ensuring fault tolerance. Each vehicle shares its plans and information on faulty states with its neighbors in a virtual-leader setting. This work was extended in [54], by merging extended Kalman filtering (EKF)-based sensor fusion for localization with distributed MPC for collision avoidance and formation tracking. Control of a quadcopter with NMPC is proposed in [55]. Local states, as well as fault parameters are estimated using unscented Kalman

filters (UKF) on each agent. Since, the internal model of vehicle dynamics is parametrized using these fault parameters, the updated internal model is shown to be able to mitigate effects of actuator fault. However, no formal proof of stability is furnished. The major drawback of the approach is that Kalman filter is known to have overshoots in its predictions, which might violate system bounds. Therefore, a potential improvement is to estimate states using constrained versions [56] of filtering algorithms.

A very interesting application of distributed multi-agent NMPC was pursued in [57], where multiple GPS-fitted robots are tasked with localizing features in an unknown environment. Hence, the objective function is maximization of local Fischer information matrix by planning a finite time trajectory which gathers the most information. The objective function is not only nonlinear, but uncertain, due to noise. Hence, the OCP is an optimal control problem with gradually identified model, as the features appear in the state vector. Simulations show remarkable improvement over some existing algorithms. Additionally, constraints are also applied for collision avoidance by declaring the uncertainty ellipse around the identified feature as a no-fly zone. However, there are quite a few shortcomings in this pioneering work. Firstly, no stability results were provided for this approach. Secondly, the multiple agents do not share information with each other, nor coordinate their tasks, which may lead to agents duplicating the same effort, and collisions. Discovering more features leads to growth of the state vector which will make the OCP harder to solve. Therefore, there should be mechanism to limit

the size of the state vector. And the use of unconstrained estimation may lead to violation of system bounds.

Autonomous agents working in a cooperative team can work in coordination with each other only if there is some communication among them. Even though their dynamics is decoupled from each other, the information structure and cooperation goals couples them in the distributed control architecture. Since, communication bandwidth is limited, no information can travel immediately. The amount of delay in reception (also known as latency) depends on the communication protocol, network traffic, congestion, bandwidth of medium etc. Along with this, the information received must be situation in time of broadcast, which can be difficult if the clocks at the two agents are not synchronized, itself a non trivial issue. Also, the sampling time of two agents might be different, and multi-rate information needs to be processed for optimization. Since, cooperative control is intrinsically tied to communication and information flow, these are important elements in control design.

Pioneering theoretical work on extending distributed NMPC framework to a group of autonomous vehicles receiving delayed information (delay is fixed) from their neighbors was recently presented in ([58]-[59]). Rigorous stability analysis is used to establish regional input-to-state (ISS), extending the work on NMPC of single systems in [60]. The delayed state information is projected in the prediction horizon using a *forward forgetting-factor*. In effect, it means that each agent assumes that the states of its neighbors will asymptotically go to zero (or equilib-

rium) and uses this assumed prediction to plan its own trajectory. Hence, there is no need for agents to know their neighbors' dynamics, but agents are assumed to have synchronous clocks and same sampling time. However, no explicit conflict resolution is considered and it appears that the scheme may fail during aggressive manoeuvres. This is because all states in a system do not settle down to target set at the same exponential rate (dictated by forgetting factor) and during aggressive manoeuvres, the assumption of smooth asymptotic trajectory may not hold.

NMPC based formation control in leader-follower formulation is shown in [61] to be tolerant to limited communication failure, provided that the network is strongly connected (i.e. each agent communicate with all other team members). In [50], using cost penalties for obstacle avoidance and penalty combined with priority strategy collision avoidance in the NMPC framework, the neighbors' randomly delayed information is projected in the prediction horizon by linear recurrence. No stability proofs are furnished in both cases.

Another approach for the same problem is taken in [62], where some members of the team develop fault in communication systems, so that trajectory broadcast by them is received after a fixed delay. It is assumed that all agents have dynamic models of every other agent in the team. It is assumed that after developing fault in communication system, the faulty agent will limit its control authority to predefined limits, which are known to all agents a priori. Obviously, when delayed information is received, the first part of received trajectory is intact, but the "tail" is missing. Using dynamic model of the agent having faulty communication, the

receiving agents simulate all possible trajectories of the faulty agent in the tail segment, or a so-called “tube” regional in the tail segment. Then the worst case trajectory, from a collision avoidance point of view is selected in the cost function of the receiving agent [63]. This method has many limitations. The computation of tube region is computationally heavy, and may take too long to calculate for multiple input systems. Then, there is also the need for each agent to know the dynamics of all team members, and their hard limits on control authority. Also, the agents’ clocks are assumed to be synchronized. To alleviate the online computation load, the tube region can be calculated off line and retrieved for online implementation [55]. However, the authors do not mention how could one possibly calculate tubes for all feasible trajectories. It should be pointed out that even though the approach seems promising, no stability proofs are provided.

The same authors extended their work to distributively and adaptively allocate available bandwidth among agents being controlled by delay tolerant distributed NMPC [64]. It is assumed there is no uncertainty in dynamic model or sensor noise, and states are measurable without delay. All agents are assumed to know the dynamic model of all other agents and their clocks are synchronized. Moreover, the tube calculation technique for tail-segment estimation due to delay [55] is abandoned in this work, and it’s cost is simply removed from the cost function. Surprisingly, no theoretical justification is provided for this. The delay in communication between two vehicles is inversely proportional to the bandwidth allocated to that channel. For distributed dynamic bandwidth allocation, each

vehicle calculates the error in NMPC calculation of all of its neighbors due to delay caused by allocated bandwidth. Then, bandwidth is allocated to neighbors by solving a large scale nonlinear optimization problem minimizing some measure of these errors, and rigorous proof for its convergence based on linearized models is furnished. This approach is very promising, however it computationally very expensive and no convergence or stability proof for the overall NMPC/bandwidth allocation algorithm is provided. Also, the stability proofs are applicable to agents which can be represented by single linear models for the entire trajectory, which is not feasible for many autonomous vehicles.

1.2.3 Gaps in Current Body of Work

It should be noted that this literature survey was focused on nonlinear model predictive control (NMPC) for robust multi-agent control of dynamically decoupled systems, like autonomous vehicles. There is a huge body of work pertaining to other control techniques for formation control (see [65] and [22]), including linear MPC. There is also a considerable amount of literature on NMPC for dynamically coupled systems (see [66] and [67]), for example chemical process plants. However, these are outside the scope of this work. It is noteworthy that work in this focus area is very recent, with preliminary work starting only in 2001, and formal proofs with delay tolerance beginning to appear as recently as 2008. Therefore, it is not surprising that the body of literature in this regard is relatively small, and offers many fertile avenues for research and development. We found the following areas

where we can contribute to the current body of work:

- i. *Conservativeness of Existing Algorithms.* The first area of improvement in the current body of work is theoretical establishment of stability and feasibility for cooperative distributed multi-agent NMPC for uncoupled systems. Even though the stability proofs furnished in the seminal work of [59] are rigorously derived using terminal constraint to prove input to state stability (ISS), the results are very conservative. The algorithm and stability theorems are applicable to trivial trajectories, without any guarantee for collision avoidance or robustness properties. Many of the other algorithms which have been proposed lack any theoretical justification from stability standpoint.
- ii. *Limited Bandwidth Algorithms* which require propagation of entire trajectory to neighbors require exchange of large data packets. Reduction of packet size or utilizing more efficiently the limited bandwidth is another area where only preliminary and very conservative results are available [64].
- iii. *Robustness* to faults, noise, uncertainty is considered in very adhoc manner in the literature. There has been a very recent attempt to prove practical stability of NMPC coupled with extended Kalman filter (EKF) based state estimation for single system in the presence of non-vanishing errors with deterministic model and no disturbance or measurement noise [68]. We will consider simultaneous presence of several sources of noise, including those mentioned above.

1.3 Problem Statement

This thesis addresses the formation control of teams of mobile robot - or multi-agent system of autonomous vehicles - by providing a rigorous generalized framework for distributed model predictive control of constrained nonlinear systems. We address leader-follower formation control of constrained autonomous vehicles operating in an environment where communication bandwidth is limited and transmission delays are present, along with other sources of uncertainty and disturbances. A number of sources of uncertainty are taken into account to provide robustness to the algorithms developed. In existing literature, usually only measurement / estimation errors or model mismatch are taken into account. We consider the simultaneous presence of six sources of uncertainty

- i. error in estimating current state,
- ii. error in estimating current external input (disturbance or external information),
- iii. error in predicting future system state due to model mismatch,
- iv. error in predicting future external input due to disturbance model mismatch (disturbance model is another uncertain dynamic system with unknown input),
- v. error in approximating trajectory due to data compression, and
- vi. error in approximating the last segments (tail) of the compressed trajectory due to propagation delays.

We provide detailed feasibility and stability analysis to closed form analytic expressions relating the growth of uncertainty along the prediction horizon, and its effect on recursive feasibility and robust stability. In particular the objective is to be able to simultaneously plan the trajectory and drive a formation of cooperative autonomous agents to accomplish assigned missions in a safe and stable manner, such that collisions are reliably avoided. The dynamical models of autonomous vehicles are uncertain and subject to an externally driven disturbance system. The agents are heterogeneous in dynamics, and can therefore have different discretization times and sampling rates. Moreover, the bandwidth of communication channel is limited and needs to be utilized efficiently. The communication channel is also subject to random delays. Our objective is to design stable distributed NMPC controllers for collision free formation control tasks, robust to these sources of uncertainties, for different network topologies.

1.4 Research Contribution

The contributions of this paper are non-trivial in the following aspects.

- i. Existing literature mostly considers either modeling uncertainty with perfect measurements or measurement noise with perfect model. The proposed approach provides a unified framework for dealing with both types of uncertainties, along with the inclusion of a non-additive disturbance with uncertain dynamics and unknown input.
- ii. Input-to-state stability (ISS) framework in existing literature is extended with

Theorem 3.2.2 to cater for the combination of uncertainties mentioned above.

- iii. New bounds on prediction error growth along the prediction horizon have been derived (Lemma 3.2.1) based on the bounds on components of the combined uncertainty. In addition, constraint tightening for robust satisfaction of original constraints in the presence of this combination of uncertainties (Theorem 3.2.1) is also a new development.
- iv. Recursive feasibility is ensured by the newly developed Theorem 3.1 which relates it to the size of the one-step controllable set to the terminal region.
- v. Terminal constraint region is maximized (Theorem 4.3.1) based on PLDI based LMIs, and warm started with a novel approach involving algebraic Riccati equations.
- vi. One-step controllable set and robust output feasible set are determined based on min-max optimization (Algorithm 6) rather than the existing set based approaches.
- vii. One main and five component new algorithms are presented for constraint tightening, terminal region optimization, determining feasibility and online optimization.
- viii. Robustness to inaccuracy in communicated trajectories is explicitly taken into account, resulting in practical stability instead of asymptotic stability in existing literature.

- ix. Collision avoidance is also explicitly catered for. A novel modification of potential field method is proposed, based on a novel spatial filter, whose feasibility and stability is rigorously proved.
- x. New generalized input to state practical stability (ISpS) and generalized small gain conditions are derived for the distributed controller.
- xi. Unlike existing literature, the stability results of this chapter are not limited to strongly connected networks. It is shown even a weakly connected network topology for multiple agents can be designed for fleet-wide stability.

The contributions of this paper resulted in the following peer-reviewed research.

1. S. El-Ferik, B. A. Siddiqui, and F. L. Lewis, Distributed Nonlinear MPC Formation Control with Limited Bandwidth, in American Control Conference, Washington, DC, 17-19 Jun. 2013, pp. 63886393. [73]. [Adjudged as the best presentation in the session].
2. S. El-Ferik, B. Siddiqui, R. B. Mansour, and F. Al-Sunni, Dual Submarine Leak Detection System, U.S. Patent 8 499 617, Aug 6, 2013. [19]. [Awarded 4th prize in innovation track and 5th Students' Conference organized by Ministry of Higher Education (MoHE) at Mecca, April 2013].
3. S. El-Ferik, B. A. Siddiqui, and F. L. Lewis, Distributed Nonlinear MPC of Multi-Agent Systems with Data Compression and Random Delays, IEEE Transactions on Automatic Control, Oct. 2014, accepted for publication.

4. S. El-Ferik and B. A. Siddiqi, “Algorithms and System for Collaborative Multi-agent Robust Predictive Control with Data Compression”, submitted to US Patent Office, December 2014.
5. S. El-Ferik and B. A. Siddiqi, “Method for Determining Robust Constraints and Optimum Parameters for Nonlinear Predictive Control”, submitted to US Patent Office, December 2014
6. S. El-Ferik, B. A. Siddiqui, and F. Lewis, Constraint Tightened Robust Non-linear Predictive Control with Uncertain Disturbance Model, *Automatica*, Dec. 2014, submitted, under review. [84]

1.5 Thesis Organization

This chapter (Chapter 1) introduced the problems to be studied in this chapter in a comprehensive manner, first by motivating the reader about the significance of multi-agent control systems and how they relate to nature, the problems and challenges involved. A detailed literature review provides insights into avenues where research is still lacking and where this work can help bridge the gaps by providing a generalized framework for robust, distributed NMPC control design methodology. The research problem is clearly stated along with details of the research methodology followed in this work.

Chapter 2 motivates the reason nonlinear discrete-time systems are the focus of this research. Some useful set theoretic and functional analysis tools are intro-

duced , including the concept of set invariance, comparison functions and a useful property of these functions. Different notions of nonlinear stability analysis are also introduced. Modern concepts of input-to-state and input-to-state practical stability are also introduced. An important new result in the form of Theorem 2.5.2 is presented which forms the cornerstone of later development.

Chapter 3 presents new results in nonlinear MPC control with robustness against a number of sources of uncertainty. The main NMPC algorithm and one of its five component algorithms to address constraint tightening and online optimization are introduced in this chapter. Algorithm 1 includes offline components and online optimization of the recursive finite horizon OCP 3.2.1. It shows that due to uncertainties, only practical stability (ISpS) can be ensured, and the amount of tolerable disturbance is bounded by the size of the one-step controllability set to the terminal constraint region. An extended numerical example was introduced in two parts. Closed form analytic expressions of all nonlinear functions and Lipschitz constants are provided along with a simulation example for constraint tightening Algorithm 2.

Chapter 4 presents new results in terminal region maximization and feasibility set estimation of robust nonlinear MPC algorithm. We presented four algorithms terminal region optimization, terminal control law design and determining maximum robust output feasible set. Terminal region is maximized based on polytopic linear difference inclusions (PLDI) by Algorithms 5-4. One-step controllable set and robust output feasible set are calculated using Algorithm 5-6. Hence, this

chapter completed the development of all components of Algorithm 1. To increase robustness and initial feasibility region, the terminal region was maximized with theoretically derived methods for warm starting the algorithm. Moreover, min-max optimization to find the maximum initial feasibility set for the worst case realization of uncertainties as also described. Simulations based on the extended nonlinear oscillator were used to validate the theoretical results.

Chapter 5 , we address the problem of leader-follower formation control of constrained autonomous vehicles subject to propagation delays and uncertainties, building on the development in previous chapters. Limited network throughput demands reduction in packet size. The proposed approach achieves formation tracking through NMPC such that each agent performs local optimization based on planned approximate trajectories received from its neighbors. The trajectory is compressed using neural networks, which is shown to reduce the packet size considerably. Moreover, the method allows the agents to be heterogeneous, make asynchronous measurements and have different local optimization parameters. A method for estimating the tail of trajectory not available due to delays is also furnished. Collision avoidance is achieved by formulating a novel spatial-filtered potential field which is activated in a “zone of safety” around the agent’s trajectory. New theoretical results are presented along with validating simulations for different network topologies.

Finally, the thesis is concluded in Chapter 6, summarizing the contributions of this work along with interesting future research directions.

CHAPTER 2

NOTIONS OF STABILITY IN NONLINEAR SYSTEMS

2.1 Introduction

Analysis and design of nonlinear dynamical systems and their control laws in electrical, mechanical, aerospace, biological or any other engineering system requires a wide range of mathematical tools, especially those pertaining to notions of stability and control. This chapter serves as the generalized mathematical foundation of later theoretical development particularized to study of distributed nonlinear model predictive control. We introduce important concepts such as comparison functions, Lyapunov's method, input-state and practical stability. We will focus on deterministic discrete-time nonlinear systems, for ease of relating to digital implementation. We present an important new result in input-to-state practical stability, which is very general and will serve as the foundation of NMPC

framework in later chapters.

As made clear in later chapters, information from other members of the team is treated by each agent as external inputs. Besides not being controllable from the point of view of the agents, these external inputs are also uncertain. Therefore asymptotic stability is very difficult to achieve, and we have to resort to practical stability criteria. Also, since external inputs are present, we have to use the relatively modern concept of input to state stability (ISS) to analyze dependence of system response in terms of external input magnitude. ISS was introduced in the 90s by Sontag [70]. It utilizes comparison functions to characterize the Lyapunov function and establish stability. ISS is equivalent to asymptotic stability of a ball around the origin whose radius is a function of the norm of the applied control input [71]. Therefore, zero-input (unforced system) means asymptotic stability of the origin. Due to its ability to handle external inputs, ISS has been widely used as a framework for robust control design [72]. Since asymptotic stability is not achievable in many practical situations, extensions of the original ISS to cover robustness issues have also appeared. Among them is input-to-state practical stability (ISpS) [73] and integral ISS (iISS) [74]. ISpS is a more general property than iISS, and will therefore be the focus of this and following chapters. Practical stability means that even with zero-input, some uncertainty may make the equilibrium unapproachable, and we can only ensure asymptotic stability of a ball around the equilibrium whose radius is a function of the magnitude of uncertainty. We will provide a new result on ISpS, after introducing several concepts which lead

up to it. In later chapters, we will develop it further to formulate a small-gain theorem and develop a general framework for distributed NMPC.

Chapter Organization General nonlinear systems are compared with their linear approximations, and the contrast between continuous-time and discrete-time descriptions with their pros and cons are discussed in sections 2.2-2.3. Then some useful set theoretic and functional analysis tools are introduced in section 2.4, including the concept of set invariance, comparison functions and the useful Lemma 2.4.1. Different notions of stability analysis are introduced in section 2.5. Modern concepts of input-to-state and input-to-state practical stability are introduced. An important new result in the form of Theorem 2.5.2 is presented which forms the cornerstone of later development. Finally, salient features of the chapter are concluded in the final section.

2.2 Linear versus Nonlinear Systems

In general all dynamical systems are described by nonlinear difference (discrete-time) or differential (continuous-time) equations, if all phenomena related to their dynamics are considered and no approximation is made. We will deal with systems that can be modeled by a finite number of coupled first-order non-autonomous

(state equation is an explicit function of time) difference equations

$$\begin{aligned}
 x_{1,t+1} &= f_1(t, x_{1,t}, \dots, x_{n,t}, u_{1,t}, \dots, u_{m,t}, w_{1,t}, \dots, w_{p,t}) \\
 &\vdots \\
 x_{n,t+1} &= f_n(t, x_{1,t}, \dots, x_{n,t}, u_{1,t}, \dots, u_{m,t}, w_{1,t}, \dots, w_{p,t})
 \end{aligned} \tag{2.1}$$

where $x_{i,t} \in \mathbb{R}^n$, $u_{j,t} \in \mathbb{R}^m$ and $w_{k,t} \in \mathbb{R}^p$ are the i^{th} system state, j^{th} internal input and k^{th} external input respectively, at time instant $t \in \mathbb{Z}_{\geq 0}$, and f_i are locally Lipschitz maps (see Definition 2.4.13) for $i = 1, \dots, n$, $j = 1, \dots, m$ and $k = 1, \dots, p$. Internal input u can be considered the manipulable control variable, whereas w can be an external input, like disturbance etc. to the system. We will use a vector notation for these equations for compactness. Let $x_t = [x_{1,t}, \dots, x_{n,t}]^T$, $u_t = [u_{1,t}, \dots, u_{m,t}]^T$, $w_t = [w_{1,t}, \dots, w_{p,t}]^T$ and $f(x_t, u_t) = [f_1(t, x_t, u_t), \dots, f_n(x_t, w_t)]^T$,

$$x_{t+1} = f(t, x_t, u_t, w_t) \tag{2.2}$$

However, most nonlinear systems can be approximated reasonably well by linear models, linearized about some set point in the state space. A common linearization of (2.2) is representation in terms of first difference (derivative) around some set point $(\bar{x}, \bar{u}, \bar{w})$.

$$x_{t+1} = A(t)x_t + B(t)u_t + E(t)w_t \tag{2.3}$$

where, $A = \frac{\partial f}{\partial x}(t, \bar{x}, \bar{u}, \bar{w})$, $B = \frac{\partial f}{\partial u}(t, \bar{x}, \bar{u}, \bar{w})$ and $E = \frac{\partial f}{\partial w}(t, \bar{x}, \bar{u}, \bar{w})$ are Jacobean matrices of the system. Linear systems are far easier to analyze and control, due to a wide variety of easy to use tools, such as root-locus and Nyquist plots, even for sophisticated and high order linear models. Indeed, many practitioners do not feel the need to abandon well-understood linear analysis for the more complex nonlinear model. However, linearization has its limitations. Firstly, linear model is generally only valid in some neighborhood of the set point, whereas nonlinear models are globally applicable throughout the state-space. Another reason for engineers to study nonlinear models is that often the dynamics of linear models is not rich enough to predict phenomena such as multiple equilibria, limit cycles, bifurcation, synchronization and frequency entrainment, chaotic behavior, finite escape time, subharmonic and almost-periodic oscillations etc ([75], [76]). These phenomena and other rich insight into system dynamics can be predicted with nonlinear models. In other cases, it is not even possible to linearize (2.2), though one may resort to more complex parameter-varying or time-varying linear representations, with increasing difficulty in analysis and control design. Therefore, even though linear analysis and design is more tractable, in many cases it is more desirable - if not necessary - to design controllers and analyze systems using nonlinear tools.

2.3 Discrete- versus Continuous-time models

As mentioned in Section 2.2, system dynamics can be modeled in two alternative frameworks: in continuous time with differential equations or in discrete-time with difference equations. Continuous time ranges over the entire real-number line. This is how all dynamic variables evolve in nature. However, this is often not how we measure them, especially in this age. In most digital circuits, the continuous variables are measured by sampling them at discrete intervals of time. Moreover, most controllers today are implemented on embedded digital computing hardware making it necessary to have a discrete-time description of the controller. Controllers designed in discrete-time can be directly implemented in digital form on embedded computers [77]. Digital control offers several distinct advantages over analog (continuous) controllers, including inexpensive hardware, reconfigurable software, scalability, adaptability, less prone to noise etc. Another advantage not yet obvious is that the optimization problem with discrete-time model is easier to solve than continuous model in MPC, as the number of decision variables is countable. Therefore, in this thesis we will focus on nonlinear discrete time system models.

However, one must caution that design of controller in discrete-time is often more complex than continuous-time design, since the first difference of Lyapunov function in discrete-time is quadratic in the state variables, as opposed to being linear in the continuous case [77].

2.4 Some Mathematical Theory Concepts

Set theory and functional analysis are important tools in nonlinear and robust control theory. In future chapters we will be making extensive use of them. Therefore, in order to make the thesis self-contained, a concise introduction to some of these concepts is rendered below.

2.4.1 Set Theoretic Concepts

Set theory is the branch of mathematical logic that studies sets, which are collections of (mathematical) objects. Let \mathbb{R} , $\mathbb{R}_{\geq 0}$, \mathbb{Z} , $\mathbb{Z}_{\geq 0}$ denote real, non-negative real, integer and non-negative integer sets of numbers, respectively. Given a signal x , let $x_{t,t+N}$ be the discrete-time sequence from time instant t to $t + N$. In the following, we introduce a few concepts from set theory which will be useful for later development.

Definition 2.4.1 (Compact Sets) A set is *closed* if and only if it contains all of its limit points. A set is *bounded* if all its points lie within finite distance of each other. A closed and bounded set is said to be *compact*.

Definition 2.4.2 (Interior Set and Point) All points in a set excluding its boundary is called the interior of the set, i.e. $\mathbf{int} A \triangleq \{x : x \in A \setminus \partial A\}$. Members of the interior set are called interior points.

For a set $A \subseteq \mathbb{R}^n$, the *point to set distance* from $\zeta \in \mathbb{R}^n$ to A is denoted by $\text{dist}(\zeta, A) \triangleq \inf \{|\eta - \zeta|, \eta \in A\}$, and if A is a closed set, its boundary is denoted by ∂A .

Definition 2.4.3 (Set Difference) For two sets $A, B \subseteq \mathbb{R}^n$, their set difference is denoted by $A \setminus B \triangleq \{x : x \in A, x \notin B\}$, and their distance is denoted by $\text{dist}(A, B) \triangleq \inf \{d(\zeta, A), \zeta \in B\}$

Definition 2.4.4 (Minkowski (Pontryagin) Difference and Sum) For two sets $A, B \subseteq \mathbb{R}^n$, the Pontryagin (or Minkowski) difference between them is defined as

$$A \sim B \triangleq \{x \in \mathbb{R}^n : x + y \in A, \forall y \in B\}. \quad (2.4)$$

The Minkowski (or vector) sum of these two sets is defined as

$$A \oplus B \triangleq \{x + y \in \mathbb{R}^n \forall x \in A, y \in B\}. \quad (2.5)$$

Definition 2.4.5 (Indicator Function) The indicator function of a subset A of a set X is a function $\mathbf{1}_A : X \rightarrow \{0, 1\}$ defined as:

$$\mathbf{1}_A(x) = \begin{cases} 1 & \text{if } x \in A, \\ 0 & \text{if } x \notin A. \end{cases} \quad (2.6)$$

Set Invariance Theory

Set invariance is a fundamental concept in design of robust controllers for constrained systems. Set invariance is strictly connected with (Lyapunov) stability.

We will briefly introduce some of its fundamental concepts. Consider the following

discrete-time nonlinear system

$$x_{t+1} = f(x_t, u_t, w, t) \quad (2.7)$$

with $f(0, 0, 0) = 0$ i.e. the origin is an equilibrium point and $x_t \in X \subset \mathbb{R}^n$, $u_t \in U \subset \mathbb{R}^r$ and $w_t \in W \subset \mathbb{R}^p$ are the system state, input and external (or ‘disturbance’) input respectively. Sets X , U and W are compact, containing the origin as an interior point.

Definition 2.4.6 (Admissible and Allowable Inputs) An *admissible* control input is one which satisfies input constraints $u \in U$, while an *allowable* disturbance is contained in its constraint set $w \in W$.

It is now possible to state basic concepts of invariance.

Definition 2.4.7 (Robust Positively Invariant Set) A set $\Xi \subseteq X$ is called robust positively invariant (RPI) for system (2.7), if $\bar{f}(x_t, u_t) \in \Xi$ for every $x_t \in \Xi$, if the control is admissible ($u_t \in U$) and disturbance input is admissible ($w_t \in W$).

In other words, if the system reaches an RPI set, its future evolution remains inside that set. We often need to determine the subset of state constraint set X which is compatible with some feedback control law.

Definition 2.4.8 (Robust Input Admissible Set) Given a feedback control law (CL) $u_{t+l} = k(x_{t+l})$ for system (2.7), the robust input admissible (also known as Robust Positive Control Invariant in case of state feedback) set $X_{CL} \subseteq X$ is

defined as

$$X_{CL} \triangleq \{x_{t+l} : x_{t+l+1} \in X, k(x_{t+l}) \in U, w_{t+l} \in W\} \quad (2.8)$$

for $l \geq 0$, with closed loop dynamics

$$x_{t+1} = f(x_t, k(x_t), w, t) \quad (2.9)$$

Reachability and controllability are important concept in constrained robust control. We study the problem of determining the subset of state space which can be reached using an admissible control sequence to any given target set, while guaranteeing that the state constraints will be satisfied along the trajectory for all allowable disturbance sequences. This is a more comprehensive problem than classical interpretations of reachability and controllability problems in unconstrained linear systems.

Definition 2.4.9 (One-Step Robust Controllable Set) Given a set $\Omega \subseteq X$, the robust 1-step robust controllable set to Ω is denoted by $\mathcal{C}_1(\Omega, X)$. It is the set of all states in X which can be steered to Ω by applying an admissible control in exactly one step, for all allowable disturbances.

$$\mathcal{C}_1(\Omega, X) \triangleq \{x_t \in X : f(x_t, u_t, w_t) \in \Omega, u_t \in U, w_t \in W\} \quad (2.10)$$

$\mathcal{C}_1(\Omega)$ is also called the *predecessor* set of Ω in the literature. One-step controllable sets have the rather obvious property of monotonicity [78], i.e.

$$\Omega \subseteq \bar{\Omega} \implies \mathcal{C}_1(\Omega) \subseteq \mathcal{C}_1(\bar{\Omega}).$$

Definition 2.4.10 (*N-Step Robust Controllable Set*) Given a set $\Omega \subseteq X$, the robust I -step robust controllable set to Ω is denoted by $\mathcal{C}_N(\Omega, X)$. It is the largest set of states in X which can be steered to Ω by applying an admissible control sequence in exactly N steps, for all allowable disturbances.

$$\mathcal{C}_N(\Omega, X) \triangleq \{x_t \in X : x_{t,t+N+1} \in \Omega, u_{t,t+N} \in U, w_{t,t+N} \in W\} \quad (2.11)$$

Definition 2.4.11 (*N-Step Robust Stabilizable Set*) If the N -step controllable set $\mathcal{C}_N(\Omega, X)$ in (2.11) is also RPI, then it is called the N -step robust stabilizable set to Ω , denoted by $\mathcal{S}_N(\Omega, X)$. It is the set of all sets in X which can be steered to Ω in N steps or less for all allowable disturbances. Since Ω is RPI, the state remains in Ω after entering it.

$$\mathcal{S}_N(\Omega, X) \triangleq \{x_t \in X : x_{t,t+l} \in \Omega, u_{t,t+l} \in U, w_{t,t+l} \in W, \forall 0 \leq l \leq N\} \quad (2.12)$$

Stabilizability is of course a weaker condition than controllability, like its interpretation in linear unconstrained systems. This is a very useful result in “dual mode” MPC control, which is the subject of this thesis.

2.4.2 Functional Analysis Concepts

Functional analysis is a branch of mathematical analysis that studies vector spaces. It has its roots in calculus of variations, which was the precursor of optimal control - which in turn is the precursor of MPC! A vector space is a mathematical structure formed by a collection of (real-valued) vectors, which may be added together and multiplied by scalars. A vector space on which a *norm* is defined is called *normed vector space*.

Definition 2.4.12 (Vector Norm) A function $|v|_p$ of a vector v is called its norm if

- i. $|v|_p > 0, \forall v \neq 0$,
- ii. for any positive scalar $c \in \mathbb{R}_{\geq 0}$ we have $|cv|_p = c|v|_p$, and
- iii. it satisfies *triangle inequalities* for any two vectors v and w

$$|v + w|_p \leq |v|_p + |w|_p \tag{2.13}$$

$$|v - w|_p \geq |v|_p - |w|_p \tag{2.14}$$

Let absolute value of a vector $v \in \mathbb{R}^n$ be denoted by $\mathbf{abs}(v)$. The p-norm is defined as $|v|_p \triangleq \left(\sum_{i=1}^n \mathbf{abs}(v)^p \right)^{1/p}$. The p-norm is generic: $p = 1$ defines the L_1 or *taxicab* norm denoted as $|\cdot|_1$, $p = 2$ defines the L_2 or *Euclidean* norm denoted as $|\cdot|$ and $p \rightarrow \infty$ is the L_∞ norm denoted by $|\cdot|_\infty$. The taxicab norm is just the summation of absolute values of elements of v , Euclidean norm is the notion of

distance in vector space and infinity norm is maximum absolute value of elements of the vector, i.e. $|v|_\infty \triangleq \max\{abs(x_1), \dots, abs(x_n)\}$. Weighted norm of a vector x for a positive definite matrix P is denoted as $|x|_P = x^T P x$.

For a discrete-time series $\phi = [\phi_0, \phi_1, \dots]^T$, we define $\|\phi\| \triangleq \sup_{l \geq 0} \{|\phi_l|\}$ and $\|\phi_{[t]}\| \triangleq \sup_{0 \leq l \leq t} \{|\phi_l|\}$.

Definition 2.4.13 (Local Continuity) For any $u \in \mathbb{R}^m$, the function $f(x, u)$ is locally (Lipschitz) continuous w.r.t. $x \in X$, if for some *Lipschitz constant* $L_{fx} \in \mathbb{R}_{\geq 0}$

$$|f(x_1, u) - f(x_2, u)| \leq L_{fx}|x_1 - x_2|, \quad \forall x \in X$$

If $X = \mathbb{R}^n$, the continuity is global. The identity function is denoted by $\mathcal{I} : \mathbb{R} \rightarrow \mathbb{R}$, functional composition of two functions γ_1 and γ_2 by $\gamma_1 \circ \gamma_2$ and function inverse of function α by α^{-1} . A vector valued function of the form $f(x_1, \dots, x_n) = A_1 x_1 + \dots + A_n x_n + b$ is called an *affine function*, where x_i can be scalars or vectors, coefficients A_i can be scalars or matrices and constant b is a scalar or vector.

Comparison Functions

We also make extensive use of class \mathcal{K} , \mathcal{K}_∞ and \mathcal{KL} functions commonly used in nonlinear analysis. A function $\alpha : [0, a) \rightarrow [0, \infty)$ is said to belong to class \mathcal{K} , if it is continuous, strictly increasing and $\alpha(0) = 0$. It belongs to class \mathcal{K}_∞ , if $\alpha(r) \rightarrow \infty$ as $r \rightarrow \infty$ and $a \rightarrow \infty$. A function $\beta(r, s) : [0, a) \times [0, \infty) \rightarrow [0, \infty)$ is said to belong to class \mathcal{KL} , if for each fixed $s \geq 0$, the mapping $\beta(\cdot, s)$ belongs to class \mathcal{K} , and for each fixed $r \geq 0$, the mapping $\beta(r, \cdot)$ is non-increasing and

$\beta(r, s) \rightarrow 0$ as $s \rightarrow \infty$ [75].

Examples of comparison functions include: $\alpha(r) = \frac{1}{a-r}, \forall 0 < r < a$ belongs to class \mathcal{K} -functions, $\alpha(r) = r, \forall r > 0$ belongs to class \mathcal{K}_∞ -functions and $\beta(r, s) = r/s$ belongs to class \mathcal{KL} -functions. Comparison functions have some important properties which will be used in later development. Some of them are reproduced here without proof ([75], [79]). The last property is very important and original to this thesis, so the proof for it will be rendered at the end of this section. Let $\alpha_{1,2}$ belong class \mathcal{K} -function, $\alpha_{3,4} \in \mathcal{K}_\infty$ and $\beta \in \mathcal{KL}$. Then the following hold for $r_1, r_2, r_3, r, s > 0$

- $\alpha_1^{-1} \in \mathcal{K}$ and $\alpha_3^{-1} \in \mathcal{K}_\infty$
- $\alpha_1 \circ \alpha_2 \in \mathcal{K}$ and $\alpha_3 \circ \alpha_4 \in \mathcal{K}_\infty$
- $\alpha_1 \circ \beta(\alpha_2(r_1), s) \in \mathcal{KL}$
- $\max(\alpha_1(r_1), \alpha_2(r_1)) \in \mathcal{K}$ and $\max(\alpha_3(r_1), \alpha_4(r_1)) \in \mathcal{K}_\infty$
- $\min(\alpha_1(r_1), \alpha_2(r_1)) \in \mathcal{K}$ and $\min(\alpha_3(r_1), \alpha_4(r_1)) \in \mathcal{K}_\infty$
- $\alpha_1\left(\frac{r_1+r_2}{2}\right) \leq \alpha_1(r_1) + \alpha_1(r_2)$
- $\alpha_1(r_1) + \alpha_2(r_2) \leq \alpha_1(r_1 + r_2) + \alpha_2(r_1 + r_2)$
- $\min\left(\alpha_1\left(\frac{r_1+r_2}{2}\right), \alpha_2\left(\frac{r_1+r_2}{2}\right)\right) \leq \alpha_1(r_1) + \alpha_2(r_2)$
- For any $\alpha_3(r_1) < \alpha_4(r_1), \forall a > r_1 > 0$, the function $\alpha_5 \triangleq \alpha_4 - \alpha_3$ belongs to class \mathcal{K} . Similarly, for any $\alpha_3(r_1) < r_1, \forall a > r_1 > 0$, the function $\alpha_6 \triangleq \mathcal{I} - \alpha_3$ belongs to class \mathcal{K}

Since \mathcal{K}_∞ -functions are a class of \mathcal{K} -functions; hence all the properties above can be extended to \mathcal{K}_∞ -functions. Finally, we state and prove an important property which will be used in later development.

Lemma 2.4.1 *Let, $\underline{\alpha}(r) \triangleq \min(\alpha(r/3), \sigma(r/3), \mu(r/3))$, where $\underline{\alpha}, \alpha, \sigma, \mu \in \mathcal{K}_\infty$.*

Then,

$$\underline{\alpha}(r_1 + r_2 + r_3) \leq \alpha(r_1) + \sigma(r_2) + \mu(r_3) \quad (2.15)$$

Proof. Let, $r \triangleq r_1 + r_2 + r_3$. If, $r_1 \geq r_2, r_1 \geq r_3$ then, $r_1 \geq r/3$, and hence

$$\alpha(r/3) \leq \alpha(r_1) \leq \alpha(r_1) + \sigma(r_2) + \mu(r_3)$$

But, if $r_2 \geq r_1, r_2 \geq r_3$. Then, $r_2 \geq r/3$, and hence

$$\sigma(r/3) \leq \sigma(r_2) \leq \alpha(r_1) + \sigma(r_2) + \mu(r_3)$$

Similarly, if $r_3 \geq r_1, r_3 \geq r_2$, then

$$\mu(r/3) \leq \mu(r_3) \leq \alpha(r_1) + \sigma(r_2) + \mu(r_3)$$

Combining the three inequalities above, we obtain inequality (2.15). █

2.5 Notions of Stability

Stability theory plays a central role in systems analysis and control design. We discuss stability for discrete-time systems, but the same definitions also hold for continuous-time systems with trivial modifications. There are several notions of stability, e.g. equilibrium point/set stability, input-state stability, input-output stability etc. In this thesis, we will be dealing mostly with input-to-state stability (ISS) and input-to-state practical stability (ISpS), and therefore explain these concepts in more detail than other notions of stability.

Definition 2.5.1 (Equilibrium Point) Set-point (t, \bar{x}, \bar{u}) is said to be an equilibrium point of system (2.2), if $x_{t+1} = x_t, \forall x_t = \bar{x}, u_t = \bar{u}, t \geq t_0$.

For linear systems, the only possible equilibrium point is $(t_0, \bar{x}, \bar{u}) = (0, 0, 0)$, but for nonlinear systems, (t_0, \bar{x}, \bar{u}) may be nonzero - or even an equilibrium set, such as a limit cycle [77].

2.5.1 Stability of System with Feedback and no External Input

For the systems in which there is no external inputs $w_t \equiv 0, \forall t \geq 0$ below, it is useful to consider that a feedback control law exists such that $u_t = \Theta(x_t)$, such that (2.2) can be written as

$$x_{t+1} = \bar{g}(t, x_t) \tag{2.16}$$

such that the x_e can be considered an equilibrium point for system (2.16), which is equivalent to the set point $(\bar{x}_t, \Theta(\bar{x}_t), 0)$ for system (2.2).

Definition 2.5.2 (Lyapunov Stability) Point x_e is Lyapunov stable (often simply referred to as stable) at t_0 , if for every $\epsilon > 0$, there exists a $\delta(\epsilon, x_{t_0}) > 0$, such that $|x_{t_0} - x_e| < \delta \implies |x_t - x_e| < \epsilon$ for $t > t_0$.

Lyapunov stable equilibrium means that solutions starting close (within a distance δ) to the equilibrium remain close (within a distance ϵ) to it for all future time. Note that this must hold for any ϵ one may desire, i.e. x_t should be kept arbitrarily close to x_e by starting sufficiently close to it.

Definition 2.5.3 (Asymptotically Stability) Point x_e is locally asymptotically stable (LAS) at t_0 , if there exists a compact set $x_e \ni D \subset \mathbb{R}^n$ if $x_{t_0} \in D \implies \lim_{t \rightarrow \infty} |x_t - x_e| \rightarrow 0$. It is said to be globally asymptotically stable (GAS) if $D = \mathbb{R}^n$.

Asymptotic stability means that solutions that start close to the equilibrium point not only remain close in the future, but also eventually converge to the equilibrium.

Definition 2.5.4 (Exponential Stability) Point x_e is exponentially stable at t_0 if it is asymptotically stable and there exist $M > 0, a > 0$, such that $x_{t_0} \in D \implies |x_t - x_e| \leq M |x_{t_0} - x_e| e^{-a(t-t_0)}$ for $t \geq t_0$.

It is obvious that exponential stability is a special case of asymptotic stability.

Definition 2.5.5 (Practically Stable/ Ultimately Bounded) Equilibrium point x_e is ultimately bounded (UB) or practically stable (pS) after settling time

T_s if for $x_{t_0} \in D$, there exist $c > 0, T_s > t_0$ such that $\|x_t - x_e\| \leq c$ for all $t \geq T_s + t_0$ [80].

Thus, for pS with settling time or UB, the state reached and stays within a neighborhood of the equilibrium after some time $T_s + t_0$. All definitions above are called uniformly stable/bounded if the stability condition does not depend on t_0 . Of course, all autonomous systems ($f(x, u, w)$ or $\bar{g}(x)$ does not depend on t) are uniformly stable if they are stable.

Remark 2.5.1 Exponential and asymptotic stability are very strong properties, and quite difficult to obtain in closed-loop, due to presence of unknown though bounded external disturbances and/or uncertainty. Lyapunov stability is a weaker condition, but still difficult to achieve, since it requires the state to be taken arbitrarily close (ϵ) to equilibrium, but starting close enough (δ) to it. However, practical stability is a much weaker and easier to achieve condition as, unlike Lyapunov stability, bound c cannot be made arbitrarily small by choosing an arbitrarily close initial condition (ϵ). In practice, bound c depends on the magnitude of external input/disturbance.

For linear systems, asymptotic stability requires all closed loop poles to be inside the unit disc. Lyapunov stability requires all poles to be either inside or on the unit disc, but no repeated poles on the unit disc (marginal stability). For nonlinear or non-autonomous (time-varying) systems, stability is not so straight-forward to determine. To investigate stability and design control of nonlinear systems, one has to resort to (direct) Lyapunov method.

Lyapunov Stability Analysis

Let the system (2.16) be autonomous (time invariant), i.e.

$$x_{t+1} = \bar{g}(x_t) \quad (2.17)$$

Without loss of generality, we can consider $x_e = 0 \ni D \subset \mathbb{R}^n$ to be an equilibrium point. For non-zero equilibrium, trivial modification of state variables can make the origin an equilibrium point.

Definition 2.5.6 (Generalized Lyapunov Function) A scalar function $V(x) : \mathbb{R}^n \rightarrow \mathbb{R}_{\geq 0}$ with continuous partial differences is a Lyapunov function for the system (2.17) and equilibrium $x_e = 0 \ni D \subset \mathbb{R}^n$, such that there exist class \mathcal{K} -functions $\alpha_{1,2}$ and constants $c_{1,2}, \bar{c} \geq 0$ so that the following conditions hold

$$V(x) \geq c_1 \alpha_1(|x_t|) \quad \forall x \in D \quad (2.18)$$

$$\Delta V_t \triangleq V(\bar{g}(x_t)) - V(x_t) \leq -c_2 \alpha_2(|x_t|) + \bar{c} \quad \forall x \in D \quad (2.19)$$

Based on this generalized definition of Lyapunov function, we can now state the following theorem.

Theorem 2.5.1 *If there exists a Lyapunov function according to definition 2.5.6, then the equilibrium $x_e = 0 \ni D \subset \mathbb{R}^n$ is locally*

i Lyapunov stable if $c_{1,2}, \bar{c} = 0$, such that $V(0) = 0, V(x) \geq 0$ for $x \in D \setminus \{0\}$

ii *Asymptotically stable (LAS) if $c_{1,2}, \bar{c} = 0$, such that $V(0) = 0, V(x) > 0$ for $x \in D \setminus \{0\}$*

iii *Practically stable if $c_{1,2}, \bar{c} > 0$ for some bound c .*

We present this theorem without proof, because Lyapunov and asymptotic stability proofs are readily available (e.g. in [75]), and proof for practical stability is similar to proof of the more general ISpS theorem in the next section.

Corollary 2.5.1 (Global Stability) *To obtain global stability from Theorem 2.5.1, set $D = \mathbb{R}^n$.*

Example 2.5.1 (Bounds on quadratic Function) Consider a Lyapunov function $V(x) = x^T Q x$, with $Q \in \mathbb{R}^{n \times n}$ a positive definite (p.d.) matrix for system (2.17). It can be easily shown that

$$\underline{\alpha}(\|x\|) \leq V(x) \leq \bar{\alpha}(\|x\|)$$

where $\alpha, \bar{\alpha} \in \mathcal{K}_\infty$ with $\underline{\alpha}(\cdot) = \lambda_{\min}(Q)$ and $\bar{\alpha}(\cdot) = \lambda_{\max}(Q)$, corresponding to extreme eigenvalues of Q .

For collaborative control, this notion of stability which ignores the effect of external inputs is not sufficient. We will model the information shared between agents as external input w , and will therefore require the notion of input-state stability.

2.5.2 Stability of System with Feedback and External Input

Dependence of state trajectory on magnitude of input - especially an input which cannot be manipulated, e.g. external disturbance - is an important issue in system analysis. For linear systems, one can resort to consideration of system gains and operator-theoretic approach, for example H_∞ and H_2 control. For nonlinear systems however, there is still debate about suitable formulation of stability in terms of input perturbation. A widely used concept is that of input-to-state stability (ISS) and its extensions, first introduced by Sontag [70]. ISS is similar to asymptotic stability in that the zero-input trajectory is asymptotically stable. Therefore, all development below is more general and can be particularized to results of the previous section.

Consider the discrete-time nonlinear system (2.2) which is autonomous and supplied with appropriate feedback $u = \Theta(x)$, such that

$$x_{t+1} = \bar{f}(x_t, w_t) \tag{2.20}$$

with $f(0,0) = 0$ i.e. the origin is an equilibrium point. $x_t \in V \subset \mathbb{R}^n$ and $w_t \in W \subset \mathbb{R}^r$ are the system state and input respectively. We will use the following definitions in the course of this thesis.

Definition 2.5.7 (Input-to-State practical Stability (ISpS)) If Ξ is compact, RPI and contains the origin as an interior point, the system (2.20) is said

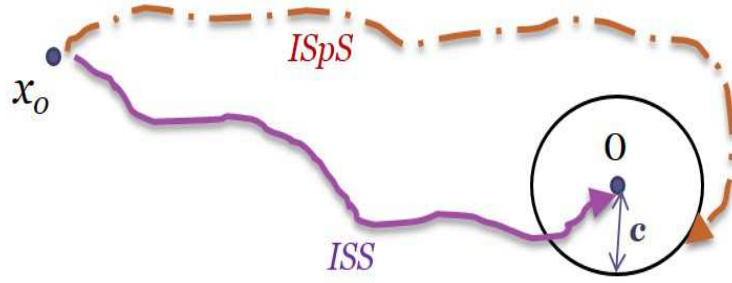


Figure 2.1: Illustration of difference between ISS (asymptotic) and ISpS (practical) stability.

to be regionally ISpS [71] in Ξ for $t \geq 0, x_0 \in \Xi$ and $w \subset W$, and there exists a \mathcal{KL} -function β , a \mathcal{K} -function γ and a constant $c > 0$ such that

$$|x_t(x_0, w)| \leq \beta(|x_0|, t) + \gamma(\|w\|) + c \quad (2.21)$$

Definition 2.5.8 (Input-to-State Stability (ISS)) If in the inequality (2.21), $c \equiv 0$, then system (2.20) is said to be regionally ISS in Ξ [71].

The difference between the ISS (asymptotic) stability and ISpS (practical) stability is illustrated in the phase portrait of Fig. 2.1.

- Remark 2.5.2**
- I. ISS implies ISpS, but converse is not true, since an ISS system with 0-input, i.e. $w_k = 0, \forall k \geq 0$ implies asymptotic stability to the origin, while for an ISpS system, 0-input implies asymptotic stability to a compact set (ball of radius c) containing the origin [81].
 - II. ISpS is equivalent to ISS extended to point-to-set distance from the state to a proper compact invariant set for the system [71].

III. Set of ISpS systems includes the set of systems that are ISS but the converse is not true.

IV. In this thesis, the stability analysis will demonstrate that according to the proposed control approach, closed-loop dynamics is ISpS, not ISS, due to the presence of a range of uncertainties. In fact, even the error present is neural network approximation error in compressing trajectories, only ISpS can be ensured, as we showed in [73], even though this uncertainty does not affect open-loop dynamics. Thus, in this study, c in equation (2.21) is not zero but function of the NN estimation error which is bounded due to properties of NN as universal approximator [77].

Lyapunov-like Stability Analysis

We state an important new result in regional input-to-state practical stability. This general result will form the cornerstone of later development. We first formulate a generalized version of the Lyapunov function.

Definition 2.5.9 (ISpS Lyapunov function) $V : \mathbb{R}^n \rightarrow \mathbb{R}_{\geq 0}$ is an ISpS Lyapunov function for (2.20) in Ξ , if for suitable functions $\alpha_{1,2,3}, \sigma_3 \in \mathcal{K}_\infty$, $\sigma_{1,2} \in \mathcal{K}$ and positive constants $\bar{c}, \bar{c} > 0$, there exists a compact and RPI set $\Xi \ni 0$ and another RPI set $\Omega \subset \Xi$ with origin as an interior-point, such that the following conditions hold.

$$V(x_t, w_t) \geq \alpha_1(|x_t|), \quad \forall x_t \in \Xi \quad (2.22)$$

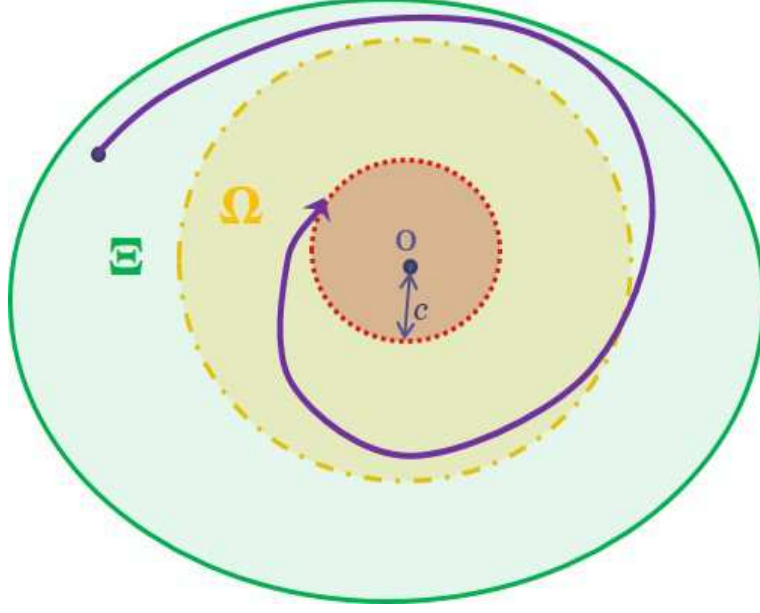


Figure 2.2: Illustration of solution sets for ISpS Stability.

$$\begin{aligned}
 V(f(x_t, w_t), w_{t+1}) - V(x_t, w_t) &\leq \\
 -\alpha_2(|x_t|) + \sigma_1(|w_t|) + \sigma_2(|w_{t+1}|) + \bar{c}, \quad \forall x_t \in \Xi
 \end{aligned} \tag{2.23}$$

$$V(x_t, w_t) \leq \alpha_3(|x_t|) + \sigma_3(|w_t|) + \bar{c}, \quad \forall x_t \in \Omega \tag{2.24}$$

for all $w_{t,t+1} \in W$.

We are now in a position to state the general ISpS result. Relationship between sets in definitions above are illustrated in Fig. 2.2.

Theorem 2.5.2 *If system (2.20) admits an ISpS-Lyapunov function in Ξ , then it is regional ISpS and satisfies condition ((2.21)), with $\beta(r, s) \triangleq \alpha_1^{-1}(3\hat{\beta}(3\alpha_3(r), s))$, $\gamma(s) \triangleq \alpha_1^{-1}(3(\hat{\gamma}(3\sum_{i=1}^3\sigma_i(s)) + \hat{\beta}(3\sigma_3(s), 0)))$ and $c \triangleq \alpha_1^{-1}(3(\hat{\beta}(3(\bar{c}+d), 0) + \alpha_1^{-1}\hat{\gamma}(\mu(3\bar{c})) + \alpha_1^{-1}\hat{\gamma}(3\bar{c})))$, where $\mu, \hat{\gamma} \in \mathcal{K}_\infty$ while $\hat{\beta} \in \mathcal{KL}$.*

Proof. Let $\bar{\alpha}_3(s) \triangleq \alpha_3(s) + \sigma_3(s) + s \in \mathcal{K}_\infty$. Then, (2.24) implies that

$$V(x_t, w_t) \leq \bar{\alpha}_3(|x_t| + |w_t| + \bar{c}), \quad \forall x_t \in \Omega, w_t \in W \quad (2.25)$$

But, from Lemma 2.4.1,

$$\underline{\alpha}_2(|x_t| + |w_t| + \bar{c}) \leq \alpha_2(|x_t|) + \sigma_3(|w_t|) + \mu(\bar{c}) \quad (2.26)$$

where $\underline{\alpha}_2(s) \triangleq \min(\alpha_2(s/3), \sigma_3(s/3), \mu(s/3))$. Combining ((2.25))-((2.26)) leads to

$$\begin{aligned} \underline{\alpha}_2(s) \circ \bar{\alpha}_3^{-1}(V(x_t, w_t)) &\leq \alpha_2(|x_t|) + \sigma_3(|w_t|) + \mu(\bar{c}) \\ -\alpha_2(|x_t|) &\leq -\alpha_4(V(x_t, w_t)) + \sigma_3(|w_t|) + \mu(\bar{c}) \end{aligned} \quad (2.27)$$

where $\alpha_4(s) \triangleq \underline{\alpha}_2(s) \circ \bar{\alpha}_3^{-1}(s) \in \mathcal{K}_\infty$. Consider ((2.24)) and ((2.27)):

$$\begin{aligned} V(f(x_t, w_t), w_{t+1}) - V(x_t, w_t) &\leq -\alpha_4(|V(x_t, w_t)|) + \sigma_1(|w_t|) \\ &\quad , \quad +\sigma_3(|w_t|) + \sigma_2(|w_{t+1}|) + \mu(\bar{c}) + \bar{c} \end{aligned} \quad (2.28)$$

where $x_t \in \Omega, \forall w_t, w_{t+1} \in W$. Since $|w_t| \leq \|w_{[t]}\|, |w_{t+1}| \leq \|w_{[t+1]}\|$, let $\hat{w} \triangleq \max(\|w_{[t]}\|, \|w_{[t+1]}\|)$ and define $\omega(\hat{w}, \bar{c}, \bar{c}) \triangleq \sum_{i=1}^3 \sigma_i(\hat{w}) + \mu(\bar{c}) + \bar{c}$. Therefore,

$$V(f(x_t, w_t), w_{t+1}) \leq (Id - \alpha_4)(V(x_t, w_t)) + \omega(\hat{w}, \bar{c}, \bar{c}) \quad (2.29)$$

Let ρ be a \mathcal{K}_∞ function, such that $(Id - \rho)$ is also a \mathcal{K}_∞ function, e.g. $\rho(s) = s/k, \forall k \in \mathbb{Z}_{>1}$ and define a compact set $D \subset \Omega \subset \Xi$ containing the origin such that

$$D \triangleq \{x \mid d(x, d\Omega) > d_1, V(x_t, w_t) \leq \hat{\gamma}(\omega)\} \quad (2.30)$$

where, $\hat{\gamma} \triangleq \alpha_4^{-1} \circ \rho^{-1} \in \mathcal{K}_\infty$. Hence, assuming that $(Id - \alpha_4)$ is also \mathcal{K}_∞ function, and letting $x_t \in D$,

$$V(f(x_t, w_t), w_{t+1}) \leq (Id - \alpha_4) \circ \hat{\gamma}(\omega) + \omega, \forall x_t \in D \quad (2.31)$$

By adding and subtracting $\rho \circ \alpha_4 \circ \hat{\gamma}(\omega)$ from ((2.29)), one has

$$V(f(x_t, w_t), w_{t+1}) \leq \hat{\gamma}(\omega) - (\mathcal{I} - \rho) \circ \alpha_4 \circ \hat{\gamma}(\omega) + \omega - \rho \circ \alpha_4 \circ \hat{\gamma}(\omega)$$

But, $\rho \circ \alpha_4 \circ \hat{\gamma}(\omega) = \omega$. Hence,

$$\begin{aligned} V(f(x_t, w_t), w_{t+1}) &\leq \hat{\gamma}(\omega) - (Id - \rho)\alpha_4 \circ \hat{\gamma}(\omega) \\ &\leq \hat{\gamma}(\omega) \end{aligned} \quad (2.32)$$

Thus, D is a robust positive invariant (RPI) set, and states starting within D remain inside it. In addition, D is attractive for state starting in $\Omega \setminus D$. Hence, if $x_t \in \Omega \setminus D$, then from ((2.30)) it is clear that $V(x_t, w_t) > \hat{\gamma}(\omega)$ and

$$\rho \circ \alpha_4(V(x_t, w_t)) > \omega, \quad \forall x_t \in \Omega \setminus D, w_t \in W \quad (2.33)$$

But, from ((2.27)):

$$\alpha_4(V(x_t, w_t)) \leq \alpha_2(|x_t|) + \sigma_3(|w_t|) + \mu(\bar{c}), \quad \forall x_t \in \Omega \quad (2.34)$$

Using ((2.33)), one gets:

$$\omega \leq \rho \circ (\alpha_2(|x_t|) + \sigma_3(|w_t|) + \mu(\bar{c})), \quad \forall x_t \in \Omega \setminus D$$

However, $Id > \rho$, for $(Id - \rho) > 0$. Thus,

$$\begin{aligned} \omega &\leq \alpha_2(|x_t|) + \sigma_3(|w_t|) + \mu(\bar{c}) \\ \sum_{i=1}^3 \sigma_i(\hat{w}) + \mu(\bar{c}) + \bar{c} &\leq \alpha_2(|x_t|) + \sigma_3(\hat{w}) + \mu(\bar{c}) \end{aligned} \quad (2.35)$$

And,

$$\begin{aligned} \sigma_1(\hat{w}) + \sigma_2(\hat{w}) + \bar{c} &\leq \alpha_2(|x_t|) \\ \sigma_1(w_t) + \sigma_2(w_{t+1}) + \bar{c} &\leq \alpha_2(|x_t|) \end{aligned} \quad (2.36)$$

where $x_t \in \Omega \setminus D$. Using ((2.23)), one has:

$$V(f(x_t, w_t), w_{t+1}) - V(x_t, w_t) < 0, \quad \forall x_t \in \Omega \setminus D \quad (2.37)$$

Therefore, starting from $\Omega \setminus D$, the state enters D in a finite time and then remains within D since D is RPI. Consequently, T_2 exists such that

$$x_{T_2}(x_2, w_2) \in D, \quad \forall x_2 \in \Omega \setminus D \quad (2.38)$$

Similarly, starting from $x_1 \in \Xi \setminus \Omega$, we will now show the state enters Ω in finite time, i.e. a time T_1 exists such that

$$x_{T_1}(x_1, w_1) \in \Omega, \quad \forall x_1 \in \Xi \setminus \Omega \quad (2.39)$$

To prove this, consider the fact that $|x_1| \geq |x_2|$, so that there exists d_2 such that $\alpha_2(|x_1|) \geq \alpha_2(|x_2|) + d_2$. Now taking into account ((2.36)),

$$\begin{aligned} \sigma_1(\hat{w}) + \sigma_2(\hat{w}) + \bar{c} &< \alpha_2(|x_2|) \leq \alpha_2(|x_1|) - d_2 \\ -\alpha_2(|x_1|) + \sigma_1(\hat{w}) + \sigma_2(\hat{w}) + \bar{c} &< -d_2 \end{aligned} \quad (2.40)$$

where, $x_1 \in \Xi \setminus \Omega$ and $x_2 \in \Omega \setminus D$. When seen in conjunction with ((2.23)),

$$V(f(x_t, w_t), w_{t+1}) - V(x_t, w_t) < -d_2, \quad \forall x_t \in \Xi \setminus \Omega \quad (2.41)$$

This proves the assertion in ((2.39)). Hence, a state x_t starting in Ξ will enter $\Omega \setminus D$ in finite time, and from there it will enter D in finite time as well, where it shall remain for D is RPI.

Using a standard comparison lemma (see e.g. [82]), there exist a \mathcal{KL} function $\hat{\beta}(r, s)$ and a \mathcal{K} function $\hat{\gamma}$ such that

$$V(x_t, w_t) \leq \max(\beta(V(x_0, w_0), t), \hat{\gamma}(\omega(\|w_{[t]}\|), \bar{c}, \bar{c})) \quad (2.42)$$

where $x_t \in \Xi$, $w_{[t]} \in W$, and $\omega \triangleq \sum_{i=1}^3 \sigma_i(\hat{w}) + \mu(\bar{c}) + \bar{c}$.

Since, $V(x_1, w_1) \geq V(x_2, w_2)$ for $x_1 \in \Xi \setminus \Omega$ and $x_2 \in \Omega$ as Ω is RPI, then there exists d such that $V(x_1, w_1) \leq V(x_2, w_2) + d$. Therefore and in conjunction with ((2.24)), one has

$$V(x_0, w_0) \leq \alpha_3(|x_0|) + \sigma_3(|w_0|) + d_3, \quad \forall x_0 \in \Xi, w_0 \in W \quad (2.43)$$

where $d_3 \triangleq \bar{c} + d$. Now ((2.42)) can be written as

$$V(x_t, w_t) \leq \max(\beta(\alpha_3(|x_0|) + \sigma_3(|w_0|) + d_3, t), \hat{\gamma}(\omega)) \quad (2.44)$$

We have the property for any \mathcal{K} -function $\hat{\alpha}(r)$

$$\hat{\alpha}(r_1 + r_2 + r_3) \leq \hat{\alpha}(3 \max(r_1, r_2, r_3)) \leq \hat{\alpha}(3r_1) + \hat{\alpha}(3r_2) + \hat{\alpha}(3r_3) \quad (2.45)$$

Applying (2.45) to (2.44), one gets

$$V(x_t, w_t) \leq \max(\hat{\beta}(3\alpha_3(|x_0|), t) + \hat{\beta}(3\sigma_3(|w_0|), t) + \hat{\beta}(3d_3, t), \hat{\gamma}(\omega)) \quad (2.46)$$

where $x_t \in \Xi$, $w_{[t]} \in W \forall t \geq 0$. Thus, using (2.45) and noting that $\hat{\beta}(\cdot, t) \leq \hat{\beta}(\cdot, 0)$, one has

$$\begin{aligned}
V(x_t, w_t) &\leq \hat{\beta}(3\alpha_3(|x_0|), t) + \hat{\beta}(3\sigma_3(|w_0|), t) \\
&\quad + \hat{\beta}(3d_3, t) + \hat{\gamma}\left(\sum_{i=1}^3 \sigma_i(\hat{w}) + \mu(\bar{c}) + \bar{c}\right) \\
&\leq \hat{\beta}(3\alpha_3(|x_0|), t) \\
&\quad + \hat{\gamma}\left(3 \sum_{i=1}^3 \sigma_i(\|w_{[t]}\|)\right) + \hat{\beta}(3\sigma_3(\|w_{[t]}\|), 0) \\
&\quad + \hat{\beta}(3d_3, 0) + \hat{\gamma}(\mu(3\bar{c})) + \hat{\gamma}(3\bar{c})
\end{aligned} \tag{2.47}$$

Using ((2.22)) leads to

$$\begin{aligned}
\alpha_1(|x_t|) &\leq \hat{\beta}(3\alpha_3(|x_0|), t) + \\
&\quad + \hat{\gamma}\left(3 \sum_{i=1}^3 \sigma_i(\|w_{[t]}\|)\right) + \hat{\beta}(3\sigma_3(\|w_{[t]}\|), 0) \\
&\quad + \hat{\beta}(3d_3, 0) + \hat{\gamma}(\mu(3\bar{c})) + \hat{\gamma}(3\bar{c})
\end{aligned} \tag{2.48}$$

Hence, applying (2.45) again and noting that $\alpha^{-1}(r) \in \mathcal{K}$, the system ((2.20)) is regional ISpS in Ξ , i.e.

$$|x_t| \leq \beta(|x_0|, t) + \gamma(\|w_{[t]}\|) + c, \quad \forall x_t \in \Xi, w_{[t]} \in W$$

where, $\beta(r, s) \triangleq \alpha_1^{-1}(3\hat{\beta}(3\alpha_3(r), s))$, $\gamma(s) \triangleq \alpha_1^{-1}(3(\hat{\gamma}(3 \sum_{i=1}^3 \sigma_i(s)) + \hat{\beta}(3\sigma_3(s), 0)))$ and $c \triangleq \alpha_1^{-1}(3(\hat{\beta}(3(\bar{c} + d), 0) + \alpha_1^{-1}\hat{\gamma}(\mu(3\bar{c})) + \alpha_1^{-1}\hat{\gamma}(3\bar{c})))$ ▀

The proof above is very general can combined with the definitions of ISS and ISpS in this section, can be particularized not only to prove ISS, but the properties of Theorem 2.5.1 as well. Theorem 2.5.2 is completely general and it will serve as the foundation on which more particular results of NMPC in the coming sections

will be based.

2.6 Chapter Conclusion

In this chapter we introduced some important concepts in nonlinear system analysis. Linear and continuous-time system descriptions were found to be more convenient frameworks for stability analysis and control design, but practical reasons were given to motivate the focus of this thesis on nonlinear discrete-time autonomous systems. Commonly used Lyapunov methods and stability notions for feedback systems without external disturbance were introduced and shown to be inadequate for the more realistic scenario of uncertainty and disturbance prone control systems. This motivated the notion of input-to-state stability (ISS) and its extension to practical stability (ISpS). It is shown that ISpS is a general framework from which other particular results can be extracted. Finally Theorem 2.5.2 is stated and rigorously proved to form the cornerstone of future development of distributed NMPC framework in the coming chapters.

CHAPTER 3

ROBUST NONLINEAR MPC CONTROL

3.1 Introduction

This chapter is the first step towards establishing a distributed nonlinear model predictive control (NMPC) strategy for fleet of autonomous vehicles. Various control techniques exist for design of control of vehicles. Depending on complexity of model of the vehicle, its mission profile, hardware, computational resources, uncertainty, disturbances, and real world constraints, many different control algorithms have been developed and applied to mobile robots for the purpose of navigation. These include both linear and nonlinear techniques, including but not limited to proportional-integral-derivative (PID), linear quadratic regulator (LQR), linear quadratic Gaussian (LQG), H_∞ , L_2 , adaptive, gain-scheduling, neural-network (NN), fuzzy, model predictive control (MPC) etc. All of these algorithms have

their merits and demerits. Some, like PID are very straight-forward but not robust, others like LQR are optimal but for an infinite horizon, still others like NN require prior training of the controller or at least persistent excitation (which is required for adaptive control).

However, a disadvantage common to all of the controllers above is that there is no explicit mechanism in them to handle system or control constraints, and those which are optimal in some sense are optimized for an infinite future time. Real systems have constraints on the system states and manipulable control inputs as well, e.g. limitations on maximum power, actuation limits, minimum speed (e.g. in aircraft), physical boundaries, etc. The only control architecture which simultaneously caters to all system constraints is a family of controllers called MPC. Both industry and academia have enthusiastically pursued and applied control designs based on MPC concepts. Most techniques other than MPC resort to ad-hoc methods for dealing with constraints, e.g. anti-windup techniques. Flexible constraint handling capabilities of MPC are a unique feature, and there is flexibility to formulate the online optimal control objective can be formulated as 1-, 2-, ∞ -norm etc. Virtually the same architecture can be carried over to nonlinear systems as well. MPC also has inherent robustness qualities, which can be further improved quite easily [83]. MPC technology has found wide application in diverse areas like process, petrochemical, chemical, food processing, manufacturing, aerospace, robotics, etc. It is the standard approach for implementing constrained, multi-variable control.

In this chapter, a robust model predictive control scheme for constrained discrete-time nonlinear systems affected by several bounded uncertainties is considered. States and disturbances are measured with noise, and both system and disturbance models are also uncertain. The objective is to guarantee the robust satisfaction of state constraints, ensure recursive feasibility and stability despite the combined effect of these uncertainties. For that, restricted constraint sets are introduced to satisfy state constraints for the perturbed system. In our approach, we derive several conditions based on bounds on each component of uncertainty. Feasibility and stability of the algorithm is proportional to the size of the terminal region and the one-step controllable set to this region. Theoretical development shows that due to uncertainties, only practical stability (ISpS) can be ensured by using suitably selected cost functional for MPC optimization.

3.1.1 Chapter Contributions

The contributions of this chapter are non-trivial in the following aspects, which are under review in Automatica [84].

- i. Existing literature mostly considers either modeling uncertainty with perfect measurements [85] or measurement noise with perfectly well known statistics [68]. The proposed approach provides a unified framework for dealing with both types of uncertainties, along with the inclusion of a non-additive disturbance with uncertain dynamics and unknown input.
- ii. Input-to-state practical stability framework in existing literature is extended

with Theorem 3.2.2 to cater for the combination of uncertainties mentioned above.

- iii. New bounds on prediction error growth along the prediction horizon have been derived (Lemma 3.2.1) based on the bounds on components of the combined uncertainty. In addition, constraint tightening for robust satisfaction of original constraints in the presence of this combination of uncertainties (Theorem 3.2.1) is also a new development.
- iv. Recursive feasibility is ensured by the newly developed Theorem 3.1 which relates it to the size of the one-step controllable set to the terminal region.
- v. Two new algorithms are presented for constraint tightening and online optimization.

Chapter Organization An introduction to nonlinear MPC technique is provided in Section 3.2, with a discussion on merits / demerits of NMPC and its comparison with other optimal control approaches. We also formulate the robust NMPC problem in terms of the cost function, its components and the role of uncertainties, and propose the solution in terms of Algorithm 1. The constraint tightening approach for robustifying the NMPC Algorithm is formulated in Section 3.2.5, by deriving bounds on growth of uncertainty in prediction of state and disturbance due to contribution of various components of the combined uncertainty (Algorithm 2). Based on these bounds on prediction and the minimum size of one-step controllability set to the terminal constraint set, conditions of recursive

feasibility for Algorithm 1 are derived in Section 3.2.6. The final component of theoretical framework of this chapter is stability analysis for Algorithm 1, which is carried out in Section 3.2.7, where stability of both the nominal system and actual (perturbed) system is evaluated. Finally, a numerical example is introduced in Section 3.3, which is used to illustrate application of Algorithm 2 in this chapter. The example is extended in Chapter 4.

3.2 Nonlinear Model Predictive Control

Model Predictive Control is a family of controllers in which there an explicit dynamic model of the system or process to be controlled is directly used to predict and optimize its response for some finite time in the future. MPC was first introduced in the late 1960s as a nonlinear control framework for industrial applications (mostly process control) [86]. When the dynamic model of the system used for prediction is linear, the technique is called Linear MPC, even though the optimization problem is invariably nonlinear. Similarly, when prediction dynamic model is nonlinear, the entire control scheme is called nonlinear model predictive control (NMPC). It is worth noting that this is slight abuse of notion, since both linear and nonlinear constrained MPC are nonlinear control techniques (since control is an implicit and nonlinear function of the state). Existing body of work, however, treats linear and nonlinear MPC separately, mainly due to the different theoretical tools needed to prove the closed-loop stability in the two frameworks.

3.2.1 Advantages and Disadvantages

The concept behind this scheme is simple and controller tuning can be achieved by persons not well versed with control engineering, and the concept has evolved to a mature level [87]. It is a model based control process, like linear quadratic, pole placement and adaptive control, however MPC has many remarkable features [88], some of which are:

- 1. A wide variety of processes can be controlled, including non-minimum phase, unstable, time delays and non-linear plants.
- It can be easily extended to multiple input / multiple output (MIMO) plants.
- It is robust to modeling errors to some extent.
- It is relatively easy to tune.
- Process model can be finite impulse response (FIR), step response, transfer function, state space or even non-linear. This is in contrast to linear quadratic (LQ) or pole-placement control.
- Predictive control can cater for process constraints during the controller design itself. It is the most attractive feature of MPC.
- It is an open design framework, i.e. within its broader framework the controller can be designed in a variety of ways, and it can be fused with other control schemes, such as adaptive control.

- Known and unknown disturbances can also be catered for in the design process.
- Since MPC is predictive in nature, if the reference set-point trajectory is known in advance (e.g. landing trajectory), it too can be used in the controller design by looking ahead for the trajectory.
- Due to its constraint handling, model updatability and inherent robustness it has been proposed and implemented for reconfigurable and fault tolerant control.

It was for these properties precisely, that it was brought into use in the industry about 15 years before stability proofs were established for it [89]. However, MPC techniques also have some disadvantages, namely

- Increased computational burden due to the requirement to solve an online optimization problem every sampling instant.
- Having a nonlinear model for prediction makes the constrained optimization problem non-convex, making the problem harder to solve.
- Stability requirements are less intuitive.

However, in recent years, there has been remarkable progress towards mitigating all of the above mentioned disadvantages. We will now first introduce the basic algorithm of NMPC, and discuss these merits and demerits further after that

3.2.2 Problem Formulation

Consider an agent (vehicle) having nonlinear discrete-time dynamics

$$x_{t+1} = f(x_t, u_t, w_t) \quad (3.1)$$

and the nonlinear output is

$$y_t = h(x_t) \quad (3.2)$$

Internal states x_t , outputs y_t , local control inputs u_t and external inputs w_t belong to the following constrained convex sets:

$$\begin{aligned} x_t \in X \subset \mathbb{R}^n, & \quad X \triangleq \{x : x_{\min} \leq x \leq x_{\max} > 0\} \\ y_t \in Y \subset \mathbb{R}^q, & \quad Y \triangleq \{y : y_{\min} \leq y \leq y_{\max} > 0\} \\ u_t \in U \subset \mathbb{R}^m, & \quad U \triangleq \{u : u_{\min} \leq u \leq u_{\max} > 0\} \\ w_t \in W \subset \mathbb{R}^p, & \quad W \triangleq \{w : w_{\min} \leq w \leq w_{\max} > 0\} \end{aligned} \quad (3.3)$$

External input w will be later used to model the information communicated by other members of the team or obstacles. In the current context of a single vehicle, we can utilize it to model any disturbance affecting the agent (e.g. wing gust, water current, turbulence etc.) or information about obstacle it has to avoid. The disturbance evolves according to the following nonlinear mapping

$$w_{t+1} = g(w_t, \phi_t) \quad (3.4)$$

where ϕ is an unknown input vector, possibly random. Since w_t is not additive, we can also use it represent plant uncertainty. Let the actual state of the system be x_t , while the state predicted by model (3.5) at time t for future time instant $t + l$ by $\tilde{x}_{t,t+l}$. We assume that our model of the system is not perfect, such that the *nominal* model actually used for state prediction is

$$\tilde{x}_{t+1} = \tilde{f}(\tilde{x}_t, u_t, \tilde{w}_t) \quad (3.5)$$

Often, not all states are directly measurable, and when they are sensors may produce an output corrupted with noise and this lead to uncertainty. Therefore, the measured output is

$$\tilde{y}_t = y_t + \xi_{y_t}, \quad \underline{\xi}_y \leq |\xi_{y_t}| \leq \bar{\xi}_y \quad (3.6)$$

Therefore, given the outputs measured by sensors, there is an need to estimate the states in a manner such that the effect of noise and uncertainty are mitigated. In this chapter, we assume a mechanism of state estimation exists, such that the state is estimated with some bounded error ξ_x , such that

$$\tilde{x}_t = \tilde{x}_{t|t-1} + K_t(\tilde{y}_t - h(\tilde{x}_{t|t-1})) \quad (3.7)$$

where K_t is time varying nonlinear filter, which is assumed to be available and $\tilde{x}_{t|t-1}$ is the *prior* estimate. In ths thesis, we assume that this filter exists, such

that

$$\tilde{x}_t = x_t + \xi_{x_t}, \quad \underline{\xi}_x \leq |\xi_{x_t}| \leq \bar{\xi}_x \quad (3.8)$$

Moreover, assume that we have another estimator for w , which produces the estimate \tilde{w} , such that

$$\tilde{w}_t = w_t + \xi_{w_t}, \quad \underline{\xi}_w \leq |\xi_{w_t}| \leq \bar{\xi}_w \quad (3.9)$$

We assume that we do not have exact knowledge of the evolution of $w_{t,t+Np}$, and that can only have an approximation $\tilde{w}_{t,t+Np}$ of it using a nominal model $\tilde{g}(\cdot)$ given by

$$\tilde{w}_{t+1} = \tilde{g}(\tilde{w}_t), \quad (3.10)$$

such that there is a bounded *disturbance transition uncertainty* due to disturbance model mismatch

$$\tilde{g}(w_t) = g(w_t, \phi_t) + e_{w_t}, \quad \underline{e}_w \leq |e_{w_t}| \leq \bar{e}_w, \quad (3.11)$$

Similarly, we assume that system model mismatch leads to *system transition uncertainty* $e_{x_t} \triangleq \tilde{f}(x_t, u_t, w_t) - f(x_t, u_t, w_t)$, such that

$$\tilde{f}(x_t, u_t, w_t) = f(x_t, u_t, w_t) + e_{x_t}, \quad \underline{e}_x \leq |e_{x_t}| \leq \bar{e}_x \quad (3.12)$$

Now, due to uncertainty, the constraint sets (3.3) for x and w will be 'larger' than constraints sets for \tilde{x} and \tilde{w} , such that

$$\tilde{x}_t \in \tilde{X}_t(\bar{e}_x, \bar{\xi}_x, \bar{e}_w, \bar{\xi}_w) \subset X, \tilde{y}_t \in \tilde{Y}_t(\bar{v}) \subset Y, \quad \tilde{w}_t \in \tilde{W}_t(\bar{\xi}_w, \bar{e}_w) \subset W \quad (3.13)$$

The exact definition of these '*tightened*' constraint sets is deferred to Section 3.2.5. Normally NMPC is used for state regulation, i.e. to it will is usually to steer the state to the origin or to an equilibrium state $x_r = r$, where r is a constant reference. This is generally true for process industries. However, in mobile robotics, The control objective depends on the mission profile of the vehicle, as the target state may evolve over time, rather than being constant. Tracking and path tracking are two fundamental control problems in mobile robotics. For tracking problems, the objective is to converge to a time-varying reference trajectory $x_d(t)$ designed separately. On the other hand, in path following applications, the objective is to follow a reference path parameterized by geometric parameters rather than time. The path following problem can be reduced to state regulation task [90]. Therefore, we will explain the control strategy of MPC using regulation problem as an example. Based on the control objective, let the vehicle have the finite-horizon optimization cost function given by

$$\begin{aligned} J_t(\tilde{x}, u, \tilde{w}, N_c, N_p, k_f) = & \sum_{l=t}^{t+N_c-1} [h(\tilde{x}_l, u_l) + q(\tilde{x}_l, \tilde{w}_l)] \\ & + \sum_{l=t+N_c}^{t+N_p-1} [(k_f(\tilde{x}_l) + q(\tilde{x}_l, \tilde{w}_l))] + h_f(\tilde{x}_{t+N_p}), \end{aligned} \quad (3.14)$$

where N_p and N_c are prediction and control horizons. Cost function (3.14) consists of transition cost h , terminal cost h_f and robustness cost q (due to the effect of external input). Control sequence $u_{t,t+N_p}$ consists of two parts, $u_{t,t+N_c-1}$ and $u_{t+N_c,t+N_p-1}$. The latter part is generated by terminal (also called *auxiliary*) control law $u_l = k_f(\tilde{x}_l)$ for $l \geq N_c$, while the former is finite horizon optimal control $u_{t,t+N_p}$ which is the solution of the optimization problem 3.2.1.

Problem 3.2.1 (Finite Horizon Optimal Control Problem (FHOCP))

At every instant $t \geq 0$, given prediction and control horizons $N_p, N_c \in \mathbb{Z}_{\geq 0}$, terminal control $k_f(\tilde{x}) : \mathbb{R}^n \rightarrow \mathbb{R}^m$, state estimate \tilde{x}_t and disturbance estimate \tilde{w}_t , find the optimal control sequence $u_{t,t+N_c-1}^o$, which minimizes the finite horizon cost (3.14)

$$u_{t,t+N_c-1}^o = \arg \min_{u \in U} J_t(\tilde{x}_t, \tilde{w}_{t,t+N_p}, u_{t,t+N_p}, N_c, N_p), \quad (3.15)$$

subject to

I. nominal state dynamics (3.5)

II. nominal disturbance dynamics (3.10)

III. Control constraint (3.3) and the tightened constraint sets (3.13)

IV. Terminal state \tilde{x}_{t+N_p} is constrained to an invariant terminal set $X_f \in \tilde{X}_{t+N_c}$, i.e.

$$\tilde{x}_{t+l} \in X_f, \quad \forall l = N_c, \dots, N_p \quad (3.16)$$

Definition 3.2.1 *Suboptimal sequence $u_{t,t+N_c-1}$ satisfying the constraints (3.1), (3.3) and (3.16) is called feasible control.*

In other words, a control input is feasible if and only if it provides a feasible solution to the finite horizon optimal control problem 3.2.1. Hence if a control input is admissible ($u \in U$), it is not necessarily feasible. For a given state the set of feasible inputs is a subset of the admissible inputs.

3.2.3 Receding Horizon Strategy

The loop is closed by implementing only the first element of $u_{t,t+N_c-1}^0$ at each instant, such that the NLMPC implicit control law becomes

$$\Theta_t(\tilde{x}, \tilde{w}) = u_t^0(\tilde{x}_t, \tilde{w}_t, N_p, N_c) \quad (3.17)$$

and the closed loop dynamics becomes

$$x_{t+1} = f(x_t, \Theta_t(\tilde{x}, \tilde{w}), w_t) = f_c(x_t, w_t) \quad (3.18)$$

with closed loop nonlinear map $f_c(x, w)$. This process is repeated every sampling instant, as illustrated in Fig. 3.2. The overall control architecture is shown in Fig. 3.1. To summarize, at time t , current state is sampled and an estimate of the disturbance is made, then cost (3.14) is minimized over a finite horizon N_p , using N_c control adjustments and pre-computed terminal control law k_f , such that system constraints (3.1)-(3.3) are satisfied in addition to state remaining in

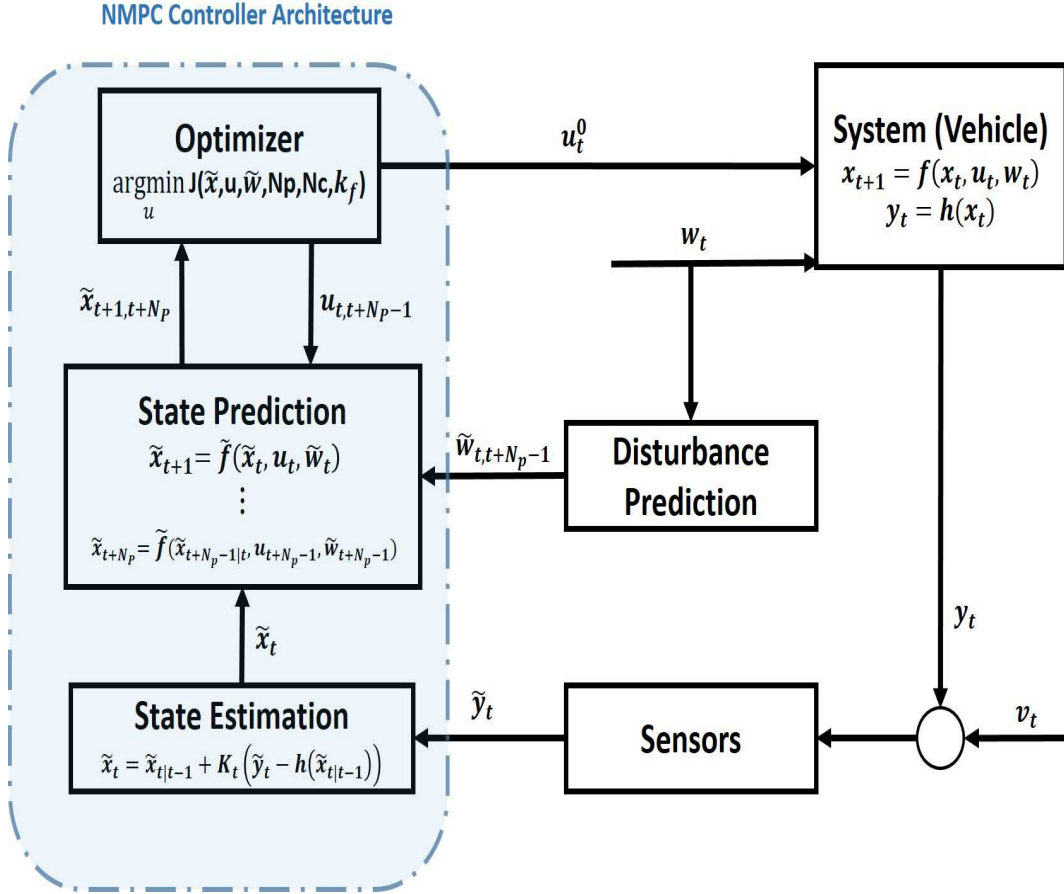


Figure 3.1: Complete architecture of the NMPC controller for Single Vehicle. Optimizer output consists of the optimization of first $N_C - 1$ steps of control sequence appended with $N_P - N_C - 1$ steps of terminal controller $k_f(x)$. (This art is original; copyrights belong to the author).

an invariant terminal set X_f . Only the first step of this optimized control sequence is implemented. Then the plant state is sampled again and the same optimization problem 3.2.1 is solved again, yielding re-optimized control. Prediction horizon keeps being shifted forward and for this reason MPC is also called receding horizon control (RHC), though this is a slight abuse of notation (RH strategy along with model based optimization together forms the MPC strategy).

In this thesis, we have developed a comprehensive strategy for robust non-linear model predictive control, elucidated in Algorithm 1. There two classes

Algorithm 1 Robust NMPC Control with Constraint Tightening

- 1: **Input** nominal model $\tilde{f}(\tilde{x}, u, 0)$, nominal constraints (3.3), RH cost (3.14) and error bounds (3.7)- (3.12).
 - 2: **procedure** OFFLINE OPTIMIZATION
 - 3: **Tighten** constraints using Algorithm 2 for robustness.
 - 4: **Determine** optimized terminal set X_f and terminal control k_f using Algorithm 3
 - 5: **Warm-start** Algorithm 5 with Algorithm 4.
 - 6: **Determine** One-step controllability set $\mathcal{C}_1(X_f)$ to ensure recursive feasibility using Algorithm 5.
 - 7: **Determine** Robust output feasibility set X_{MPC} using Algorithm 6.
 - 8: **end procedure**
 - 9: **Start** system time at t , $l = 0$
 - 10: **while** Target state is not reached **do**
 - 11: **procedure** (Online Optimization)
 - 12: Measure outputs \tilde{y}_{t+l} and disturbance \tilde{w}_{t+l}
 - 13: **Estimate** state \tilde{x}_{t+l} and disturbance \tilde{w}_{t+l}
 - 14: **Solve** finite horizon OCP 3.2.1 at $t + l$ for control $u_{t+1,t+l+N_c}^0$
 - 15: **Implement** first element of optimized control u_t^0
 - 16: **end procedure** System clock advances, $l = l + 1$
 - 17: **end while**
-

of optimization problems solved in Algorithm 1: offline and online. This overall algorithm consists of various ingredient algorithms which will be duly explained in the following sections of this and the next chapter.

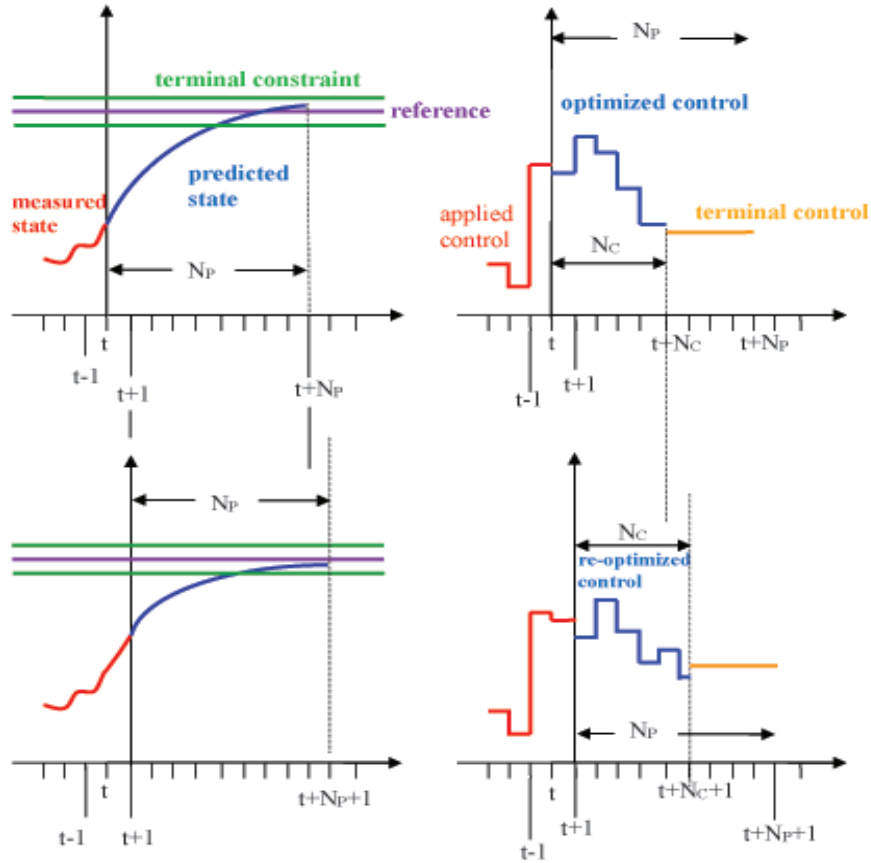


Figure 3.2: Basic concepts of Model Predictive Control. (Clockwise from top left): estimated (red) and predicted (blue) state at t for $\tilde{x}_{t,t+N_p}$, along with terminal constraint set X_f ; applied (red), optimized (blue) and terminal (orange) control input at time t ; applied, optimized and terminal control input at time $t + 1$ (first element of optimized control at t was applied at $t + 1$); estimated and predicted state at $t + 1$ for $\tilde{x}_{t+1,t+N_{p+1}}$. (This art is original; copyrights belong to the author).

3.2.4 Comparison with other Optimal Control Techniques

The main difference between conventional optimal control techniques and MPC is the fact that the control law in former is pre-computed, while MPC requires online control optimization. Even though, now the overriding reason for resorting to MPC is its explicit constraint handling capabilities, its initial appeal amongst practitioners was the applicability to multi variable systems (many early formulations did not even consider constraints). Apart from that, it can be argued that MPC is an alternate formulation of classical optimal control. However, most other formulations of optimal control e.g. LQR/G (H_2), H_∞ linear optimal control consider infinite horizon (unconstrained) optimization problem computed offline for all (unconstrained) states. MPC, on the other hand solves an open-loop, finite-horizon constrained optimization problem online at every sampling instant for the measured (constrained) state. The finite horizon is required to be reasonable short, mainly to

1. allow computation of the control input within the sampling interval, and
2. reduce prediction errors, since errors in prediction due to uncertainty grows with prediction horizon.

Therefore, the difference is more in implementation than in the concept and formulation [38]. In fact, the MPC strategy of applying the first step of the optimized control sequence can be argued to having its roots in Dynamic Programming theory [40]. However, it is worth noting that the abject failure of many optimal control techniques (such as LQR) in industrial applications was their inadequacies

in handling constraints, nonlinearities and uncertainty. These real world issues are handled very well by MPC which led to its popularity among practitioners. In the following section, we will determine requirements of stability for NMPC, and based on these, derive appropriate values of design parameters of the control law.

3.2.5 Robustness of NMPC Algorithm

If there was no uncertainty about system dynamics or no disturbance was present, one will expect the prediction to be accurate and therefore there would be no need to measure and optimize at every sampling instant. In that case one could simply apply the entire optimized sequence $u_{N_P-1}^0$ and re-optimize after every $N_P - 1$ time steps. However, in the real world, one can never measure or model with absolute precision and accuracy, and external disturbances are always present, even in very controlled laboratory environments. Therefore, in the real world the system dynamics does not exactly match the predicted behavior. Maintenance of acceptable performance and stability in presence of uncertainty and disturbances is called *robustness*. One way to deal with it is to sample and re-optimize every sampling instant in the receding horizon strategy of NMPC described above. This lends NMPC the *inherent robustness* property, if the magnitude of uncertainty or disturbance is sufficiently small and if the FHOCP is unconstrained. Simultaneous presence of constraints and disturbances - even if non-persistent - can make an MPC controller infeasible and unstable, even if it is stabilizing for the nominal case

[91]. However, this inherent robustness may not guarantee acceptable performance (it has even been shown that stabilizing NMPC designed for constrained nominal model may exhibit zero-robustness [92]) and one needs to improve the robustness credentials of NMPC by taking more deliberate steps in that direction.

Explicitly incorporating uncertainties and disturbances in the design of NMPC control law is not trivial, as one needs to ensure performance, stability and constraint non-violation for all possible realizations of uncertainty/disturbance. Different approaches have been suggested in the literature in this regard. We will review some of them, before choosing the *constraint tightening* robustness technique for reasons made clear later. We will make a few standard MPC assumptions on initial feasibility and continuity.

Assumption 3.2.1 (Feasible Initial Set) *There exists a compact robust output feasible set $X_{MPC} \subseteq X$, which is the set of initial states for which optimal control problem 3.2.1 is feasible.*

This is an assumption of initial feasibility of the FHOCP 3.2.1. We need this to prove *recursive* (also called *iterative*) *feasibility* later. Note that Assumption 3.2.1 is fairly standard in MPC literature (e.g. see [93], [59] etc.).

Assumption 3.2.2 (L. Continuity of Transition Maps) . *We assume that transition maps $\tilde{f}(\cdot)$ and $\tilde{g}(\cdot)$ are locally Lipschitz continuous, such that*

I. $\tilde{f}(0, 0, 0) = 0$ and $\tilde{f} \in C^2$, i.e. the nominal map is twice differentiable.

II. $\tilde{g}(0) = 0$

$$\begin{aligned}
\text{III. } & |\tilde{f}(x_1, u_1, w_1) - \tilde{f}(x_2, u_2, w_2)| \leq L_{fx}|x_1 - x_2| + L_{fu}|u_1 - u_2| + L_{fw}|w_1 - w_2| \\
& \text{for } x_1, x_2 \in X, u_1, u_2 \in U \text{ and } w_1, w_2 \in W.
\end{aligned}$$

$$\text{IV. } |\tilde{g}(w_1) - \tilde{g}(w_2)| \leq L_{gw}|w_1 - w_2|, \text{ for } w_1, w_2 \in W$$

These assumptions are fairly standard and satisfied for most estimation models.

Min-Max Optimization based Robustness Approach

In min-max MPC controllers [79], the cost functional is minimized for the worst possible realizations of the uncertainty over the prediction horizon at each time instant. This is often the most computationally the most expensive approach, and even the reduced conservatism by its proponents is contested [91]. Practically, min-max robust NMPC is limited to systems with small size or very slow dynamics. This approach, however, suffers from two major drawbacks (i) the resulting optimization problem is computationally more expensive even if it is possible to design minmax controllers with a finite-dimensional parameterization; (ii) the minmax paradigm of optimizing performance for the worst-case disturbance represents an unrealistic scenario and may yield poor performance whenever the disturbance realization gets close to zero. For the above reasons, a more sensible approach seems to minimize the nominal performance index while imposing constraint fulfillment for all admissible disturbances, presented in the next section.

Constraint Tightening Robustness Approach

Satisfying constraints along the horizon depends on the future realization of the uncertainties, which are random. By assuming Lipschitz continuity of the nominal disturbance and state models (Assumptions 3.2.2), it is possible to compute bounds on effect of the evolving uncertainties on the system. Since, our system consists of many possible sources of uncertainty, the bound calculated will be much more involved and comprehensive than those presented in existing literature (e.g. [94] and [85]). The idea of constraint tightening for robustifying MPC algorithms was introduced in 2001 by Chisci *et al* in [91]. This seminal work presented the idea that, for constrained linear systems

“Robustness against persistent bounded disturbances can be enforced by inserting in the predictive controller suitable constraint restrictions. The robust predictive controller obtained in this way guarantees, for all admissible disturbances, constraint fulfillment and asymptotic state regulation, i.e. convergence of the state to a minimal robust invariant set, provided that the initial state is feasible.”

Marruedo *et al* extended this idea to nonlinear systems in the next year [94].

Lemma 3.2.1 (Bounded Prediction Errors) *Given the following estimation and transition error bounds*

- i. Estimation error bounds $\bar{\xi}_x, \bar{\xi}_w \in \mathbb{R}_{\geq 0}$ defined in (3.8)-(3.9),*
- ii. One step transition error bounds $\bar{e}_x, \bar{e}_w \in \mathbb{R}_{\geq 0}$ defined in (3.12)- (3.11),*

and Lipschitz constants L_{fx} , L_{fc} and L_{gw} defined in Assumption 3.2.2, then the l -step prediction errors in predicting $x_{t,t+Np}$ and $w_{t,t+Np}$ are bounded by

$$|w_{t+l} - \tilde{w}_{t+l}| \leq L_{gw}^l \bar{\xi}_w + \bar{e}_w \frac{L_{gw}^l - 1}{L_{gw} - 1}, \quad (3.19)$$

$$\begin{aligned} |x_{t+l} - \tilde{x}_{t+l}| &\leq L_{fx}^l \bar{\xi}_x + \bar{e}_x \frac{L_{fx}^l - 1}{L_{fx} - 1} + \bar{\xi}_w L_{fw} \frac{L_{fx}^l - L_{gw}^l}{L_{fx} - L_{gw}} \\ &\quad + \bar{e}_w \frac{L_{fw}}{L_{gw} - 1} \left(\frac{L_{fx}^l - L_{gw}^l}{L_{fx} - L_{gw}} - \frac{L_{fx}^l - 1}{L_{fx} - 1} \right), \end{aligned} \quad (3.20)$$

for $l = 0, \dots, N_P$, and $L_{fx}, L_{gw} \neq 1$ and $L_{fx} \neq L_{gw}$.

Proof. Let us first look at the prediction error for the disturbance. From (3.9), we have for $l = 0$

$$|w_t - \tilde{w}_t| = \xi_{w_t} \leq \bar{\xi}_w$$

At the next sampling instant, i.e. $l = 1$, we have from (3.4), (3.10), (3.9) and (3.11)

$$\begin{aligned} |w_{t+1} - \tilde{w}_{t+1}| &= |g(w_t, \phi_t) - \tilde{g}(\tilde{w}_t)| \\ &= |\tilde{g}(w_t) + e_{w_t} - \tilde{g}(\tilde{w}_t)| \\ &\leq |\tilde{g}(w_t) - \tilde{g}(\tilde{w}_t)| + \bar{e}_w \end{aligned}$$

But, in view of Assumption 3.2.2

$$|w_{t+1} - \tilde{w}_{t+1}| \leq L_{gw} |w_t - \tilde{w}_t| + \bar{e}_w \leq L_{gw} \bar{\xi}_w + \bar{e}_w \quad (3.21)$$

At next sampling instant when $l = 2$,

$$\begin{aligned}
|w_{t+2} - \tilde{w}_{t+2}| &= |g(w_{t+1}, \phi_{t+1}) - \tilde{g}(\tilde{w}_{t+1})| \\
&= |\tilde{g}(w_{t+1}) - \tilde{g}(\tilde{w}_{t+1}) + e_{w_{t+1}}| \\
&\leq |\tilde{g}(w_t) - \tilde{g}(\tilde{w}_t)| + \bar{e}_w \\
&\leq L_{gw}|w_{t+1} - \tilde{w}_{t+1}| + \bar{e}_w
\end{aligned}$$

Substituting (3.21)

$$|w_{t+2} - \tilde{w}_{t+2}| \leq L_{gw} (L_{gw}\bar{\xi}_w + \bar{e}_w) + \bar{e}_w \leq \bar{\xi}_w L_{gw}^2 + \bar{e}_w (L_{gw} + 1) \quad (3.22)$$

Finally, following the same development as above, we can show that for $l = 3$

$$|w_{t+3} - \tilde{w}_{t+3}| \leq \bar{\xi}_w L_{gw}^3 + \bar{e}_w (L_{gw}^2 + L_{gw} + 1) \quad (3.23)$$

So generalizing from (3.21)-(3.23) for l -step ahead prediction

$$|w_{t+l} - \tilde{w}_{t+l}| \leq \bar{\xi}_w L_{gw}^l + \bar{e}_w \left(\sum_{k=0}^{l-1} L_{gw}^k \right) = \bar{\xi}_w L_{gw}^l + \bar{e}_w \frac{L_{gw}^l - 1}{L_{gw} - 1},$$

which proves (3.19).

Now, consider prediction error for system state. From (3.8), we have for $l = 0$

$$|x_t - \tilde{x}_t| = \xi_{x_t} \leq \bar{\xi}_x$$

At the next sampling instant, i.e. $l = 1$, we have from (3.1), (3.5), (3.8) and (3.12)

$$\begin{aligned}
|x_{t+1} - \tilde{x}_{t+1}| &= |f(x_t, u_t, w_t) - \tilde{f}(\tilde{x}_t, u_t, \tilde{w}_t)| \\
&= |\tilde{f}(x_t, u_t, w_t) + e_{x_t} - \tilde{f}(\tilde{x}_t, u_t, \tilde{w}_t)| \\
&\leq |\tilde{f}(x_t, u_t, w_t) - \tilde{f}(\tilde{x}_t, u_t, \tilde{w}_t)| + \bar{e}_x
\end{aligned}$$

But, in view of Assumption 3.2.2

$$|x_{t+1} - \tilde{x}_{t+1}| \leq L_{fx}|x_t - \tilde{x}_t| + L_{fw}|w_t - \tilde{w}_t| + \bar{e}_x \leq L_{fx}\bar{\xi}_x + L_{fw}\bar{\xi}_w + \bar{e}_x \quad (3.24)$$

At next sampling instant when $l = 2$,

$$\begin{aligned}
|x_{t+2} - \tilde{x}_{t+2}| &= |f(x_{t+1}, u_{t+1}, w_{t+1}) - \tilde{f}(\tilde{x}_{t+1}, u_{t+1}, \tilde{w}_{t+1})| \\
&= |\tilde{f}(x_{t+1}, u_{t+1}, w_{t+1}) - \tilde{f}(\tilde{x}_{t+1}, u_{t+1}, \tilde{w}_{t+1}) + e_{x_{t+1}}| \\
&\leq L_{fx}|x_{t+1} - \tilde{x}_{t+1}| + L_{fw}|w_{t+1} - \tilde{w}_{t+1}| + \bar{e}_x
\end{aligned}$$

Substituting (3.21) and (3.24)

$$\begin{aligned}
|x_{t+2} - \tilde{x}_{t+2}| &\leq L_{fx} (L_{fx}\bar{\xi}_x + L_{fw}\bar{\xi}_w + \bar{e}_x) + L_{fw} (L_{gw}\bar{\xi}_w + \bar{e}_w) + \bar{e}_x \\
&\leq L_{fx}^2\bar{\xi}_x + \bar{e}_x (L_{fx} + 1) + \bar{\xi}_w L_{fw} (L_{fx} + L_{gw}) + L_{fw}\bar{e}_w
\end{aligned} \quad (3.25)$$

Finally, following the same development as above, we can show that for $l = 3, 4, 5$

$$\begin{aligned}
|x_{t+3} - \tilde{x}_{t+3}| &\leq \bar{\xi}_x L_{fx}^3 + \bar{e}_x (L_{fx}^2 + L_{fx} + 1) \\
&\quad + \bar{\xi}_w L_{fw} (L_{fx}^2 + L_{fx} L_{gw} + L_{gw}^2) + \bar{e}_w L_{fw} (L_{fx} + L_{gw} + 1) \\
|x_{t+4} - \tilde{x}_{t+4}| &\leq \bar{\xi}_x L_{fx}^4 + \bar{e}_x (L_{fx}^3 + L_{fx}^2 + L_{fx} + 1) \\
&\quad + \bar{\xi}_w L_{fw} (L_{fx}^3 + L_{fx}^2 L_{gw} + L_{fx} L_{gw}^2 + L_{gw}^3) \\
&\quad + \bar{e}_w L_{fw} (L_{fx}^2 + L_{fx} L_{gw} + L_{fx} L_{gw} + L_{gw}^2 + 1) \\
|x_{t+5} - \tilde{x}_{t+5}| &\leq \bar{\xi}_x L_{fx}^5 + \bar{e}_x (L_{fx}^4 + L_{fx}^3 + L_{fx}^2 + L_{fx} + 1) \\
&\quad + \bar{\xi}_w L_{fw} (L_{fx}^4 + L_{fx}^3 L_{gw} + L_{fx}^2 L_{gw}^2 + L_{fx} L_{gw}^3 + L_{gw}^4) \\
&\quad + \bar{e}_w L_{fw} \left(\begin{array}{l} L_{fx}^3 + L_{fx}^2 L_{gw} + L_{fx}^2 + L_{fx} (L_{gw}^2 + L_{gw} + 1) \\ + L_{gw}^3 + L_{gw}^2 + L_{gw} + 1 \end{array} \right)
\end{aligned} \tag{3.26}$$

We are now in a position to generalize from (3.24)-(3.26) for l -step ahead prediction

$$\begin{aligned}
|x_{t+l} - \tilde{x}_{t+l}| &\leq \bar{\xi}_x L_{fx}^l + \bar{e}_x \sum_{k=0}^{k=l-1} L_{fx}^k + \bar{\xi}_w L_{fw} L_{fx}^{l-1} \sum_{k=0}^{k=l-1} \left(\frac{L_{gw}}{L_{fx}} \right)^k \\
&\quad + \bar{e}_w L_{fw} L_{fx}^{l-1} \sum_{j=0}^{j=l-1} \left(\frac{\sum_{k=0}^{k=j} L_{gw}^k}{L_{fx}^j} \right)
\end{aligned}$$

Using geometric series sum formulation

$$\begin{aligned}
|x_{t+l} - \tilde{x}_{t+l}| &\leq \bar{\xi}_x L_{fx}^l + \bar{e}_x \frac{L_{fx}^l - 1}{L_{fx} - 1} + \bar{\xi}_w L_{fw} \frac{L_{fx}^l - L_{gw}^l}{L_{fx} - L_{gw}} \\
&\quad + \bar{e}_w \frac{L_{fw} L_{fx}^{l-1}}{L_{gw} - 1} \sum_{j=0}^{j=l-1} \left(\frac{L_{gw}^j}{L_{fx}^j} - \frac{1}{L_{fx}^j} \right)
\end{aligned}$$

Summing the geometric series once more will result in (3.20) after minor manipulation, which proves the lemma. ■

Remark 3.2.1 *This results seems a bit conservative at fist sight. We will clarify this is not necessarily the case.*

- i. Lemma 3.2.1 is limited for $L_{fx}, L_{gw} \neq 1$ and $L_{fx} \neq L_{gw}$. However, only trivial modification is needed to reformulate the result for $L_{fx}, L_{gw} = 1$ and $L_{fx} = L_{gw}$. For example, $(L_{gw}^l - 1)/(L_{gw} - 1)$ can be replaced by the geometric series $\sum_{k=0}^{l-1} L_{gw}^k$ in case of $L_{gw} = 1$. Other cases can also be easily worked by following the development of the proof above.*
- ii. It is worth mentioning that prediction error bounds (3.19) and (3.20) are rather conservative, due to Lipschitz constants being used. Several methods have been suggested to reduce Lipschitz conservatism by pre-compensation, using different norms (other than Euclidean) and online estimation of local Lipschitz constant [94].*

We will claim an important result which will be proven in Chapter 4.

Claim 3.2.1 (Terminal Set and Terminal Control) *There exists an terminal control $k_f(\tilde{x}_l) \in U, \forall l = N_C, \dots, N_P - 1$, application of which to the nominal plant $\tilde{x}_{t+l} = \tilde{f}(\tilde{x}_l, k_f(\tilde{x}_l), 0)$ ensures that a terminal constraint set X_f is robust positively invariant (RPI) i.e. $x_l \in X_f$ and $\tilde{x}_l \in X_f, \forall l = t + N_C + 1, \dots, t + N_P$ for any $\tilde{x}_{t+N_C} \in X_f$, such that*

I. The rate of convergence of nominal state \tilde{x} under control $k_f(\tilde{x})$ is lower bounded by

$$\begin{aligned} \left| \tilde{f}(\tilde{x}_{t+l+1}, k_f(\tilde{x}_{t+l+1})) - \tilde{x}_{t+l+1} \right| &\geq \bar{\xi}_x L_{fx}^l (L_{fx} - 1) + \bar{e}_x L_{fx}^l + \\ &\quad \bar{\xi}_w L_{fw} \frac{L_{fx}^l (L_{fx} - 1) - L_{gw}^l (L_{gw} - 1)}{L_{fx} - L_{gw}} + \\ &\quad \bar{e}_w \frac{L_{fw}}{L_{gw} - 1} \left(\frac{L_{fx}^l (L_{fx} - 1) - L_{gw}^l (L_{fx} - 1)}{L_{fx} - L_{gw}} - L_{fx}^l \right), \end{aligned} \quad (3.27)$$

for $l = N_C - 1 \dots N_P - 2$, and (b) there exists $a \in \mathbb{Z}_{\geq 0}$ and $0 \leq Q_f \in \mathbb{R}^{n \times n}$ such that

$$\tilde{x}^T Q_f \tilde{x} \leq a, \quad \forall \tilde{x} \in X_f \quad (3.28)$$

By considering the effect of the prediction uncertainty bounds on the FHOCP constraints, it is possible to guarantee that state/output evolution of the actual system will be admissible as well. Recall the definitions of Pontryagin difference from Section 2.4 and Euclidean ball from Section 4.2.1.

Theorem 3.2.1 (Constraint Tightening) *With actual constraints X and W defined in (3.3), let the **tightened constraints** be given by*

$$\tilde{X}_{t+l} \triangleq X \sim \mathcal{B}^n(\bar{\rho}_{x_{t+l}}), \quad (3.29)$$

$$\tilde{W}_{t+l} \triangleq W \sim \mathcal{B}^n(\bar{\rho}_{w_{t+l}}), \quad (3.30)$$

for $l = 0, \dots, N_P$, where $\bar{\rho}_x$ and $\bar{\rho}_w$ are prediction error bounds from Lemma 3.2.1

defined as

$$\begin{aligned} \bar{\rho}_{x_{t+l}} \triangleq & L_{fx}^l \bar{\xi}_x + \bar{e}_x \frac{L_{fx}^l - 1}{L_{fx} - 1} + \bar{\xi}_w L_{fw} \frac{L_{fx}^l - L_{gw}^l}{L_{fx} - L_{gw}} \\ & + \bar{e}_w \frac{L_{fw}}{L_{gw} - 1} \left(\frac{L_{fx}^l - L_{gw}^l}{L_{fx} - L_{gw}} - \frac{L_{fx}^l - 1}{L_{fx} - 1} \right), \end{aligned} \quad (3.31)$$

$$\bar{\rho}_{w_{t+l}} \triangleq L_{gw}^l \bar{\xi}_w + \bar{e}_w \frac{L_{gw}^l - 1}{L_{gw} - 1}, \quad (3.32)$$

Then, any (in general suboptimal) admissible control sequence $u_{t,t+N_C-1}$ and terminal control $u_{t+N_C,t+N_P-1} = k_f(\tilde{x}_{t+N_C,t+N_P-1})$ which is feasible ($\tilde{x}_{t+l} \in \tilde{X}_{t+l}$, $u_{t,t+N_P-1} \in U$ and $\tilde{w}_{t+l} \in \tilde{W}_{t+l}$) with respect to tightened constraints (3.29)-(3.30) applied to the actual system (3.1), guarantees the satisfaction of original constraints (3.3), i.e. $x_{t+l} \in X$ and $w_{t+l} \in W$ for $l = 0, \dots, N_P$ and $x_t \in X_{MPC}$.

Proof. The proof will be divided in two parts.

- (a) Given state and disturbance estimates, \tilde{x}_t estimate \tilde{w}_t respectively, let us first consider the error in state prediction by applying the first $N_C - 1$ steps of a feasible sequence, i.e. $u_{t,t+N_C-1}$. Consider the error bounds defined in (3.7)-(3.12). Let us hypothesize that the realization of uncertainties is instead bounded by

$$\begin{aligned} |\tilde{x}_t - x_t| &= |\xi_{x_t}| \leq \xi'_x < \bar{\xi}_x, \\ |\tilde{w}_t - w_t| &= |\xi_{w_t}| \leq \xi'_w < \bar{\xi}_w, \\ |\tilde{f}(x_t, u_t, w_t) - f(x_t, u_t, w_t)| &= |e_{x_t}| \leq e'_x < \bar{e}_x \\ |\tilde{g}(w_t) - g(w_t, \phi_t)| &= |e_{w_t}| \leq e'_w < \bar{e}_w, \end{aligned}$$

Then, following the same development as in the proof of Lemma 3.2.1, we

can show that

$$|x_{t+l} - \tilde{x}_{t+l}| \leq \rho'_{x_{t+l}} \triangleq L_{fx}^l \xi'_x + e'_x \frac{L_{fx}^l - 1}{L_{fx} - 1} + \xi'_w L_{fw} \frac{L_{fx}^l - L_{gw}^l}{L_{fx} - L_{gw}} \\ + e'_w \frac{L_{fw}}{L_{gw} - 1} \left(\frac{L_{fx}^l - L_{gw}^l}{L_{fx} - L_{gw}} - \frac{L_{fx}^l - 1}{L_{fx} - 1} \right),$$

for $l = 0, \dots, N_C$. Therefore, applying the triangle inequality

$$|x_{t+l}| \leq |\tilde{x}_{t+l}| + \rho'_x$$

Since $\tilde{x}_{t+l} \in \tilde{X}_{t+l}$, therefore

$$x_{t+l} \in \tilde{X}_{t+l} \oplus \mathcal{B}^n(\rho'_{x_{t+l}})$$

Comparing with (3.29) and (3.31), it is obvious that $\rho'_{x_{t+l}} < \bar{\rho}_{x_{t+l}}$ and hence

$\mathcal{B}^n(\rho'_{x_{t+l}}) \subset \mathcal{B}^n(\bar{\rho}_{x_{t+l}})$. Therefore,

$$x_{t+l} \in \tilde{X}_{t+l} \oplus \mathcal{B}^n(\bar{\rho}_{x_{t+l}})$$

But, from the definition of tightened constraints in (3.29), we gather that

$X = \tilde{X}_{t+l} \oplus \mathcal{B}^n(\bar{\rho}_{x_{t+l}})$. Hence, we have proven that

$$x_{t+l} \in X, \quad \forall l = 0, \dots, N_C$$

(b) Given state and disturbance prediction $\tilde{x}_{t+N_C} \in X_f \subseteq \tilde{X}_{t+N_C}$ and $\tilde{w}_{t+N_C} \in$

\tilde{W}_{t+N_C} respectively, consider the error in state prediction by applying the

terminal sequence $u_{t,t_{N_C-1}} = k - f(\tilde{x}_{t,t_{N_C-1}})$. Consider the prediction error bounds defined in (3.31). The rate of growth of prediction error can be calculated as follows. For $l = N_C - 1 \dots N_P - 2$, we have

$$\begin{aligned} x_{t+l+2} - \tilde{x}_{t+l+2} - (x_{t+l+1} - \tilde{x}_{t+l+1}) &= f(x_{t+l+1}, k_f(\tilde{x}_{t+l+1}), w_{t+l+1}) \\ &\quad - \tilde{f}(\tilde{x}_{t+l+1}, k_f(\tilde{x}_{t+l+1}), 0) - f(x_{t+l}, k_f(\tilde{x}_{t+l}), w_{t+l}) + \tilde{f}(\tilde{x}_{t+l}, k_f(\tilde{x}_{t+l}), 0) \end{aligned}$$

Rearranging these terms and using Assumption 3.2.2,

$$\begin{aligned} (x_{t+l+2} - x_{t+l+1}) - (\tilde{x}_{t+l+2} - \tilde{x}_{t+l+1}) &\leq L_{fx}\xi_{x_{t+l+1}} + L_{fw}\xi_{w_{t+l+1}} + e_{x_{t+l+1}} \\ &\quad - (L_{fx}\xi_{x_{t+l}} + L_{fw}\xi_{w_{t+l}} + e_{x_{t+l}}) \end{aligned}$$

Using the definition of prediction error bounds in Theorem 3.2.1

$$(x_{t+l+2} - x_{t+l+1}) - (\tilde{x}_{t+l+2} - \tilde{x}_{t+l+1}) \leq \bar{\rho}_{x_{t+l+1}} - \bar{\rho}_{x_{t+l}}$$

But, comparing with the rate of convergence of the nominal system under the action of terminal control as described in Claim 3.2.1, it is obvious that

$$-(\tilde{x}_{t+l+1} - \tilde{x}_{t+l+2}) + (\bar{\rho}_{x_{t+l}} - \bar{\rho}_{x_{t+l+1}}) \leq -\epsilon \text{ for some } \epsilon \geq 0. \text{ Therefore,}$$

$$|x_{t+l+2} - x_{t+l+1}| \leq -\epsilon$$

Using triangular inequality,

$$|x_{t+l+2}| \leq |x_{t+l+1}| - \epsilon \tag{3.33}$$

Now, for $l = N_C - 1$, we have that $x_{t+N_C} \in X$ from part 1 of this proof, hence

$$x_{t+N_C+1} \in X \sim \mathcal{B}^n(\epsilon)$$

Since $X \sim \mathcal{B}^n(\epsilon)$, this means $X \sim \mathcal{B}^n(\epsilon) \subseteq X$ and hence $|x_{t+N_C+1}| \in X$.

Recursively repeating this procedure, we can show that

$$x_{t+l} \in X, \quad \forall l = N_C + 1, \dots, N_P$$

Therefore, combining both parts of this proof, we have proved that if the nominal state satisfies tightened constraints ($\tilde{x}_{t+l} \in \tilde{X}_{t+l}$), the actual constraints ($\tilde{x}_{t+l} \in \tilde{X}_{t+l}$) are also satisfied throughout the prediction horizon $l = 0, \dots, N_P$, as long as initial feasibility is provided ($x_t \in X_{MPC}$). ▀

Remark 3.2.2 *Constraint tightening (3.29)-(3.30) is novel as it is the first time that such a variety of uncertainty contributions have been considered simultaneously. Remarkably, the external input is not a constant or random unknown as is usually assumed, but here it is considered to evolve according to an uncertain nonlinear map. Besides, estimation errors and prediction errors are also considered. This leads to very general bounds on prediction error, which can be specialized to specific cases (e.g. perfect measurement will mean $\xi_x \rightarrow 0$). Also worthy of note is the fact that we have not considered the model mismatch to be state-dependent as in [85], as it does not have obvious practical application in mobile robotics. In fact, if the system is very nonlinear, one cannot expect modeling error to reduce*

with state, as in many cases larger state amplitude offers better model fidelity.

The constraint tightening procedure is summarized in the algorithm below.

Algorithm 2 Constraint Tightening

- 1: **Given** (i) nominal models $\tilde{f}(\tilde{x}, u, \tilde{w})$, $\tilde{g}(\tilde{w})$, (ii) uncertainty bounds $\bar{\xi}_x$, $\bar{\xi}_w$, \bar{e}_x , $\bar{e}_x w$, and (iii) horizons N_C , N_P .
 - 2: **procedure** CONSTRAINT TIGHTENING
 - 3: **Calculate** Lipschitz constants of nonlinear maps $\tilde{f}(\tilde{x}, u, \tilde{w})$ and $\tilde{g}(\tilde{w})$.
 - 4: **Calculate** the prediction error bounds in (3.31) and (3.32).
 - 5: **Tighten** the constraints by Pontryagin difference as given in (3.29)-(3.30).
 - 6: **end procedure**
-

3.2.6 Robust Recursive Feasibility of NMPC Algorithm

We defined the robust output feasible set X_{MPC} in Assumption 3.2.1 as the set of initial states for which the OCP 3.2.1 is feasible. However, finding this set or even guaranteeing feasibility for constrained nonlinear FHOCP is not a trivial task. In MPC however, the initial feasibility is not enough to prove feasibility of the receding horizon optimal control problem. We must prove recursive feasibility, i.e. at every sampling instant, the FHOCP is feasible. We will assume that initially, the problem has a feasible solution, as stated in Assumption 3.2.1.

Definition 3.2.2 (One-Step Controllable Set of X_f) *The one-step controllability set to the terminal constraint set X_f is defined as*

$$\mathcal{C}_1(X_f, \tilde{X}_{t+N_C}) \triangleq \left\{ \tilde{x} \in \tilde{X}_{t+N_C} : \tilde{f}(\tilde{x}, u, \tilde{w}) \in X_f, u \in U, \tilde{w} \in \tilde{W} \right\} \quad (3.34)$$

Let us also define $\bar{d} \triangleq \text{dist}(\tilde{X}_{t+N_C} \setminus \mathcal{C}_1(X_f, \tilde{X}_{t+N_C}), X_f)$.

Numerical computation of $\mathcal{C}(X, X_f)$ is very difficult. There have been some attempts nonetheless for efficient approximation of the one-step controllability set, such as [95]. We will present a method to calculate the terminal region and its one-step controllability set in this regard in Chapter 4.

Assumption 3.2.3 (Feasibility Bounds on Uncertainties) *The following bounds apply to the allowable uncertainties ($L_{fx} \neq L_{gw}$)*

I. *Lower bound on uncertainty growth*

$$\bar{\rho}_{x_{t+l}} - \bar{\rho}_{x_{t+l-1}} \geq L_{fx}^{l-1} \left(\underline{\xi}_x \right) + L_{fw} \frac{L_{fx}^{l-1} - L_{gw}^{l-1}}{L_{fx} - L_{gw}} \left(\underline{\xi}_w \right) \quad (3.35)$$

for $l = 1, \dots, N_C$.

II. *Uncertainties are upper bounded by minimum size of one-step controllability set to terminal constraint set*

$$\begin{pmatrix} L_{fx}^{N_C-1} \left((L_{fx} + 1) \bar{\xi}_x + L_{fw} \bar{\xi}_w + \bar{e}_x \right) + \\ L_{fw} \frac{L_{fx}^{N_C-1} - L_{gw}^{N_C-1}}{L_{fx} - L_{gw}} \left((L_{gw} + 1) \bar{\xi}_w + \bar{e}_w \right) \end{pmatrix} \leq \bar{d} \quad (3.36)$$

For the case where $L_{fx} = L_{gw}$, the assumption above can be easily reformulated as shown in Remark 3.2.1. Recursive feasibility and robust positive invariance of feasible region X_{MPC} will now be stated and proven.

Theorem 3.1 (Recursive Feasibility) *Under Assumptions 3.2.2 and 3.2.3, terminal control (Claim 3.2.1), suitable bounds on uncertainties (Assumption*

3.2.3) and tightened constraints (Theorem 3.2.1), given the feasibility of initial state $\tilde{x}_t \in X_{MPC}$ (Assumption 3.2.1), the FHOCP 3.2.1 is recursively feasible.

Proof. We need to show that given an initially feasible state $\tilde{x}_t \in X_{MPC}$ at time instant t , there exists a feasible solution for the FHOCP 3.2.1 at $t + 1$, and by induction for the entire horizon. We will carry out the proof in two steps. Therefore, suppose that at time instant t , there exists an optimal control solution $u_{t,t+N_c-1|t}^0$. In particular at $t + 1$, there is a possibly feasible sequence $u'_{t+1,t+N_c|t+1} = \text{col}[u_{t+1,t+N_c-1|t}^0, u'_{t+N_c}]$, where u'_{t+N_c} is a feasible control action. We will have to show that (a) $u'_{t+1,t+N_c-1|t+1} = \text{col}[u_{t+1,t+N_c-1|t}^0, u'_{t+N_c}]$ is feasible for the tightened constraints (3.29), and (b) u'_{t+N_c} exists.

(a) To prove $\tilde{x}_{t+l,t+N_c|t+1} \in \tilde{X}_{t+l|t+1}$ for $l = 1, \dots, N_C$: Given estimations for state $\tilde{x}_t|t$ and disturbance $\tilde{w}_t|t$ at t , we mentioned that there exists the feasible control $u_{t,t+N_c-1|t}^0$ which state and disturbance predictions $\tilde{x}_{t,t+N_c|t}$ and $\tilde{w}_{t+l,t+N_c|t}$ respectively, using nominal maps (3.5) and (3.10). At $t + 1$, new estimations $\tilde{x}_{t+1|t+1}$ and $\tilde{w}_{t+1|t+1}$ are made, such that the new predictions using the old sequence $u'_{t+1,t+N_c-1|t+1} = u_{t+1,t+N_c-1|t}^0$ are $\tilde{x}_{t+1,t+N_c|t+1}$ and $\tilde{w}_{t+l,t+N_c|t+1}$. We can write

$$\begin{aligned} & \tilde{x}_{t+l|t+1} - \tilde{x}_{t+l|t} \\ &= \tilde{f}(\tilde{x}_{t+l-1|t+1}, u_{t+l-1|t}^0, \tilde{w}_{t+l-1|t+1}) - \tilde{f}(\tilde{x}_{t+l-1|t}, u_{t+l-1|t}^0, \tilde{w}_{t+l-1|t}) \\ &\leq \left| \tilde{f}(\tilde{x}_{t+l-1|t+1}, u_{t+l-1|t}^0, \tilde{w}_{t+l-1|t+1}) - \tilde{f}(\tilde{x}_{t+l-1|t}, u_{t+l-1|t}^0, \tilde{w}_{t+l-1|t}) \right| \end{aligned}$$

Using Assumption 3.2.2,

$$\tilde{x}_{t+l|t+1} - \tilde{x}_{t+l|t} \leq L_{fx} |\tilde{x}_{t+l-1|t+1} - \tilde{x}_{t+l-1|t}| + L_{fw} |\tilde{w}_{t+l-1|t+1} - \tilde{w}_{t+l-1|t}|$$

Using the same recursion we can write

$$\begin{aligned} \tilde{x}_{t+l|t+1} - \tilde{x}_{t+l|t} &\leq L_{fx}^2 |\tilde{x}_{t+l-2|t+1} - \tilde{x}_{t+l-2|t}| \\ &\quad + L_{fw} (L_{fx} + L_{gw}) |\tilde{w}_{t+l-2|t+1} - \tilde{w}_{t+l-2|t}| \\ &\leq L_{fx}^3 |\tilde{x}_{t+l-3|t+1} - \tilde{x}_{t+l-3|t}| \\ &\quad + L_{fw} (L_{fx}^2 + L_{fx} L_{gw} + L_{gw}^2) |\tilde{w}_{t+l-3|t+1} - \tilde{w}_{t+l-3|t}| \\ &\leq L_{fx}^4 |\tilde{x}_{t+l-4|t+1} - \tilde{x}_{t+l-4|t}| \\ &\quad + L_{fw} (L_{fx}^3 + L_{fx}^2 L_{gw} + L_{fx} L_{gw}^2 + L_{gw}^3) |\tilde{w}_{t+l-4|t+1} - \tilde{w}_{t+l-4|t}| \end{aligned}$$

This can be generalized as

$$\begin{aligned} \tilde{x}_{t+l|t+1} - \tilde{x}_{t+l|t} &\leq L_{fx}^{l-1} |\tilde{x}_{t+1|t+1} - \tilde{x}_{t+1|t}| \\ &\quad + L_{fw} \frac{L_{fx}^{l-1} - L_{gw}^{l-1}}{L_{fx} - L_{gw}} |\tilde{w}_{t+1|t+1} - \tilde{w}_{t+1|t}|, \end{aligned} \tag{3.37}$$

for $l = 1, \dots, N_c - 1$. Now, since we have assumed that $\tilde{x}_{t+l|t} \in \tilde{X}_{t+l|t} \triangleq X \sim$

$\mathcal{B}^n(\bar{\rho}_{x_{t+l|t}})$, with $\bar{\rho}_{x_{t+l|t}}$ given as (3.31), this means

$$\begin{aligned} \tilde{x}_{t+l|t+1} &\in X \sim \mathcal{B}^n(\bar{\rho}_{x_{t+l|t}}) \\ &\oplus \mathcal{B}^n \left(L_{fx}^{l-1} |\tilde{x}_{t+1|t+1} - \tilde{x}_{t+1|t}| + L_{fw} \frac{L_{fx}^{l-1} - L_{gw}^{l-1}}{L_{fx} - L_{gw}} |\tilde{w}_{t+1|t+1} - \tilde{w}_{t+1|t}| \right) \end{aligned} \tag{3.38}$$

However, we need to prove $\tilde{x}_{t+l,t+N_c|t+1} \in \tilde{X}_{t+l|t+1} \triangleq X \sim \mathcal{B}^n(\bar{\rho}_{x_{t+l|t+1}})$. For

this to be true, we should have

$$\bar{\rho}_{x_{t+l|t+1}} \leq \bar{\rho}_{x_{t+l|t}} - L_{fx}^{l-1} |\tilde{x}_{t+1|t+1} - \tilde{x}_{t+1|t}| - L_{fw} \frac{L_{fx}^{l-1} - L_{gw}^{l-1}}{L_{fx} - L_{gw}} |\tilde{w}_{t+1|t+1} - \tilde{w}_{t+1|t}| \quad (3.39)$$

But, since $\bar{\rho}_{x_{t+l|t+1}} = \bar{\rho}_{x_{t+l-1|t}}$, we can write the inequality above as

$$\bar{\rho}_{x_{t+l|t}} - \bar{\rho}_{x_{t+l-1|t}} \geq L_{fx}^{l-1} |\tilde{x}_{t+1|t+1} - \tilde{x}_{t+1|t}| + L_{fw} \frac{L_{fx}^{l-1} - L_{gw}^{l-1}}{L_{fx} - L_{gw}} |\tilde{w}_{t+1|t+1} - \tilde{w}_{t+1|t}|$$

Adding and subtracting actual state x_{t+l} and disturbance w_{t+l} ,

$$\begin{aligned} \bar{\rho}_{x_{t+l|t}} - \bar{\rho}_{x_{t+l-1|t}} &\geq L_{fx}^{l-1} |(\tilde{x}_{t+1|t+1} - x_{t+1}) - (\tilde{x}_{t+1|t} - x_{t+1})| \\ &\quad + L_{fw} \frac{L_{fx}^{l-1} - L_{gw}^{l-1}}{L_{fx} - L_{gw}} |(\tilde{w}_{t+1|t+1} - w_{t+1}) - (\tilde{w}_{t+1|t} - w_{t+1})| \end{aligned}$$

Using triangle inequality,

$$\begin{aligned} \bar{\rho}_{x_{t+l|t}} - \bar{\rho}_{x_{t+l-1|t}} &\geq L_{fx}^{l-1} \left| |\tilde{x}_{t+1|t} - x_{t+1}| - |\tilde{x}_{t+1|t+1} - x_{t+1}| \right| \\ &\quad + L_{fw} \frac{L_{fx}^{l-1} - L_{gw}^{l-1}}{L_{fx} - L_{gw}} \left| |\tilde{w}_{t+1|t} - w_{t+1}| - |\tilde{w}_{t+1|t+1} - w_{t+1}| \right| \\ &\geq L_{fx}^{l-1} |\tilde{x}_{t+1|t+1} - x_{t+1}| + L_{fw} \frac{L_{fx}^{l-1} - L_{gw}^{l-1}}{L_{fx} - L_{gw}} |\tilde{w}_{t+1|t+1} - w_{t+1}| \end{aligned}$$

Since we take fresh samples at $t + 1$, estimation error's lower bounds are given by (3.8) and (3.9). This leads to inequality (3.35). Since this proves the inequality (3.39), we can substitute it in (3.38) as

$$\tilde{x}_{t+l|t+1} \in X \sim \mathcal{B}^n(\bar{\rho}_{x_{t+l-1|t}}) \subseteq X \sim \mathcal{B}^n(\bar{\rho}_{x_{t+l|t+1}}) \stackrel{\Delta}{=} \tilde{X}_{t+l|t+1} \quad (3.40)$$

for $l = 1, \dots, N_C$. This completes the first part of the proof.

- (b) To prove $\tilde{x}_{t+N_C+1|t+1} \in X_f \subseteq \tilde{X}_{t+N_C+1|t+N_C+1}$: We will start with rewriting inequality (3.37).

$$\begin{aligned}
\tilde{x}_{t+N_C|t+1} - \tilde{x}_{t+N_C|t} &\leq L_{fx}^{N_C-1} \left| (\tilde{x}_{t+1|t+1} - x_{t+1}) - (\tilde{x}_{t+1|t} - x_{t+1}) \right| \\
&\quad + L_{fw} \frac{L_{fx}^{N_C-1} - L_{gw}^{N_C-1}}{L_{fx} - L_{gw}} \left| (\tilde{w}_{t+1|t+1} - w_{t+1}) - (\tilde{w}_{t+1|t} - w_{t+1}) \right| \\
&\leq L_{fx}^{N_C-1} \left| |\tilde{x}_{t+1|t+1} - x_{t+1}| + |\tilde{x}_{t+1|t} - x_{t+1}| \right| \\
&\quad + L_{fw} \frac{L_{fx}^{N_C-1} - L_{gw}^{N_C-1}}{L_{fx} - L_{gw}} \left| |\tilde{w}_{t+1|t+1} - w_{t+1}| + |\tilde{w}_{t+1|t} - w_{t+1}| \right|
\end{aligned}$$

Since upper bounds on accumulated prediction errors are given by (3.19)-(3.20) and (3.31)-(3.32),

$$\begin{aligned}
\tilde{x}_{t+N_C|t+1} - \tilde{x}_{t+N_C|t} &\leq L_{fx}^{N_C-1} \left| \bar{\rho}_{x_{t+1|t+1}} + \bar{\rho}_{x_{t+1|t}} \right| \\
&\quad + L_{fw} \frac{L_{fx}^{N_C-1} - L_{gw}^{N_C-1}}{L_{fx} - L_{gw}} \left| \bar{\rho}_{w_{t+1|t+1}} + \bar{\rho}_{w_{t+1|t}} \right|
\end{aligned}$$

We have $\bar{\rho}_{x_{t+1|t+1}} = \bar{\rho}_{x_{t|t}}$ and $\bar{\rho}_{w_{t+1|t+1}} = \bar{\rho}_{w_{t|t}}$. Hence,

$$\begin{aligned}
\tilde{x}_{t+N_C|t+1} - \tilde{x}_{t+N_C|t} &\leq L_{fx}^{N_C-1} \left| (L_{fx} + 1)\bar{\xi}_x + L_{fw}\bar{\xi}_w + \bar{e}_x \right| \\
&\quad + L_{fw} \frac{L_{fx}^{N_C-1} - L_{gw}^{N_C-1}}{L_{fx} - L_{gw}} \left| (L_{gw} + 1)\bar{\xi}_w + \bar{e}_w \right|
\end{aligned} \tag{3.41}$$

From Assumption 3.2.3, let

$$L_{fx}^{N_C-1} \left| (L_{fx} + 1)\bar{\xi}_x + L_{fw}\bar{\xi}_w + \bar{e}_x \right| + L_{fw} \frac{L_{fx}^{N_C-1} - L_{gw}^{N_C-1}}{L_{fx} - L_{gw}} \left| (L_{gw} + 1)\bar{\xi}_w + \bar{e}_w \right| \leq \bar{d}$$

Now, since we have assumed that $\tilde{x}_{t+N_C|t} \in X_f$, with $\bar{\rho}_{x_{t+1|t}}$ given as (3.31),

this means

$$\tilde{x}_{t+N_c|t+1} \in X_f \oplus \mathcal{B}^n(\bar{d}) \triangleq \mathcal{C}_1(X_f, X)$$

Hence, there exists a feasible control $u'_{t+N_c} \in U$, such that $\tilde{x}_{t+N_c+1|t+1} \in X_f \subseteq \tilde{X}_{t+N_c+1|t+N_c+1}$. This completes the proof. █

Remark 3.2.3 *It can be seen from the inequality (3.35) that the lower bound on growth of uncertainties depends on the lower bounds on estimation errors. If these lower bounds are zero (which is often the case), this condition on uncertainty growth is always satisfied. It is apparent from the foregoing that ensuring recursive feasibility is dependent on two factors:*

1. *finding the set of initial states X_{MPC} for which feasible control solutions exist,*
2. *finding the minimum size \bar{d} of one-step robust controllability set $\mathcal{C}_1(X_f)$.*

We present a novel algorithm for determining the robust one-step controllability set to X_f and an iterative scheme for determining X_{MPC} in Chapter 4.

3.2.7 Robust Stability of NMPC Algorithm

Even if the system model being controlled is linear, presence of constraints make the control problem nonlinear [75]. Therefore, Lyapunov and Dynamic Programming analysis are natural tools for determining stability of the NMPC controllers.

As pointed above, NMPC inherits many features of classical optimal control, therefore many concepts like Hamilton-Bellman-Jacobi theory, Bellman's 'curse of dimensionality', calculus of variations etc. have direct correspondence in MPC theory. In fact, one can calculate offline static optimal controllers for finite horizon optimality of unconstrained linear time-invariant (LTI) systems using the same arguments as those that apply to stability requirements of NMPC [38]. It is another matter that we are not interested in unconstrained LTI systems. Constrained nonlinear systems optimized over finite horizon is much more involved and challenging.

Asymptotic ISS for MPC schemes can be shown in case of additive, vanishing disturbance [96]. However, [79] proves that only ISpS can be guaranteed a priori in case of non-vanishing (not decaying with state) uncertainties. In the proposed approach, the uncertainty in predicting ξ_x and ξ_w are non-vanishing and one can only guarantee ISpS. One method to ensure closed-loop stability of MPC [38] is by specifying a terminal cost h_f and a terminal constraint set, such that control switches to terminal or auxiliary control k_f upon the system entering X_f during control horizon N_c . We consider the stability of the system with respect to uncertain external input by exploiting Theorem 2.5.2. We will introduce some useful assumptions and justify them.

Assumption 3.2.4 (Cost Lipschitz Continuity) *We assume that $k_f(\cdot)$, $h(\cdot)$, $q(\cdot)$ and $h_f(\cdot)$ are locally Lipschitz continuous and there are nonlinear functions relating to the cost components.*

- I. $|k_f(\tilde{x})| \leq L_{k_f}|\tilde{x}|$, for $\tilde{x} \in \tilde{X}_f$
- II. $|h(\tilde{x}, u)| \leq L_{hx}|\tilde{x}| + L_{hu}|u|$, for $\tilde{x} \in \tilde{X}_t$ and $u \in U$
- III. $0 \leq |q(\tilde{x}, \tilde{w})| \leq L_{qx}|\tilde{x}| + L_{qw}|\tilde{w}|$, for $x \in \tilde{X}_t$ and $w \in \tilde{W}_t$
- IV. $|h_f(\tilde{x})| \leq L_{hf}|\tilde{x}|$ for $\tilde{x} \in \tilde{X}_f$
- V. $\alpha_1(|\tilde{x}_t|) \leq h(\tilde{x}_t, u_t)$, for $\tilde{x} \in \tilde{X}_t$.
- VI. $\alpha_{1,f}(|\tilde{x}_t|) \leq h_f(\tilde{x}_t) \leq \alpha_{2,f}(|\tilde{x}_t|)$, for all $\tilde{x}_t \in \tilde{X}_t$,

with positive local Lipschitz constants L_{k_f} , L_{hx} , L_{hu} , L_{qx} , L_{qw} and L_{hf} .

These continuity assumptions are not restrictive. Local Lipschitz conditions and nonlinear bounds are satisfied by most quadratic cost functions, as shown in Example 3.3.1. Hence, with the above development, we have explicit relations for all parameters (in terms of designer chosen variables) mentioned in Assumption 3.2.4.

Remark 3.2.4 *Due to the use of Lipschitz constants, nonlinear bounds in Assumption 3.2.4 are conservative. Similarly, as noted in [59], small-gain condition may turn out to be conservative in practice as it is typical of these kind of results. On the other hand, the generality of the problem makes it rather difficult to obtain tighter conditions without introducing more restrictive assumptions on the structure of the dynamics and on the cost function.*

We will prove the stability of the nominal system first and show that even the nominal system is only practically stable (ISpS). We will then treat the robust

stability of the actual system, and show that only ultimate boundedness (ISpS) can be guaranteed for the uncertain, perturbed system.

Stability of Nominal System with Nominal Disturbance Model

In this section we will investigate stability of the nominal system (3.5) with nominal disturbance model (3.10) under the receding horizon control strategy. We will show that it is practically stable and converges to a region around target state. It will be extended in the next section for the uncertain perturbed system (3.1). We will introduce a few definitions which will be proven later.

Lemma 3.2.2 (Technical) *With reference to Definition 2.5.9, the following hold for practical stability of the nominal system (3.5) with nominal disturbance model (3.10) under RH control (3.17),*

$$(i). \quad \alpha_1(s) = \alpha_2(s) \triangleq \min h(s, 0)$$

$$(ii). \quad \alpha_3(s) \triangleq \alpha_{2,f}(L_{fx}^{N_p} s) + (L_{hx} + L_{hu}L_{kf} + L_{qx}) \frac{(L_{fx})^{N_p-1}}{L_{fx}-1} s$$

$$(iii). \quad \sigma_1(s) \triangleq \left(\begin{array}{l} \frac{L_{qx}+L_{hx}}{L_{fx}-L_{gw}} \left(\frac{L_{fx}^{N_p-1}-1}{L_{fx}-1} - \frac{L_{gw}^{N_p-1}-1}{L_{gw}-1} \right) + \frac{L_{gw}^{N_p-1}-1}{L_{gw}-1} \frac{L_{qw}}{L_{fw}} \\ + \frac{L_{hu}L_{kf}}{L_{fx}-L_{gw}} \left(\frac{L_{fx}^{N_p-1}-L_{fx}^{N_c}}{L_{fx}-1} - \frac{L_{gw}^{N_p-1}-L_{gw}^{N_c}}{L_{gw}-1} \right) \\ + \frac{L_{fx}^{N_p-1}-L_{gw}^{N_p-1}}{L_{fx}-L_{gw}} \end{array} \right) L_{fw} (L_{gw} s)$$

$$(iv). \quad \sigma_2(s) \triangleq \sigma_1 \left(\frac{s}{L_{gw}} \right) + \psi(s)$$

$$(v). \quad \sigma_3(s) \triangleq L_{qw} \frac{(L_{gw})^{N_p-1}}{L_{gw}-1} s$$

$$(vi). \quad \bar{c} \triangleq \left(\begin{array}{l} \frac{L_{fx}^{N_p-1}-1}{L_{fx}-1} (L_{qx} + L_{hx}) \\ + L_{hu}L_{kf} \frac{L_{fx}^{N_p-1}-L_{fx}^{N_c}}{L_{fx}-1} + L_{fx}^{N_p-1} \end{array} \right) c_1 + L_{hu} |u_{\max} - u_{\min}|$$

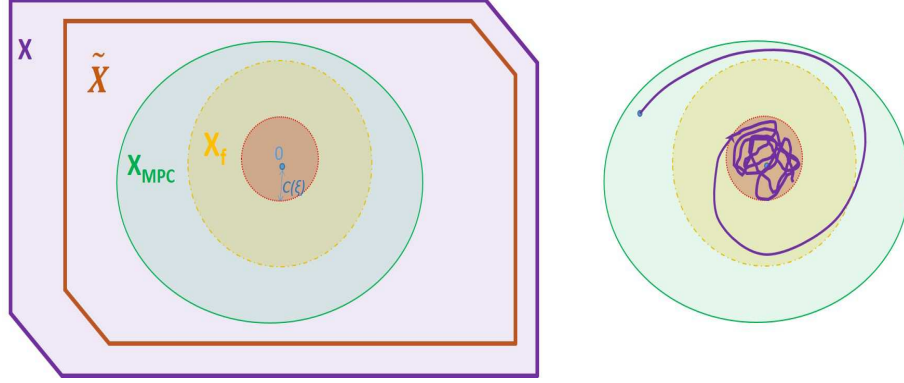


Figure 3.3: Illustration of sets introduced in Theorem 3.2.2 and feasible trajectories. State constraint set X , tightened constraint set \tilde{X} , terminal set X_f and uncertainty ball $\mathcal{B}^n(c)$ are shown (left); a feasible trajectory is also shown (right).

(vii). $\bar{c} = 0$,

where $c_1 \triangleq \bar{\xi}_x + L_{fx}\bar{\xi}_x + L_{fw}\bar{\xi}_w + \bar{e}_x$.

Figure 3.3 illustrates the sets introduced in this chapter and feasible trajectory.

Theorem 3.2.2 (Stability of Nominal System) *Let there be a terminal set $\tilde{X}_f \subset \tilde{X}$ and auxiliary control $k_f(x)$ according to Claim 3.2.1, such that Assumptions 3.2.1, 3.2.2, 3.2.3 and 3.2.4 hold. If the following condition holds for some $\psi \in \mathcal{K}$*

$$h_f\left(\tilde{f}(\tilde{x}, k_f(\tilde{x}))\right) - h_f(\tilde{x}) \leq -h(\tilde{x}, k_f(\tilde{x})) - q(\tilde{x}, \tilde{w}) + \psi(|\tilde{w}|), \quad (3.42)$$

for all $\tilde{x} \in X_f$ and $\tilde{w} \in \tilde{W}$, then the nominal system (3.5) under NMPC optimal control (3.17) which optimizes cost (3.14) admits the optimal value of cost functional $V_t(\tilde{x}_t, u_t, \tilde{w}_t) = J_t(\tilde{x}_t, u_{t,t+N_p}^0, \tilde{w}_t)$ as an ISpS Lyapunov function. It is therefore input-to-state practically stable (ISpS) for all initial states within the robust output feasible set $X_{MPC} \subseteq X$.

Proof. We need to prove that $V_t(\tilde{x}_{t|t}, u_t, \tilde{w}_{t|t}) = J_t(\tilde{x}_{t|t}, u_{t,t+N_p|t}^0, \tilde{w}_{t|t})$ is an ISS Lyapunov function in X_{MPC} . From (3.14), the optimal cost is given as

$$\begin{aligned}
V_t(\tilde{x}_{t|t}, u_{t,t+N_c-1|t}^o, \tilde{w}_{t|t}) &= h(\tilde{x}_{t|t}, u_{t|t}^o) + q(\tilde{x}_{t|t}, \tilde{w}_{t|t}) \\
&+ \sum_{l=t+1}^{t+N_c-1} [h(\tilde{x}_{l|t}, u_{l|t}^o) + q(\tilde{x}_{l|t}, \tilde{w}_{l|t})] \\
&+ \sum_{l=t+N_c}^{t+N_p-1} [h(\tilde{x}_{l|t}, u_{l|t}^o) + q(\tilde{x}_{l|t}, \tilde{w}_{l|t})] + h_f(\tilde{x}_{t+N_p|t}) \quad (3.43)
\end{aligned}$$

The lower bound on $V_t(\tilde{x}_{t|t}, u_{t|t}, \tilde{w}_{t|t})$ is obviously given by (Assumption 3.2.4)

$$\alpha_1(|\tilde{x}_{t|t}|) \leq V_t(\tilde{x}_{t|t}, u_{t,t+N_p|t}^o, \tilde{w}_{t|t}), \quad \forall \tilde{x}_{t|t} \in \tilde{X}_{t|t} \supseteq X, \tilde{w}_{t|t} \in \tilde{W}_{t|t} \subseteq W \quad (3.44)$$

By Assumption 3.2.1, X_{MPC} is not empty. In fact, the control sequence $\tilde{u}_{t,t+N_c-1|t} = [k_f(\tilde{x}_{t|t}), \dots, k_f(\tilde{x}_{t+N_c-1|t})]^T$ is feasible (but in general suboptimal) for any $\tilde{x}_t|t \in X_f$. Using Assumptions 3.2.2 and 3.2.4

$$\begin{aligned}
V_t(\tilde{x}_{t|t}, u_{t,t+N_c-1|t}^o, \tilde{w}_{t|t}) &\leq J_t(\tilde{x}_{t|t}, \tilde{u}_{t,t+N_c-1|t}, \tilde{w}_{t|t}) \\
&= \sum_{l=t}^{t+N_p-1} [h(\tilde{x}_{l|t}, \tilde{u}_{l|t}) + q(\tilde{x}_{l|t}, \tilde{w}_{l|t})] + h_f(|\tilde{x}_{t+N_p|t}|) \\
&\leq \sum_{l=t}^{t+N_p-1} [L_{hx} |\tilde{x}_{l|t}| + L_{hu} |k_f(\tilde{x}_{l|t})| + L_{qx} |\tilde{x}_{l|t}| + L_{qw} |\tilde{w}_{l|t}|] + \alpha_{2,f}(|\tilde{x}_{t+N_p|t}|) \\
&\leq \sum_{l=t}^{t+N_p-1} [(L_{hx} + L_{hu}L_{kf} + L_{qx}) |\tilde{x}_{l|t}| + L_{qw} |\tilde{w}_{l|t}|] + \alpha_{2,f}(|\tilde{x}_{t+N_p|t}|) \\
&\leq \sum_{l=t}^{t+N_p-1} [(L_{hx} + L_{hu}L_{kf} + L_{qx}) L_{fx}^{l-t} |\tilde{x}_{t|t}| + L_{qw} L_{gw}^{l-t} |\tilde{w}_{t|t}|] + \alpha_{2,f} \left((L_{fx})^{N_p} |\tilde{x}_{t|t}| \right)
\end{aligned}$$

Summing the geometric series, we obtain

$$\begin{aligned}
V_t(\tilde{x}_{t|t}, u_{t,t+N_c-1|t}^o, \tilde{w}_{t|t}) & \\
& \leq (L_{hx} + L_{hu}L_{kf} + L_{qx}) \frac{(L_{fx})^{N_p} - 1}{L_{fx} - 1} |\tilde{x}_{t|t}| \\
& + L_{qw} \frac{(L_{gw})^{N_p} - 1}{L_{gw} - 1} |\tilde{w}_{t|t}| + \alpha_{2,f} \left((L_{fx})^{N_p} |\tilde{x}_{t|t}| \right) \\
& \leq \alpha_3(|\tilde{x}_{t|t}|) + \sigma_3(|\tilde{w}_{t|t}|) + \bar{c} \quad (3.45)
\end{aligned}$$

for $\tilde{x}_{t|t} \in X_f$ and $\tilde{w}_{t|t} \in \tilde{W}_{t|t}$. It is obvious that α_3 , σ_3 and \bar{c} are as defined in Lemma 3.2.2. For (3.45) to hold, $L_{fx}, L_{gw} \neq 1$. However, following the reasons explained in Remark 3.2.1, in the very special case of $L_{fx} = 1$ and/or $L_{gx} = 1$, minor modifications are required (3.45).

Refer to Assumption 3.2.3 and the result expressed in Theorem 3.1, which states that given the optimal control sequence $u_{t,t+N_c-1|t}^o$ at time t for $\tilde{x}_t \in \tilde{X}_t$, there exists at least one feasible control $u'_{t+1,t+N_c|t+1} = [u_{t+1,t+N_c-1|t}^o, u'_{t+N_c|t+1}]^T$ at $t+1$, where $u'_{t+N_c|t+1} \in U$ is such that $\tilde{x}_{t+N_c+1|t+1} \in X_f$ any $x_t \in X_{MPC}$. Also, note that since new measurements are made at $t+1$, nominal estimates $x_{t+1|t+1}$ and $w_{t+1|t+1}$ at $t+1$ are different than the estimates $x_{t+1|t}$ and $w_{t+1|t}$, even though the same model is used for prediction. The cost of using this (suboptimal, in general) control is

$$\begin{aligned}
V_{t+1}(\tilde{x}_{t+1|t+1}, u_{t+1,t+N_c|t+1}^o, \tilde{w}_{t+1|t+1}) & \leq J(\tilde{x}_{t+1}, \tilde{w}_{t+1}, u'_{t+1,t+N_c|t+1}, N_C, N_P) \\
& = \sum_{l=t+1}^{t+N_c} [h(\tilde{x}_{l|t+1}, u'_{l|t+1}) + q(\tilde{x}_{l|t+1}, \tilde{w}_{l|t+1})]
\end{aligned}$$

$$\begin{aligned}
& + \sum_{l=t+Nc+1}^{t+Np} [h(\tilde{x}_{l|t+1}, k_f(\tilde{x}_{l|t+1})) + q(x_{l|t+1}, \tilde{w}_{l|t+1})] + h_f(\tilde{x}_{t+Np+1|t+1}) \\
& = \sum_{l=t+1}^{t+Nc-1} [h(\tilde{x}_{l|t+1}, u_{l|t}^o) + q(\tilde{x}_{l|t+1}, \tilde{w}_{l|t+1})] \\
& + h(\tilde{x}_{t+Nc|t+1}, u'_{t+Nc|t+1}) + q(\tilde{x}_{t+Nc|t+1}, \tilde{w}_{t+Nc|t+1}) \\
& + \sum_{l=t+Nc+1}^{t+Np} [h(\tilde{x}_{l|t+1}, k_f(\tilde{x}_{l|t+1})) + q(x_{l|t+1}, \tilde{w}_{l|t+1})] \\
& + h_f(\tilde{f}(\tilde{x}_{t+Np|t+1}, k_f(\tilde{x}_{t+Np|t+1}))) \quad (3.46)
\end{aligned}$$

Add and subtract (3.43) from (3.46).

$$\begin{aligned}
& V_{t+1}(\tilde{x}_{t+1|t+1}, u_{t+1,t+Nc|t+1}^o \tilde{w}_{t+1|t+1}) \\
& \leq V_t(\tilde{x}_{t|t}, u_{t,t+Nc-1|t}^o, \tilde{w}_{t|t}) - h(\tilde{x}_{t|t}, u_{t|t}^o) - q(\tilde{x}_{t|t}, \tilde{w}_{t|t}) \\
& + \sum_{l=t+1}^{t+Nc-1} [h(\tilde{x}_{l|t+1}, u_{l|t}^o) - h(\tilde{x}_{l|t}, u_{l|t}^o) + q(\tilde{x}_{l|t+1}, \tilde{w}_{l|t+1}) - q(\tilde{x}_{l|t}, \tilde{w}_{l|t})] \\
& + h(\tilde{x}_{t+Nc|t+1}, u'_{t+Nc|t+1}) - h(\tilde{x}_{t+Nc|t}, k_f(\tilde{x}_{t+Nc|t})) \\
& + q(\tilde{x}_{t+Nc|t+1}, \tilde{w}_{t+Nc|t+1}) - q(\tilde{x}_{t+Nc|t}, \tilde{w}_{t+Nc|t}) \\
& + \sum_{l=t+Nc+1}^{t+Np-1} \left[\begin{aligned} & h(\tilde{x}_{l|t+1}, k_f(\tilde{x}_{l|t+1})) - h(\tilde{x}_{l|t}, k_f(\tilde{x}_{l|t})) \\ & + q(x_{l|t+1}, \tilde{w}_{l|t+1}) - q(\tilde{x}_{l|t}, \tilde{w}_{l|t}) \end{aligned} \right] \\
& + h(\tilde{x}_{t+Np|t+1}, k_f(\tilde{x}_{t+Np|t+1})) + q(\tilde{x}_{t+Np|t+1}, \tilde{w}_{t+Np|t+1}) \\
& + h_f(\tilde{f}(\tilde{x}_{t+Np|t+1}, k_f(\tilde{x}_{t+Np|t+1}))) - h_f(\tilde{x}_{t+Np|t}) \quad (3.47)
\end{aligned}$$

Now, we compute upper limits on the components of (3.47). From Assumptions 3.2.4 and 3.2.2, and inequality (3.37) for $l = 1, \dots, N_C - 1$

$$\begin{aligned} |h(\tilde{x}_{t+l|t+1}, u_{t+l|t}^o) - h(\tilde{x}_{t+l|t}, u_{t+l|t}^o)| &\leq L_{hx} |\tilde{x}_{t+l|t+1} - \tilde{x}_{l|t}| \\ &\leq L_{hx} \left(\begin{aligned} &L_{fx}^{l-1} |\tilde{x}_{t+1|t+1} - \tilde{x}_{t+1|t}| \\ &+ L_{fw} \frac{L_{fx}^{l-1} - L_{gw}^{l-1}}{L_{fx} - L_{gw}} |\tilde{w}_{t+1|t+1} - \tilde{w}_{t+1|t}| \end{aligned} \right) \end{aligned}$$

But, utilizing Lemma 3.2.1,

$$\begin{aligned} |\tilde{x}_{t+1|t+1} - \tilde{x}_{t+1|t}| &= |\tilde{x}_{t+1|t+1} - x_{t+1} - \tilde{x}_{t+1|t} + x_{t+1}| \\ &\leq |\tilde{x}_{t+1|t+1} - x_{t+1}| + |\tilde{x}_{t+1|t} - x_{t+1}| \leq \bar{\xi}_x + L_{fx} \bar{\xi}_x + L_{fw} \bar{\xi}_w + \bar{e}_x \end{aligned}$$

Therefore,

$$\begin{aligned} |h(\tilde{x}_{t+l|t+1}, u_{t+l|t}^o) - h(\tilde{x}_{t+l|t}, u_{l|t}^o)| &\leq L_{hx} L_{fx}^{l-1} (\bar{\xi}_x + L_{fx} \bar{\xi}_x + L_{fw} \bar{\xi}_w + \bar{e}_x) \\ &\quad + L_{hx} L_{fw} \frac{L_{fx}^{l-1} - L_{gw}^{l-1}}{L_{fx} - L_{gw}} (|\tilde{w}_{t+1|t+1}| + L_{fx} |\tilde{w}_{l|t}|) \quad (3.48) \end{aligned}$$

for $l = 1, \dots, N_C - 1$. Using the treatment of (3.48)

$$\begin{aligned} |q(\tilde{x}_{t+l|t+1}, \tilde{w}_{t+l|t+1}) - q(\tilde{x}_{t+l|t}, \tilde{w}_{t+l|t})| &\leq L_{qx} (|\tilde{x}_{t+l|t+1} - \tilde{x}_{l|t}|) + L_{qw} (|\tilde{w}_{t+l|t+1}| + |\tilde{w}_{l|t}|) \\ &\leq L_{qx} \left(\begin{aligned} &L_{fx}^{l-1} (\bar{\xi}_x + L_{fx} \bar{\xi}_x + L_{fw} \bar{\xi}_w + \bar{e}_x) \\ &+ L_{fw} \frac{L_{fx}^{l-1} - L_{gw}^{l-1}}{L_{fx} - L_{gw}} (L_{gw} |\tilde{w}_{l|t}| + |\tilde{w}_{t+1|t+1}|) \end{aligned} \right) \end{aligned}$$

$$+ L_{qw}L_{gw}^{l-1} (L_{gw}|\tilde{w}_{t|t}| + |\tilde{w}_{t+1|t+1}|) \quad (3.49)$$

$l = 1, \dots, N_P - 1$. Similarly,

$$\begin{aligned} & \left| h(\tilde{x}_{t+l|t+1}, k_f(\tilde{x}_{t+l|t+1})) - h(\tilde{x}_{t+l|t}, k_f(\tilde{x}_{t+l|t})) \right| \\ & \leq L_{hx} (|\tilde{x}_{t+l|t+1} - \tilde{x}_{t+l|t}|) + L_{hu}L_{kf} (|\tilde{x}_{t+l|t+1} - \tilde{x}_{t+l|t}|) \\ & \leq (L_{hx} + L_{hu}L_{kf}) \left(\begin{array}{l} L_{fx}^{l-1} (\bar{\xi}_x + L_{fx}\bar{\xi}_x + L_{fw}\bar{\xi}_w + \bar{e}_x) \\ + L_{fw} \frac{L_{fx}^{l-1} - L_{gw}^{l-1}}{L_{fx} - L_{gw}} (L_{gw} |\tilde{w}_{t|t}| + |\tilde{w}_{t+1|t+1}|) \end{array} \right) \quad (3.50) \end{aligned}$$

for $l = N_C + 1, \dots, N_P - 1$. Consider (3.41) for the difference between transition costs at N_C .

$$\begin{aligned} & \left| h(\tilde{x}_{t+N_C|t+1}, u'_{t+N_C|t+1}) - h(\tilde{x}_{t+N_C|t}, k_f(\tilde{x}_{t+N_C|t})) \right| \\ & \leq L_{hx} (|\tilde{x}_{t+l|t+1} - \tilde{x}_{l|t}|) + L_{hu} (|u'_{t+N_C|t+1} - k_f(\tilde{x}_{t+N_C|t})|) \\ & \leq L_{hx}L_{fx}^{N_C-1} (\bar{\xi}_x + L_{fx}\bar{\xi}_x + L_{fw}\bar{\xi}_w + \bar{e}_x) + L_{hu} |u_{\max} - u_{\min}| \\ & \quad + L_{hx}L_{fw} \frac{L_{fx}^{N_C-1} - L_{gw}^{N_C-1}}{L_{fx} - L_{gw}} (L_{gw} |\tilde{w}_{t|t}| + |\tilde{w}_{t+1|t+1}|) \quad (3.51) \end{aligned}$$

and finally,

$$\begin{aligned} & \left| h_f(\tilde{x}_{t+N_P|t+1}) - h_f(\tilde{x}_{t+N_P|t}) \right| \leq L_{hf} |\tilde{x}_{t+N_P|t+1} - \tilde{x}_{t+N_P|t}| \\ & \Rightarrow h_f(\tilde{x}_{t+N_P|t+1}) - h_f(\tilde{x}_{t+N_P|t}) \leq L_{hf} |\tilde{x}_{t+N_P|t+1} - \tilde{x}_{t+N_P|t}| \\ & \Rightarrow -h_f(\tilde{x}_{t+N_P|t}) \leq -h_f(\tilde{x}_{t+N_P|t+1}) + L_{fx}^{N_P-1} (\bar{\xi}_x + L_{fx}\bar{\xi}_x + L_{fw}\bar{\xi}_w + \bar{e}_x) \end{aligned}$$

$$+ L_{fw} \frac{L_{fx}^{Np-1} - L_{gw}^{Np-1}}{L_{fx} - L_{gw}} (L_{gw} |\tilde{w}_{t|t}| + |\tilde{w}_{t+1|t+1}|) \quad (3.52)$$

Substituting inequalities (3.48) - (3.52) in (3.47), we can write

$$\begin{aligned} & V_{t+1}(\tilde{x}_{t+1|t+1}, u_{t+1,t+Nc|t+1}^o, \tilde{w}_{t+1|t+1}) - V_t(\tilde{x}_{t|t}, u_{t,t+Nc-1|t}^o, \tilde{w}_{t|t}) \\ & \leq -h(\tilde{x}_{t|t}, u_{t|t}^o) - q(\tilde{x}_{t|t}, \tilde{w}_{t|t}) \\ & \quad + \sum_{l=1}^{Np-1} \left[\begin{aligned} & L_{fx}^{l-1} (L_{qx} + L_{hx}) (\bar{\xi}_x + L_{fx} \bar{\xi}_x + L_{fw} \bar{\xi}_w + \bar{e}_x) \\ & + \frac{L_{fx}^{l-1} - L_{gw}^{l-1}}{L_{fx} - L_{gw}} (L_{qx} + L_{hx}) L_{fw} (L_{gw} |\tilde{w}_{t|t}| + |\tilde{w}_{t+1|t+1}|) \\ & + L_{qw} L_{gw}^{l-1} (L_{gw} |\tilde{w}_{t|t}| + |\tilde{w}_{t+1|t+1}|) \end{aligned} \right] \\ & \quad + L_{hu} |u_{\max} - u_{\min}| \\ & \quad + \sum_{l=Nc+1}^{Np-1} \left[(L_{hu} L_{kf}) \left(\begin{aligned} & L_{fx}^{l-1} (\bar{\xi}_x + L_{fx} \bar{\xi}_x + L_{fw} \bar{\xi}_w + \bar{e}_x) \\ & + L_{fw} \frac{L_{fx}^{l-1} - L_{gw}^{l-1}}{L_{fx} - L_{gw}} (L_{gw} |\tilde{w}_{t|t}| + |\tilde{w}_{t+1|t+1}|) \end{aligned} \right) \right] \\ & + L_{fx}^{Np-1} (\bar{\xi}_x + L_{fx} \bar{\xi}_x + L_{fw} \bar{\xi}_w + \bar{e}_x) + L_{fw} \frac{L_{fx}^{Np-1} - L_{gw}^{Np-1}}{L_{fx} - L_{gw}} (L_{gw} |\tilde{w}_{t|t}| + |\tilde{w}_{t+1|t+1}|) \\ & \quad + h(\tilde{x}_{t+Np|t+1}, k_f(\tilde{x}_{t+Np|t+1})) + q(\tilde{x}_{t+Np|t+1}, \tilde{w}_{t+Np|t+1}) \\ & \quad + h_f(\tilde{f}(\tilde{x}_{t+Np|t+1}, k_f(\tilde{x}_{t+Np|t+1}))) - h_f(\tilde{x}_{t+Np|t+1}) \end{aligned}$$

Noting that $q(\tilde{x}_{t|t}, \tilde{w}_{t|t}) \geq 0$ and condition (3.42), we obtain

$$V_{t+1}(\tilde{x}_{t+1|t+1}, u_{t+1,t+Nc|t+1}^o, \tilde{w}_{t+1|t+1}) - V_t(\tilde{x}_{t|t}, u_{t,t+Nc-1|t}^o, \tilde{w}_{t|t}) \leq -h(\tilde{x}_{t|t}, u_{t|t}^o)$$

$$\begin{aligned}
& \left(\begin{aligned}
& \frac{L_{qx}+L_{hx}}{L_{fx}-L_{gw}} \left(\frac{L_{fx}^{Np-1}-1}{L_{fx}-1} - \frac{L_{gw}^{Np-1}-1}{L_{gw}-1} \right) L_{fw} (L_{gw} |\tilde{w}_{t|t}| + |\tilde{w}_{t+1|t+1}|) \\
& + \frac{L_{gw}^{Np-1}-1}{L_{gw}-1} L_{qw} (L_{gw} |\tilde{w}_{t|t}| + |\tilde{w}_{t+1|t+1}|) \\
& + \frac{L_{hu}L_{kf}}{L_{fx}-L_{gw}} \left(\frac{L_{fx}^{Np-1}-L_{fx}^{Nc}}{L_{fx}-1} - \frac{L_{gw}^{Np-1}-L_{gw}^{Nc}}{L_{gw}-1} \right) L_{fw} (L_{gw} |\tilde{w}_{t|t}| + |\tilde{w}_{t+1|t+1}|) \\
& + L_{fw} \frac{L_{fx}^{Np-1}-L_{gw}^{Np-1}}{L_{fx}-L_{gw}} (L_{gw} |\tilde{w}_{t|t}| + |\tilde{w}_{t+1|t+1}|) + \psi (|\tilde{w}_{t+1|t+1}|)
\end{aligned} \right) \\
& + \left(\begin{aligned}
& \frac{L_{fx}^{Np-1}-1}{L_{fx}-1} (L_{qx} + L_{hx}) (\bar{\xi}_x + L_{fx}\bar{\xi}_x + L_{fw}\bar{\xi}_w + \bar{e}_x) \\
& + L_{hu}L_{kf} \frac{L_{fx}^{Np-1}-L_{fx}^{Nc}}{L_{fx}-1} (\bar{\xi}_x + L_{fx}\bar{\xi}_x + L_{fw}\bar{\xi}_w + \bar{e}_x) \\
& + L_{fx}^{Np-1} (\bar{\xi}_x + L_{fx}\bar{\xi}_x + L_{fw}\bar{\xi}_w + \bar{e}_x) + L_{hu} |u_{\max} - u_{\min}|
\end{aligned} \right)
\end{aligned}$$

Since $\alpha_1(|\tilde{x}|) \leq h(\tilde{x}, u)$ (Assumption 3.2.4), we can now write

$$\begin{aligned}
& V_{t+1}(\tilde{x}_{t+1|t+1}, u_{t+1,t+Nc|t+1}^o, \tilde{w}_{t+1|t+1}) - V_t(\tilde{x}_{t|t}, u_{t,t+Nc-1|t}^o, \tilde{w}_{t|t}) \\
& \leq -\alpha_2(|\tilde{x}_t|) + \sigma_1(|\tilde{w}_t|) + \sigma_2(|\tilde{w}_{t+1}|) + \bar{c} \\
& \quad \forall \tilde{x}_t \in X_{MPC}, \forall \tilde{w}_t \in \tilde{W}_t, \tilde{w}_{t+1} \in \tilde{W}_{t+1}, \quad (3.53)
\end{aligned}$$

where α_2 , σ_1 , σ_2 , and \bar{c} are as defined in Lemma 3.2.2. Hence, in view of Theorem 2.5.2 and inequalities (3.44), (3.45) and (3.53), the nominal system (3.5)-(3.10) under RH optimal control (3.17) is ISpS in X_{MPC} . Hence, in reference to Theorem 2.5.2, we can write

$$|\tilde{x}_{t+l|t+l}| \leq \tilde{\beta} (|\tilde{x}_{t|t}|, l) + \tilde{\gamma} (\|\tilde{w}_{[t+l|t+l]}\|) + \tilde{c} \quad (3.54)$$

according to the definitions given in Theorem 2.5.2. █

Remark 3.2.5 *Practical (ISpS) stability of nominal system model coupled with*

nominal disturbance model under proposed NMPC controller was demonstrated. Some remarks are in order.

R-I. For comparison, consider the ISS stability of the nonlinear system under additive disturbance studied in [59]. However, Theorem 3.2.2 considers the nominal system with nominal disturbance model. We do not have a strict structural requirement on the nominal disturbance model (3.10), unlike [59] which assumes a linear asymptotically stable disturbance model.

R-II. Stability of nominal system does not necessarily translate into same margin of stability and convergence for the actual system with disturbances and uncertainties. In the next section we will study stability of the perturbed dynamics, and show that ultimate boundedness (ISpS) can be achieved, albeit with different bounds.

Stability of Uncertain and Perturbed System

In the previous section, we showed practical (ultimately bounded) stability of the nominal system under NMPC control. However, we are more interested in the trajectory of the actual uncertain and perturbed system in closed loop. We will see that due to recursive feasibility and constraint tightening, the ISpS results for nominal system are easily translated into corresponding ISpS stability for the perturbed system. The treatment below is inspired from [97].

Theorem 3.2.3 (ISpS Stability of Perturbed and Uncertain System) *If the nominal system (3.5) with nominal disturbance model (3.10) is ISpS stable*

within tightened constraint sets (3.13) under RH control law (3.17), then the uncertain system (3.1) perturbed with external input (3.4) under the same control (3.17) is also ISpS stable.

Proof. Let us start from the result derived in the last section, i.e practical stability of the nominal system under RH control law. At every instant, new measurements are taken and hence we have from (3.6)

$$\begin{aligned} |x_{t+l} - \tilde{x}_{t+l|t+l}| &\leq \bar{\xi}_x \\ x_{t+l} - \tilde{x}_{t+l|t+l} &\leq \bar{\xi}_x \\ |\tilde{x}_{t+l|t+l}| &\geq |x_{t+l} - \bar{\xi}_x| \geq |x_{t+l}| - |\bar{\xi}_x| \end{aligned}$$

Put this in (3.54),

$$|x_{t+l}| \leq \tilde{\beta}(|\tilde{x}_{t+l|t+l}|, l) + \tilde{\gamma}(\|\tilde{w}_{[t+l|t+l]}\|) + \tilde{c} + \bar{\xi}_x \quad (3.55)$$

Similarly,

$$|x_t - \tilde{x}_{t|t}| \leq \bar{\xi}_x \Rightarrow |\tilde{x}_{t|t}| \leq |x_t| + \bar{\xi}_x$$

Put this in (3.55), and apply properties of comparison functions from Section 2.4.2.

$$\begin{aligned} |x_{t+l}| &\leq \tilde{\beta}(|x_t| + \bar{\xi}_x, l) + \tilde{\gamma}(\|\tilde{w}_{[t+l|t+l]}\|) + \tilde{c} + \bar{\xi}_x \\ &\leq \tilde{\beta}(2|x_t|, l) + \tilde{\gamma}(\|\tilde{w}_{[t+l|t+l]}\|) + \tilde{c} + \bar{\xi}_x + \tilde{\beta}(2\bar{\xi}_x, 0) \end{aligned} \quad (3.56)$$

Now, from (3.9),

$$\begin{aligned} \|\tilde{w}_{t,t+l|t+l}\| &\triangleq \sup_{0 \leq k \leq l} \{|\tilde{w}_{t+k|t+k}|\} \leq \sup_{0 \leq k \leq l} \{|w_{t+k}| + \bar{\xi}_w\} \\ &= \sup_{0 \leq k \leq l} \{|w_{t+k}|\} + \bar{\xi}_w = \|w_{t,t+l}\| + \bar{\xi}_w \end{aligned}$$

Put this back in (3.2.7)

$$\begin{aligned} |x_{t+l}| &\leq \tilde{\beta}(2|x_t|, l) + \tilde{\gamma}(\|w_{t,t+l}\| + \bar{\xi}) + \tilde{c} + \bar{\xi} + \tilde{\beta}(2\bar{\xi}_x, 0) \\ &\leq \tilde{\beta}(2|x_t|, l) + \tilde{\gamma}(2\|w_{t,t+l}\|) + \tilde{c} + \bar{\xi} + \tilde{\beta}(2\bar{\xi}_x, 0) + \tilde{\gamma}(2\bar{\xi}_w) \end{aligned}$$

Hence, we can now write

$$|x_{t+l}| \leq \beta(|x_t|, l) + \gamma(\|w_{t,t+l}\|) + c \tag{3.57}$$

with $\beta(r, s) \triangleq \tilde{\beta}(2r, s)$, $\gamma(s) = \tilde{\gamma}(2s)$ and $c \triangleq \tilde{c} + \bar{\xi} + \tilde{\beta}(2\bar{\xi}_x, 0) + \tilde{\gamma}(2\bar{\xi}_w)$.

Therefore, in view of (3.57), the perturbed system (3.5) under RH control law (3.17) is also ISpS stable. █

3.3 Illustrative Examples: Quadratic Cost and Constraint Tightening

In many cases the cost functional in MPC is quadratic. We will see that in this case, we can derive explicit analytic forms of Lipschitz constants and other bounds

in the development above. We will furnish two examples, one analytic and another numerical to elucidate the theory developed in this chapter.

Example 3.3.1 (Bounds and L. Constants of Quadratic Cost) *If the cost functional is quadratic, such as*

$$J_t(\tilde{x}, u, \tilde{w}, N_c, N_p, k_f) = (\tilde{x}_{t,t+N_p})^T Q_f (\tilde{x}_{t,t+N_p}) + \sum_{l=t}^{t+N_p-1} \left[\begin{array}{l} (\tilde{x}_l)^T Q (\tilde{x}_l) + (u_l)^T R (u_l) \\ + (\tilde{x}_l - \tilde{f}(0, 0, \tilde{w}_l))^T S (\tilde{x}_l - \tilde{f}(0, 0, \tilde{w}_l)) \end{array} \right] \quad (3.58)$$

with positive definite matrices Q , R , S and Q_f , then the Lipschitz constants and nonlinear bounds in Assumption 3.2.4 can be explicitly found in terms of system and design variables. Lipschitz constants L_{fx} , L_{fu} and L_{gw} of state and disturbance models can be determined easily after examining the model. Comparing (3.58) with cost functional (3.14), it is easy to see that $h(\tilde{x}, u) = |\tilde{x}|_Q + |u|_R$, $q(\tilde{x}, \tilde{w}) = |\tilde{x} - \tilde{f}(0, 0, \tilde{w}_{l-1})|_S$ and $h_f(\tilde{x}_{t+N_p}) = |\tilde{x}_{t+N_p}|_{Q_f}$. Continuing from Example (2.5.1), we can show that (using nomenclature of Assumption 3.2.4 and Lemma 3.2.2). Let $\lambda_{\Pi_{\min}}$ and $\lambda_{\Pi_{\max}}$ are the minimum and maximum eigenvalues of the p.d. matrix Π . Constraint values x_{\max} , u_{\max} and w_{\max} are defined in (3.3). Here, $|\tilde{x}|_{\max} \triangleq \max(|x_{\min}|, |x_{\max}|)$ and similarly defined for u and \tilde{w} .

$$I. \quad \alpha_1(|\tilde{x}|) = \alpha_2(|\tilde{x}|) = \lambda_{Q_{\min}} |\tilde{x}|^2$$

$$II. \quad \alpha_{1f}(|\tilde{x}|) = \lambda_{Q_{f,\min}} |\tilde{x}|^2$$

$$III. \quad \alpha_{2f}(|\tilde{x}|) = \lambda_{Q_{f,\max}} |\tilde{x}|^2$$

IV. $L_{hx} = \lambda_{Q_{\max}} |\tilde{x}|_{\max}$

V. $L_{hu} = \lambda_{R_{\max}} |u|_{\max}$

VI. From triangular inequality $|\tilde{x} - \tilde{f}(0, 0, \tilde{w}_l)|_S \leq |\tilde{x}|_S + |\tilde{f}(0, 0, \tilde{w}_l)|_S$, hence we have $L_{qx} = \lambda_{S_{\max}} |\tilde{x}|_{\max}$

VII. Similarly, $L_{qw} = \lambda_{S_{\max}} L_{fw}^2 |\tilde{w}|_{\max}$

VIII. From (3.28), $x^T Q_f x \leq a$ for $\tilde{x} \in X_f$, therefore $|\tilde{x}| \leq \sqrt{a/\lambda_{Q_f, \max}}, \forall \tilde{x} \in X_f$.

Therefore, $L_{hf} = \sqrt{a\lambda_{Q_f, \max}}$.

IX. $L_{kf} = \lambda_{k_{f\max}} \sqrt{a/\lambda_{Q_f, \max}}$, where $\lambda_{k_{f\max}}$ is the maximum eigenvalue of $K^T K$, if the terminal control is given by $k_f(\tilde{x}) = K^T \tilde{x}$.

Inserting these values in Lemma 3.2.2 gives explicit expressions for the remaining nonlinear functions described in this chapter.

Next, we consider a numerical example (inspired by [95]) which further illustrates these concepts introduced in this chapter. We will consider constraint tightening of a simple nonlinear oscillator.

Example 3.3.2 (Nonlinear Oscillator: Part I (Constraint Tightening))

Consider an unstable second order nonlinear oscillator. The perturbed system is given as

$$\begin{aligned} x_{(1)_{t+1}} &= x_{(1)_t} + 0.051 [-x_{(2)_t} + 0.4902 (1 + x_{(1)_t}) u_t] + w_{(1)_t} \\ x_{(2)_{t+1}} &= x_{(2)_t} + 0.049 [x_{(1)_t} + 0.5102 (1 - 4x_{(2)_t}) u_t] + w_{(2)_t}, \end{aligned} \tag{3.59}$$

where subscript (i) denote the i -th component of a vector. The external input (disturbance) is driven by the following system

$$w_{t+1} = 10^{-3}w_t + \phi_t \quad (3.60)$$

where $|\phi_t| \leq 10^{-4}$ is a normally distributed noise. Constraints are given as below

$$\begin{aligned} U &= \{u \in \mathbb{R} : -2 \leq u \leq 2\} \\ X &= \{x \in \mathbb{R} : -0.4 \leq x_{(1)} \leq 0.225, -0.49 \leq x_{(2)} \leq 0.175\} \\ W &= \{w_{(1,2)} \in \mathbb{R} : -5 \times 10^{-3} \leq w_{(1,2)} \leq 5 \times 10^{-3}\} \end{aligned} \quad (3.61)$$

We assume that the model available to us is

$$\begin{aligned} \tilde{x}_{(1)_{t+1}} &= \tilde{x}_{(1)_t} + 0.05 [-\tilde{x}_{(2)_t} + 0.5 (1 + \tilde{x}_{(1)_t}) u_t] + \tilde{w}_{(1)_t} \\ \tilde{x}_{(2)_{t+1}} &= \tilde{x}_{(2)_t} + 0.05 [\tilde{x}_{(1)_t} + 0.5 (1 - 4\tilde{x}_{(2)_t}) u_t] + \tilde{w}_{(2)_t}, \end{aligned} \quad (3.62)$$

while the model of disturbance is

$$\tilde{w}_{t+1} = 1.01 \times 10^{-3} \tilde{w}_t \quad (3.63)$$

We also assume that the estimation errors are bounded by

$$\begin{aligned} |x_t - \tilde{x}_{t|t}| &\leq \bar{\xi}_x = 10^{-5} \\ |w_t - \tilde{w}_{t|t}| &\leq \bar{\xi}_w = 10^{-5} \end{aligned} \quad (3.64)$$

We can write (3.62) as

$$\begin{aligned}\tilde{x}_{t+1} &= \begin{bmatrix} 1 + 0.025u_t & -0.05 \\ 0.05 & 1 - 0.1u_t \end{bmatrix} \tilde{x}_t + 0.025 \begin{bmatrix} 1 + \tilde{x}_{(1)_t} \\ 1 - 4\tilde{x}_{(2)_t} \end{bmatrix} u_t + \tilde{w}_t \\ &= \tilde{A}_t \tilde{x}_t + \tilde{B}_t u_t + \tilde{D}_t \tilde{w}_t \quad (3.65)\end{aligned}$$

Let the cost functional be given by (3.58) in Example (3.3.1), with the following $Q = 0.1 \times I_2$, $R = 1$, $S = 10^{-3} I_2$, $N_P = 12$ and $N_c = 5$. Continuing from Example (3.3.1),

- I. $L_{fx} = 1.189$. This is given by $\max_t \left(\mathbf{abs} \left(\mathbf{eig} \left(\tilde{A}_t \right) \right) \right)$.
- II. $L_{fu} = 0.0801$. This is given by $\left| \tilde{B}_t \right|$.
- III. $L_{fw} = 1.4142$, given by $\left| \tilde{D}_t \right|$
- IV. $L_{gw} = 1.01 \times 10^{-3}$
- V. $\alpha_1(|r|) = \alpha_2(|r|) = \lambda_{Q_{\min}} |r|^2 = 0.1 |r|^2$
- VI. $L_{hx} = 0.06325$, given by $\lambda_{Q_{\max}} |\tilde{x}|_{\max}$.
- VII. $L_{hu} = 2$, given by $\lambda_{R_{\max}} |u|_{\max}$
- VIII. $L_{qx} = 6.325 \times 10^{-4}$, given by $\lambda_{S_{\max}} |\tilde{x}|_{\max}$
- IX. $L_{qw} = 1.414 \times 10^{-5}$, given by $L_{qw} = \lambda_{S_{\max}} L_{fw}^2 |\tilde{w}|_{\max}$
- X. $\bar{e}_x = 6.325 \times 10^{-4}$, as $|f(x, u, w) - \tilde{f}(x, u, w)| \leq 10^{-3} |x|$

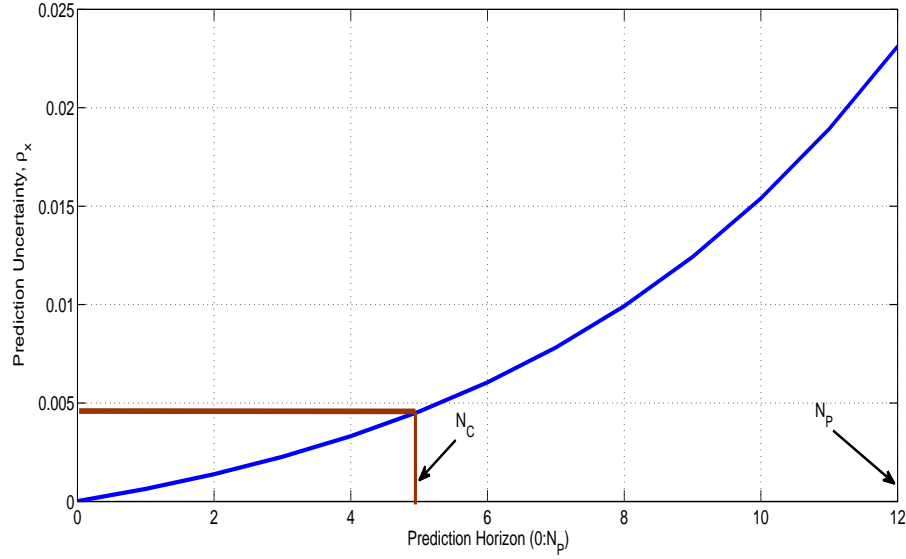


Figure 3.4: Growth of state prediction error along the horizon. Value at N_C is marked in brown.

$$XI. \quad \bar{e}_w = 5 \times 10^{-8}, \text{ as } |f(x, u, w) - \tilde{f}(x, u, w)| \leq 10^{-5}|w|$$

We are now in a position to find the shrunk constraints given in Theorem 3.2.1.

Substituting the above values in (3.31)

$$\begin{aligned} \bar{\rho}_{x_{t+l}} &= (1.189)^l \times 10^{-5} + 3.3 \times 10^{-3} \left((1.189)^l - 1 \right) \\ &+ 5.95 \times 10^{-8} \left((1.189)^l - (1.01 \times 10^{-3})^l \right) \\ &+ 3.745 \times 10^{-8} \left((1.189)^l - 1 - 0.159 \left((1.189)^l - (1.01 \times 10^{-3})^l \right) \right) \end{aligned} \quad (3.66)$$

The growth of prediction uncertainty is depicted in Fig. 3.4. It can be seen that the growth is exponential, which limits the maximum horizon which can be employed while ensuring feasibility. Constraints are tightened according to Theorem 3.2.1, as shown in Fig. 3.5. It can be seen how the growth of prediction error effects the of constraint shrinkage.

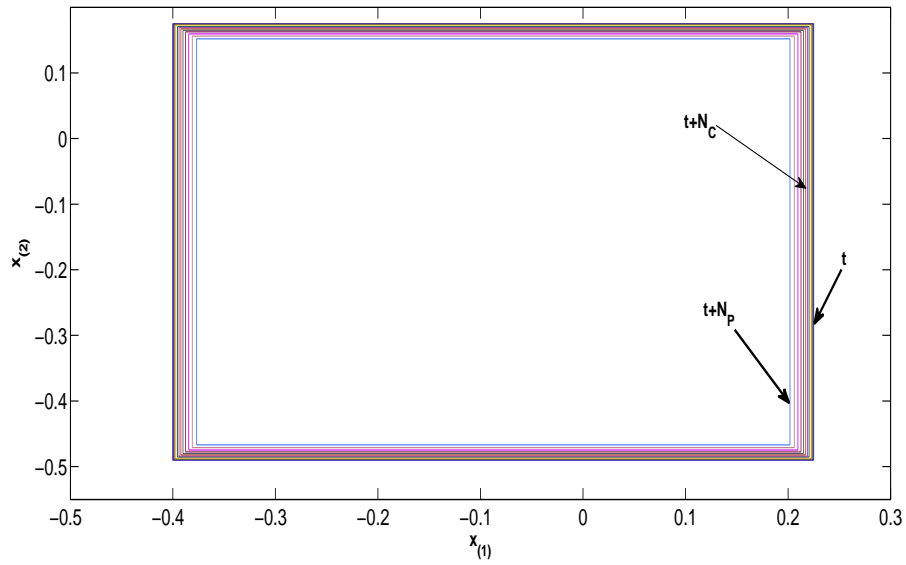


Figure 3.5: Constraint tightening for the nonlinear oscillator of Example (3.3.2). Notice the exponential increase in shrinkage of constraints with increasing horizon.

3.4 Conclusion

This chapter presented new results in nonlinear MPC control with robustness against a number of sources of uncertainty. The main NMPC algorithm and one of its five component algorithms to address constraint tightening and online optimization are introduced in this chapter. Algorithm 1 includes offline components and online optimization of the recursive finite horizon OCP 3.2.1. We showed that due to uncertainties, only practical stability (ISpS) can be ensured, and the amount of tolerable disturbance is bounded by the size of the one-step controllability set to the terminal constraint region. An extended numerical example was introduced in two parts. Closed form analytic expressions of all nonlinear functions and Lipschitz constants are provided along with a simulation example for constraint tightening Algorithm 2.

CHAPTER 4

OPTIMIZATION OF TERMINAL, CONTROLLABLE AND FEASIBLE SETS

4.1 Introduction

In the previous chapter, we laid the foundation blocks of the robust NMPC algorithm introduced in this thesis. However, details of several ingredients were deliberately postponed. We talked about the terminal set constraint and its associated terminal control law, but assumed its existence in Claim 3.2.1 for expediting development of the mathematical framework. Similarly, we assumed the existence of feasible initial conditions in Assumption 3.2.1. We also assumed the knowledge of one-step controllable set to the terminal set in Definition 3.2.2. All three of these assumptions are justified and quantified in this chapter. We do so by using the

convenient and highly developed framework of convex optimization, particularly the mathematically adept Linear Matrix Inequalities (LMI) form.

4.1.1 Chapter Contributions

The contributions of this chapter are non-trivial in the following aspects, which are under review in Automatica [84].

- i. Terminal constraint region is maximized (Theorem 4.3.1) based on PLDI based LMIs, and warm started with a novel approach involving algebraic Riccati equations.
- ii. One-step controllable set and robust output feasible set are determined based on min-max optimization (Algorithm 6) rather than the existing set based approaches [78].
- iii. Four new algorithms are presented for terminal region optimization and determining feasibility.
- iv. Important guidelines on the choice of components of cot function, especially the robustness cost are provided due to unprecedented insight gained in development of this chapter.

Chapter Organization Most of the algorithms in this chapter are based on convex optimization, for which a brief primer is provided in Section 4.2. A methodology (Algorithms 3-4) for simultaneous optimization of terminal control law and

maximization of terminal constraint set is developed in Section 4.3. The numerical example first introduced in Section 3.3 is extended to show application of Algorithms 3-4. As mentioned in the last chapter, recursive feasibility is related to the minimum size of the one-step controllability set to the terminal region. This one-step controllable set is determined with Algorithm 5 developed in Section 4.4. Having verified condition for recursive stability, in Section 4.5 the robust output feasible set for the nonlinear system under Algorithm 1 is determined using Algorithm 6. Since all ingredients of Algorithm 1 have now been developed, the algorithm is finally applied to extended example of the nonlinear oscillator in Section 4.6.

4.2 Introduction to Convex Analysis

Convex analysis is the branch of mathematics that studies properties of convex functions convex sets. It has application in optimization and therefore of relevance to MPC. In this chapter we will utilize this tool to determine terminal (auxiliary) control laws and maximizing the terminal region. Symbols used in this introductory section should not be confused with ones used in the rest of the chapter dealing with the main algorithm. Given a scalar $c \in [0, 1]$, vectors $u, v \in S \subseteq \mathbb{R}^n$, the set $S \subseteq \mathbb{R}^n$ is a convex (or affine) set and real valued vector function $s(\cdot)$ is a convex function if

$$cx + (1 - c)y \in S \tag{4.1}$$

$$f(cx + (1 - c)y) \leq cf(x) + (1 - c)f(y) \tag{4.2}$$

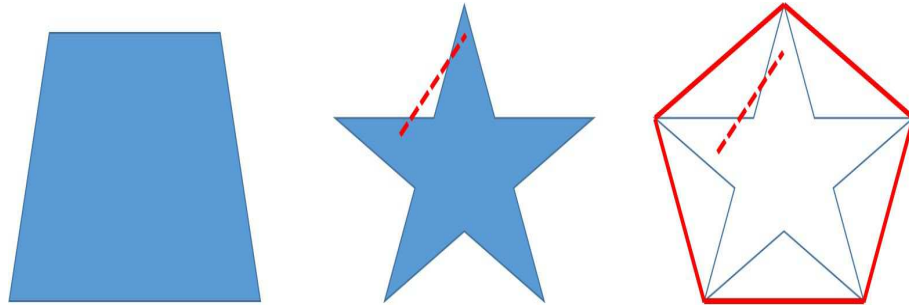


Figure 4.1: Convex and nonconvex sets. Left. The polyhedron is convex. Middle. The star shaped set is not convex, since the line segment (dotted) between the two points in the set is not contained in the set. Right. The pentagon in red is a convex hull of the non-convex star shaped set. (This art is original, copyrights belong to author).

A function is convex if and only if its epigraph (region above its graph) is a convex set. Given some non-negative scalars $c_1, \dots, c_k \in \mathbb{R}_{\geq 0}$ such that $\sum_{i=1}^k c_i = 1$, the vector $\sum_{i=1}^k c_i x_i, \forall x_i \in \mathbb{R}^n$ is called a *convex combination*. The *convex hull* of set S is the set of all convex combinations of vectors in S , i.e.

$$\mathbf{Co} S \triangleq \left\{ \sum_{i=1}^k c_i x_i : x_i \in S, c_i \geq 0, i = 1, \dots, k, \sum_{i=1}^k c_i x_i = 1 \right\} \quad (4.3)$$

It is obvious that convex hulls are also convex.

4.2.1 Examples of Convex Sets

Balls and ellipsoids are also examples of convex sets. A *Euclidean ball* (or just ball) of radius $c \in \mathbb{R}_{>0}$ and centered at $x_c \in \mathbb{R}^n$ is denoted as

$$\mathcal{B}^n(x_c, c) \triangleq \{x \in \mathbb{R}^n : |x - x_c| \leq c\} \quad (4.4)$$

A ball centered at the origin ($x_c = 0$) is simply written as $\mathcal{B}^n(c)$. Given a p.d. matrix $P > 0$, an *ellipsoid* centered at x_c is denoted by

$$\mathcal{E}^n(x_c, P) \triangleq \{x \in \mathbb{R}^n : (x - x_c)^T P (x - x_c) \leq c\} \quad (4.5)$$

for some positive scalar c . The lengths of semi-axes of \mathcal{E} are given by $\sqrt{\lambda_i}$, where λ_i are the eigenvalues of cP^{-1} and $i = 1, \dots, n$. The volume of \mathcal{E} is equal to $\frac{4}{3}\pi\sqrt{\det(P/c)^{-1}}$.

Another important class of convex sets is *polyhedra*. A polyhedron is defined as the solution set of a finite number of linear equalities and inequalities, such that

$$\mathcal{P}^n(A, b, C, d) \triangleq \{x : Ax \preceq b, Cx = d\} \quad (4.6)$$

where $x \in \mathbb{R}^n$, $b \in \mathbb{R}^m$, $d \in \mathbb{R}^p$ are vectors and $A \in \mathbb{R}^{m \times n}$, $C \in \mathbb{R}^{p \times n}$ are matrices representing m inequalities and p equalities. The symbol \preceq denotes *vector inequality* or *component-wise inequality* in \mathbb{R}^m . Convex hull is also a polyhedron, therefore both terms are used alternatively. A closed polyhedron is called a *polytope*. This distinction between polyhedra and polytopes is reversed by some authors, but we will adhere to our definition above [98]. The Minkowski sum of line segments in any dimension forms a type of polytope called *zonotope*.

4.2.2 Convex Optimization and LMIs

Minimization of a convex function subject to convex constraints is called convex optimization. Such problems have special mathematical structure which lends them to very efficient numerical algorithms, such as the interior-point and ellipsoid methods. Maximization problems are simply the minimization of the negative of the objective function above. Least squares, linear programming (LP), semidefinite programming (SDP) etc. are all convex optimization problems. The generic convex optimization problem is

Problem 4.2.1 (General Convex Optimization Problem) *Find the optimum x^0 that minimizes convex function $f(x) : \mathbb{R}^n \rightarrow \mathbb{R}_{\geq 0}$*

$$x^0 = \underset{x}{\operatorname{arg\,min}} f(x)$$

subject to convex set $X \subseteq \mathbb{R}^n$ and convex function $g_i(x), h_i(x) : \mathbb{R}^n \rightarrow \mathbb{R}$ constraints

$$x \in X \tag{4.7}$$

$$g_i(x) \preceq 0_m, \quad i = 1, \dots, m \quad h_i(x) = 0_p, \quad i = 1, \dots, p \tag{4.8}$$

Convex optimization problems of a very wide variety are efficiently solved using linear matrix inequalities (LMIs) [99], which deal with matrix variables. LMIs were first introduced by Lyapunov in his celebrated work on stability at the dawn

of the 20th century. An LMI has the form

$$A(x) \triangleq A_0 + \sum_{i=1}^m x_i A_i > B \quad (4.9)$$

where $x = \{x_1, \dots, x_m\} \in \mathbb{R}^m$ is a real valued vector variable, $A_i = A_i^T \in \mathbb{R}^{n \times n}$ are symmetric matrix variables and $B \in \mathbb{R}^{n \times n}$ is positive semi-definite (p.s.d.) matrix i.e. $B \geq 0$. Positive matrix means that all eigenvalues of the matrix are positive and p.s.d. means all eigenvalues are non-negative. LMI (4.9) is called a convex constraint on x . Nonlinear convex inequalities (such as those in Problem 4.2.1) can be converted to converted to LMI form using *Schur complements*.

Definition 4.2.1 (Schur Complement) *Given matrices $A \in \mathbb{R}^{n \times n}$, $B \in \mathbb{R}^{n \times m}$, $C \in \mathbb{R}^{m \times n}$, $D \in \mathbb{R}^{m \times m}$ and D is invertible. Then,*

$$F = \begin{bmatrix} A & B \\ C & D \end{bmatrix} > 0$$

is equivalent to

$$G = A - BD^{-1}C > 0$$

where $G \in \mathbb{R}^{m \times m}$ is the Schur complement of block D of matrix $F \in \mathbb{R}^{(n+m) \times (n+m)}$.

These concepts will now be used as tools for convex optimization of terminal region and control design.

4.3 Terminal Control Design and Maximization of Terminal Constraint Set

Points consisting of extreme or boundary values of constrained variables are called extreme or vertex points of the system. For example if $\tilde{x} \leq 2$, $u \leq 3$, then $(2, 3)$ is a vertex point of the system.

4.3.1 Re-parametrization of Constraints

We defined the terminal region as $X_f = \{\tilde{x} : \tilde{x}^T Q_f \tilde{x} \leq a\}$. Now, let us the parametrize the state and control constraints (3.3) as follows.

$$|z_v| \leq b_v, \quad \forall v = 1, \dots, \bar{v}, \quad (4.10)$$

where

$$z_v = c_v x + d_v u \quad (4.11)$$

and \bar{v} is the number of constraints. Therefore, the set

$$Z = \left\{ \begin{bmatrix} \tilde{x} \\ u \end{bmatrix}^T \in \mathbb{R}^{n+m} : |z_v| \leq b_v, b_v > 0, v = 1, \dots, \bar{v} \right\} \quad (4.12)$$

defines the set of allowable states and controls. In fact, we can scale these constraints by $b_v = 1$ for $v = 1, \dots, \bar{v}$ without loss of generality. Suppose, we can

have a polytope $M \subseteq Z$ defined by

$$M = \left\{ \begin{bmatrix} \tilde{x} & u \end{bmatrix}^T \in \mathbb{R}^{n+m} : \bar{c}_v \tilde{x} + \bar{d}_v u \leq 1, v = 1, \dots, \hat{v} \right\}. \quad (4.13)$$

In general $\bar{v} \neq \hat{v}$. Notice that in this setting, if there is an upper and lower bound on a variable, these bounds will appear as two separate bounds, i.e. $\bar{v} = 2^{(n+m)}$, where n and m is the size of state and control vector respectively. Suppose there are two states and one control variable with only upper and lower bounds, then $\bar{v} = 2^3 = 8$. When a linear terminal control $u = K_v \tilde{x} \in U$ for $\tilde{x} \in X_f$ is considered, the state and input constraints are defined in $\tilde{X}_f \subseteq \tilde{X}_{t+N_c}$, such that

$$\tilde{X}_f = \{ \tilde{x} \in \mathbb{R}^n : p_v \tilde{x} \leq 1, v = 1, \dots, \hat{v} \}, \quad (4.14)$$

where $p_v \triangleq (\bar{c}_v + \bar{d}_v)$. We will show that X_f is contained in \tilde{X}_f .

Lemma 4.3.1 (Technical) *Let the allowable set of states \tilde{X}_f be given as (4.14).*

The ellipsoid $X_f(a) = \{ \tilde{x} : \tilde{x}^T Q_f \tilde{x} \leq a \}$ is contained in the set \tilde{X}_f , such that $X_f \subseteq \tilde{X}_f \subseteq \tilde{X}_{t+N_c}$, iff

$$p_v (a Q_f^{-1}) p_v^T \leq 1, \quad \forall v = 1, \dots, \hat{v} \quad (4.15)$$

Proof. For $\tilde{x} \in X_f$, it holds that $\tilde{x}^T Q_f \tilde{x} \leq a$. Therefore,

$$\tilde{x} \tilde{x}^T Q_f \tilde{x} \tilde{x}^T \leq a \tilde{x} \tilde{x}^T \Rightarrow \tilde{x} \tilde{x}^T \leq a Q_f^{-1} \quad (4.16)$$

However, for $\hat{x} \in \tilde{X}_f$, condition (4.14) holds i.e.

$$p_v \hat{x} \leq 1 \Rightarrow p_v (\hat{x} \hat{x}^T) p_v^T \leq 1, \forall v = 1, \dots, \hat{v} \quad (4.17)$$

However, from (4.16), $\hat{x} \in X_f$ holds if and only if $p_v (aQ_f^{-1}) p_v^T \leq 1$ for $v = 1, \dots, \hat{v}$, and thus $X_f \subseteq \tilde{X}_f$. Also, since $\bar{d}_v \tilde{x}_v \geq K_v \tilde{x}_v \in U$, it is obvious that $\tilde{X}_f \subseteq \tilde{X}_{t+N_C}$.

Hence the result. ■

4.3.2 Terminal Control Design for Linearization around Vertex Points

It is clear that the most important aspect of determining the stability of the system (3.1) under RH control law (3.17) is the terminal inequality (3.42). To satisfy this, we propose an algorithm for maximizing the terminal region and designing terminal control which is based on global linearization of the nominal system. We will first state an important result based on (3.42) about stabilizing general linearization of the nominal system, before describing the main method.

Let $A_v \triangleq \left. \frac{\partial \tilde{f}}{\partial \tilde{x}} \right|_{\tilde{x}=\tilde{x}_v, u=u_v, \tilde{w}=\tilde{w}_v}$ and $B_v \triangleq \left. \frac{\partial \tilde{f}}{\partial u} \right|_{\tilde{x}=\tilde{x}_v, u=u_v, \tilde{w}=\tilde{w}_v}$ be linearization about an arbitrary point in the terminal set X_f .

Lemma 4.3.2 (Stabilization of Arbitrary Points in X_f) *Under Assumption 3.2.2, let the cost functional be quadratic, as defined in (3.58). Also, assume that there exists a p.d. matrix $\tilde{S} > 0$, such that $-q(\tilde{x}, \tilde{w}) + \psi(|\tilde{w}|) \leq \tilde{x}^T \tilde{S} \tilde{x}$, for $\tilde{x} \in X_f$ and allowable disturbances $\tilde{w} \in \tilde{W}_{t+l}$, $\forall l = N_C, \dots, N_P$. Then, there*

exists a terminal control law $u = K_v \tilde{x}$, for $\tilde{x} \in X_f$, and terminal constraint set X_f as defined in Claim 3.2.1, such that the closed loop general linearization $A_{CL_v} \triangleq A_v + B_v K_v$ of the nominal system (3.5) is locally stable. Let $\tilde{Q} \triangleq Q + K_v^T R K_v - \tilde{S}$. Stability of the point $\tilde{x} = \tilde{x}_v, u = u_v, \tilde{w} = \tilde{w}_v$ is ensured with desired rate of convergence hata, if the following Lyapunov LMI holds

$$A_{CL_v}^T Q_f A_{CL_v} - Q_f + \tilde{Q} \leq 0 \quad (4.18)$$

subject to:

$$Q + K_v^T R K_v - \tilde{S} > \hat{a} I_n, \quad (4.19)$$

$$k_f(\tilde{x}) = K_v \tilde{x} \in U \quad (4.20)$$

and

$$\tilde{x}^T Q_f \tilde{x} \leq a \quad (4.21)$$

Rate of convergence \hat{a} is obtained from (3.27).

Proof. We know the nominal system (3.5) with nominal disturbance model (3.10) is stable if condition (3.42) holds in X_f . Rewriting (3.42) in terms of quadratic cost (3.58)

$$h_f \left(\tilde{f}(\tilde{x}, k_f(\tilde{x})) \right) - h_f(\tilde{x}) \leq -\tilde{x}^T (Q + K_v^T R K_v) \tilde{x} - q(\tilde{x}, \tilde{w}) + \psi(|\tilde{w}|)$$

But, since $-q(\tilde{x}, \tilde{w}) + \psi(|\tilde{w}|) \leq \tilde{x}^T \tilde{S} \tilde{x}$, we can write

$$\tilde{f}(\tilde{x}, k_f(\tilde{x}))^T Q_f \tilde{f}(\tilde{x}, k_f(\tilde{x})) - \tilde{x}^T Q_f \tilde{x} \leq -\tilde{x}^T \left(Q + K_v^T R K_v - \tilde{S} \right) \tilde{x} \quad (4.22)$$

Therefore for the region $X_f = \{ \tilde{x} : \tilde{x}^T Q_f \tilde{x} \leq \hat{a} \}$ to be invariant, we need $Q + K_v^T R K_v - \tilde{S} > 0$. However, we need a minimum rate of convergence \hat{a} , such that

$$-\tilde{x}^T \left(Q + K_v^T R K_v - \tilde{S} \right) \tilde{x} \leq -\tilde{x}^T (\hat{a} I_n) \tilde{x}$$

which is equivalent to (4.19). Now, 'near' the point where the system is linearized, $\tilde{f}(\tilde{x}, k_f(\tilde{x})) \approx A_{CL_v} \tilde{x}$. Therefore, we can rewrite (4.22) as

$$\tilde{x}^T \left(A_{CL_v}^T Q_f A_{CL_v} - Q_f \right) \tilde{x} \leq -\tilde{x}^T \tilde{Q} \tilde{x},$$

which is equivalent to (4.18), for $\tilde{Q} \triangleq Q + K_v^T R K_v - \tilde{S}$. Finally, the constraint (4.20) ensures control constraints are obeyed, while also ensuring existence of an upper bound on h_f i.e. $\tilde{x}^T Q_f \tilde{x} \leq a$. ■

Remark 4.3.1 *The result above gives us some important guidelines.*

- I. *The requirement $-q(\tilde{x}, \tilde{w}) + \psi(|\tilde{w}|) \leq \tilde{x}^T \tilde{S} \tilde{x}$ and (4.19) provide guidelines on selection of weight $S \in \mathbb{R}^{n \times n}$ on the external input. In general $Q \gg S$.*
- II. *If one can find $X_f \in \tilde{X}_{t+N_P}$ by putting $Q + K_v^T R K_v - \tilde{S} > 0$, then there is no need to enforce the rate constraint of form (4.19), since, the invariance of X_f will ensure tightened constraints are not violated from $t + N_C$ to $t + N_P$.*

This will be the case in most circumstances, so as a guideline it is better solve without the rate condition, initially.

4.3.3 Terminal Region Optimization

Even though we hinted at the method to find $k_f = K_v \tilde{x}$, we did not mention how exactly to find Q_f , or indeed what are the points $\tilde{x}_v \in X_f$. One way to solve (4.18) is by solving the equality $A_{CL_v}^T Q_f A_{CL_v} - Q_f + \tilde{Q} = 0$ with linearization at $\tilde{x}_v = 0, u = 0$, by using efficient discrete algebraic Riccati equation (DARE) algorithms, but this does not fix a , and it does not mean that the region itself has been maximized. In this section we will present analytical and algorithmic results to maximize the terminal region, while simultaneously solving for the control law, without the results being based on linearizing the origin alone.

Suppose that for each point (\tilde{x}, u) , there is a matrix $F(x, u) \in \Omega(M)$, such that the LDI of the nonlinear system (3.5) with no disturbance, i.e. $\tilde{x} + t + 1 = \tilde{f}(\tilde{x}_t, u_t, 0)$ within the set $M \in \mathbb{R}^{n+m}$ defined by (4.13) is given as

$$\Omega(M) = \left\{ F \triangleq \begin{bmatrix} A & B \end{bmatrix} \triangleq \begin{bmatrix} \frac{\partial \tilde{f}}{\partial \tilde{x}} & \frac{\partial \tilde{f}}{\partial u} \end{bmatrix}, [\tilde{x} \quad u]^T \in M \right\} \quad (4.23)$$

The minimum convex polytope which contains the set $\Omega(M)$ is called a polytopic linear difference inclusion (PLDI), and is described by a list of its vertex (or extreme) matrices. The PLDI $\mathbf{Co}\Omega(M)$ is given by

$$\mathbf{Co}\Omega(M) \triangleq \mathbf{Co} \left\{ \begin{bmatrix} A_1 & B_1 \end{bmatrix}, \begin{bmatrix} A_2 & B_2 \end{bmatrix}, \dots, \begin{bmatrix} A_{\hat{v}} & B_{\hat{v}} \end{bmatrix} \right\}$$

$$= \left\{ F \in \mathbb{R}^{n \times (n+m)} : F = \sum_{v=1}^{v=\hat{v}} \phi_v \begin{bmatrix} A_v & B_v \end{bmatrix}, 0 < \phi_v < 1, \sum_{v=1}^{v=\hat{v}} \phi_v = 1 \right\} \quad (4.24)$$

for $v = 1, \dots, \hat{v}$. The nonlinear system $\tilde{x} + t + 1 = \tilde{f}(\tilde{x}_t, u_t, 0)$ can be described by the PLDI (4.3.3). Suppose that $K_v \in \mathbb{R}^{m \times n}$ is a time invariant feedback gain of the v^{th} vertex system, then the control law of the entire PLDI system (4.3.3) (and by implication the nonlinear system itself) can be given as the wighted average of controllers of the designed for for all \bar{v} vertices [100], i.e.

$$K = \sum_{v=1}^{v=\hat{v}} \phi_v K_v \quad (4.25)$$

Substitute (4.25) in (4.3.3), we obtain the closed loop system

$$\tilde{x}_{t+1} = A_{CL} \tilde{x}_t = \sum_{v=1}^{v=\hat{v}} \phi_v \begin{bmatrix} A_v & B_v K \end{bmatrix} = \sum_{i=1}^{i=\hat{v}} \left[\phi_i \sum_{j=1}^{j=\hat{v}} \begin{bmatrix} A_i & B_i \phi_j K_j \end{bmatrix} \right] \quad (4.26)$$

Based on the PLDI of nonlinear system (3.1), maximization of the terminal region subject to (4.18) and (4.15) can be formulated as a linear matrix inequality (LMI) problem. Very efficient methods for solving LMI based convex optimization problems exist [98], and hence this is a very attractive feature of the algorithm presented in this chapter. The convex OCP for maximizing the terminal constraint set is presented below.

Problem 4.3.1 (Maximization of Terminal Constraint Set) *The volume of terminal constraint set $X_f(a) = \{\tilde{x} : \tilde{x}^T Q_f \tilde{x} \leq a\}$ for $a > 0$, within set M defined in (4.13) with cost functional (3.58), is maximized for matrix variables*

$W_1 \triangleq Q_f^{-1} \in \mathbb{R}^{n \times n}$ and $W_2 \triangleq KQ_f^{-1} \in \mathbb{R}^{m \times n}$ by solving

$$\min_{W_1, W_2, a} \log \det (aW_1)^{-1} \quad (4.27)$$

subject to

$$W_1 = W_1^T > 0, \quad (4.28)$$

$$a > 0, \quad (4.29)$$

$$\begin{bmatrix} W_1 & (A_v W_1 + B_v W_2)^T & W_1 (Q - \tilde{S})^{1/2} & W_2^T R^{1/2} \\ * & W_1 & 0 & 0 \\ * & * & I & 0 \\ * & * & * & I \end{bmatrix} \geq 0 \quad (4.30)$$

for $v = 1, \dots, \bar{v}$.

$$\begin{bmatrix} 1/a & \bar{c}_v W_1 + \bar{d}_v W_2 \\ * & W_1 \end{bmatrix} \geq 0 \quad (4.31)$$

for $v = 1, \dots, \hat{v}$. Matrix \tilde{S} is defined in Lemma 4.3.2. Additionally, if it is required to converge with a given rate \hat{a} , then the OCP is subject to another condition

$$\begin{bmatrix} -\left(Q - \left(\tilde{S} + \hat{a}I_n\right)\right) & W_2^T \\ * & R^{-1} \end{bmatrix} \geq 0 \quad (4.32)$$

We will now prove the result below, that the arguments (W_1 , W_2 and a) which minimize (4.27) result in maximum volume of X_f , while being stabilizing and obeying state/control constraints (4.13).

Theorem 4.3.1 *Given the PLDI of the nonlinear system (3.5) is described by (4.3.3) within the set M defined in (4.13), and matrices $W_1 \in \mathbb{R}^{n \times n}$, $W_2 \in \mathbb{R}^{m \times n}$ and scalar $a \in \mathbb{R}_{\geq 0}$, which are the solution of the convex OCP 4.3.1, then the following postulates are true*

- i. $Q_f = W_1^{-1}$, such that the volume of ellipsoid $X_f(a) = \{\tilde{x} : \tilde{x}^T Q_f \tilde{x} \leq a\}$ is maximized.*
- ii. $X_f \in \tilde{X}_f \in \tilde{X}_{t+Nc}$*
- iii. Terminal control law $k_f(\tilde{x}) = K\tilde{x}$ for $\tilde{x} \in X_f$, such that*

$$K = W_2 W_1^{-1} \tag{4.33}$$

satisfies the control constraints $K\tilde{x} \in U$ and stabilizes the nonlinear system (3.5) with zero external input.

- iv. If required, the controller (4.33) makes the closed loop system converge with at least the desired rate \hat{a} .*

Proof. The proof will be carried out in four parts as there are as many postulates to prove in Theorem 4.3.1.

- i. Given a p.d. matrix $Q_f > 0$, an ellipsoid centered at origin is denoted by $X_f(a, Q_f) = \{\tilde{x} : \tilde{x}^T Q_f \tilde{x} \leq a\}$ for some positive scalar a . The volume of X_f is proportional to $(\det(a^{-1}Q_f))^{-\frac{1}{2}}$. Maximizing the volume is therefore the same as minimizing $\det(a^{-1}Q_f)$. But, $W_1 = Q_f^{-1}$, this is equivalent to*

minimizing $\det(aW_1)^{-1}$. However, the objective $\det(aW_1)^{-1}$ (which is to be minimized) is not convex, but monotonic transformations can make this OCP convex. One alternative is the logarithmic transform, leading instead to minimization of $-\log \det(aW_1)$, proving postulate (i).

- ii. From Lemma 4.3.1, $X_f \in \tilde{X}_f \in \tilde{X}_{t+Nc}$, when (4.15) holds, from which we have

$$p_v (aQ_f^{-1}) p_v^T \leq 1, \quad \forall v = 1, \dots, \hat{v},$$

$$(\bar{c}_v Q_f^{-1} + \bar{d}_v K) Q_f^{-1} Q_f Q_f^{-1} (\bar{c}_v + \bar{d}_v K) \leq 1/a,$$

$$1/a - (\bar{c}_v Q_f^{-1} + \bar{d}_v K Q_f^{-1}) Q_f (\bar{c}_v Q_f^{-1} + \bar{d}_v K Q_f^{-1}) \geq 0$$

Applying Schur's complement results in

$$\begin{bmatrix} 1/a & \bar{c}_v Q_f^{-1} + \bar{d}_v K Q_f^{-1} \\ * & Q_f^{-1} \end{bmatrix} \geq 0$$

Substituting $W_1 = Q_f^{-1}$ and (4.33) results in (4.31), which proves the postulate (ii).

- iii. For stability we require the closed loop system to satisfy the Lyapunov inequality (4.18), from which we have

$$Q_f \geq (A_v + B_v K)^T Q_f (A_v + B_v K) + Q + K^T R K - \tilde{S}$$

Post- and pre-multiply by $W_1 = Q_f^{-1}$ and substitute (4.18) in the expression above, we obtain

$$W_1 \geq (A_v W_1 + B_v W_2)^T W_1^{-1} (A_v W_1 + B_v W_2) + W_1 (Q - \tilde{S}) W_1 + W_2 R W_2$$

Applying Schur complement,

$$\begin{bmatrix} W_1 - W_1 (Q - \tilde{S}) W_1 - W_2 R W_2 & (A_v W_1 + B_v W_2)^T \\ * & W_1 \end{bmatrix} \geq 0,$$

$$\begin{bmatrix} W_1 & (A_v W_1 + B_v W_2)^T \\ * & W_1 \end{bmatrix} - \begin{bmatrix} W_1 (Q - \tilde{S}) W_1 + W_2 R W_2 & 0 \\ * & 0 \end{bmatrix} \geq 0$$

The last inequality can be written as

$$\begin{bmatrix} W_1 & (A_v W_1 + B_v W_2)^T \\ * & W_1 \end{bmatrix} - \begin{bmatrix} W_1 (Q - \tilde{S})^{\frac{1}{2}} & W_2 R^{\frac{1}{2}} \\ 0 & 0 \end{bmatrix} \begin{bmatrix} I & 0 \\ 0 & I \end{bmatrix}^{-1} \begin{bmatrix} W_1 (Q - \tilde{S})^{\frac{1}{2}} & 0 \\ W_2 R^{\frac{1}{2}} & 0 \end{bmatrix}$$

Applying Schur complement once again results in (4.30), which proves postulate (iii).

- iv. Applying Schur complement to (4.19) directly results in (4.32), which proves postulate (iv).

By Relaxation Theorem [99], it is clear that proving these properties at vertex

points prove them for the whole PLDI (4.3.3) and hence for the nonlinear system (3.5) with zero external input as well. █

4.3.4 Description of Terminal Region Optimization Algorithms

We are now in a position to gather all of our results in a concise algorithm. Efficient algorithms exist for solving the volume maximization convex problem. This

Algorithm 3 Optimizing Terminal Region and Control

- 1: **Given** nominal model $\tilde{f}(\tilde{x}, u, 0)$ and cost weights Q , R and S .
 - 2: **Select** $\tilde{S} \in \mathbb{R}^{n \times n}$, such that $-q(\tilde{x}, \tilde{w}) + \psi(\tilde{w}) \leq \tilde{x}^T \tilde{S} \tilde{x}$
 - 3: **Get** initial guess values of Q_f as Q_f^∞ and K as K^∞ by Algorithm 4
 - 4: **procedure** CONVEX OPTIMIZATION
 - 5: **Solve** convex OCP 4.3.1 subject to (4.28)-(4.31).
 - 6: **if** $X_f \subset \tilde{X}_{t+Np}$ **then**
 - 7: Go to 11
 - 8: **else**
 - 9: **Solve** convex OCP (4.3.1) subject to (4.28)-(4.32).
 - 10: **end if**
 - 11: **end procedure** End algorithm; accept optimal values of Q_f , K and a .
-

is the basic algorithm, for which we did not mention how the optimization routine is initialized. Most modern software packages (see the examples in the next section) select the initial iterate internally. For example, the SDPT3 semidefinite programming package [101] algorithms can start with an infeasible starting point, as the algorithms try to achieve feasibility and optimality of its iterates simultaneously. However, the performance of these algorithms is quite sensitive to the choice of the initial iterate. Reasonable initial guesses is often crucial, especially in non-convex optimization. It is advisable to choose an initial iterate that at

least has the same order of magnitude as the optimal solution [102].

Therefore, we have developed a methodology to provide a reasonably good initial guess of optimization variables to warm-start Algorithm 3. It is based on the fact that (4.30) can be approximated as the discrete version of linear quadratic regulator (DLQR) [103], when $a = 1$. Therefore, we solve the following discrete-time algebraic Riccati equations (DARE) at each vertex point:

$$Q_{f_v}^\infty = (Q - \tilde{S}) + A_v^T \left(Q_{f_v}^\infty + Q_{f_v}^\infty B_v (R + B_v^T Q_{f_v}^\infty B_v)^{-1} B_v^T Q_{f_v}^\infty \right) A_v, \quad (4.34)$$

where $Q_{f_v}^\infty$ is the solution of the DARE above. The control gain computed from (4.34) is given as

$$K_v^\infty = (R + B_v^T Q_{f_v}^\infty B_v)^{-1} B_v^T Q_{f_v}^\infty A_v \quad (4.35)$$

Obviously, we will have \bar{v} values of $Q_{f_v}^\infty$ and K_v^∞ . Therefore, we will solve another optimization problem that finds the maximum volume ellipsoid which is confined in the intersection of all the \bar{v} vertex ellipsoids. This will serve as the initial guess for $W_1^0 = (Q_{f_v}^\infty)^{-1}$. It is important to note that the initial guess is based on solution of unconstrained algebraic Riccati equations (4.34). Therefore, we formulate the following convex OCP by exploiting the S-procedure [104].

Problem 4.3.2 [*Warm-Start for Algorithm 3*] *Given \bar{v} vertex ellipsoids $\mathcal{E}_v^n(Q_{f_v}^\infty) \triangleq \{\tilde{x} \in \mathbb{R}^n : \tilde{x}^T Q_{f_v}^\infty \tilde{x} \leq 1\}$ which are solutions of (4.34), the maximum volume ellipsoid in the intersection of all \mathcal{E}_v^n is obtained by solving the following*

convex OCP for some Lagrangian variables t_v

$$\min_{\tilde{W}_\infty} -\log \det \tilde{W}^\infty \quad (4.36)$$

subject to

$$\tilde{W}^\infty > 0 \quad (4.37)$$

$$1 \geq t_v \geq 0 \quad (4.38)$$

$$t_v \tilde{W}_v^\infty - \tilde{W}^\infty \geq 0 \quad (4.39)$$

for v, \dots, \bar{v} . Here $\tilde{W}^\infty \triangleq (Q_f^\infty)^{-1}$ and $\tilde{W}_v^\infty \triangleq (Q_{f_v}^\infty)^{-1}$.

The warm-start procedure is listed in Algorithm 4

Algorithm 4 Warm-Start Procedure for Algorithm 3

- 1: **procedure** CONVEX OPTIMIZATION
 - 2: **Solve** Riccati equations (4.34) for vertex values of $Q_{f_v}^\infty$
 - 3: **Solve** convex OCP 4.3.2 to obtain Q_f^∞ .
 - 4: **Claculate** K^∞ by solving (4.35) for Q_f^∞ at A_0 and B_0 , i.e. linearization of origin
 - 5: **end procedure** End algorithm and pass Q_f^∞ and K^∞ to Algorithm 3
-

4.3.5 Illustrative Example on Terminal Region Optimization

We will now proceed to continue the example of nonlinear oscillator introduced in the previous chapter. In this work, we used the semi-definite programming packages LogDetPPA [105], SDPT3-4.0 [101] and PENBMI [106], running on the optimization toolbox YALMIP [107].

Table 4.1: Parameters of Constraint Set for Terminal Optimization

| v | $\tilde{x}_{(1)}$ | $\tilde{x}_{(2)}$ | u | \bar{c}_v | \bar{d}_v |
|-----|-------------------|-------------------|-----|-----------------|-------------|
| 1 | min | - | - | $[-8.89 \ 0]$ | 0 |
| 2 | max | - | - | $[\ 8.89 \ 0]$ | 0 |
| 3 | - | min | - | $[0 \ -8.89]$ | 0 |
| 4 | - | max | - | $[0 \ 8.89]$ | 0 |
| 5 | - | - | min | $[0 \ 0]$ | -0.5 |
| 6 | - | - | max | $[0 \ 0]$ | 0.5 |

Example 4.3.1 (Nonlinear Oscillator: Part II (Optimizing X_f)) Recall

Example 3.3.2, where we illustrated the constraint tightening Algorithm 2. To proceed, we need to first specify the set $M \subset Z$ within which the OCP 4.3.1 is feasible. This can be checked by starting from Z and making the constraints tighter progressively till the problem becomes feasible. Therefore, we take the set $M \subset Z$ as $2 \leq u \leq 2$, $-0.1125 \leq \tilde{x}_{(1)} \leq 0.1125$ and $-0.1125 \leq \tilde{x}_{(2)} \leq 0.1125$.

Therefore, the values of parameters of the normalized set

$$M = \left\{ \left[\begin{array}{ccc} \tilde{x}_{(1)} & \tilde{x}_{(2)} & u \end{array} \right]^T \in \mathbb{R}^{n+m} : \bar{c}_v \tilde{x} + \bar{d}_v u \leq 1, v = 1, \dots, 6 \right\}$$

are given in Table 4.1. The general linearization of the system is

$$\begin{bmatrix} \tilde{x}_{(1)_{t+1}} \\ \tilde{x}_{(2)_{t+1}} \end{bmatrix} = \begin{bmatrix} 1 + 0.025u_t & -0.05 \\ 0.05 & 1 - 0.1u_t \end{bmatrix} \begin{bmatrix} \tilde{x}_{(1)_t} \\ \tilde{x}_{(2)_t} \end{bmatrix} + 0.025 \begin{bmatrix} 1 + \tilde{x}_{(1)_t} \\ 1 - 4\tilde{x}_{(2)_t} \end{bmatrix} u_t \quad (4.40)$$

There are $\bar{v} = 2^3 = 8$ vertex systems, which are listed in Table 4.2. Since we have to choose \tilde{S} such that $-q(\tilde{x}, \tilde{w}) > +\psi(|\tilde{w}|) \leq \tilde{x}^T \tilde{S} \tilde{x}$, let us choose $\tilde{S} = 10 \cdot S = 10^{-2} I_2$. To warm start the algorithm, we solve DAREs (4.34)-(4.35) at

Table 4.2: Vertex Matrices of Nonlinear Oscillator System

| v | $\tilde{x}_{(1)}$ | $\tilde{x}_{(2)}$ | u | A_v | | B_v | |
|-----|-------------------|-------------------|-----|-------|-------|--------|--|
| 1 | min | min | min | 0.95 | -0.05 | 0.0222 | |
| | | | | 0.05 | 1.20 | 0.0294 | |
| 2 | max | min | min | 0.95 | -0.05 | 0.0278 | |
| | | | | 0.05 | 1.20 | 0.0294 | |
| 3 | min | max | min | 0.95 | -0.05 | 0.0222 | |
| | | | | 0.05 | 1.20 | 0.0206 | |
| 4 | max | max | min | 1.05 | -0.05 | 0.0278 | |
| | | | | 0.05 | 0.80 | 0.0206 | |
| 5 | min | min | max | 1.05 | -0.05 | 0.0222 | |
| | | | | 0.05 | 0.80 | 0.0294 | |
| 6 | max | min | max | 1.05 | -0.05 | 0.0278 | |
| | | | | 0.05 | 0.80 | 0.0294 | |
| 7 | min | max | max | 1.05 | -0.05 | 0.0222 | |
| | | | | 0.05 | 0.80 | 0.0206 | |
| 8 | max | max | max | 1.05 | -0.05 | 0.0278 | |
| | | | | 0.05 | 0.80 | 0.0206 | |

each vertex system listed in Table 4.2. Numerical values of the vertex solutions of DAREs (4.34) are listed in Table . The initial guess about terminal region Q_f is found by solving OCP 4.3.2. The procedure is illustrated in Figure 4.2. Numerical value of the initial guess Q_f^∞ is

$$Q_f^\infty = \begin{bmatrix} 342.04 & 69.16 \\ 69.16 & 670.08 \end{bmatrix} \quad (4.41)$$

The linearization of origin $(0, 0)$ is obtained from (4.40) as follows

$$A_0 = \begin{bmatrix} 1 & -0.05 \\ 0.05 & 1 \end{bmatrix} \begin{bmatrix} \tilde{x}_{(1)_t} \\ \tilde{x}_{(2)_t} \end{bmatrix}, \quad B_0 = \begin{bmatrix} 0.025 \\ 0.025 \end{bmatrix} u_t$$

Initial iterate of the the control gain K is found by solving (4.35) at A_0 and B_0 ,

Table 4.3: Solutions of Riccati Equations at Vertex Points

| v | $Q_{f_v}^\infty$ | | $(K_v^\infty)^T$ | $\text{eig}(A_v + B_v K_v^\infty)$ | $\text{eig}(A_v + B_v K)$ |
|-----|------------------|--------|------------------|------------------------------------|---------------------------|
| 1 | 16.26 | 73.79 | -2.13 | (0.96, 0.84) | (0.98, -0.20) |
| | 73.79 | 362.54 | -10.31 | | |
| 2 | 15.16 | 68.83 | -2.06 | (0.96, 0.84) | (0.99, -0.27) |
| | 68.83 | 340.15 | -9.99 | | |
| 3 | 28.86 | 134.63 | -2.85 | (0.96, 0.84) | (0.99, 0.12) |
| | 134.63 | 656.40 | -13.88 | | |
| 4 | 26.32 | 122.85 | -2.75 | (0.96, 0.84) | 0.99, 0.05 |
| | 122.85 | 601.76 | -13.29 | | |
| 5 | 314.34 | -65.66 | -4.85 | (0.96, 0.81) | 0.99, -0.50 |
| | -65.66 | 13.98 | 1.01 | | |
| 6 | 172.88 | -36.07 | -3.60 | (0.96, 0.81) | (0.98, -0.55) |
| | -36.07 | 7.80 | 0.75 | | |
| 7 | 253.54 | -53.91 | -4.36 | (0.96, 0.81) | (0.97, -0.15) |
| | -53.91 | 11.31 | 0.91 | | |
| 8 | 147.21 | -30.70 | -3.33 | (0.96, 0.81) | (0.95, -0.20) |
| | -30.70 | 6.67 | 0.69 | | |

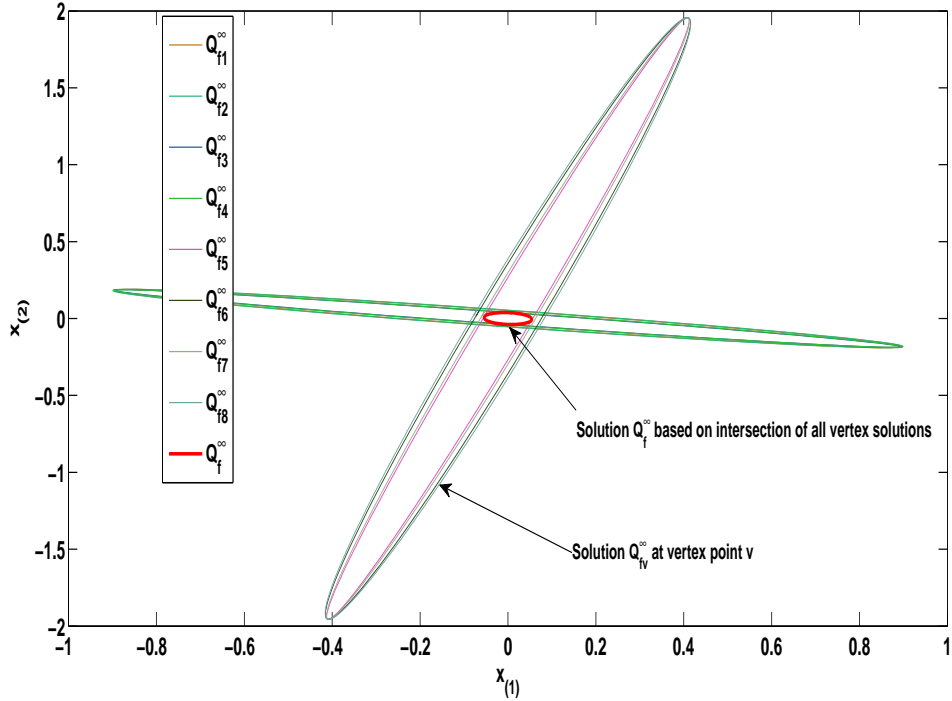


Figure 4.2: Warm Start Ellipsoids used in Algorithm 4 applied to Example 4.3.1

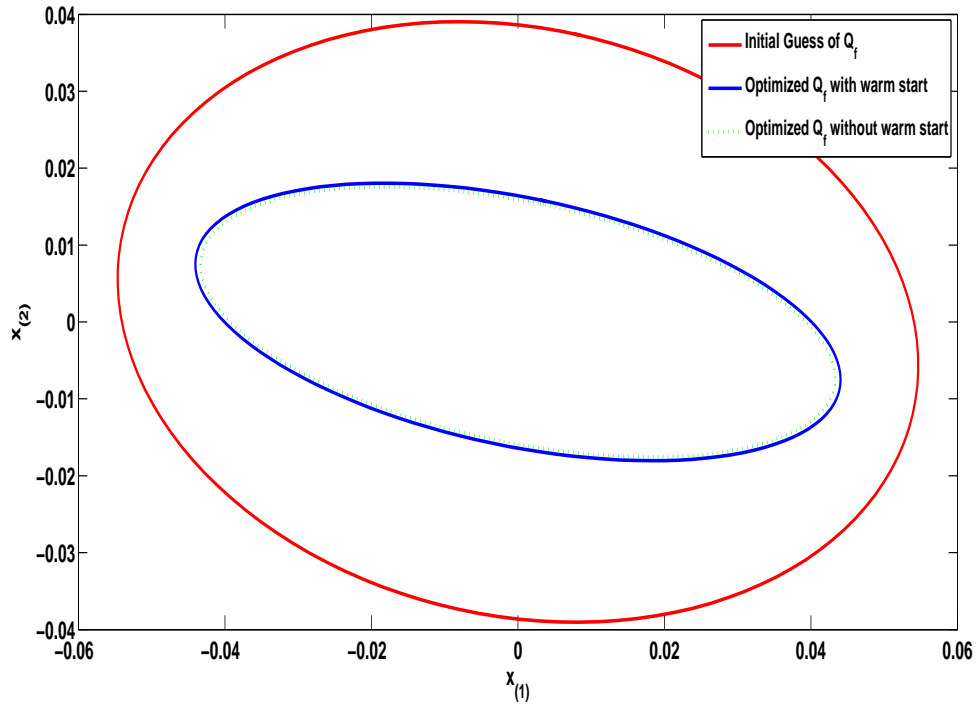


Figure 4.3: Optimized terminal region using Algorithm 3 applied to Example 4.3.1. Results both with and without warm starting with Algorithm 4 are shown

and the result is

$$K^\infty = (R + B_0^T Q_f^\infty B_0)^{-1} B_0^T Q_f^\infty A_0 = \begin{bmatrix} -6.52 & -10.45 \end{bmatrix}$$

Now, using these initial iterates, Algorithm 3 can be used to solve for optimum parameters of the terminal region. We have taken $a = 1$, though it can take other non-negative values as well. The optimized results are given below and illustrated in Fig. 4.3.

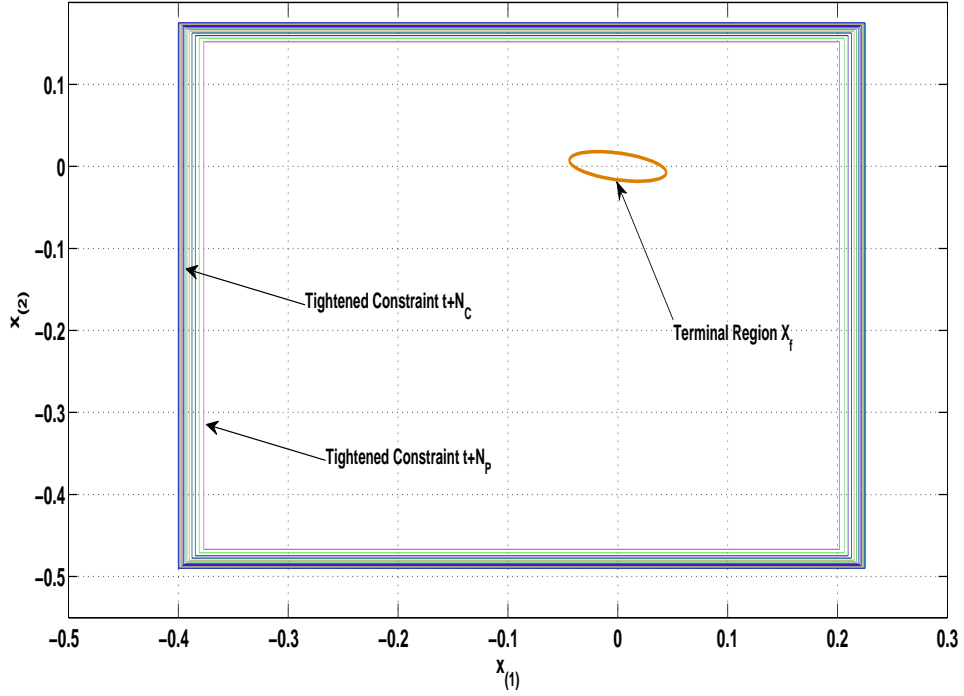


Figure 4.4: Terminal region X_f optimized with Algorithms 3-4 for Example 4.3.1. Tightened constraints from Algorithm 2 are also shown

$$Q_f = \begin{bmatrix} 6222.7 & 631.1 \\ 631.1 & 3709.7 \end{bmatrix}, \quad K = \begin{bmatrix} -11.66 & -36.33 \end{bmatrix} \quad (4.42)$$

As one can see from Fig. 4.3, there is a slight improvement by using warm starting, which results in a larger terminal region. Also, it can be observed from the last column of Table 4.3, the optimized value of terminal control gain K is stabilizing for every point of the terminal region. For perspective, the terminal region $X_f = \tilde{x}^T Q_f \tilde{x} \leq 1$ is shown in the allowable state space in Fig. 4.4.

4.4 Determination of 1-Step Controllable Set to Terminal Constraint Set

Recall that the maximum allowable uncertainty is bounded by the minimum size of the 1-step controllable set to X_f , denoted by $\mathcal{C}_1(X_f)$ as given by (3.36). In particular, this bound (3.36) on uncertainty was shown to ensure recursive feasibility. Therefore, it is imperative to determine the minimum size of $\mathcal{C}_1(X_f)$, defined below

Definition 4.4.1 *The minimum size of 1-step controllability set to terminal set X_f is defined as*

$$\bar{d} \triangleq \text{dist}(\tilde{X}_{t+N_c} \setminus \mathcal{C}_1(X_f, \tilde{X}_{t+N_c}), X_f) \quad (4.43)$$

The relationship between \tilde{X}_{t+N_c} , $\mathcal{C}_1(X_f)$ and \bar{d} is illustrated in Fig. 4.5. It is clear that to find \bar{d} , we must know the topology of $\mathcal{C}_1(X_f)$. There are various techniques for estimating one-step controllability to given sets. A conservative set-based estimation of $\mathcal{C}_1(X_f)$ by iteratively computing convex inner approximations of $\mathcal{C}_1(X_f)$ is presented in [95]. However, the effect of disturbance on size of $\mathcal{C}_1(\cdot)$ is not considered. Another set-based approach [108] is based on Minkowski difference between a collection of polytopes for calculating one-step robust with polytopic additive uncertainties. A similar approach solved as a mixed-integer feasibility program is presented in [78]. Set based approaches are however conservative, providing only inner approximations. We propose an explicit method based on min-max optimization to give better estimates of $\mathcal{C}_1(X_f)$.

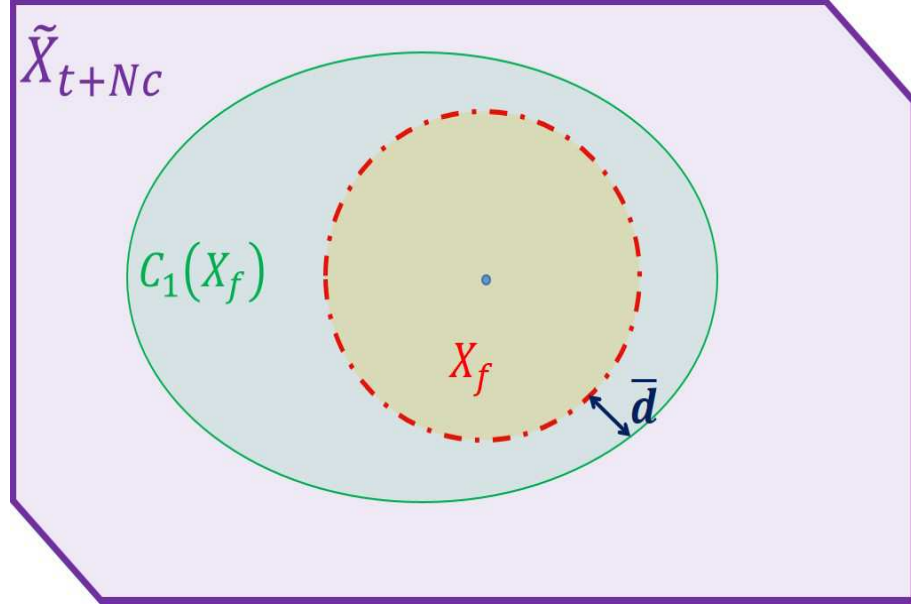


Figure 4.5: Relationship between tightened constraint \tilde{X}_{t+Nc} , terminal set X_f and minimum size \bar{d} of 1-step controllable set $\mathcal{C}_1(X_f)$ to X_f .

Let the boundary of X_f and $\mathcal{C}_1(X_f)$ be denoted by $\partial(X_f)$ and $x_c^i \in \partial(\mathcal{C}_1(X_f))$

respectively. We propose the following algorithm for this purpose.

Algorithm 5 Determining One Step Controllable Set to X_f

- 1: **Divide** the boundary of terminal set $\partial(X_f)$ into \bar{N} steps.
 - 2: **Solve** OCP 4.4.1 to find points $\tilde{x}_c^i \in \partial(\mathcal{C}_1(X_f))$ for $i = 1, \dots, \bar{N}$.
 - 3: **Calculate** minimum size of $\mathcal{C}_1(X_f)$ as $\bar{d} = \min(|\tilde{x}_{c_1}^1 - \tilde{x}_f^1|, \dots, |\tilde{x}_{c_1}^{\bar{N}} - \tilde{x}_f^{\bar{N}}|)$ for $\tilde{x}_f^i \in \partial(X_f)$ and $i = 1, \dots, \bar{N}$.
-

Problem 4.4.1 (Min-Max Optimization of One-Step Robust Controllability Set $\mathcal{C}_1(X_f)$)

Given the target set X_f , tightened constraints defined in (3.29)-(3.30) and nominal constraints (3.3), let the boundary of X_f be discretized appropriately into \bar{N} point $\tilde{x}_f^i \in \partial(X_f)$ for $i = 1, \dots, \bar{N}$. Then, the one-step robust controllability set $\mathcal{C}_1(X_f)$ is obtained by solving the following \bar{N} min-max OCPs

$$\tilde{x}_{c_1}^i = \max_w \left(\min_u \left(-\log \left(\tilde{x}_{c_1}^i Q_f \tilde{x}_{c_1}^i \right) \right) \right) \quad (4.44)$$

for $i = 1, \dots, \bar{N}$, subject to

$$\tilde{x}_f^i = \tilde{f}(\tilde{x}_{c_1}^i, u, \tilde{w}) \quad (4.45)$$

$$1 - \tilde{x}_{c_1}^i Q_f \tilde{x}_{c_1}^i \leq 0 \quad (4.46)$$

$$\tilde{x}_{c_1}^i \in \tilde{X}_{N_{c-1}}, \quad u \in U, \quad \tilde{w} \in \tilde{W}_{N_{c-1}} \quad (4.47)$$

The boundary of $\mathcal{C}_1(X_f)$ is given as $\partial(\mathcal{C}_1(X_f)) = \{\tilde{x}_{c_1}^i, \forall i = 1, \dots, \bar{N}\}$.

Notice that even though cost functional (4.44) is convex, the overall OCP is not convex due to presence of nonlinear constraints (4.45)-(4.46). Due to non-convexity, it is important to have a good initial guess. This can be easily accomplished by choosing initial guess in the sector of state space where the half space containing x_f^i lies. This will be further illustrated in Example 4.4.1. Cost functional (4.44) is the convex form of $(\tilde{x}_{c_1}^i Q_f \tilde{x}_{c_1}^i)^{-1}$, minimizing which maximizes the distance from $X_f = \{\tilde{x} : \tilde{x} Q_f \tilde{x} \leq 1\}$. Constraint (4.45) ensures that $\tilde{x}_{c_1}^i$ is the point from which the point $\tilde{x}_f^i \in \partial(X_f)$ can be reached in exactly one step. Constraint (4.46) ensures that is outside X_f . Finally, the cost is (4.44) is minimized with control u , but maximized with respect to the disturbance \tilde{w} to account for the worst case of disturbance input.

Algorithm 5 is computationally expensive, but these are optimizations carried out offline, therefore computational time is not very important. We will now apply the algorithm to an the nonlinear oscillator example from previous sections.

Example 4.4.1 (Nonlinear Oscillator: Part III (Determining $\mathcal{C}_1(X_f)$))

We optimized the terminal constraint region X_f in Example 4.3.1. In this example

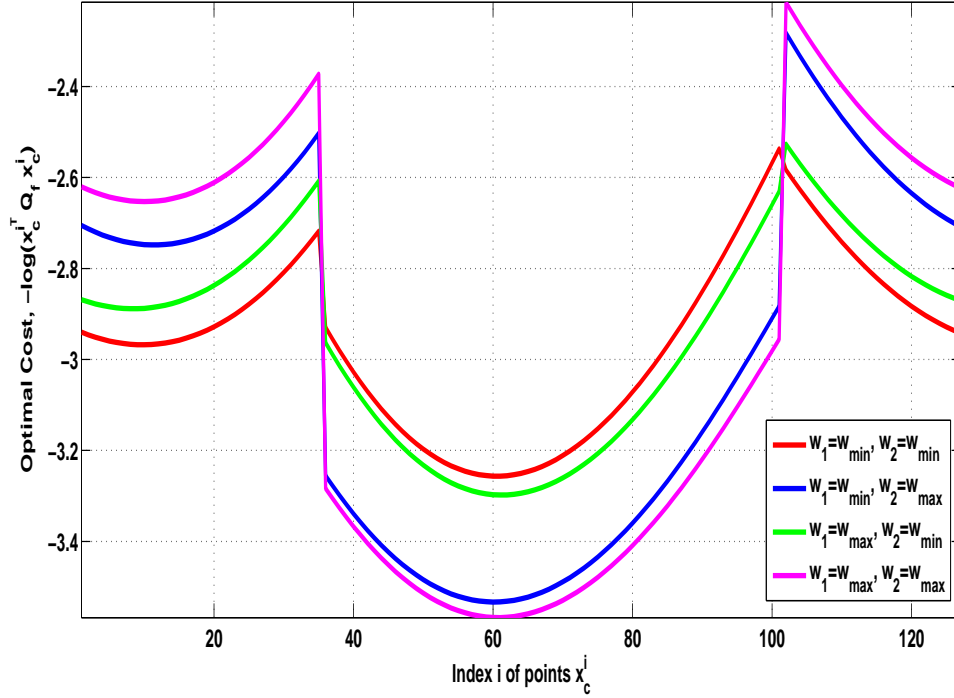


Figure 4.6: Optimal Cost from (4.44) for $i = 1, \dots, \bar{N}$ with various disturbance levels using Algorithm 5 for Example 4.4.1. Notice the cost does not change monotonously with disturbance level.

we will apply Algorithm 5 to determined the one-step robust controllability set to terminal set X_f . We begin by noting from Example 3.3.2 that ($N_C = 5$)

$$\tilde{x}_{c_1}^i \in \tilde{X}_4 = \left\{ \left[\begin{array}{cc} -0.398 & -0.488 \end{array} \right]^T \leq \tilde{x}_{c_1}^i \leq \left[\begin{array}{cc} 0.223 & 0.173 \end{array} \right]^T \right\}$$

$$u \in U = \{-2 \leq u \leq 2\}$$

$$\tilde{w} \in \tilde{W}_{N_C-1} = \{-5 \times 10^{-3} \leq \tilde{w}_{1,2} \leq 5 \times 10^{-3}\} \quad (4.48)$$

for $i = 1, \dots, \bar{N}$. The metric $\tilde{x}_c^i{}^T Q_f \tilde{x}_c^i$ from (4.44) for $i = 1, \dots, \bar{N}$ with various disturbance levels is shown in Fig. 4.6. Applying these values to the non-linear oscillator (3.62), we obtain the boundary of one-step controllability set

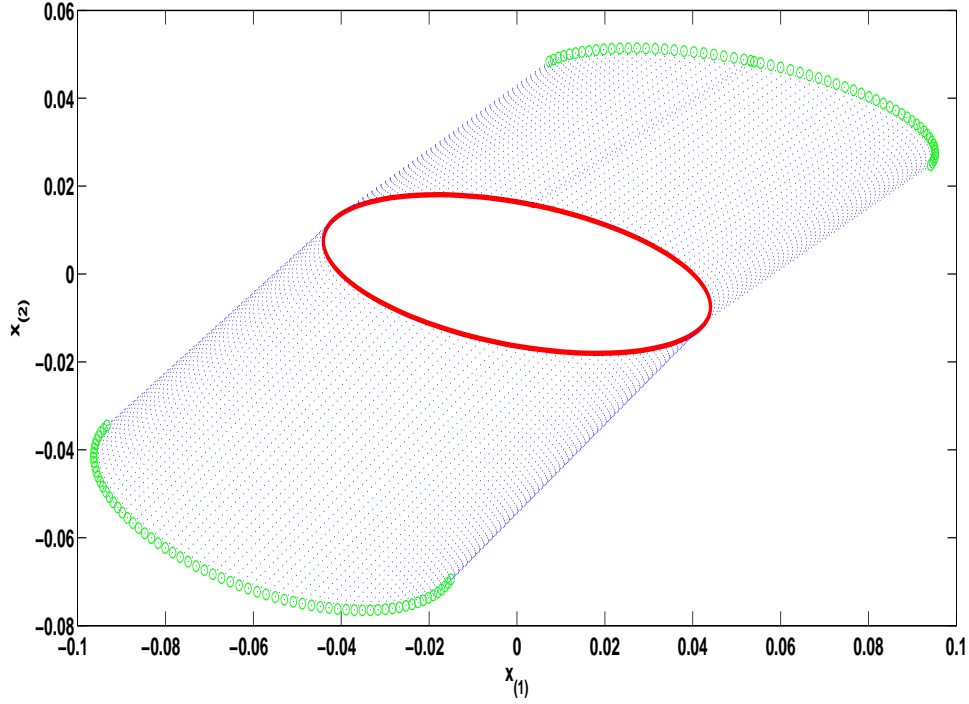


Figure 4.7: Boundary points of one-step controllability set calculated using Algorithm 5 for Example 4.4.1. The target set X_f is shown in solid red, the boundary points $\tilde{x}_c \in \partial(\mathcal{C}_1(X_f))$ in green circles, and the one-step trajectories (starting from green circles) in dotted blue lines.

$\tilde{x}_c^i \in \partial(\mathcal{C}_1(X_f))$ for $i = 1, \dots, \bar{N}$ shown in Fig. 4.7. Initial guess for \tilde{x}_c^i is chosen according the direction of the vector normal to the ellipsoid surface at point $\tilde{x}_f \delta X_f$. We are now in a position to calculate the minimum size of $\mathcal{C}_1(X_f)$ as follows

$$\bar{d} = \min_i (|\tilde{x}_{c_1}^i - \tilde{x}_f^i|), \forall i = 1, \dots, \bar{N} = 6.18 \times 10^{-2} \quad (4.49)$$

Calculating the inequality (3.36) for recursive feasibility

$$\begin{pmatrix} L_{fx}^{Nc-1} ((L_{fx} + 1) \bar{\xi}_x + L_{fw} \bar{\xi}_w + \bar{e}_x) + \\ L_{fw} \frac{L_{fx}^{Nc-1} - L_{gw}^{Nc-1}}{L_{fx} - L_{gw}} ((L_{gw} + 1) \bar{\xi}_w + \bar{e}_w) \end{pmatrix} =$$

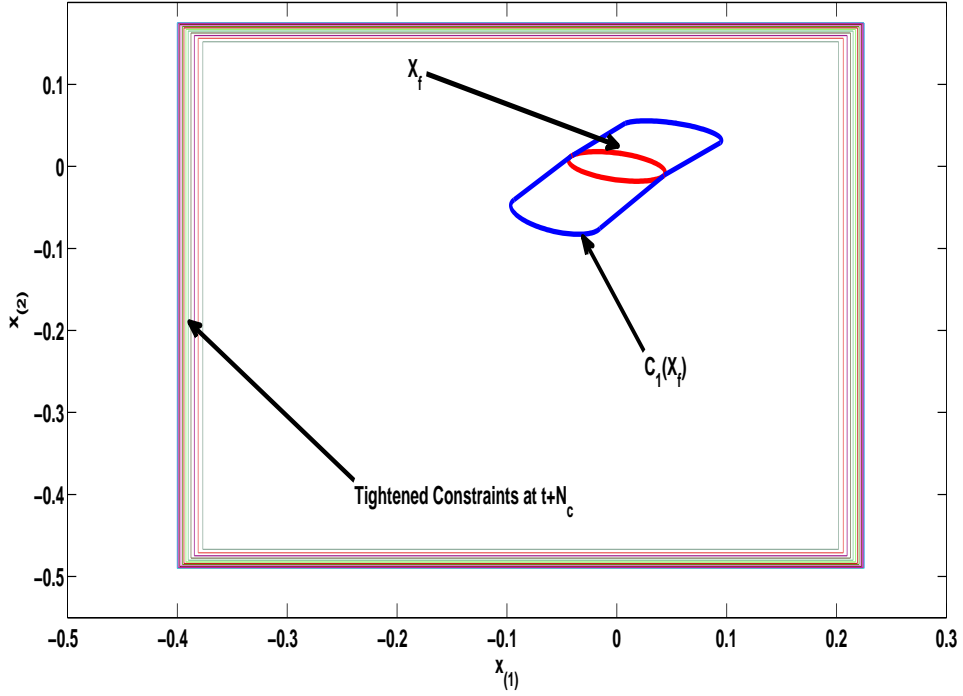


Figure 4.8: One-step controllability set $\mathcal{C}_1(X_f)$ calculated using Algorithm 5 for Example 4.4.1. Also shown are target set X_f and tightened constraints, for perspective.

$$\begin{aligned} & \left(\begin{array}{l} 1.189^4 (2.189 \times 10^{-5} + 1.414 \times 10^{-5} + 6.325 \times 10^{-4}) + \\ 1.414 \frac{1.189^4 - (1.01 \times 10^{-3})^4}{1.189 - 1.01 \times 10^{-3}} (2.01 \times 10^{-8} + 5 \times 10^{-8}) \end{array} \right) \\ & = 1.34 \times 10^{-3} \leq \bar{d} = 6.18 \times 10^{-2} \end{aligned}$$

Therefore, it is clear that recursive feasibility is ensured. The one-step set $\mathcal{C}_1(X_f)$ is shown in Fig. 4.8 along with X_f and constraints to get a perspective on its size.

4.5 Determination of Robust Output Feasible

Set X_{MPC}

In the last section we applied Algorithm 5 to find the one-step robust controllability set $\mathcal{C}_1(X_f)$. This proved useful in determining recursive feasibility of the nonlinear MPC scheme. In this section, we will extend Algorithm 5 to solve for the entire feasibility region of for the MPC algorithm. This will form the final ingredient of the NMPC Algorithm developed in Chapter 3. For development in this chapter, we will state a few postulates, sometimes without proof as they are straightforward, to help in developing the main algorithm of this section.

Postulate 4.5.1 *Robust one-step controllability set $\mathcal{C}(X_f)$ contains the target set X_f , i.e. $X_f \subset \mathcal{C}(X_f)$.*

Proof. According to Theorem 7 of [109], X_f is RPI, if and only if $X_f \subset \mathcal{C}(X_f)$, and since we have proven in Theorem 4.3.1 that X_f is RPI, therefore Postulate 4.5.1 follows. █

Postulate 4.5.2 *Robust one-step controllability set $\mathcal{C}(X_f)$ to the terminal set X_f is contained in the one-step controllability set of robust output feasible set X_{MPC} , i.e.*

$$\mathcal{C}_1(X_f) \subseteq \mathcal{C}_1(X_{MPC}^-) \tag{4.50}$$

Proof. Recall from Definition 2.4.9 that one-step controllable sets possess monotonicity, i.e. $\Omega \subseteq \bar{\Omega} \implies \mathcal{C}_1(\Omega) \subseteq \mathcal{C}_1(\bar{\Omega})$. Now, we know that $X_f \subset X_{MPC}$, and hence $\mathcal{C}_1(X_f) \subseteq \mathcal{C}_1(X_{MPC}^-)$. █

Postulate 4.5.3 *Robust one-step controllability set $\mathcal{C}(X_f)$ to the terminal set X_f can be written as a finite union of polyhedra.*

Proof. This holds because X_f is convex (RPI) $X_f \subset \mathcal{C}(X_f)$ according to Postulate 4.5.1. Therefore $\mathcal{C}(X_f)$ is compact and can be divided into intersecting polyhedra. █

Postulate 4.5.4 *The one-step controllable set operator can be used recursively to define l -step controllable set $\mathcal{C}_l(X_f)$ as follows (for $l \geq 2$).*

$$\mathcal{C}_l(X_f) = \mathcal{C}_1(\mathcal{C}_{l-1}(X_f)) \quad (4.51)$$

This follows from dynamic programming like arguments for overlapping subproblems.

Postulate 4.5.5 *The boundary of target set, i.e. $\partial(X_f)$ is included in the one step controllable set $\mathcal{C}_1(X_f)$.*

$$\partial(X_f) \subset \mathcal{C}_1(X_f) \quad (4.52)$$

This result is obvious, since we require the states in $\mathcal{C}_1(X_f)$ to at least reach X_f in one step. Based on these postulates we can state our main result.

Theorem 4.5.1 *Given the terminal set X_f , tightened constraints $\tilde{x} \in \tilde{X}_{t+l}$, $\tilde{w} \in \tilde{W}_{t+l}$ for $l = 1, \dots, N_C$ and control constraint $u \in U$, the robust feasibility set is obtained by N_C applications of the one-step controllable set operator $\mathcal{C}_\infty(\cdot)$ by*

recursively solving OCP 4.4.1, such that

$$X_{MPC} = \bigcup_{l=2}^{l=N_c} \mathcal{C}_1(\mathcal{C}_{l-1}(X_f)) \cup \mathcal{C}_1(X_f) \cup X_f \quad (4.53)$$

Proof. From Postulate 4.5.4, we have that

$$\mathcal{C}_2(X_f) = \mathcal{C}_1(\mathcal{C}_1(X_f))$$

Similarly, $\mathcal{C}_3(X_f) = \mathcal{C}_1(\mathcal{C}_2(X_f))$, but from the expression above

$$\mathcal{C}_1(X_f) = \mathcal{C}_1(\mathcal{C}_1(\mathcal{C}_1(X_f)))$$

We can therefore generalize this expression as follows

$$X_{MPC} = \mathcal{C}_1(\mathcal{C}_{N_c-1}(X_f)) = \mathcal{C}_1(\mathcal{C}_1(\mathcal{C}_{N_c-2}(X_f))) \dots = \mathcal{C}_1(\mathcal{C}_1(\dots \mathcal{C}_1(X_f))) \quad (4.54)$$

Also, from Postulate 4.5.5, we have $\partial(X_f) \subset \mathcal{C}_1(X_f)$. Applying this to the recursive set operation of (4.54), we obtain

$$\partial(\mathcal{C}_{N_c-1}(X_f)) \subset \mathcal{C}_1(\mathcal{C}_{N_c-1}(X_f))$$

$$\partial(\mathcal{C}_{N_c-2}(X_f)) \subset \mathcal{C}_1(\mathcal{C}_{N_c-2}(X_f)), \dots, \subset \partial(X_f) \subset \mathcal{C}_1(X_f)$$

But, since $X_{MPC} = \mathcal{C}_1(\mathcal{C}_{N_C-1}(X_f))$, we can write

$$X_{MPC} = \mathcal{C}_1(\mathcal{C}_{N_C-1}(X_f)) \cup \mathcal{C}_1(\mathcal{C}_{N_C-2}(X_f)) \cup \dots \cup \mathcal{C}_1(X_f) \cup X_f$$

which is the same as (4.53) and hence the result. █

With this theoretical development, we can now state the procedure for recursively solving for robust output feasibility set X_{MPC} .

Algorithm 6 Determining Feasibility Region X_{MPC}

- 1: **Determine** $\mathcal{C}_1(X_f)$ by using Algorithm 5, given as $\tilde{x}_{c_1}^i \in \partial(\mathcal{C}_1(X_f))$ for $i = 1, \dots, \bar{N}$.
 - 2: **procedure** RECURSIVE ESTIMATION OF X_{MPC}
 - 3: **for** $l = 2, \dots, N_C$ **do**
 - 4: **if** $l = 2$ **then**
 - 5: **Solve** OCP 4.4.1 with target set $\mathcal{C}_1(X_f)$ to obtain $\mathcal{C}_2(X_f) = \mathcal{C}_1(\mathcal{C}_1(X_f))$
 - 6: **else**
 - 7: **Solve** OCP 4.4.1 with target set $\mathcal{C}_{l-1}(X_f)$ to obtain $\mathcal{C}_l(X_f) = \mathcal{C}_1(\mathcal{C}_{l-1}(X_f))$
 - 8: **end if**
 - 9: **end for**
 - 10: **Determine** X_{MPC} according to (4.53).
 - 11: **end procedure**
-

Remark 4.5.1 *The method given in Algorithms 5-6 is computationally demanding. However, all algorithms in this chapter are for used offline in the proposed MPC scheme, therefore computational burden is not an overriding concern. However, we must provide the caveat that choosing initial conditions for higher dimension systems is far less intuitive. In that case Algorithms 5-6 should be implemented in a heuristic (non gradient based approaches) to avoid the problems of local minima.*

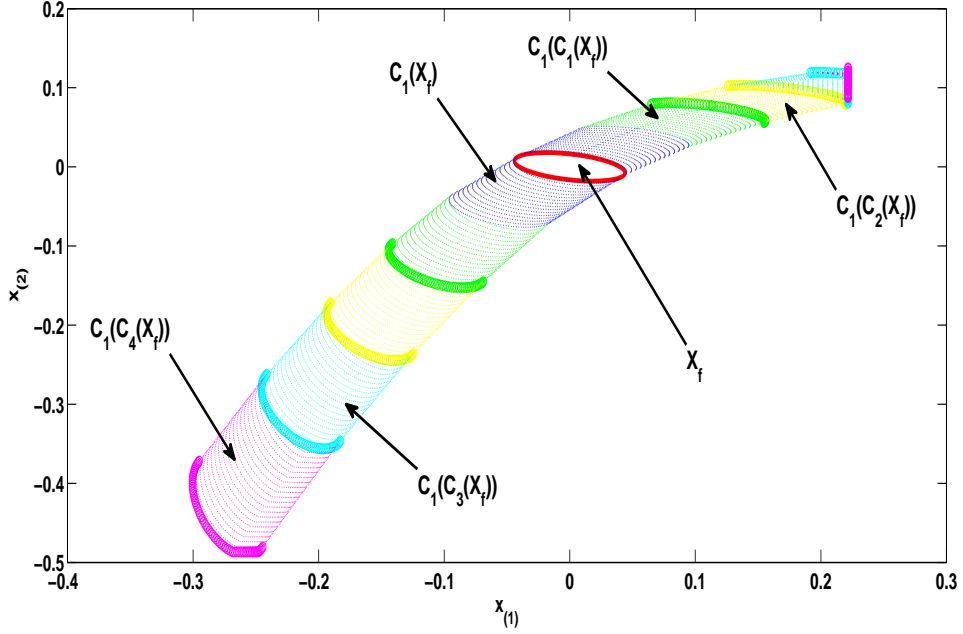


Figure 4.9: Recursive one-step controllable sets in Example 4.5.1. Circles indicate set boundary points and dotted lines show one step trajectories between boundaries of successive sets.

Example 4.5.1 (Nonlinear Oscillator: Part IV (Determining X_{MPC}))

Continuing our example of the nonlinear oscillator, we recall that we determined $C_1(X_f)$ in Example 4.4.1. Here, we will apply Algorithm 6 to find the robust output feasible set X_{MPC} . Using the same parameters as in previous examples, the iterative one-step controllability sets $C_{\downarrow}(C_{\downarrow-\infty}(\mathcal{X}_f))$, $\forall l = 2, \dots, (N_C = 5)$ are shown in Fig. 4.9. $C_{\infty}(\mathcal{X}_f)$ was calculated in Example 4.4.1. It can be observed that the sets are not symmetric about the terminal set X_f , which is due to asymmetric state constraints (see Fig. 4.11), as well as nonlinear dynamics. It is also seen that only a subspace of constrained state space is feasible for OCP 3.2.1. Optimal cost (4.44) for boundary of each set $\partial C_l(X_f)$, $\forall l = 1, \dots, N_C$ is shown in Fig. 4.10. Being closest to X_f , $C_{\infty}(\mathcal{X}_f)$ has the highest cost. Fig. 4.11 shows the

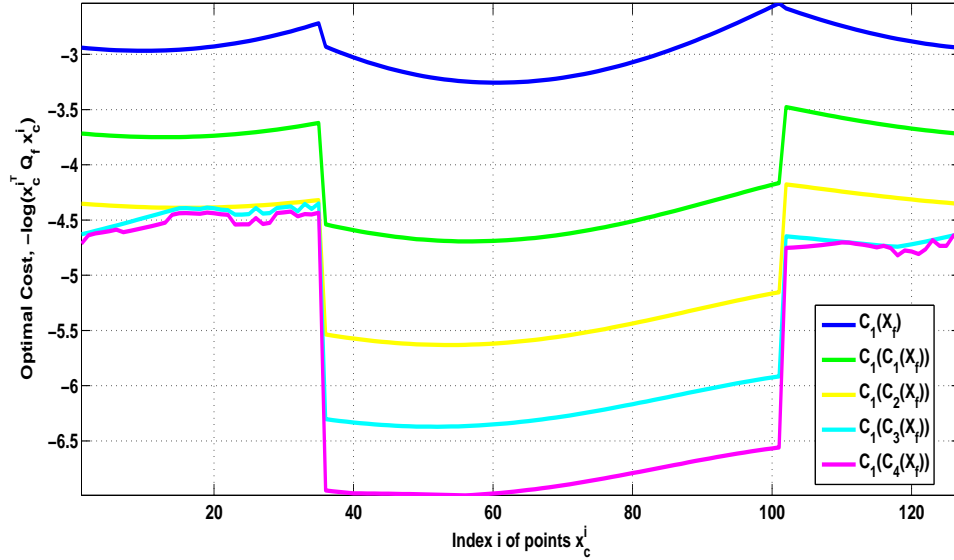


Figure 4.10: Optimal Cost from (4.44) for boundary points of 1-step Controllable Sets $\mathcal{C}_\downarrow(\mathcal{C}_{\downarrow-\infty}(\mathcal{X}_1))$, using Algorithm 6 for Example 4.5.1.

robust output feasible set X_{MPC} along with tightened constrained \tilde{X}_{t+N_c} . It is observed that boundary of X_{MPC} coincides with tightened state constraint set boundary $\partial\tilde{X}_{t+N_c}$. This estimation of the set of initial feasible state is much less conservative than the one given in [110] due to explicit inclusion of constraints in the optimization.

4.6 Illustrative Example of Overall Robust NMPC Scheme (Algorithm 1)

We have now fully developed all the ingredients of Algorithm 1. Examples 3.3.2-4.5.1 showed the application of ingredient Algorithms 2-6 on a nonlinear oscillator (3.59). Therefore, in this section we apply Algorithm 1 on the same system.

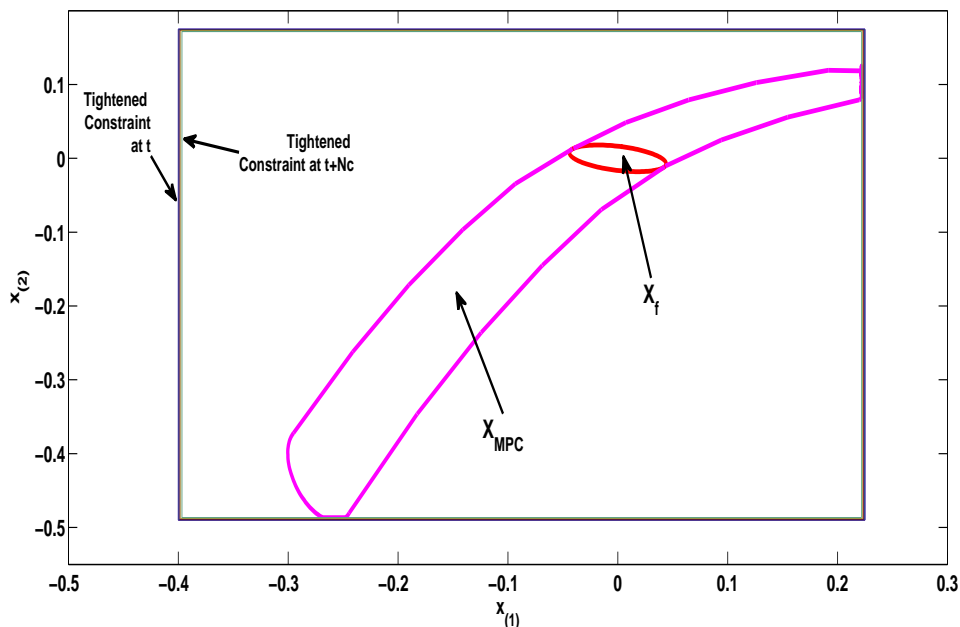


Figure 4.11: Robust Output Feasible Set X_{MPC} with Tightened Constraints. Boundaries of X_{MPCC} coincide with tightened constraint \tilde{X}_{t+Nc} .

Example 4.6.1 *We can now implement the online part of Algorithm 1, implemented using `fmincon` package of Matlab [111]. The initial condition is chosen as $\tilde{x}_t = [-0.25 \ -0.4]^T \in X_{MPC}$. The goal is to regulate the state to the origin, without violating any constraints. Fig. 4.12 shows the state trajectory in the phase plane, along with terminal region X_f and tightened constraints (inner most set is \tilde{X}_{t+Np} and outermost is \tilde{X}_t). It can be observed that the state does not converge to zero, since Theorem 3.2.3 only guaranteed practical stability. Evolution of the states with time is shown in Fig. 4.13, where it is again clear that the state does not converge to the origin due to the presence of uncertainty. The control input calculated by application of Algorithm 1 is shown in Fig. 4.14. The figure shows how the maximum control authority is utilized initially without violation of this*

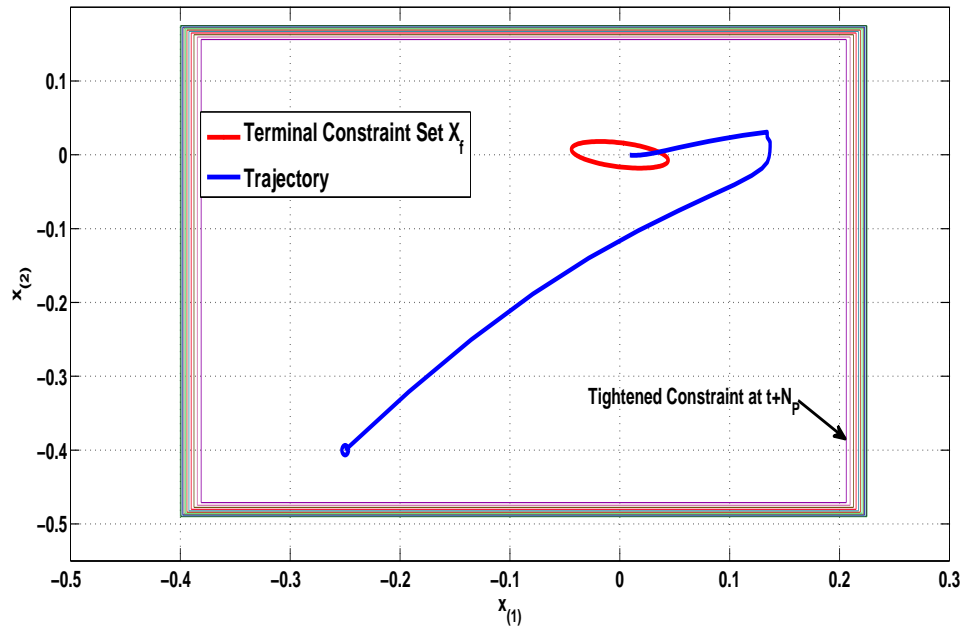


Figure 4.12: State trajectory in phase plane for Example 4.6.1, solved with Algorithm 1. Notice that the state does not converge to the origin. Also shown is the terminal constraint set (red dotted) and tightened constrain sets.

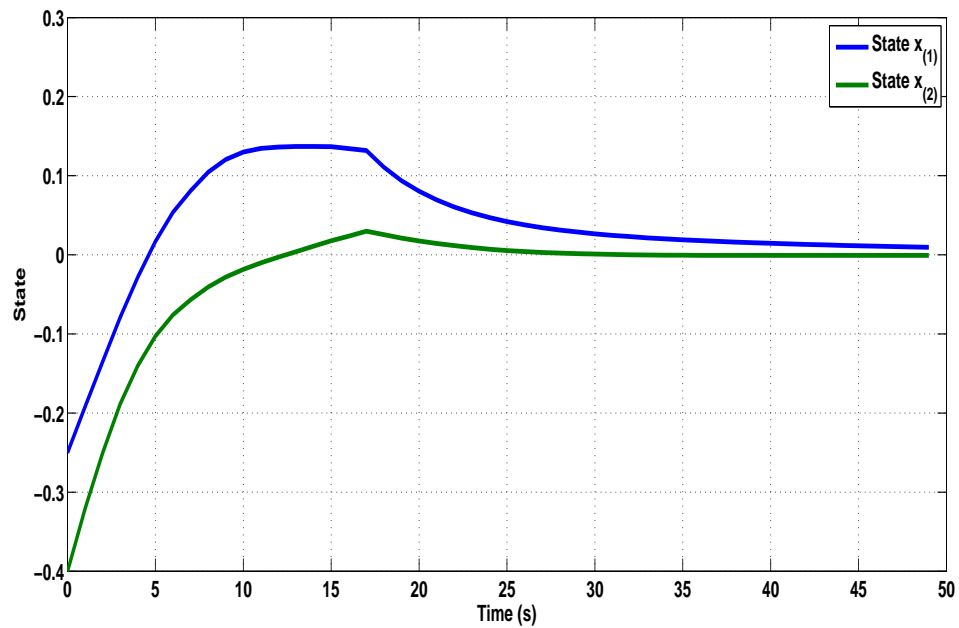


Figure 4.13: Time evolution of states for Example 4.6.1. Notice that the state does not converge to the origin.

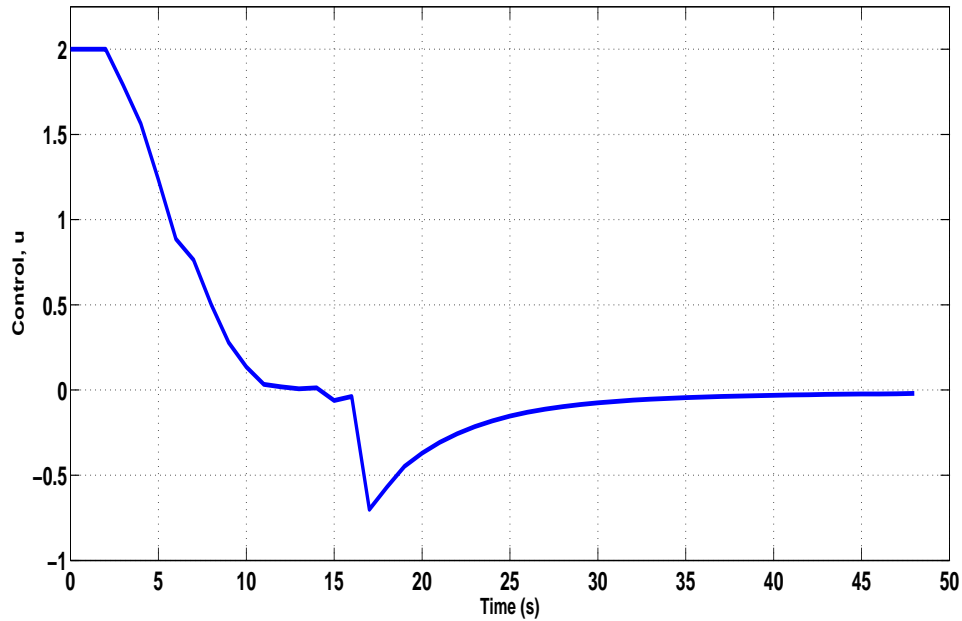


Figure 4.14: Control history for Example 4.6.1. Notice that maximum control authority is utilized by Algorithm 1.

constraint, which is a unique feature of NMPC. Fig. 4.15 shows the evolution of cost functional (3.58), which decreases monotonously, as expected. Computation time for offline part of Algorithm 1 was 320 seconds and for 50 seconds of simulation, the online algorithm took 39 seconds of computation time, on an Intel Core i5-4210U 2.7 GHz machine with 4 GB memory. This is adequate for online implementation, and can be further improved with dedicated code and hardware. Table 4.4 gives the breakdown of the computational time for various components of Algorithm 1. The offline algorithms take the most time to compute, but the online algorithm takes 0.8 seconds to simulate every second of simulation.

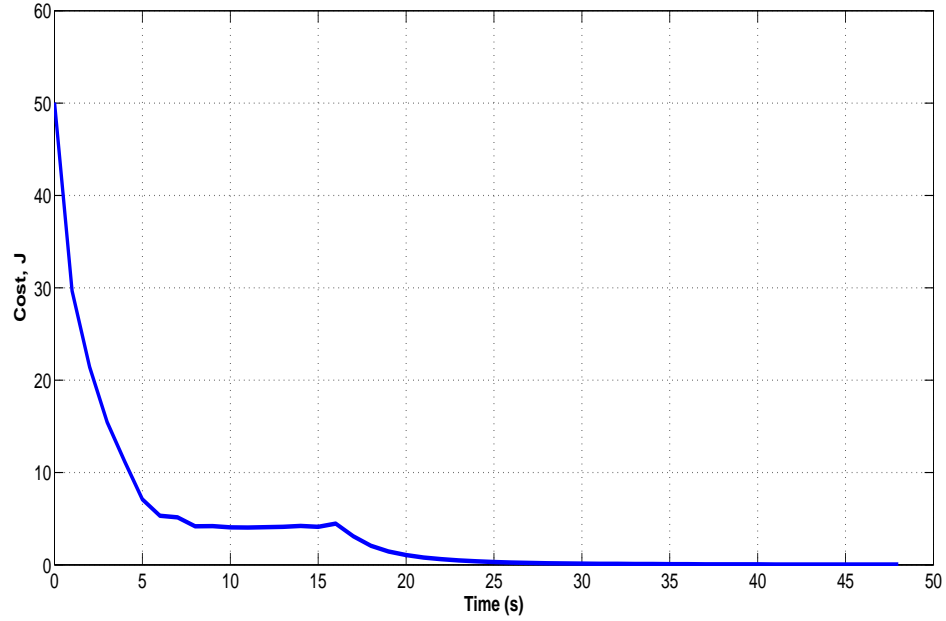


Figure 4.15: Evolution of Optimization Cost Function for Example 4.6.1.

Table 4.4: Computational Times of Algorithms 1-6 for Examples 3.3.2-4.6.1

| S. No. | Algorithm | Computational Time (s) |
|--------|--|------------------------|
| 1 | Algorithm 2 (offline) | 0.004 |
| 2 | Algorithms 3-4 (offline) | 5.286 |
| 3 | Algorithm 5 (offline) | 62.779 |
| 4 | Algorithm 6 (offline) | 251.117 |
| 5 | Algorithm 1 online part (50 s simulation) | 38.535 |

4.7 Conclusion

In this chapter, we presented new results in terminal region maximization and feasibility set estimation of robust nonlinear MPC algorithm. We presented four algorithms terminal region optimization, terminal control law design and determining maximum robust output feasible set. Terminal region is maximized based on polytopic linear difference inclusions (PLDI) by Algorithms 5-4. One-step controllable set and robust output feasible set are calculated using Algorithm 5-6. Hence, this chapter completed the development of all components of Algorithm 1. Moreover, theoretical development in Chapter 3 showed that due to uncertainties, only practical stability can be ensured, and the amount of tolerable disturbance is bounded by the size of one-step controllability set to terminal constraint region. Hence, to increase robustness and feasibility region, the terminal region was maximized with theoretically derived methods for warm starting the algorithm. Moreover, min-max optimization to find the maximum initial feasibility set for the worst case realization of uncertainties as also described. Simulations were used to validate the theoretical results. In the next chapter, we will extend the results so far for the multi-agent case for cooperative control.

CHAPTER 5

FORMATION CONTROL BASED ON ROBUST DISTRIBUTED NMPC

5.1 Introduction

With increasing computational power in affordable deployable packages, advanced control techniques like NMPC have been implemented on mobile robots in challenging environments [112]. NMPC has the unique feature of being able to handle constraints on state and control variables, which are invariably present in mobile robots. These constraints may be minimum speed (aerial vehicles), maximum speed, maximum acceleration dictated by structural integrity, throttle and steering control limits etc. The robust NMPC framework we developed in Chapters 3-4 can be easily applied to single autonomous vehicles, and it can handle mea-

surement noise as well as modeling uncertainty and external disturbance. In this chapter, we will extend the framework for systems consisting of multiple agents.

Chapter Organization The chapter is organized as follows: The problem is introduced in Section 5.2, and an outline of the proposed solution is provided. An important new result in the form of Theorem 5.5.1 is presented, which forms the basis of the rest of the development in this chapter. Also presented are the novel data compression and collision avoidance schemes. In Section 5.5, Theorem 2.5.2 is extended to prove stability of Algorithm 7 in several new theorems and lemmas. These theoretical results are validated in extensive simulations presented in Section 5.6. Finally, a summary of the chapter is presented along with recommendations for future research directions.

5.1.1 Centralized versus Distributed Cooperative Control

As mentioned in Chapter 1, most biological systems are not only interconnected, but in many cases, individual agents often cooperate with each other to obtain a mutually beneficial goal. Recently, with advances in cheap sensors and actuators, mobile robots have become ubiquitous in academia and research institutions. Cooperative control in a team of autonomous vehicles can be thought of as distributed control of dynamically decoupled cooperating systems [59]. Cooperation has been defined as a close relationship among all agents in the team with information sharing playing an important role [22]. Therefore, cooperative tasks may be performed in three manners [113], depending on how information is exchanged,

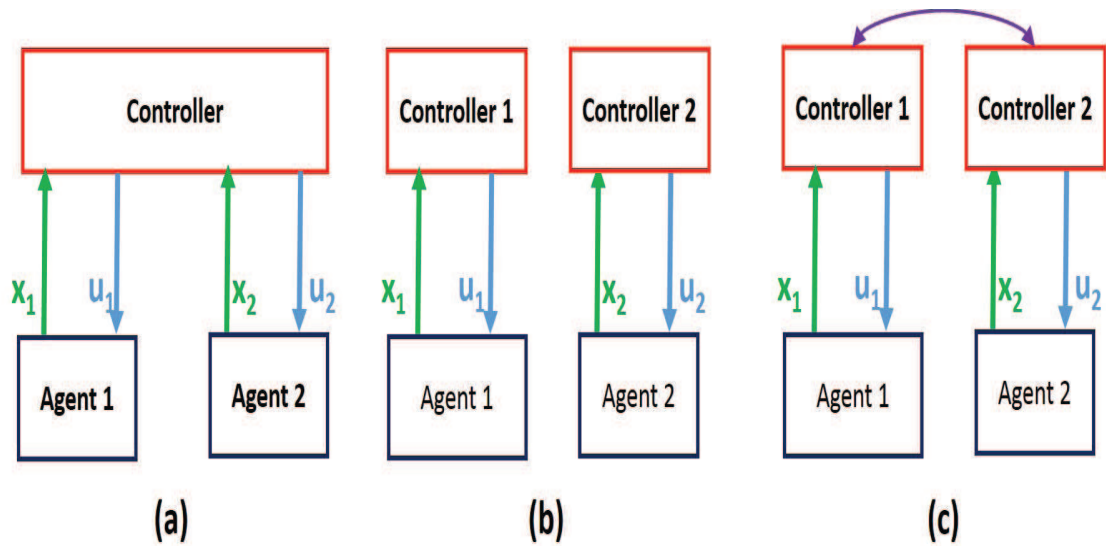


Figure 5.1: Centralized (a), decentralized (b) and (c) distributed control of multi-agent systems. Notice the information exchange between agents in the three settings.

depicted in Fig. 5.1.

- Centralized control. All information is collected at a single hub which also computes control for all agents.
- Decentralized control. No information exchange among agents; control actions are based only on local measurements by each agent.
- Distributed control. Agents have access to information from other agents, which is used in calculation of control action computed locally by each agent.

Centralized control is the framework we developed in Chapters 3-4. It has the advantage of being a control architecture which has been studied since the beginning of automatic control and therefore many control design methods are available. However, it has sever limitations due to the necessity to maintain communication of all agents with the central hub, the failure of which usually means failure of

the entire control systems. Also, as the number of variables increase, centralized control becomes increasingly difficult to calculate and synthesize. If the agents are spread over a large area or wirelessly connected, such as aircraft formations, it may become very difficult to maintain communication or handle large amount of data over a limited bandwidth budget. Decentralized control is the other extreme in which no information is exchanged with other agents. This is the simplest approach and works if the interconnection among system variables is weak or the systems have a certain structure [114]. However, in general it is limited to a certain class of systems, often at the cost of reduced performance. Distributed control is an architecture which is between these two extremes. Control is calculated locally but information from other agents is incorporated in control synthesis. In terms of performance, it is lower than the performance of centralized control but better than decentralized control, but in terms of computational burden it is much less demanding than centralized control. In many multi-agent problems, distributed control is often the architecture of choice due to practical considerations and acceptable performance at lower computational and bandwidth requirements. In this work we will consider the distributed control of a fleet of autonomous agents.

5.1.2 Introduction to Graph Theory

Information exchange among networked vehicles is conveniently modeled by directed or undirected graphs [65]. An information graph is a set of nodes A^i and edges connecting pairs of these nodes. If order of pairing in an edge $E(A^i, A^j)$,

where $i, j = 1, \dots, N, i \neq j$ is ordered (meaning information flow is from one node to the other only, and not vice versa), it is called a directed graph, but if the order is unimportant (two way communication), it is an undirected graph. If a weight is assigned to every edge in the graph, it is called a weighted graph. A path is a sequence of edges from one node to get to another in the direction of information flow. In this work, we consider general mixed graphs (i.e. having both directed and undirected edges).

Let's define the connectivity matrix as $\Gamma = [\gamma_{ij}]$, where $\gamma_{ij} > 0$ if $(A^i, A^j) \in E$ and 0 otherwise. By convention $\gamma_{ii} = 0$, i.e. there are no self-loops. The neighborhood of a node A^i is $G^i : \{A^j : \gamma_{ij} > 0\} \cup \{A^j : \gamma_{ji} > 0\}$. The diagonal matrix $D = [d_{ij}]$ where $d_{ij} \triangleq \sum_{j \in G^i} \gamma_{ij}$ is called the weighted in-degree of node A^i , i.e. the row sum of Γ at row i . The graph's Laplacian matrix is $L \triangleq D - \Gamma$, which has all row sums equal to zero.

5.1.3 Formation Control

Often the main task in multi-vehicle cooperative control is formation [50]. Formations control means the ability to move the entire fleet with a common speed and heading. This invariably means that the vehicles in the team should be able to either sense the states of team members, or receive state information from other team members. In most cases however, the communication occurs wirelessly as the agents are spread over a large area or it is not possible to maintain tethered connection network due to movement of vehicles and presence of obstacles. Also

due to mobile nature of these vehicles, the on-board computational power is limited due to size and power budgets. Therefore, distributed control is often the only practical control architecture. There are three basic elements in multi-agent formation control [24].

- i. Cohesion: attraction to distant neighbors up to a reachable distance.
- ii. Alignment: velocity and average heading agreement with neighbors.
- iii. Separation: repulsion from neighbors within some minimal distance. This is also called collision avoidance.

Formation control without collision avoidance is also called state synchronization. In [28], a dynamic neural network based adaptive control scheme for distributed fleet state synchronization, without the need to know local or leader (nonlinear) dynamics. Lyapunov analysis is used to derive tuning rules, with the implicit need for persistent excitation, for both strongly connected and weakly (simply) connected networks. However, delays, asynchronous measurements, collision avoidance and limits on control actuation forces are not considered. In a similar approach, synchronization of nonlinear Lagrangian systems with linear-in-parameter model uncertainties has been solved using distributed adaptive back-stepping and adaptive redesign [29]. But unlike [28], all agents are assumed to have access to group reference trajectory, which constitutes a further limitation. Synchronization of a fleet of nonlinear Euler-Lagrangian systems has also been achieved using distributed H_∞ controllers robust to model uncertainties and disturbances in fixed and switching network topologies guaranteeing input to state stability (ISS) [30].

A prevalent technique for formation control of both linear and nonlinear systems is model predictive control (MPC), also known as receding horizon control (RHC) for its inherent ability to handle constraints, incorporation of non-local information and reconfigurability. Few attempts at centralized NMPC have been made (e.g. [31]-[32]), but all suffer from computational complexity and time, both being two major impediments towards its perusal. Work on multi-agent formation control using MPC was pioneered at Caltech in 2001 [33]. He considered distributed NMPC for leader-less synchronization of agents with constrained, continuous dynamics. All agents had access to the dynamic model of every other agent as well as the virtual leader. Stability was ensured using terminal set and linear terminal control technique [34]. However, no delay was considered. This work has been extended later in [35] by requiring each agent to transmit its optimum control trajectory at every sampling instant to its neighbors. Each vehicle's control is determined by solving an NMPC problem that minimizes a local cost function, which considers the received control trajectories and models of its neighbors. For stability, it is required that the actual trajectory of each vehicle does not deviate too much from the one it transmitted to its neighbors. Hence, no account is taken of model uncertainties and delays. The need to know neighbors' dynamic models was removed in a recent work [36], by communicating state error trajectories to immediate neighbors, instead of vehicle trajectories. However, the results are conservative in that only a queue or string formation is considered. In another direction, the results of [33] were extended using graph theory to spec-

ify distributed NMPC cost functions for agents, and ensuring collision avoidance by repelling potential field [44]. In a similar vein, [45] considered collision and obstacle avoidance in a pursuit-evasion game among multiple vehicles by adding repulsive potential fields to local NMPC cost function and using current position and velocity of other vehicles to predict their future trajectories. However, the author did not provide stability proofs and ignored robustness issues. In [46], feedback linearization is used in the terminal set of NMPC, but only collision avoidance is considered in formation, without stability proofs.

Recently, [58]-[59] distributed NMPC was considered for a group of agents receiving delayed input from their neighbors. The delayed information is projected in the prediction horizon using a *forward forgetting-factor*. For a fleet of underwater vehicles [53], decentralized MPC was proposed, while ensuring fault tolerance. Each vehicle shares its plans and information on faulty states with its neighbors in a virtual-leader setting. This work was extended in [54], to take into account extended Kalman filtering (EKF)-based sensor fusion for localization in addition to distributed MPC for collision avoidance and formation tracking. In [50], using penalties for obstacle/collision avoidance in the NMPC framework, the neighbors' randomly delayed information is projected in the prediction horizon by linear recurrence.

In this chapter, we address the problem of leader-follower formation control of constrained autonomous vehicles subject to propagation delays. Limited network throughput demands reduction in packet size. The proposed approach achieves

formation tracking through NMPC such that each agent performs local optimization based on planned approximate trajectories received from its neighbors. Since exchanging the entire horizon will increase packet size proportional to length of prediction horizon, the trajectory is compressed using neural networks, which is shown to reduce the packet size considerably. Moreover, the method allows the agents to be heterogeneous, make asynchronous measurements and have different local optimization parameters. Correction for propagation delays is achieved by time-stamping each communication packet [115]. Collision avoidance is achieved by formulating a novel spatial-filtered potential field which is activated in a “zone of safety” around the agent’s trajectory. New theoretical results are presented along with validating simulations.

5.1.4 Chapter Contributions

This chapter extends the work in [59] and contributes to the literature with the following original results, which resulted in several publications [73], [19] etc. mentioned in Chapter 1.

- Robustness to inaccuracy in communicated trajectories is explicitly taken into account, resulting in practical stability instead of asymptotic stability as in [59].
- An unprecedented number of sources of uncertainty is simultaneously considered, with explicit analytic closed form expressions for contribution of each source in uncertainty growth.

- Collision avoidance is also explicitly catered for. A novel modification of potential field method is proposed. Unlike [45], our potential field is multiplicative, based on a spatial filter and stability is rigorously proved.
- New input to state practical stability (ISpS) and generalized small gain conditions are derived, with explicit closed form expressions rendering great insight into the role of each source of uncertainty in reducing feasibility and stability.
- Unlike [59], the stability results of this chapter are not limited to strongly connected networks. It is shown even a weakly connected network topology for multiple agents can be designed for fleet-wide stability.

5.2 Problem Formulation

Consider a set of N agents, where each agent is denoted as A^i with $i = 1, \dots, N$. Each agent has the following open loop nonlinear discrete-time dynamics described by

$$x_{t+1}^i = f_o^i(x_t^i, u_t^i), \quad \forall t \geq 0, \quad i = 1, \dots, N, \quad (5.1)$$

where f_o^i is a nonlinear map for local open loop dynamics. x_t^i and u_t^i are states and controls local to agent A^i . These variables belong to the following constraint

sets :

$$\begin{aligned} x_t^i \in X^i \subset \mathbb{R}^{n^i}, & \quad X^i \triangleq \{x^i : x_{\min}^i \leq x^i \leq x_{\max}^i > 0\} \\ u_t^i \in U^i \subset \mathbb{R}^{m^i}, & \quad U^i \triangleq \{u^i : u_{\min}^i \leq u^i \leq u_{\max}^i > 0\} \end{aligned} \quad (5.2)$$

One can observe that the agents' dynamics (5.1) are decoupled from each other in open loop. This is the standard case for most formation control problems [116]. It is rare for formations to be dynamically coupled, but such cases do exist, e.g. [19]. In this thesis, we will focus on team of dynamically decoupled agents. Due to measurements corrupted with sensor noise, we assume that local states are estimated (locally) with bounded error ξ_x^i , such that

$$\tilde{x}_t^i = x_t^i + \xi_{x_t}^i, \quad \xi_x^i \leq |\xi_{x_t}^i| \leq \bar{\xi}_x^i \quad (5.3)$$

Even though the agents are dynamically decoupled, they need to cooperate with each other to perform the formation keeping task. To achieve this goal, a *cooperation* component is added to the cost functional (performance index) (5.10) of each agent. To this end, define w_t^i as an *information vector* transmitted to agent A^i by other agents in its neighborhood G^i , which consists of the states of these neighbors.

Definition 5.2.1 (Information Vector) *The external input to agent A^i in formation control task in a multi-agent system consists of state information of other*

agents in its neighborhood G^i , such that

$$w^i \triangleq \text{col}(x^j), \quad \forall j = 1, \dots, M^i, j \in G^i, j \neq i, \quad (5.4)$$

where M^i is the number of agents in the neighborhood of A^i . This external input in the form of the information vector w^i is driven by the dynamics of the neighboring systems, as below

$$w_{t+1}^i = g^i(w_t^i, \phi_t^i) \triangleq \text{col}(f_o^j(x_t^j, u_t^j)), \quad \forall j = 1, \dots, M^i, j \in G^i, j \neq i, \quad (5.5)$$

where g^i is a nonlinear map composed of nonlinear dynamics of neighboring agents and their local inputs $\phi_t^i \triangleq \text{col}(u_t^j)$. We assume that the information vector is constrained to the following set

$$w_t^i \in W^i \subset \mathbb{R}^{p^i}, \quad W^i \triangleq \{w^i : w_{\min}^i \leq w^i \leq w_{\max}^i > 0\} \quad (5.6)$$

Moreover, assume that we have an updatable approximation for w^i , which produces the approximation \tilde{w}^i , such that

$$\tilde{w}_t^i = w_t^i + \xi_{w_t}^i, \quad \underline{\xi}_w^i \leq |\xi_{w_t}^i| \leq \bar{\xi}_w^i \quad (5.7)$$

We assume that we do not have exact knowledge of the evolution of the information over the horizon i.e. $w_{t,t+N_p}^i$, and that we can only have an approximation of it $\tilde{w}_{t,t+N_p}^i$. The exact approximation method will be discussed in Section 5.2.1. Also,

let us assume that the agent A^i has nominal model $\tilde{g}(\cdot)$ of the true information vector (5.5) given by

$$\tilde{w}_{t+1}^i = \tilde{g}^i(\tilde{w}_t^i), \quad (5.8)$$

such that there is a bounded *information vector transition uncertainty* due to information vector model mismatch

$$\tilde{g}(w_t^i) = g(w_t^i, \phi_t^i) + e_{w_t}^i, \quad \underline{e}_w^i \leq |e_{w_t}^i| \leq \bar{e}_w^i, \quad (5.9)$$

Now, let the *distributed* cost function of each agent be given as

$$\begin{aligned} J_t^i \left(\tilde{x}^i, u^i, \tilde{w}^i, d^{h^i}, d^{q^i}, N_c^i, N_p^i \right) &= \sum_{l=t}^{t+N_c^i-1} \left[h^i \left(\tilde{x}_l^i, u_l^i, d^{h^i} \right) + q^i \left(\tilde{x}_l^i, \tilde{w}_l^i, d^{q^i} \right) \right] \\ &+ \sum_{l=t}^{t+N_p^i-1} \left[h^i \left(\tilde{x}_l^i, k_f^i(\tilde{x}_l^i), d^{h^i} \right) + q^i \left(\tilde{x}_l^i, \tilde{w}_l^i, d^{q^i} \right) \right] + h_f^i \left(\tilde{x}_{t,t+N_p^i}^i, d^{h^i} \right), \end{aligned} \quad (5.10)$$

where N_p^i and N_c^i are the local prediction and control horizons, respectively, according to the NMPC notation (see Fig. 3.2). The distributed cost function (5.10) consists of three components

- i. *Local transition cost* h^i , which is the cost to reach a local target state, which is embedded in the *local alignment vector* d^{h^i} .
- ii. *Cooperative cost* q^i which is the cost for agent A^i to converge to an aligned state with its neighbors $A^j \in G^i$. The cooperation goal is embedded in the *cooperative alignment vector* d^{q^i} .

iii. *Terminal cost* h_f^i is the cost of distance between the local state at $t + N_P^i$ and the local target state.

Local control sequence $u_{t,t+N_P^i}^i$ consists of two parts, $u_{t,t+N_C^i-1}^i$ and $u_{t+N_C^i,t+N_P^i-1}^i$. The latter part is generated by a *local terminal control law* $u^i = k_f^i(\tilde{x}_l^i)$ for $l \geq N_C^i$, while the former is finite horizon optimal control $u_{t,t+N_P^i}^i$ which is the solution of the optimization problem 5.2.1. Now, in spite of the agents being dynamically decoupled, states of other agents in the multi-agent system affect the control of agent A^i by virtue of the information vector \tilde{w}^i being part of its NMPC cost function (5.10). Therefore, even though the agents are decoupled in the open loop, their dynamics is coupled in close loop due to cooperation cost component in distributed cost (5.10). Therefore we can write the closed loop form of the open loop agent dynamics (5.1) as

$$x_{t+1}^i = f^i(x_t^i, u_t^i, w_t^i), \quad \forall t \geq 0, \quad i = 1, \dots, N, \quad (5.11)$$

We assume that our model of agent dynamics is not perfect, such that the *nominal* model used for control synthesis is

$$\tilde{x}_{t+1}^i = \tilde{f}^i(\tilde{x}_t^i, u_t^i, w_t^i), \quad (5.12)$$

where, the actual state of the system is x_t^i , while the state predicted by model (5.12) is \tilde{x}_t^i . This system model mismatch leads to *agent transition uncertainty*

$e_{x_t}^i \triangleq \tilde{f}^i(x_t^i, u_t^i, w_t^i) - f^i(x_t^i, u_t^i, w_t^i)$, such that

$$\tilde{f}^i(x_t, u_t, w_t) = f^i(x_t, u_t, w_t) + e_{x_t}^i, \quad \underline{e}_x^i \leq |e_{x_t}^i| \leq \bar{e}_x^i \quad (5.13)$$

Now, due to uncertainty, the constraint sets (5.2) and (5.6) for x^i and w^i will be ‘larger’ than constraint sets for \tilde{x}^i and \tilde{w}^i , such that

$$\tilde{x}_t \in \tilde{X}_t^i(\bar{e}_x^i, \bar{\xi}_x^i, \bar{e}_w^i, \bar{\xi}_w^i) \subset X^i, u_t \in U, \quad \tilde{w}_t^i \in \tilde{W}_t^i(\bar{\xi}_w^i, \bar{e}_w^i) \subset W^i \quad (5.14)$$

The exact definition of these ‘tightened’ constraint sets is given later. We will now state the distributed finite horizon control problem for NMPC.

Problem 5.2.1 (Distributed Finite Horizon Optimal Control Problem)

At every instant $t \geq 0$, given prediction and control horizons $N_p^i, N_c^i \in \mathbb{Z}_{\geq 0}$, terminal control $k_f^i(\tilde{x}^i) : \mathbb{R}^n \rightarrow \mathbb{R}^m$, state estimate \tilde{x}_t^i and information vector approximation $\tilde{w}_{t,t+N_p^i}^i$, find the optimal control sequence $u_{t,t+N_c^i-1}^{o^i}$, which minimizes the finite horizon cost (5.27)

$$u_{t,t+N_c^i-1}^{o^i} = \arg \min_{u^i \in U^i} \tilde{J}_t^i \left(\tilde{x}_t^i, \tilde{w}_{t,t+N_p^i}^i, u_{t,t+N_p^i}^i, N_c^i, N_p^i \right), \quad (5.15)$$

subject to

I. nominal state dynamics (5.12)

II. nominal information vector dynamics (5.8)

III. Tightened constraint sets (5.14)

IV. Terminal state $\tilde{x}_{t+N_p}^i$ is constrained to an invariant terminal set $X_f^i \in$

$\tilde{X}_{t+N_c}^i$, i.e.

$$\tilde{x}_{t+l}^i \in X_f^i, \quad \forall l = N_c^i, \dots, N_p^i \quad (5.16)$$

The loop is closed by implementing only the first element of $u_{t,t+N_c^i-1}^{0^i}$ at each instant, such that the NLMPC control law becomes

$$\Theta_t^i(\tilde{x}^i, \tilde{w}^i) = u_t^{0^i}(\tilde{x}_t^i, \tilde{w}_t^i, N_p^i, N_c^i) \quad (5.17)$$

and the closed loop dynamics becomes

$$x_{t+1}^i = f(x_t^i, \Theta_t^i(\tilde{x}^i, \tilde{w}^i), w_t^i) = f_c^i(x_t^i, w_t^i) \quad (5.18)$$

with local closed loop nonlinear map $f_c^i(x, w)$. This process is repeated every sampling instant, as illustrated in Fig. 3.2. To summarize, at time t , each agent A^i ($i = 1, \dots, N$) estimates its local state \tilde{x}_t^i and receives an approximation of information vector $\tilde{w}_{t,t+N_p^i}^i$ from its neighbors. Then, cost (5.10) is minimized over a finite horizon N_p^i , using N_c^i control adjustments and pre-computed terminal control law k_f^i , subject to constraints (5.14) and (5.16). Only the first element of this optimized control sequence is implemented. Then the cycle is repeated at the next sampling instant. This algorithm is stated below

Algorithm 7 Distributed NMPC Algorithm for Formation Control

- 1: **procedure** OFFLINE CONVEX AND MIN-MAX OPTIMIZATION
 - 2: **Input** $A^1, A^i \leftarrow \tilde{x}_t^i, d^{h^i}, d^{q^i}, g^i$ $\triangleright i = 1 \triangleq \text{Leader}, t = 0$
 - 3: **Tighten** constraints with Algorithm 8
 - 4: **Compute** Q_f^i and K_f^i using Algorithms 3 and 4
 - 5: **Compute** Output feasibility set X_{MPC}^i and controllability sets $\mathcal{C}_1(X_f^i)$ using Algorithms 5 and 6
 - 6: **end procedure**
 - 7: **procedure** DISTRIBUTED ONLINE RH OPTIMIZATION
 - 8: **Design** Spatially filtered potential (5.72)
 - 9: **Solve** Problem 5.2.1 at A^i for $u_{t,t+N_c^i-1}^{i^o}$
 - 10: **Train NN** Train Neural network for $\tilde{x}_{t,t+N_p}^{i^o}$
 - 11: **Implement** first element/block of $u_{t,t+N_c^i-1}^{i^o}$
 - 12: **Transmit/Receive** data packets
 - 13: **Estimate** time delay Δ_{ij}
 - 14: **Reconstruct** $\tilde{w}_{t,t+N_p^i}^i$ with received NN and estimate tail of received trajectory (5.22).
 Increment time by one sample $\triangleright t^i = t^i + T^i$
 - 15: **end procedure**
-

5.2.1 Neural Network based Trajectory Compression

For cooperation, agents transmit their planned state trajectories, $\tilde{x}_{t,t+N_p^i}^i \in \mathbb{R}^{n^i \times N_p^i}$ as mentioned in Definition 5.2.1. These communication packets are received by vehicles within the neighborhood of transmitting agents. Neighborhood may be defined based on communication range, number of channels on receiving agents etc.

Definition 5.2.2 (Neighborhood of Agents) *Each agent A^i in the team of N agents has a neighborhood $G^i = A^j, \forall j \neq i, j = 1, \dots, M^i$, consisting of M^i neighbors from which it is able to at least receive information.*

However, reception of these packets occurs after some delay Δ^{j^i} , called the *propagation delay*, which is not necessary an integer multiple of the sampling time T^i .

Table 5.1: Anatomy of a Typical Communication Packet.

| Data Register | Data |
|-------------------|---------------------------------|
| 1 | Agent identity, i |
| 2 | Time stamp, T_s^i |
| 3 | Sampling time, T^i |
| 4 to $3 + q^i$ | Neural network, \mathcal{N}^i |
| $4 + q^i$ onwards | Error correcting codes |
| Optional (leader) | Cooperation Goals |

This delay may depend on the relative range and orientation between the agents or the medium and method of communication [117]. Considering that most multi-vehicle systems are connected over wireless channels, the bandwidth allocated to each channel may be limited. Hence, there is an interest in compressing the data before sending it and then recovering it at the receiver's end. To reduce packet size, this trajectory containing $n^i \times N_p^i$ floating points is compressed by approximating it with neural network \mathcal{N}^i of q^i weights and biases, with compression factor C_w^i of

$$C_w^i = 1 - \frac{q^i + \text{overhead size}}{n^i \times N_p^i} \quad (5.19)$$

Overhead size accounts for agent identity i , time-stamp (T_s^i) and sampling time T^i etc. The leader also communicates formation geometry and way-points to followers. The typical communication packet from A^i to A^j will have the topology shown in Table 5.1. It is assumed that there exists a mechanism for synchronizing clocks, which allows delay Δ_{ji} to be estimated. NN at A^i is trained using state trajectory as output and N_p^i discrete instants as input. Using sampling rate T^j and prediction horizon N_p^j at A^j , re-sampled trajectory $\tilde{w}_t^j \in W^j \subset \mathbb{R}^{n^j \times N_p^j}$ is gen-

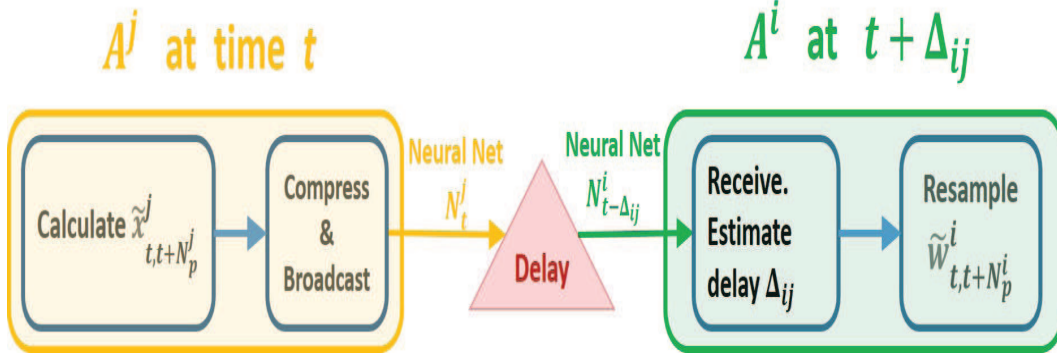


Figure 5.2: Trajectory compressed at Agent A^j is transmitted to Agent A^i , where it is received after delay Δ_{ij} and recovered using neural network.

erated using received neural network \mathcal{N}^i . If horizon is sufficiently long, states can be extrapolated with bounded error, but very long horizons are impractical due to increased computational load. Therefore, we have suggested another method of ‘extrapolation’ in the next section. If packet is delayed by more than a threshold $\bar{\Delta}$, the packet is deemed to be lost. The data compression and recovery process is depicted in Fig. 5.2. The basic universal approximation result says that any smooth function $w(t)$ can be approximated arbitrarily closely on a compact set using a two-layer NN with appropriate weights. This result has been shown using various activation functions, see [77]. In general, a single-layered NN will not provide universal approximation, but can still give acceptable performance. Let $\tilde{x}_{t,t+N_p^j}^j(\tau)$ be the trajectory optimized at A^j , then we can show [77]

$$\hat{x}_{t,t+N_p^j}^j(\tau) = \tilde{x}_{t,t+N_p^j}^j(\tau) + \xi_N^j, \quad \underline{\xi}_N^j \leq |\xi_N^j| \leq \bar{\xi}_N^j \quad (5.20)$$

where $\hat{x}^j(\tau)$ is the approximation of $x^j(\tau)$ by the NN, and $\tau \triangleq \text{col}(t, t \dots t)$ is the stack of t vector n^i times and $\bar{\xi}_{\mathcal{N}}^j \in \mathbb{R}_{\geq 0}$ is the NN function approximation error which decreases as the hidden-layer size H_L increases.

Tail Recovery and Maximum Allowable Delay

For ease of understanding, we will consider a two member team, though generalization to a larger team is trivial. Similarly, for the development here, we will assume delay Δ to be an integer multiple of sampling time T^i , though it is easy to generalize. As depicted in Fig. 5.2, the trajectory of A^j is compressed by a neural network \mathcal{N}_t^j in (5.20). This neural network \mathcal{N}_t^j is broadcast over the communication channel and received at agent A^i after some delay. Therefore, the packet when it is received at time t by A^i was actually sent at $t - \Delta_{ij}$. Let us assume there is a mechanism for estimating propagation delay Δ_{ij} . Then the neural network received $\mathcal{N}_t^i = \mathcal{N}_{t-\Delta_{ij}}^j$ is used to reconstruct trajectory as follows

$$\begin{aligned} \tilde{w}_{t-\Delta_{ij}, t+N_p^j-\Delta_{ij}}^i(\tau) &= \hat{x}_{t-\Delta_{ij}, t+N_p^j-\Delta_{ij}}^j(\tau), \\ \left| \tilde{w}_{t-\Delta_{ij}, t+N_p^j-\Delta_{ij}}^i(\tau) - \tilde{x}_{t-\Delta_{ij}, t+N_p^j-\Delta_{ij}}^j(\tau) \right| &\leq \bar{\xi}_{\mathcal{N}}^i, \end{aligned} \quad (5.21)$$

Note that at the time of reception t , from (5.21), the useful part of the trajectory is that we recover is only $\tilde{w}_{t, t+N_p^j-\Delta_{ij}}^i$. Therefore, we need to recover the “tail” of the transmitted trajectory $\tilde{w}_{t+N_p^i-\Delta_{ij}, t+N_p^i}^i$. Since we have nominal model for the

dynamics of A^j as (5.8), we can predict the tail as

$$\tilde{w}_{t+N_p^i-\Delta_{ij}+1}^i = \tilde{g}^i \left(\tilde{w}_{t+N_p^i-\Delta_{ij}}^i \right), \dots, \tilde{w}_{t+N_p^i}^i = \tilde{g}^i \left(\tilde{w}_{t+N_p^i-1}^i \right) \quad (5.22)$$

The nominal model is not perfect, hence increasing the delay will increase tail approximation error. As shown in Section 5.3.1, the approximation error will be grow with delay, such that there is an upper limit to the maximum allowable delay $\bar{\Delta}^i$. An important factor in limiting the tolerable delay is the need to ensure collision avoidance. If the approximation error is greater (or delay is greater) than an upper bound, admissible control for avoiding collision may not exist. This means that agents will get too close due to trajectory approximation error, such that collision cannot be avoided in the sense of (5.25)-(5.27) (see Section 5.2.2), i.e. if there is not enough time to maneuver to avoid collision. Consequently, we assume an upper bound on the allowable delay $\Delta_t^{ij} \leq \bar{\Delta}$, which is the worst case scenario of two agents on a direct collision course at maximum allowable speed and with minimum separation between them, i.e.

$$\bar{\Delta} \triangleq R_{\min}/v_{\max} \quad (5.23)$$

With this conservative bound on Δ_t^{ij} , there is always enough time to execute collision avoidance manoeuvres.

5.2.2 Collision Avoidance

Let us first define the “distance” between two agents as the minimum distance between the balls of uncertainty around their predicted or estimated positions at any given instant.

$$d_k^{ij} \triangleq \text{dist}(\mathcal{B}(\tilde{x}_k^i, \bar{\rho}_{x_k}^i), \mathcal{B}(\tilde{w}_k^{j_i}, \bar{\rho}_{w_k}^i),) \quad (5.24)$$

We define an agent A^i to be on collision course with at least one other agent if

$$\sum_{j \in G^i} \mathbf{1}_{(R_{\min}^i - d_k^{ij}) > 0, \forall t \leq k \leq (t + N_p^i)} > 0, \quad \forall j \neq i \quad (5.25)$$

where R_{\min} safety zone of an agent and d_k^{ij} is the Euclidean distance between agent A^i and A^j . $\sum_{j \in G^i} \mathbf{1}_{(R_{\min}^i - d_k^{ij}) > 0, \forall t \leq k \leq (t + N_p^i)}$ represents the total number of agents in collision course with agent A^i . The definition of collision course is illustrated in Fig. 5.3. A repelling potential can be formulated as:

$$\Phi_t^i = \sum_{j \in G^i} \frac{\bar{\lambda} R_{\min}^i \mathbf{1}_{(R_{\min}^i - d_k^{ij}) > 0, \forall t \leq k \leq (t + N_p^i)}}{\sum_{k=t}^{t+N_p^i} \lambda(d_k^{ij}) d_k^{ij}} \quad (5.26)$$

where $0 < \lambda_{\min} \leq \lambda(d_{ij}) \leq \lambda_{\max}$ are positive weights of a filter and are strictly decreasing in their argument, such that $\bar{\lambda} \triangleq \sum_{k=t}^{t+N_p^i} \lambda(d_k^{ij})$. To take into account agents on a possible collision course, the cost (5.10) is then modified as:

$$\tilde{J}_t^i = J_t^i (1 + \Phi_t^i) \quad (5.27)$$

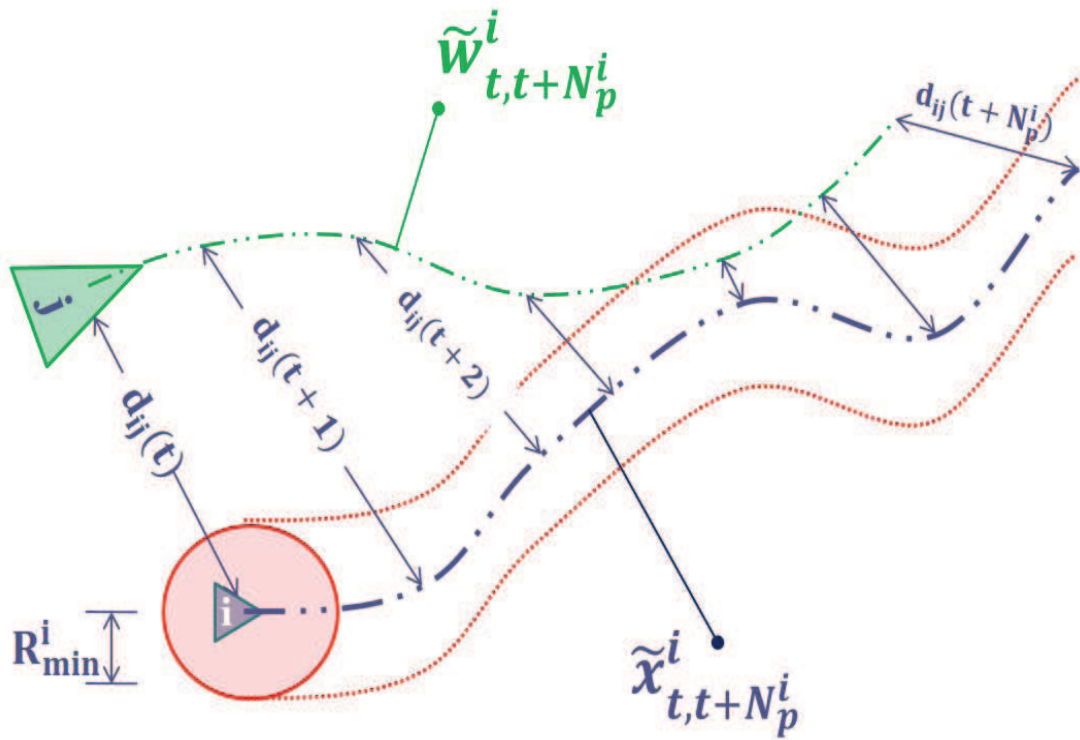


Figure 5.3: Illustration of the concept of collision course. Notice that in order to maintain clarity, the uncertainty balls $\mathcal{B}(\tilde{x}_k^i, \bar{\rho}_{x_k}^i)$ and $\mathcal{B}(\tilde{w}_k^{j_i}, \bar{\rho}_{w_k}^i)$ have not been depicted in the figure. Also, it is obvious that \tilde{w}_k^i stands for $\tilde{w}_k^{j_i}$ in the figure.

One should note that if at any instant $t \leq k \leq (t + N_p^i)$ in the prediction horizon, an agent A^i has a feasible trajectory which falls within R_{\min}^j of agent A^j , the cost of taking such a course would be increased from (5.10) to (5.27). In addition, the strength of potential field (5.26) is inversely proportional to the weighted average of the distance between the two agents

$$\bar{d}_t^{ij} = \frac{\sum_{k=t}^{t+N_p^i} \lambda(d_k^{ij}) d_k^{ij}}{\bar{\lambda}} \quad (5.28)$$

The weights λ , strictly decreasing with d_k^{ij} , ensure that the smallest separation between two agents gets the highest weight. On the other hand, taking a simple average (i.e. $\lambda \equiv 1$) or a time-based forgetting factor (λ is strictly decreasing with k , the time index), results in poor performance in collision avoidance, as trajectories which enter very late in zone R_{\min} (i.e. $R_{\min}^i - d_k^{ij} > 0, \forall k \rightarrow t + N_p^i$) have a small repelling potential (5.26), and hence not prevented from very early on. Such strategy results in agents getting very close before they start repelling each other to avoid collision, causing a loss of tracking performance. However, with the proposed cost modification as in (5.27), trajectories are immediately penalized upon falling within zone R_{\min}^j and are obviously avoided in the NMPC optimal control selection process, as depicted in Fig. 5.4. In other words, the potential (5.26) is present when feasible solutions fall inside R_{\min} . The indicator function in (5.26) acts as a “gain-scheduled” binary (0-1) variable depending on whether a feasible trajectory falls within R_{\min} . Conditions for stability of this approach are

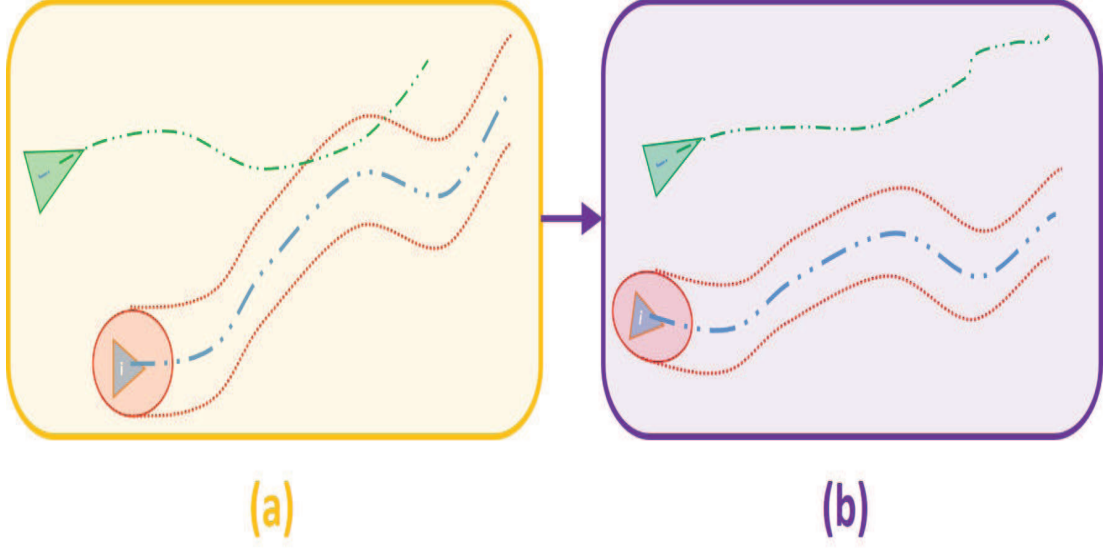


Figure 5.4: Illustration of the successful collision course. The agents were on collision course in (a), but collision avoidance mechanism pushed them away in (b).

shown in Section 5.5. We define successful collision avoidance to occur if weighted average distance between the agents on collision course is increased during the next time instant i.e.

$$\sum_{k=t}^{t+N_p^i} \lambda(d_k^{ij}) d_k^{ij} < \sum_{k=t+1}^{t+N_p^i+1} \lambda(d_k^{ij}) d_k^{ij} \quad (5.29)$$

Remark 5.2.1 *It should also be noted that since prediction uncertainty (5.30) and (5.31) increase with prediction horizon, the definition of inter-agent distance (5.24) also embeds temporal information in our novel spatially filtered potential field (5.26).*

5.3 Robustness Analysis

We will analyze the conditions for robust feasibility of the proposed multi-agent Algorithm. Therefore, the similar assumptions to the ones made in Section 3.2.5 are made.

Assumption 5.3.1 (Feasible Initial Sets) *There exist compact robust output feasible sets $X_{MPC}^i \subseteq X^i$ for each agent ($i = 1, \dots, N$), which is the set of initial states for which each optimal control problem 5.2.1 is feasible.*

This is an assumption of initial feasibility of the FHOCP 5.2.1 for each agent, which we will need to prove *recursive feasibility* later.

Assumption 5.3.2 (L. Continuity of Agent Transition Maps) . *We assume that transition maps $\tilde{f}^i(\cdot)$ and $\tilde{g}^i(\cdot)$ are locally Lipschitz continuous, such that*

I. $\tilde{f}^i(0, 0, 0) = 0$ and $\tilde{f}^i \in C^2$.

II. $\tilde{g}^i(0) = 0$

III. $|\tilde{f}^i(x_1^i, u_1^i, w_1^i) - \tilde{f}^i(x_2^i, u_2^i, w_2^i)| \leq L_{fx}^i |x_1^i - x_2^i| + L_{fu}^i |u_1^i - u_2^i| + L_{fw}^i |w_1^i - w_2^i|$
for $x_1^i, x_2^i \in X^i$, $u_1^i, u_2^i \in U^i$ and $w_1^i, w_2^i \in W^i$.

IV. $|\tilde{g}^i(w_1^i) - \tilde{g}^i(w_2^i)| \leq L_{gw}^i |w_1^i - w_2^i|$, for $w_1^i, w_2^i \in W$

Using these assumptions, we can now find the bounds used to tighten constraints for robust constraint satisfaction.

5.3.1 Constraint Tightening

Due to presence of estimation errors, prediction errors and propagation delays, we need to find bounds on the growth of errors in a way similar to the bounds derived in Section 3.2.5. However, we have to now do this in a multi-agent setting, as shown in this section.

Lemma 5.3.1 (Multi-Agent Prediction Error Bounds) *Given the following estimation and transition error bounds*

- i. Estimation error bounds $\bar{\xi}_x^i, \bar{\xi}_w^i \in \mathbb{R}_{\geq 0}$ defined in (5.3) and (5.7),*
- ii. One step transition error bounds $\bar{e}_x^i, \bar{e}_w^i \in \mathbb{R}_{\geq 0}$ defined in (5.13) and (5.9),*
- iii. Neural network approximation error $\xi_{\mathcal{N}_f}^i$, defined in (5.21).*

and Lipschitz constants defined in Assumption 5.3.2, then the l -step prediction error in predicting $x_{t,t+N_p}$ is bounded by

$$|x_{t+l}^i - \tilde{x}_{t+l}^i| \leq L_{fx}^{i,l} \bar{\xi}_x^i + \bar{e}_x^i \frac{L_{fx}^{i,l} - 1}{L_{fx}^i - 1} \quad (5.30)$$

and the l -step prediction error in predicting $w_{t,t+N_p}$ is bounded by

$$|w_{t+l}^i - \tilde{w}_{t+l}^i| = \sum_{j \in G^i} |w_{t+l}^i - \tilde{w}_{t+l}^i|_j \quad (5.31)$$

where,

$$|w_{t+l}^{ij} - \tilde{w}_{t+l}^{ij}|_j \triangleq \begin{cases} L_{fx}^{j^l} \bar{\xi}_x^j + \bar{e}_x^j \frac{L_{fx}^{j^l} - 1}{L_{fx}^j - 1} + \bar{\xi}_N^i, & \forall l = 0, \dots, N_P^j - \Delta_{ij} - 1 \\ L_{gw}^{i^{l-(N_P^i - \Delta_{ij})}} \bar{\rho}_{w, N_P^i}^i + \bar{e}_w^i \frac{L_{gw}^{i^{l-(N_P^i - \Delta_{ij})}} - 1}{L_{gw}^i - 1}, & \forall l = N_P^i - \Delta_{ij}, \dots, N_P^i \end{cases} \quad (5.32)$$

and

$$\bar{\rho}_{w, N_P^i}^i \triangleq L_{fx}^{j^{N_P^i - \Delta_{ij}}} \bar{\xi}_x^j + \bar{e}_x^j \frac{L_{fx}^{j^{N_P^i - \Delta_{ij}}} - 1}{L_{fx}^j - 1} + \bar{\xi}_N^i \quad (5.33)$$

for $i = 1, \dots, N$, $l = 0, \dots, N_P$, and $L_{fx}, L_{gw} \neq 1$.

Proof. Let us first look at the prediction error for the agent A^i . From (5.3), we have for $l = 0$

$$|x_t^i - \tilde{x}_t^i| \leq \bar{\xi}_x^i$$

At the next sampling instant, i.e. $l = 1$, we have from (5.5), (5.8), (5.7) and (5.9)

$$\begin{aligned} |x_{t+1}^i - \tilde{x}_{t+1}^i| &= \left| f^i(x_t^i, u_t^i, \tilde{w}_t^i) - \tilde{f}^i(\tilde{x}_t^i, u_t^i, \tilde{w}_t^i) \right| \\ &= \left| \tilde{f}^i(x_t^i, u_t^i, \tilde{w}_t^i) + \bar{e}_x^i - \tilde{f}^i(\tilde{x}_t^i, u_t^i, \tilde{w}_t^i) \right| \\ &\leq \left| \tilde{f}^i(x_t^i, u_t^i, \tilde{w}_t^i) + \bar{e}_x^i - \tilde{f}^i(\tilde{x}_t^i, u_t^i, \tilde{w}_t^i) \right| + \bar{e}_x^i \end{aligned}$$

But, in view of Assumption 5.3.2

$$|x_{t+1}^i - \tilde{x}_{t+1}^i| \leq L_{fx}^i |x_t^i - \tilde{x}_t^i| + \bar{e}_x^i \leq L_{fx}^i \bar{\xi}_x^i + \bar{e}_x^i \quad (5.34)$$

At next sampling instant when $l = 2$,

$$|x_{t+2}^i - \tilde{x}_{t+2}^i| \leq L_{fx}^i |x_{t+1}^i - \tilde{x}_{t+1}^i| + \bar{e}_x^i$$

Substituting (5.34)

$$|x_{t+2}^i - \tilde{x}_{t+2}^i| \leq L_{fx}^i (L_{fx}^i \bar{\xi}_x^i + \bar{e}_x^i) + \bar{e}_x^i = \bar{\xi}_x^i L_{fx}^{i2} + \bar{e}_x^i (L_{fx}^i + 1) \quad (5.35)$$

Finally, following the same development as above, we can show that for $l = 3$

$$|x_{t+3}^i - \tilde{x}_{t+3}^i| \leq \bar{\xi}_x^i L_{fx}^{i3} + \bar{e}_x^i (L_{fx}^{i2} + L_{fx}^i + 1) \quad (5.36)$$

So generalizing from (5.34)-(5.36) for l -step ahead prediction

$$|x_{t+l}^i - \tilde{x}_{t+l}^i| \leq L_{fx}^{il} \bar{\xi}_x^i + \bar{e}_x^i \left(\sum_{k=0}^{l-1} L_{fx}^{ik} \right) = L_{fx}^{il} \bar{\xi}_x^i + \bar{e}_x^i \frac{L_{fx}^{il} - 1}{L_{fx}^i - 1}$$

which proves (5.30).

Now, consider prediction error for the information vector. From (5.7). Assume that A^i receives the neural network from only A^j after a delay of Δ_{ij} sampling instants. Then, from (5.30), at $t + l$ we have

$$|x_{t+l}^j - \tilde{x}_{t+l}^j| = |w_{t+l}^j - \tilde{x}_{t+l}^j| \leq L_{fx}^{jl} \bar{\xi}_x^j + \bar{e}_x^j \frac{L_{fx}^{jl} - 1}{L_{fx}^j - 1} \quad (5.37)$$

Note that $w_{t+l}^i = x_{t+l}^j$. Now, as mentioned in Section 5.2.1, we compress $\tilde{x}_{t,t+N_p^j}^j$ with neural network \mathcal{N}^j , but the packet that arrives at A^j was compressed at $t - \Delta_{ij}$. Hence, we are only able to recover $\tilde{w}_{t-\Delta_{ij},t+N_p^j}$. From (5.21), we can write that

$$|\tilde{w}_{t+l}^i - \tilde{x}_{t+l}^j| \leq \bar{\xi}_{\mathcal{N}}^i, \quad \forall l = 0, \dots, N_p^j - \Delta_{ij}$$

Using the inequality above in (5.37), we get

$$\begin{aligned} |w_{t+l}^i - \tilde{w}_{t+l}^i| &= |w_{t+l}^i - \tilde{x}_{t+l}^j - (\tilde{w}_{t+l}^i - \tilde{x}_{t+l}^j)| \\ &\leq L_{fx}^{j,l} \bar{\xi}_x^j + \bar{e}_x^j \frac{L_{fx}^{j,l} - 1}{L_{fx}^j - 1} + \bar{\xi}_{\mathcal{N}}^i, \quad \forall l = 0, \dots, N_p^j - \Delta_{ij} \end{aligned} \quad (5.38)$$

Now, we look at the error in estimating the tail as mentioned in Section 5.2.1.

Since we estimate the tail with the nominal model of the information vector given in (5.8), using (5.22) at $l = N_p^i - \Delta_{ij} + 1$, we get

$$\begin{aligned} \left| w_{t+N_p^i-\Delta_{ij}+1}^i - \tilde{w}_{t+N_p^i-\Delta_{ij}+1}^i \right| &= \left| g^i \left(w_{t+N_p^i-\Delta_{ij}}^i, \phi_{t+N_p^i-\Delta_{ij}}^i \right) - \tilde{g}^i \left(\tilde{w}_{t+N_p^i-\Delta_{ij}}^i \right) \right| \\ &\leq \left| \tilde{g}^i \left(w_{t+N_p^i-\Delta_{ij}}^i \right) - \tilde{g}^i \left(\tilde{w}_{t+N_p^i-\Delta_{ij}}^i \right) + \bar{e}_w^i \right| \\ &\leq L_{gw}^i \left| w_{t+N_p^i-\Delta_{ij}}^i - \tilde{w}_{t+N_p^i-\Delta_{ij}}^i \right| + \bar{e}_w^i \end{aligned}$$

Now, substitute (5.38) in the inequality above

$$\left| w_{t+N_p^i-\Delta_{ij}+1}^i - \tilde{w}_{t+N_p^i-\Delta_{ij}+1}^i \right| \leq L_{gw}^i \left(L_{fx}^{j, N_p^i-\Delta_{ij}} \bar{\xi}_x^j + \bar{e}_x^j \frac{L_{fx}^{j, N_p^i-\Delta_{ij}} - 1}{L_{fx}^j - 1} + \bar{\xi}_{\mathcal{N}}^i \right) + \bar{e}_w^i$$

Using the same development as in the derivation of (5.30), we can generalize

$$\begin{aligned} |w_{t+l}^i - \tilde{w}_{t+l}^i| \leq & L_{gw}^{l-(N_p^i - \Delta_{ij})} \left(L_{fx}^{j N_p^i - \Delta_{ij}} \bar{\xi}_x^j + \bar{e}_x^j \frac{L_{fx}^{j N_p^i - \Delta_{ij}} - 1}{L_{fx}^j - 1} + \bar{\xi}_{\mathcal{N}}^i \right) \\ & + \bar{e}_w^i \frac{L_{gw}^{l-(N_p^i - \Delta_{ij})} - 1}{L_{gw}^i - 1}, \quad \forall l = t + N_p^i - \Delta_{ij}, \dots, t + N_p^i \end{aligned} \quad (5.39)$$

Therefore, combining (5.38) and (5.39) and generalizing for multiple neighbors (noting that the norm of a vector of positive values is less than the sum of the vector elements), we prove (5.31). ■

The same comments as in Remark 3.2.1 are applicable in the multi-agent case. Notice that the error growth bound are markedly different from the single agent case in Section 3.2.5. Since the nominal models of agents (5.12) are similar to the nominal model in (3.5), we will state the following without a formal proof, as it is the same as in Chapter 4.

Claim 5.3.1 (Terminal Set and Terminal Control for Agents) *There exists an terminal control $k_f^i(\tilde{x}_l^i) \in U^i, \forall l = N_C^i, \dots, N_P^i - 1$, application of which to the nominal plant $\tilde{x}_{t+l}^i = \tilde{f}(\tilde{x}_l^i, k_f(\tilde{x}_l^i), 0)$ ensures that a terminal constraint set X_f^i is robust positively invariant (RPI) i.e. $x_l^i \in X_f^i$ and $\tilde{x}_l^i \in X_f^i$, $\forall l = t + N_C^i + 1, \dots, t + N_P^i$ for any $\tilde{x}_{t+N_C^i}^i \in X_f^i$, such that*

- I. *The rate of convergence of nominal state \tilde{x} under control $k_f(\tilde{x})$ is lower bounded by*

$$\left| \tilde{f}^i(\tilde{x}_{t+l+1}, k_f(\tilde{x}_{t+l+1})) - \tilde{x}_{t+l+1}^i \right| \geq \bar{\xi}_x^i L_{fx}^{i l} (L_{fx}^i - 1) + \bar{e}_x^i L_{fx}^i, \quad (5.40)$$

for $l = N_C^i - 1 \dots N_P^i - 2$, and (b) there exists $a^i \in \mathbb{Z}_{\geq 0}$ and $0 \leq Q_f^i \in \mathbb{R}^{n^i \times n^i}$

such that

$$\tilde{x}^{iT} Q_f^i \tilde{x}^i \leq a, \quad \forall \tilde{x}^i \in X_f^i \quad (5.41)$$

By considering the effect of the prediction uncertainty bounds on the constraints, it is possible to guarantee that state evolution of the actual system will be admissible as well.

Theorem 5.3.1 (Agent Constraint Tightening) *With actual constraints X^i and W^i defined in (5.2), let the **tightened constraints** be given by*

$$\tilde{X}_{t+l}^i \triangleq X^i \sim \mathcal{B}^{n^i} \left(\bar{\rho}_{x_{t+l}}^i \right), \quad (5.42)$$

$$\tilde{W}_{t+l}^i \triangleq W^i \sim \mathcal{B}^{p^i} \left(\bar{\rho}_{w_{t+l}}^i \right), \quad (5.43)$$

for $i = 1, \dots, N$ and $l = 0, \dots, N_P^i$, where $\bar{\rho}_x^i$ is the prediction error bound in Lemma 5.3.1 defined as

$$\bar{\rho}_{x_{t+l}}^i \triangleq L_{fx}^{i,l} \bar{\xi}_x^i + \bar{e}_x^i \frac{L_{fx}^{i,l} - 1}{L_{fx}^i - 1} \quad (5.44)$$

and

$$\bar{\rho}_{w_{t+l}}^i \triangleq \sum_{j \in G^i} |w_{t+l}^i - \tilde{w}_{t+l}^i|_j, \quad (5.45)$$

with defined in $|w_{t+l}^i - \tilde{w}_{t+l}^i|_j$ defined in (5.32)-(5.33). Then, any (in general suboptimal) admissible control sequence $u_{t,t+N_C^i-1}^i$ and terminal control $u_{t+N_C^i, t+N_P^i-1}^i = k_f^i(\tilde{x}_{t+N_C^i, t+N_P^i-1}^i)$ which is feasible ($\tilde{x}_{t+l}^i \in \tilde{X}_{t+l}^i$, $u_{t,t+N_P^i-1}^i \in U^i$)

and $\tilde{w}_{t+l}^i \in \tilde{W}_{t+l}^i$) with respect to tightened constraints (5.42) applied to the actual system (5.18), guarantees the satisfaction of original constraints (5.2), i.e. $x_{t+l}^i \in X^i$ for $l = 0, \dots, N_P^i$ and $x_t^i \in X_{MPC}^i$.

Proof. The proof is very similar to the proof of Theorem 3.2.1, and therefore will not be repeated here. ▮

Remark 5.3.1 *Constraint tightening (5.42) is novel as it is the first time that such a variety of uncertainty contributions have been considered simultaneously in the multi-agent case. Remarkably, an explicit bound on growth in uncertainty is derived based on the tail reconstruction. Besides, estimation, prediction and data compression errors are also considered. This leads to very general bounds on prediction error, which can be specialized to specific cases (e.g. perfect measurement will mean $\xi_x^i \rightarrow 0$).*

The constraint tightening procedure is summarized in the algorithm below.

Algorithm 8 Agent Constraint Tightening

- 1: **Given** (I) nominal models $\tilde{f}^i(\tilde{x}^i, u^i, \tilde{w}^i)$, $\tilde{g}^i(\tilde{w}^i)$, (ii) uncertainty bounds $\bar{\xi}_x^i$, $\bar{\xi}_w^i$, $\bar{\xi}_N^i$, \bar{e}_x^i , \bar{e}_w^i and horizons N_C^i , N_P^i .
 - 2: **procedure** CONSTRAINT TIGHTENING
 - 3: **Calculate** Lipschitz constants of nonlinear maps $\tilde{f}^i(\tilde{x}^i, u^i, \tilde{w}^i)$ and $\tilde{g}^i(\tilde{w}^i)$.
 - 4: **Calculate** the prediction error bounds in (5.44) and (5.45).
 - 5: **Tighten** the constraints by Pontryagin difference as given in (5.42)-(5.43).
 - 6: **end procedure**
-

5.4 Robust Recursive Feasibility without Collision Avoidance

In this section, we assume agents are not on collision course. Later we will also consider the case where collision avoidance becomes active. We defined the robust output feasible set X_{MPC}^i in Assumption 5.3.1 as the set of initial states for which the OCP 5.2.1 is feasible. We will prove the recursive feasibility of the Algorithm using arguments very similar to those in Theorem 3.1.

Definition 5.4.1 (Agent One-Step Controllable Set of X_f^i) *The one-step controllability set to the terminal constraint set X_f^i is defined as*

$$\mathcal{C}_1^i(X_f^i, \tilde{X}_{t+N_c}^i) \triangleq \left\{ \tilde{x}^i \in \tilde{X}_{t+N_c}^i : \tilde{f}(\tilde{x}^i, u, \tilde{w}^i) \in X_f^i, u^i \in U^i, \tilde{w}_t^i \in \tilde{W}^i \right\} \quad (5.46)$$

Let us also define $\bar{d}^i \triangleq \text{dist}(\tilde{X}_{t+N_c}^i \setminus \mathcal{C}_1^i(X_f^i, \tilde{X}_{t+N_c}^i), X_f^i)$.

Numerical computation of $\mathcal{C}(X, X_f)$ will be carried out using Algorithm 5.

Assumption 5.4.1 (Feasibility Bounds on Uncertainties) *The following bounds apply to the allowable uncertainties*

I. Lower bound on uncertainty growth

$$\bar{\rho}_{x_{t+l}}^i - \bar{\rho}_{x_{t+l-1}}^i \geq L_{fx}^{i^{l-1}} \left(\underline{\xi}_x^i \right) \quad (5.47)$$

for $l = 1, \dots, N_C$.

II. *Uncertainties are upper bounded by minimum size of one-step controllability set to terminal constraint set*

$$L_{fx}^{iN_c^i-1} ((L_{fx}^i + 1) \bar{\xi}_x^i + \bar{e}_x^i) \leq \bar{d} \quad (5.48)$$

Recursive feasibility and robust positive invariance of feasible region X_{MPC}^i can now be stated.

Theorem 5.1 (Agent Recursive Feasibility without Collision Avoidance)

Under Assumptions 5.3.2 and 5.4.1, terminal control (Claim 5.3.1), suitable bounds on uncertainties (Assumption 5.4.1) and tightened constraints (Theorem 5.3.1), given the feasibility of initial state $\tilde{x}_t^i \in X_{MPC}^i$ (Assumption 5.3.1), the FHOCP 5.2.1 is recursively feasible.

Proof. The proof is similar to the proof of Theorem 3.1 and can be easily derived from the proof of that theorem, and therefore not reproduced here. ▀

Due to obvious similarities, algorithms in Chapter 4 can be utilized for determining the robust one-step controllability set to X_f^i feasibility region X_{MPC}^i .

5.5 Stability Analysis

The stability of the multi-agent team is more involved than the case of a single system. Therefore, stability analysis will be carried out in three steps.

- i. We will first ignore the interconnections and consider the stability of the agents without collision avoidance.

- ii. While still ignoring interconnections we will study the stability of agents with collision avoidance active.
- iii. We will take into consideration the interconnections among agents and study the stability of the team without collision avoidance.
- iv. Finally, we will study the stability of the team with collision avoidance active.

In the first case, the multi-agent system is very similar to the single system studied in Chapters 3-4, therefore some of the results will be stated without proof, unless required. We will build on these results to prove the stability of the team under collision avoidance.

5.5.1 Stability of Individual Agents without Collision Avoidance

In the proposed approach, the uncertainty in trajectory approximation $\xi_{\mathcal{N}}^i$ is non-vanishing, even if other sources of uncertainty are not present and therefore one can only guarantee practical (ultimately bounded) stability. We consider first the stability of individual agent A^i with respect to the information received from other agents, by exploiting Theorem 3.2.2. At this stage the interconnections are ignored, and hence information from neighbors is considered as external input. We assume at this stage that agents generate conflict free trajectories. We will make the following useful assumptions.

Assumption 5.5.1 (Distributed Cost Lipschitz Continuity) *We assume*

that components of distributed cost (5.10) $k_f^i(\cdot)$, $h^i(\cdot)$, $q^i(\cdot)$ and $h_f^i(\cdot)$ are locally Lipschitz continuous and there are nonlinear functions relating to the cost components.

$$I. \quad |k_f^i(\tilde{x}^i)| \leq L_{k_f^i} |\tilde{x}^i|, \text{ for } \tilde{x}^i \in \tilde{X}_f^i$$

$$II. \quad |h^i(\tilde{x}^i, u^i)| \leq L_{hx}^i |\tilde{x}^i| + L_{hu}^i |u^i|, \text{ for } \tilde{x}^i \in \tilde{X}_t^i \text{ and } u^i \in U^i$$

$$III. \quad 0 \leq |q^i(\tilde{x}^i, \tilde{w}^i)| \leq L_{qx}^i |\tilde{x}^i| + L_{qw}^i |\tilde{w}^i|, \text{ for } \tilde{x}^i \in \tilde{X}_t^i \text{ and } \tilde{w}^i \in \tilde{W}_t^i$$

$$IV. \quad |h_f^i(\tilde{x}^i)| \leq L_{hf}^i |\tilde{x}^i| \text{ for } \tilde{x}^i \in \tilde{X}_f^i$$

$$V. \quad \alpha_1^i(|\tilde{x}_t^i|) \leq h(\tilde{x}_t^i, u_t^i), \text{ for } \tilde{x}_t^i \in \tilde{X}_t^i.$$

$$VI. \quad \alpha_{1,f}^i(|\tilde{x}_t^i|) \leq h_f^i(\tilde{x}_t^i) \leq \alpha_{2,f}^i(|\tilde{x}_t^i|), \text{ for all } \tilde{x}_t^i \in \tilde{X}_t^i,$$

with positive local Lipschitz constants $L_{k_f}^i$, L_{hx}^i , L_{hu}^i , L_{qx}^i , L_{qw}^i and L_{hf}^i .

We will introduce a few definitions, similar to 3.2.2.

Lemma 5.5.1 (Technical) *With reference to Definition 2.5.9, the following hold for practical stability of the nominal system (5.12) with nominal disturbance model (5.8) under RH control (5.17),*

$$(i). \quad \alpha_1^i(s) = \alpha_2^i(s) \triangleq \min h^i(s, 0)$$

$$(ii). \quad \alpha_3^i(s) \triangleq \alpha_{2,f}^i(L_{fx}^{iN_p^i} s) + (L_{hx}^i + L_{hu}^i L_{kf}^i + L_{qx}^i) \frac{(L_{fx}^i)^{N_p^i} - 1}{L_{fx}^i - 1} s$$

$$(iii). \quad \sigma_1^i(s) \triangleq \frac{L_{qw}^{iN_p^i} - 1}{L_{qw}^i - 1} L_{qw}^i L_{gw} \cdot s$$

$$(iv). \quad \sigma_2^i(s) \triangleq \sigma_1^i\left(\frac{s}{L_{gw}^i}\right) + \psi^i(s)$$

$$(v). \quad \sigma_3^i(s) \triangleq L_{qw}^i \frac{(L_{gw}^i)^{N_p^i} - 1}{L_{gw}^i - 1} s$$

$$(vi). \quad \bar{c}^i \triangleq \left(\begin{array}{c} \frac{L_{fx}^{iN_p^i} - 1}{L_{fx}^i - 1} (L_{qx}^i + L_{hx}^i) \\ + L_{hu}^i L_{kf}^i \frac{L_{fx}^{iN_p^i} - L_{fx}^{iN_c^i}}{L_{fx}^i - 1} + L_{fx}^{iN_p^i} \end{array} \right) c_1^i + L_{hu}^i (|u_{\max}^i| + |u_{\min}^i|)$$

$$(vii). \quad \bar{e}^i = 0,$$

$$\text{where } c_1^i \triangleq \bar{\xi}_x^i + L_{fx}^i \bar{\xi}_x^i + \bar{e}^i.$$

With these definitions, we can now state the stability of the nominal model (5.12) without collision avoidance.

Theorem 5.5.1 *Let there be a terminal set $\tilde{X}_f^i \subset \tilde{X}^i$ and auxiliary control $k_f^i(x)$ according to Claim 5.3.1, such that Assumptions 5.3.1, 5.3.2, 5.4.1 and 5.5.1 hold.*

If the following condition holds for some $\psi \in \mathcal{K}$

$$h_f^i \left(\tilde{f}^i(\tilde{x}^i, k_f^i(\tilde{x}^i)) \right) - h_f^i(\tilde{x}^i) \leq -h^i(\tilde{x}^i, k_f^i(\tilde{x}^i)) - q^i(\tilde{x}^i, \tilde{w}^i) + \psi^i(|\tilde{w}^i|), \quad (5.49)$$

for all $\tilde{x}^i \in X_f^i$ and $\tilde{w}^i \in \tilde{W}^i$, then the nominal system (5.12) under NMPC optimal control (5.17) which optimizes cost (5.10) admits the optimal value of cost functional $V_t^i(\tilde{x}_t^i, u_t^i, \tilde{w}_t^i) = J_t^i(\tilde{x}_t^i, u_{t,t+N_p^i}^0, \tilde{w}_t^i)$ as an ISpS Lyapunov function. It is therefore input-to-state practically stable (ISpS) for all initial states within the robust output feasible set $X_{MPC}^i \subseteq X^i$.

Proof. We need to prove that $V_t^i(\tilde{x}_{t|t}^i, u_t^i, \tilde{w}_{t|t}^i) = J_t^i(\tilde{x}_{t|t}^i, u_{t,t+N_p^i}^0, \tilde{w}_{t|t}^i)$ is an ISS Lyapunov function in X_{MPC}^i . From (5.10), the optimal cost is given as

$$\begin{aligned}
V_t^i(\tilde{x}_{t|t}^i, u_{t,t+N_c-1|t}^{i\circ}, \tilde{w}_{t|t}^i) &= h^i(\tilde{x}_{t|t}^i, u_{t|t}^{i\circ}) + q^i(\tilde{x}_{t|t}^i, \tilde{w}_{t|t}^i) + \\
&\sum_{l=t+1}^{t+N_c^i-1} [h^i(\tilde{x}_{l|t}^i, u_{l|t}^{i\circ}) + q^i(\tilde{x}_{l|t}^i, \tilde{w}_{l|t}^i)] + \\
&\sum_{l=t+N_c^i}^{t+N_p^i-1} [h^i(\tilde{x}_{l|t}^i, u_{l|t}^{i\circ}) + q(\tilde{x}_{l|t}^i, \tilde{w}_{l|t}^i)] + h_f^i(\tilde{x}_{t+N_p|t}^i) \quad (5.50)
\end{aligned}$$

The lower bound on $V_t^i(\tilde{x}_{t|t}^i, u_{t|t}^i, \tilde{w}_{t|t}^i)$ is obviously given by (Assumption 5.5.1)

$$\alpha_1^i(|\tilde{x}_{t|t}^i|) \leq V_t^i(\tilde{x}_{t|t}^i, u_{t,t+N_p^i|t}^{i\circ}, \tilde{w}_{t|t}^i), \quad \forall \tilde{x}_{t|t}^i \in \tilde{X}_{t|t}^i \supseteq X^i, \tilde{w}_{t|t}^i \in \tilde{W}_{t|t}^i \subseteq W^i \quad (5.51)$$

The control sequence $\tilde{u}_{t,t+N_c^i-1|t}^i = [k_f^i(\tilde{x}_{t|t}^i), \dots, k_f^i(\tilde{x}_{t+N_c^i-1|t}^i)]^T$ is feasible (but in general suboptimal) for any $\tilde{x}_{t|t}^i \in X_f^i$. Using Assumptions 5.3.2 and 5.5.1 and steps similar to the ones in the proof of Theorem 3.2.2, we can write

$$\begin{aligned}
V_t^i(\tilde{x}_{t|t}^i, u_{t,t+N_c-1|t}^{i\circ}, \tilde{w}_{t|t}^i) &\leq (L_{hx}^i + L_{hu}^i L_{kf}^i + L_{qx}^i) \frac{(L_{fx}^i)^{N_p^i} - 1}{L_{fx}^i - 1} |\tilde{x}_{t|t}^i| \\
&+ L_{qw}^i \frac{(L_{gw}^i)^{N_p^i} - 1}{L_{gw}^i - 1} |\tilde{w}_{t|t}^i| + \alpha_{2f}^i \left((L_{fx}^i)^{N_p^i} |\tilde{x}_{t|t}^i| \right) \\
&\leq \alpha_3^i(|\tilde{x}_{t|t}^i|) + \sigma_3^i(|\tilde{w}_{t|t}^i|) + \bar{c}^i \quad (5.52)
\end{aligned}$$

for $\tilde{x}_{t|t}^i \in X_f^i$ and $\tilde{w}_{t|t}^i \in \tilde{W}_{t|t}^i$. It is obvious that α_3^i , σ_3^i and \bar{c}^i are as defined in Lemma 5.5.1. For (5.52) to hold, $L_{fx}^i, L_{gw}^i \neq 1$. However, following the reasons explained in Remark 3.2.1, in the very special case of $L_{fx} = 1$ and/or $L_{gx} = 1$, minor modifications are required (5.52). Refer to Assumption 5.4.1 and the result expressed in Theorem 5.1, which states that given the optimal control se-

quence $u_{t,t+N_c^i-1|t}^{i^0}$ at time t for $\tilde{x}_t^i \in \tilde{X}_t^i$, there exists at least one feasible control $u_{t+1,t+N_c^i|t+1}^i = [u_{t+1,t+N_c^i-1|t}^{i^0}, u_{t+N_c^i|t+1}^i]^T$ at $t+1$, where $u_{t+N_c^i|t+1}^i \in U^i$ is such that $\tilde{x}_{t+N_c^i+1|t+1}^i \in X_f^i$ any $x_t^i \in X_{MPC}^i$. Also, note that since new measurements are made at $t+1$, nominal estimates $x_{t+1|t+1}^i$ and $w_{t+1|t+1}^i$ at $t+1$ are different than the estimates $x_{t+1|t}^i$ and $w_{t+1|t}^i$, even though the same model is used for prediction. The cost of using this (suboptimal, in general) control can be shown to be

$$\begin{aligned}
V_{t+1}^i(\tilde{x}_{t+1|t+1}^i, u_{t+1,t+N_c^i|t+1}^{i^0} \tilde{w}_{t+1|t+1}^i) &\leq \\
&V_t^i(\tilde{x}_{t|t}^i, u_{t,t+N_c^i-1|t}^{i^0}, \tilde{w}_{t|t}^i) - h^i(\tilde{x}_{t|t}^i, u_{t|t}^{i^0}) - q(\tilde{x}_{t|t}^i, \tilde{w}_{t|t}^i) \\
&+ \sum_{l=t+1}^{t+N_c^i-1} [h^i(\tilde{x}_{l|t+1}^i, u_{l|t}^{i^0}) - h^i(\tilde{x}_{l|t}^i, u_{l|t}^{i^0}) + q^i(\tilde{x}_{l|t+1}^i, \tilde{w}_{l|t+1}^i) - q^i(\tilde{x}_{l|t}^i, \tilde{w}_{l|t}^i)] \\
&+ h^i(\tilde{x}_{t+N_c^i|t+1}^i, u'_{t+N_c^i|t+1}) - h^i(\tilde{x}_{t+N_c^i|t}^i, k_f^i(\tilde{x}_{t+N_c^i|t}^i)) \\
&+ q^i(\tilde{x}_{t+N_c^i|t+1}^i, \tilde{w}_{t+N_c^i|t+1}^i) - q^i(\tilde{x}_{t+N_c^i|t}^i, \tilde{w}_{t+N_c^i|t}^i) \\
&+ \sum_{l=t+N_c^i+1}^{t+N_p^i-1} \left[\begin{aligned} &h^i(\tilde{x}_{l|t+1}^i, k_f^i(\tilde{x}_{l|t+1}^i)) - h^i(\tilde{x}_{l|t}^i, k_f^i(\tilde{x}_{l|t}^i)) \\ &+ q^i(\tilde{x}_{l|t+1}^i, \tilde{w}_{l|t+1}^i) - q^i(\tilde{x}_{l|t}^i, \tilde{w}_{l|t}^i) \end{aligned} \right] \\
&+ h^i(\tilde{x}_{t+N_p^i|t+1}^i, k_f^i(\tilde{x}_{t+N_p^i|t+1}^i)) + q^i(\tilde{x}_{t+N_p^i|t+1}^i, \tilde{w}_{t+N_p^i|t+1}^i) \\
&+ h_f^i(\tilde{f}^i(\tilde{x}_{t+N_p^i|t+1}^i, k_f^i(\tilde{x}_{t+N_p^i|t+1}^i))) - h_f^i(\tilde{x}_{t+N_p^i|t}^i) \quad (5.53)
\end{aligned}$$

Now, we compute upper limits on the components of (5.53). From Assumptions 5.5.1, 5.3.2 and 5.3.1 for $l = 1, \dots, N_C - 1$, and using steps similar to the ones in proof of Theorem 3.2.2, we obtain

$$|h^i(\tilde{x}_{t+l|t+1}^i, u_{t+l|t}^{i^0}) - h^i(\tilde{x}_{t+l|t}^i, u_{t+l|t}^{i^0})| \leq L_{hx}^i L_{fx}^{i-1} (\bar{\xi}_x^i + L_{fx}^i \bar{\xi}_x^i + \bar{e}_x^i) \quad (5.54)$$

for $l = 1, \dots, N_C^i - 1$. Using the treatment of (5.54)

$$\begin{aligned} & \left| q^i(\tilde{x}_{t+l|t+1}^i, \tilde{w}_{t+l|t+1}^i) - q^i(\tilde{x}_{t+l|t}^i, \tilde{w}_{t+l|t}^i) \right| \\ & \leq L_{qx}^i L_{fx}^{i^{l-1}} (\bar{\xi}_x^i + L_{fx}^i \bar{\xi}_x^i + \bar{e}_x^i) + L_{qw}^i L_{gw}^{i^{l-1}} (L_{gw}^i |\tilde{w}_{t|t}^i| + |\tilde{w}_{t+1|t+1}^i|) \end{aligned} \quad (5.55)$$

$l = 1, \dots, N_P^i - 1$. Similarly,

$$\begin{aligned} & \left| h^i(\tilde{x}_{t+l|t+1}^i, k_f^i(\tilde{x}_{t+l|t+1}^i)) - h^i(\tilde{x}_{t+l|t}^i, k_f^i(\tilde{x}_{t+l|t}^i)) \right| \\ & \leq (L_{hx}^i + L_{hu}^i L_{kf}^i) L_{fx}^{i^{l-1}} (\bar{\xi}_x^i + L_{fx}^i \bar{\xi}_x^i + \bar{e}_x^i) \end{aligned} \quad (5.56)$$

for $l = N_C^i + 1, \dots, N_P^i - 1$. Now, the difference between transition costs at N_C^i .

$$\begin{aligned} & \left| h^i(\tilde{x}_{t+N_C^i|t+1}^i, u'_{t+N_C^i|t+1}) - h^i(\tilde{x}_{t+N_C^i|t}^i, k_f^i(\tilde{x}_{t+N_C^i|t}^i)) \right| \\ & \leq L_{hx}^i L_{fx}^{i^{N_C^i-1}} (\bar{\xi}_x^i + L_{fx}^i \bar{\xi}_x^i + \bar{e}_x^i) + L_{hu}^i (|u_{\max}^i| + |u_{\min}^i|) \end{aligned} \quad (5.57)$$

and finally we can show that

$$- h_f(\tilde{x}_{t+N_P^i|t}) \leq -h_f(\tilde{x}_{t+N_P^i|t+1}) + L_{hx}^i L_{fx}^{i^{N_P^i-1}} (\bar{\xi}_x^i + L_{fx}^i \bar{\xi}_x^i + \bar{e}_x^i) \quad (5.58)$$

Substituting inequalities (5.54) - (5.58) in (5.53) and following the steps in proof of Theorem 3.2.2, we can write

$$V_{t+1}^i(\tilde{x}_{t+1|t+1}^i, u_{t+1,t+N_C^i|t+1}^{i\circ} \tilde{w}_{t+1|t+1}^i) - V_t^i(\tilde{x}_{t|t}^i, u_{t,t+N_C^i-1|t}^{i\circ}, \tilde{w}_{t|t}^i) \leq$$

$$\begin{aligned}
& - \alpha_2^i(|\tilde{x}_t^i|) + \sigma_1^i(|\tilde{w}_t^i|) + \sigma_2^i(|\tilde{w}_{t+1}^i|) + \bar{c}^i \\
& \forall \tilde{x}_t^i \in X_{MPC}^i, \forall \tilde{w}_t^i \in \tilde{W}_t^i, \tilde{w}_{t+1}^i \in \tilde{W}_{t+1}^i, \quad (5.59)
\end{aligned}$$

where α_2^i , σ_1^i , σ_2^i , and \bar{c}^i are as defined in Lemma 5.5.1. Hence, in view of Theorem 2.5.2 and inequalities (5.51), (5.52) and (5.59), the nominal system (5.12)-(5.8) under RH optimal control (5.17) is ISpS in X_{MPC}^i . Hence, in reference to Theorem 2.5.2, we can write

$$|\tilde{x}_{t+l|t+l}^i| \leq \tilde{\beta}^i(|\tilde{x}_{t|t}^i|, l) + \tilde{\gamma}^i(\|\tilde{w}_{[t+l|t+l]}^i\|) + \bar{c}^i \quad (5.60)$$

according to the definitions given in Theorem 2.5.2. █

We have shown practical (ISpS) stability of the nominal system under NMPC control. However, we are more interested in the trajectory of the actual uncertain and perturbed system in closed loop. We will see that due to recursive feasibility and constraint tightening, the ISpS results for nominal system are easily translated into corresponding ISpS stability for the perturbed dynamics of the agent.

Theorem 5.5.2 (Stability of Uncertain Agent Dynamics) *If the nominal system (5.12) with nominal disturbance model (5.8) is ISpS stable within tightened constraint sets (5.14) under RH control law (5.17), then the uncertain system (5.18) under the same control (5.17) is also ISpS stable.*

Proof. The proof is similar to that furnished for Theorem 3.2.3, and hence not reproduced here. █

Comments made in Section 5.5.1 are also applicable here. Terminal control law and terminal region can be optimized with Algorithm 3. We will now consider the important case of stability under collision avoidance.

5.5.2 Stability of Team of Agents under NMPC, without Collision Avoidance

Extending proofs for individual agents in previous section, here we will establish a generalized small gain condition to prove stability of the interconnected system, for both strongly connected and weakly connected (with at least a spanning tree) network topologies. The result is general, not limited by the number of subsystems and the way in which subsystem gains are distributed is arbitrary. Let us now state an important small gain result for multi-agent formation control

Lemma 5.5.2 *For a team of agents A^i with dynamics (5.18), each with local ISpS Lyapunov function $V_t^i(\tilde{x}_t^i, u_t^i, \tilde{w}_t^i)$ under Theorem 5.5.1, there exist $\bar{\alpha}^i \in \mathcal{K}_\infty$ and $\bar{\rho}^i \in \mathcal{K}_\infty$ such that $\bar{\alpha}^i \triangleq (\mathcal{I} + \bar{\rho}^i) \circ \alpha_2^i(|\tilde{x}_t^i|)$ and $V_{t+1}^i(\tilde{x}_{t+1}^i, u_{t+1}^i, \tilde{w}_{t+1}^i) - V_t^i(\tilde{x}_t^i, u_t^i, \tilde{w}_t^i) \leq \bar{\alpha}^i(|\tilde{x}_t^i|)$ for $\tilde{x}_t^i \in \tilde{X}_t^i \sim \mathcal{B}^n(\tilde{c}^i)$. Let the nonlinear ISpS Lyapunov gain from A^i to $A^j \in G^i$ be denoted by the function $\bar{\gamma}_{ij}(s) : \mathcal{R}_{\geq 0} \rightarrow \mathcal{R}_{\geq 0}$ and given by*

$$\bar{\gamma}_{ij}(s) \triangleq \alpha_1^i \circ (\bar{\alpha}^i)^{-1} \circ \sigma_1^i \circ (\alpha_1^j)^{-1}(s), \quad (5.61)$$

then the multi-agent team satisfies the following small gain condition for all $t \geq 0$

$$V_t^i(\tilde{x}_t^i, u_t^i, \tilde{w}_t^i) > \max_{j \in G^i, j \neq i} \{\bar{\gamma}_{ij}(V_t^j(\tilde{x}_t^j, u_t^j, \tilde{w}_t^j))\} \quad (5.62)$$

Proof. There exists a function $\bar{\rho}^i \in \mathcal{K}_\infty$, such that considering (5.59)-(5.60) the following holds for all $\tilde{x}_t^i \in \tilde{X}_t^i \sim \mathcal{B}^n(\tilde{c}^i)$

$$\begin{aligned} V_{t+1}^i(\tilde{x}_{t+1}^i, u_{t+1}^i, \tilde{w}_{t+1}^i) - V_t^i(\tilde{x}_t^i, u_t^i, \tilde{w}_t^i) &\leq \\ &- \alpha_2^i(|\tilde{x}_t^i|) + \sigma_1^i(|\tilde{w}_t^i|) + \sigma_2^i(|\tilde{w}_{t+1}^i|) + \tilde{c}^i \leq -\bar{\rho}^i \circ \alpha_2^i(|\tilde{x}_t^i|) \end{aligned} \quad (5.63)$$

This is true since Lyapunov function $V^i(\cdot)$ has a negative gradient withing X_{MPC}^i , excluding the ball of radius \tilde{c}^i , as mentioned in Theorem 5.5.1. Hence, (5.63) will hold for the arbitrarily chosen nonlinear scaling function $\bar{\rho}^i \in \mathcal{K}_\infty$. Inequality (5.63) can be written as

$$\begin{aligned} -\alpha_2^i(|\tilde{x}_t^i|) + \sigma_1^i(|\tilde{w}_t^i|) + \sigma_2^i(|\tilde{w}_{t+1}^i|) + \tilde{c}^i &\leq \bar{\rho}^i \circ \alpha_2^i(|\tilde{x}_t^i|), \\ \sigma_1^i(|\tilde{w}_t^i|) + \sigma_2^i(|\tilde{w}_{t+1}^i|) + \tilde{c}^i &\leq (\mathcal{I} + \bar{\rho}^i) \circ \alpha_2^i(|\tilde{x}_t^i|) \end{aligned} \quad (5.64)$$

Let $\bar{\alpha}^i \triangleq (\mathcal{I} + \bar{\rho}^i) \circ \alpha_2^i(|\tilde{x}_t^i|)$. Then it is easy to show from (5.63) and (5.64) that

$$V_{t+1}^i(\tilde{x}_{t+1}^i, u_{t+1}^i, \tilde{w}_{t+1}^i) - V_t^i(\tilde{x}_t^i, u_t^i, \tilde{w}_t^i) \leq \bar{\alpha}^i(|\tilde{x}_t^i|), \quad \forall \tilde{x}_t^i \in \tilde{X}_t^i \sim \mathcal{B}^n(\tilde{c}^i) \quad (5.65)$$

Now, from (5.51) we observe that $V_t^i(\tilde{x}_t^i, u_t^i, \tilde{w}_t^i) \geq \alpha_1^i(|\tilde{x}_t^i|)$, and hence

$$\sigma_1^i(|\tilde{w}_t^i|) + \sigma_2^i(|\tilde{w}_{t+1}^i|) + \tilde{c}^i \leq \bar{\alpha}^i(|\tilde{x}_t^i|) \leq \bar{\alpha}^i \circ (\alpha_1^i)^{-1} (V_t^i(\tilde{x}_t^i, u_t^i, \tilde{w}_t^i))$$

Therefore, since $\sigma_2^i(\cdot), \tilde{c}^i \geq 0$ we can say that

$$\begin{aligned}
V_t^i(\tilde{x}_t^i, u_t^i, \tilde{w}_t^i) &\geq \alpha_1^i \circ (\bar{\alpha}^i)^{-1} (\sigma_1^i(|\tilde{w}_t^i|) + \sigma_2^i(|\tilde{w}_{t+1}^i|) + \bar{c}^i) \\
&\geq \alpha_1^i \circ (\bar{\alpha}^i)^{-1} \circ \sigma_1^i(|\tilde{w}_t^i|) \quad (5.66)
\end{aligned}$$

Now, since $w_t^i = \text{col}(x_{t,t+N_p^j}^j)$, then $|w_t^i| \geq \max_j |x_t^j| \geq |x_t^j|, \forall j \in G^i$. However, $\max(r), r \geq 0$ is also a \mathcal{K}_∞ function and for any $\alpha \in \mathcal{K}_\infty$ it is evident that maximization is commutative, i.e. $\alpha(\max(r)) \equiv \max(\alpha(r))$. Therefore, (5.66) can be written as

$$\begin{aligned}
V_t^i(\tilde{x}_t^i, u_t^i, \tilde{w}_t^i) &\geq \alpha_1^i \circ (\bar{\alpha}^i)^{-1} \circ \sigma_1^i \left(\max_j |\tilde{x}_t^j| \right) \\
&= \max_j \left(\alpha_1^i \circ (\bar{\alpha}^i)^{-1} \circ \sigma_1^i (|\tilde{x}_t^j|) \right), \quad \forall j \in G^i \quad (5.67)
\end{aligned}$$

But, from (5.51) we have $V_t^j(\tilde{x}_t^j, u_t^j, \tilde{w}_t^j) \geq \alpha_1^j(|\tilde{x}_t^j|)$, and hence

$$V_t^i(\tilde{x}_t^i, u_t^i, \tilde{w}_t^i) \geq \max_j \left(\alpha_1^i \circ (\bar{\alpha}^i)^{-1} \circ \sigma_1^i \circ (\alpha_1^j)^{-1} (V_t^j(\tilde{x}_t^j, u_t^j, \tilde{w}_t^j)) \right), \quad (5.68)$$

for $j \in G^i$. If gain $\bar{\gamma}_{ij}$ is defined as in (5.61), then (5.62) is obtained. ■

Function $\bar{\alpha}^i$ is a design 'variable' which can be freely chosen to satisfy (5.61), as shown in section 5.6. We will now use Lemma 5.5.2 to the study the stability of the team of agents connected in a team, without collision avoidance.

Theorem 5.5.3 *A team of N agents connected with a network with at least one spanning tree is ISpS stable if*

- i. each agent A^i ($i = 1, \dots, N$) has an ISpS Lyapunov function $V_t^i(\tilde{x}^i, u^i, \tilde{w}^i)$,*

ii. for each of its neighbors, agent A^i has the edge gain $\bar{\gamma}_{ij}$ defined in (5.61) for

$$j \in G^i,$$

iii. small gain condition (5.62) is satisfied.

Proof. We will carry out the proof in two steps. We will first prove the stability of strongly connected networks, and then prove the same for networks with only one spanning tree (weakly connected networks).

I. A network (graph) is strongly connected if there is a path from any node to any other node in the network. In other words, every agents has a spanning tree to every other agent in the team. In this case the connectivity gain matrix Γ of the network is irreducible. If $\bar{\mu}$ is a set of n monotone aggregation functions (MAF) operating over a vector r of n positive elements, and Γ is its irreducible gain matrix, define the gain operator $\Gamma_{\bar{\mu}} : \mathbb{R}_{\geq 0}^n \rightarrow \mathbb{R}_{\geq 0}^n$,

$$\Gamma_{\bar{\mu}} \triangleq \begin{bmatrix} r_1 \\ \vdots \\ r_n \end{bmatrix} \mapsto \begin{bmatrix} \mu_1(\bar{\gamma}_{12}(r_2), \dots, \bar{\gamma}_{1n}(r_n)) \\ \vdots \\ \mu_n(\bar{\gamma}_{n,1}(r_1), \dots, \bar{\gamma}_{n,n-1}(r_{n-1})) \end{bmatrix} \quad (5.69)$$

According to the recent generalized small gain theorems of [118], if a strongly connected network obeys the following small gain condition

$$\mathcal{I} > \Gamma_{\bar{\mu}}, \quad (5.70)$$

then it is stable in the input to state stability sense (see Theorem 5.3 of

[118]). Now, $\bar{\mu} = \max$ is a monotone aggregation function ([119]). Let $r = [V_t^1(\tilde{x}_t^1, u_t^1, \tilde{w}_t^1), \dots, V_t^N(\tilde{x}_t^N, u_t^N, \tilde{w}_t^N)]$, then the (5.70) is satisfied if:

$$\begin{aligned} & \begin{bmatrix} V_t^1(\tilde{x}_t^1, u_t^1, \tilde{w}_t^1) \\ \vdots \\ V_t^N(\tilde{x}_t^N, u_t^N, \tilde{w}_t^N) \end{bmatrix} \\ & > \begin{bmatrix} \max(\bar{\gamma}_{12}(V_t^2(\tilde{x}_t^2, u_t^2, \tilde{w}_t^2)), \dots, \bar{\gamma}_{1,N}(V_t^N(\tilde{x}_t^N, u_t^N, \tilde{w}_t^N))) \\ \vdots \\ \max(\bar{\gamma}_{N,1}(V(x_1^t, w_1^t)), \dots, \bar{\gamma}_{N,N-1}(V(x_{N-1}^t, w_{N-1}^t))) \end{bmatrix} \quad (5.71) \end{aligned}$$

This can be shown to be equivalent to (5.62). This proves stability for strongly connected teams.

II. In a weakly connected there are at least two nodes for which a directed path connecting them does not exist, but there exists at least one spanning tree. The connectivity gain matrix for a weakly connected network can be brought in upper block triangular form by appropriate re-indexing of agents, such that each upper block on the diagonal is either 0 or irreducible. Hence,

we can now rewrite the gain matrix as

$$\Gamma = \begin{bmatrix} 0 & \bar{\gamma}_{12} & \bar{\gamma}_{13} & \cdots & \bar{\gamma}_{1,\bar{M}} \\ 0 & \ddots & \bar{\gamma}_{23} & \cdots & \bar{\gamma}_{2,\bar{M}} \\ \vdots & \ddots & \ddots & \ddots & \vdots \\ & & \ddots & \ddots & \bar{\gamma}_{N-1,\bar{M}} \\ 0 & \cdots & & 0 & 0 \end{bmatrix}$$

where $\bar{M} \triangleq \max_i M^i$ is the size of neighborhood of the most connected agent.

According to Proposition 6.2 of [118], the interconnected system is stable if each upper diagonal block satisfies the small gain condition (5.70). Now, the upper diagonal blocks are

$$\bar{\Gamma}_1 = 0, \quad \bar{\Gamma}_2 = \begin{bmatrix} 0 & \bar{\gamma}_{12} \\ 0 & 0 \end{bmatrix}, \quad \bar{\Gamma}_3 = \begin{bmatrix} 0 & \bar{\gamma}_{12} & \bar{\gamma}_{13} \\ 0 & 0 & \bar{\gamma}_{23} \\ 0 & 0 & 0 \end{bmatrix}$$

$$\bar{\Gamma}_k = \begin{bmatrix} 0 & \bar{\gamma}_{12} & \bar{\gamma}_{13} & \cdots & \bar{\gamma}_{1,k} \\ 0 & \ddots & \bar{\gamma}_{21} & \cdots & \bar{\gamma}_{2,k} \\ \vdots & \ddots & \ddots & \ddots & \vdots \\ & & \ddots & \ddots & \bar{\gamma}_{k-1,k} \\ 0 & \cdots & & 0 & 0 \end{bmatrix}, \quad \bar{\Gamma}_N = \Gamma$$

Then stability is assured if each of the above blocks obey the small gain

condition (5.70) iteratively, such that

$$\begin{aligned}
r_1 > \bar{\Gamma}_{\bar{\mu}1}(r_1) &\Rightarrow V_t^1(\tilde{x}_t^1, u_t^1, \tilde{w}_t^1) > 0 \\
r_2 > \bar{\Gamma}_{\bar{\mu}2}(r_2) &\Rightarrow V_t^1(\tilde{x}_t^1, u_t^1, \tilde{w}_t^1) > \bar{\gamma}_{12}(V_t^1(\tilde{x}_t^2, u_t^2, \tilde{w}_t^2)), \\
&V_t^1(\tilde{x}_t^3, u_t^3, \tilde{w}_t^3) > 0 \\
r_3 > \bar{\Gamma}_{\bar{\mu}3}(r_3) &\Rightarrow V_t^1(\tilde{x}_t^1, u_t^1, \tilde{w}_t^1) > \max \left(\begin{array}{l} \bar{\gamma}_{12}(V_t^2(\tilde{x}_t^2, u_t^2, \tilde{w}_t^2)), \\ \bar{\gamma}_{13}(V_t^3(\tilde{x}_t^3, u_t^3, \tilde{w}_t^3)) \end{array} \right), \\
&V_t^2(\tilde{x}_t^2, u_t^2, \tilde{w}_t^2) > \bar{\gamma}_{23}(V_t^3(\tilde{x}_t^3, u_t^3, \tilde{w}_t^3)), \\
&(V_t^3(\tilde{x}_t^3, u_t^3, \tilde{w}_t^3)) > 0 \\
\vdots & \qquad \qquad \qquad \vdots
\end{aligned}$$

This iterative procedure reduces to (5.62). Hence, the team is stable irrespective of the network topology as long as it is at least weakly connected (has at least one spanning tree), provided it obeys certain small gain conditions. █

5.5.3 Stability of Individual Agents with Collision Avoidance

We can now extend the results of the previous section to prove stability of the agents under the collision avoidance scheme described in Section 5.2.2. Let $V_t^i(\tilde{x}_t^i, u_t^{i\circ}, \tilde{w}_t^i) = J_t^i(\tilde{x}_t^i, u_t^{i\circ}, \tilde{w}_t^i)$ be the local ISpS Lyapunov function for A^i without collision avoidance. Let $x_{t,t+N_p}^{i\circ}$ be the optimal solution of the cost (5.10) and $\hat{x}_{t,t+N_p}^{i\circ}$ be the optimal solution of the modified cost (5.27). We will prove that

$\dot{V}_t^i(\hat{x}_t^i, \hat{u}_t^{i^o}, \tilde{w}_t^i) = J_t^i(\hat{x}_t^{i^o}, \hat{u}_t^{i^o}, \tilde{w}_t^i)$ is also an ISpS Lyapunov function, where $\hat{u}_t^{i^o}$ is the optimal control for minimizing (5.27). It is obvious that $d_{ij}(l) \neq 0$ for at least one instant $t \leq l \leq t + N_p^i$, since otherwise would mean that the current position as well planned optimal trajectories of two agents coincide exactly, which is impossible. We assume that $\underline{\kappa}^i |\hat{x}^{i^o}| \leq |\tilde{x}^{i^o}| \leq \bar{\kappa}^i |\hat{x}^{i^o}|$, for some constants $\underline{\kappa}^i, \bar{\kappa}^i \geq 0$. This assumption is also not restrictive since both \tilde{x}^{i^o} and \hat{x}^{i^o} are finite. This leads to bounds on potential function, i.e. $\underline{\Phi}^i \leq \Phi_t^i \leq \bar{\Phi}^i$ for some constants $\underline{\Phi}^i, \bar{\Phi}^i \geq 0$. Let us introduce the following definitions

Definition 5.5.1 *For agents A^i under collision avoidance, define the following nonlinear functions*

I. $\alpha_1^i(s) \triangleq (1 + \underline{\Phi}^i)\alpha_1^i(\underline{\kappa}^i s) \in \mathcal{K}_\infty$

II. $\alpha_2^i(s) \triangleq (1 + \underline{\Phi}^i)\alpha_2^i(\underline{\kappa}^i s) \in \mathcal{K}_\infty$

III. $\sigma_{1,2}^i(s) \triangleq (1 + \bar{\Phi}^i)\sigma_{1,2}^i(s) \in \mathcal{K}$

IV. $\sigma_3^i(s) \triangleq (1 + \bar{\Phi}^i)\sigma_3^i(s) \in \mathcal{K}$

V. $\bar{c}^i \triangleq (1 + \bar{\Phi}^i)(\bar{c}^i + \varkappa^i)$

VI. $\dot{\bar{c}}^i \triangleq (1 + \bar{\Phi}^i)(\bar{c}^i + \varkappa^i)$

We can now prove the main result of this section

Theorem 5.5.4 *For an agent on collision course, the optimal trajectory $\hat{x}_{t,t+N_p^i}^{i^o}$ for modified cost (5.27) not only guarantees collision avoidance with other agents in the sense of (5.29), but also maintains input-to-state practical stability, if its*

repulsive spatial filter weights $\lambda(d_{k|t}^{ij})$ are chosen at each sampling instant t such that

$$\frac{\lambda_{\max,t}^i}{\lambda_{\min,t}^i} < \frac{\underline{r}^i(|x_t|)}{\left((N_p^i - 1)(L_{hx}^i + L_{qx}^i) + L_{hf}\right) \left(N_p^i R_{\min}^i + N_p^i (N_p^i - 1)v_{\max}\right)} \triangleq \bar{a}_t \quad (5.72)$$

Proof. The proof consists of two parts. We first show that negative gradient of modified cost (5.27) lies in the direction of expanding weighted average distance \bar{d}_t^{ij} between agents on collision course. Hence, the optimal trajectory $\hat{x}_{t,t+N_p^i}^{i\circ}$ reaches the terminal set by avoiding collision in the sense of (5.29). Next, we will show that the optimal trajectory in that direction is also ISpS stable. From (5.27), we can see that

$$\frac{\partial J_t^i}{\partial \bar{d}_t^{ij}} = \frac{\partial J_t^i}{\partial \bar{d}_t^{ij}} (1 + \Phi_t^i) + J_t^i \frac{\partial \Phi_t^i}{\partial \bar{d}_t^{ij}}$$

Since $\partial \Phi_t^i / \partial \bar{d}_t^{ij} = -\Phi_t^i / \bar{d}_t^{ij} < 0$ and $\Phi_t^i > 0$, in order to have negative gradient of cost in direction of increasing inter-agent distance i.e. $\partial J_t^i / \partial \bar{d}_t^{ij} < 0$, we have

$$\frac{\partial J_t^i}{\partial \bar{d}_t^{ij}} < \frac{\Phi_t^i}{1 + \Phi_t^i} \frac{J_t^i}{\bar{d}_t^{ij}} < \frac{J_t^i}{\bar{d}_t^{ij}}$$

Since $J_t^i, \bar{d}_t^{ij} > 0$, this condition can be satisfied if

$$\max \left| \frac{\partial J_t^i}{\partial \bar{d}_t^{ij}} \right| < \frac{\min(J_t^i)}{\max(\bar{d}_t^{ij})} \quad (5.73)$$

For RHS, note that by chain rule of differentiation

$$\frac{\partial J_t^i}{\partial \bar{d}_t^{ij}} = \sum_{l=t}^{t+N_p^i} \frac{\partial J_t^i}{\partial \tilde{x}_l^i} \frac{\partial \tilde{x}_l^i}{\partial d_l^{ij}} \frac{\partial d_l^{ij}}{\partial \bar{d}_t^{ij}}$$

Now, using the triangle inequality,

$$\left| \frac{\partial J_t^i}{\partial \bar{d}_t^{ij}} \right| \leq \sum_{l=t}^{t+N_p^i} \left| \frac{\partial J_t^i}{\partial \tilde{x}_l^i} \right| \left| \frac{\partial \tilde{x}_l^i}{\partial d_l^{ij}} \right| \left| \frac{\partial d_l^{ij}}{\partial \bar{d}_t^{ij}} \right|$$

With slight abuse of notation we can write $d_l^{ij} = |\tilde{x}_l^i - \tilde{w}_l^j|$. For given neighbor trajectory $\tilde{w}_l^j = \tilde{x}_l^j, \forall j \in G^i$, we have $\partial d_l^{ij} / \partial \tilde{x}_l^i = (\tilde{x}_l^i - \tilde{w}_l^i) / d_l^{ij}$ such that $|\partial d_l^{ij} / \partial \tilde{x}_l^i| =$

1. Similarly, $\partial \bar{d}_t^{ij} / \partial d_l^{ij} = \lambda_l^i$, which results in

$$\left| \frac{\partial J_t^i}{\partial \bar{d}_t^{ij}} \right| \leq \sum_{l=t}^{t+N_p^i} \frac{1}{\lambda_l^i} \left| \frac{\partial J_t^i}{\partial \tilde{x}_l^i} \right| < \frac{1}{\lambda_{\min,t}^i} \sum_{l=t}^{t+N_p^i} \left| \frac{\partial J_t^i}{\partial \tilde{x}_l^i} \right|$$

Now, from (5.10), we get

$$\begin{aligned} \max \left| \frac{\partial J_t^i}{\partial \bar{d}_t^{ij}} \right| &< \frac{1}{\lambda_{\min,t}^i} \left(\sum_{l=t}^{t+N_p^i-1} \left(\left| \frac{\partial h_l^i}{\partial \tilde{x}_l^i} \right| + \left| \frac{\partial q_l^i}{\partial \tilde{x}_l^i} \right| \right) + \left| \frac{\partial h_{f,t+N_p^i}^i}{\partial \tilde{x}_{t+N_p^i}^i} \right| \right) \\ &< \frac{1}{\lambda_{\min,t}^i} \left(\sum_{l=t}^{t+N_p^i-1} (L_h^i + L_q^i) + L_{hf}^i \right) < \frac{(N_p^i - 1)(L_h^i + L_q^i) + L_{hf}^i}{\lambda_{\min,t}^i} \quad (5.74) \end{aligned}$$

Now, maximum $\bar{d}^i j_t$ can occur when the minimum distance between agents on collision course is R_{\min}^i and then move away from each other at v_{\max} , i.e.

$$\max(\bar{d}_t^{ij}) = \sum_{k=t}^{t+N_p^i} \lambda_k^i (R_{\min}^i + 2(k-t)v_{\max}) < \lambda_{\max,t}^i (N_p^i R_{\min}^i + N_p^i (N_p^i - 1)v_{\max}).$$

Also, as noted in Theorem 5.5.1, $\min(J_t^i) \leq V_t^i \leq \underline{r}^i(|\tilde{x}_t^i|)$. This can be combined with

(5.74) to result in the condition specified in (5.72). Hence, the minimum of modified cost lies in the direction of collision avoidance in the sense of (5.29). Since any feasible trajectory for cost (5.10) is also feasible for modified cost (5.27) and the reachable set is compact, an optimum almost always exists, unless there is not enough time to manoeuvre (to cater for which we have placed a conservative bound on $\Delta_t^{ij} \leq \bar{\Delta}$) for $t \geq 0$.

For the next part of this proof, note that $\hat{J}(\hat{x}_t^{i^\circ}, u_t^{i^\circ}, \tilde{w}_t^i) \leq \hat{J}(\tilde{x}_t^{i^\circ}, \hat{u}_t^{i^\circ}, \tilde{w}_t^i)$ and $J(\tilde{x}_t^{i^\circ}, u_t^{i^\circ}, \tilde{w}_t^i) \leq J(\hat{x}_t^{i^\circ}, \hat{u}_t^{i^\circ}, \tilde{w}_t^i)$, since $\hat{x}_{t,t+N_p^i}^{i^\circ}$ is admissible but suboptimal control for minimization of (5.10) and $\tilde{x}_{t,t+N_p^i}^{i^\circ}$ is suboptimal for (5.27). For conciseness, we will ignore the difference between V and J in this section and also drop the $^\circ$ symbol for optimal values. From Theorem 5.5.1, we have $\alpha_1^i(|\tilde{x}_t^i|) \leq V_t^i(\tilde{x}_t^i, u^i - t, \tilde{w}_t^i)$, which gives $\alpha_1^i(\underline{\kappa}^i|\hat{x}_t^i|) \leq V(\tilde{x}_t^i, u_t^i, \tilde{w}_t^i) \leq V(\hat{x}_t^i, u_t^i, \tilde{w}_t^i)$. Combining this with (5.27) and defining $\acute{\alpha}_1^i(s) \triangleq (1 + \underline{\Phi}^i)\alpha_1^i(\underline{\kappa}^i s) \in \mathcal{K}_\infty$, we get

$$\acute{\alpha}_1^i(|\hat{x}_t^i|) \leq \acute{V}(\hat{x}_t^i, u_t^i, \tilde{w}_t^i) \quad (5.75)$$

Let $V(\hat{x}_t^i, u_t^i, \tilde{w}_t^i) - V(\tilde{x}_t^i, u_t^i, \tilde{w}_t^i) \leq \varkappa^i$ for some constant $\varkappa^i > 0$. Combining this with (3.53) and defining $\acute{\alpha}_3^i(s) \triangleq (1 + \bar{\Phi}^i)\alpha_3^i(\bar{\kappa}^i s) \in \mathcal{K}_\infty$, $\acute{\sigma}_3(s) \triangleq (1 + \bar{\Phi}^i)\sigma_3(s) \in \mathcal{K}$ and $\acute{c}^i \triangleq (1 + \bar{\Phi}^i)(\bar{c}^i + \varkappa^i)$, we get

$$\acute{V}(\hat{x}_t^i, u_t^i, \tilde{w}_t^i) \leq \acute{\alpha}_3(|\hat{x}_t^i|) + \acute{\sigma}_3(|\tilde{w}_t^i|) + \acute{c}^i \quad (5.76)$$

Using (3.45), (5.27), and defining $\acute{\alpha}_2^i(s) \triangleq (1 + \Phi^i)\alpha_2^i(\kappa^i s) \in \mathcal{K}_\infty = \acute{\alpha}_1^i(|x_t^i|)$, $\acute{\sigma}_{1,2}(s) \triangleq (1 + \bar{\Phi}^i)\sigma_{1,2}(s) \in \mathcal{K}$, $\acute{c}^i \triangleq (1 + \bar{\Phi}^i)(\bar{c}^i + \varkappa^i)$, we get:

$$\begin{aligned} \Upsilon_{t+1}^i \acute{V}(x_{t+1}^i, u_{t+1}^i, \tilde{w}_{t+1}^i) - \acute{V}(x_t^i, u_t^i, \tilde{w}_t^i) \\ \leq -\acute{\alpha}_2(|x_t^i|) + \acute{\sigma}_1(|\tilde{w}_t^i|) + \acute{\sigma}_2(|\tilde{w}_{t+1}^i|) + \acute{c}^i \end{aligned} \quad (5.77)$$

where, $\Upsilon_{t+1}^i \triangleq \frac{1+\Phi_{t+1}^i}{1+\Phi_t^i}$. From (5.26), $\Upsilon_{t+1}^i \geq 1$ if (5.29) holds and we can write:

$$\begin{aligned} \acute{V}(x_{t+1}^i, u_{t+1}^i, \tilde{w}_{t+1}^i) - \acute{V}(x_t^i, u_t^i, \tilde{w}_t^i) \\ \leq -\acute{\alpha}_2(|x_t^i|) + \acute{\sigma}_1(|\tilde{w}_t^i|) + \acute{\sigma}_2(|\tilde{w}_{t+1}^i|) + \acute{c}^i \end{aligned} \quad (5.78)$$

Hence, considering (5.75), (5.76) and (5.78), agent A^i is ISpS according to Theorem 2.5.2 and moves towards its goal in an optimal manner while avoiding collision with other agents. █

Corollary 1 *If spatial filter for collision avoidance is shaped as a geometric progression $\lambda_{k|t}^i = \lambda_{\max,t}^i r_t^l$ such that $d_l^{ij} > d_{l+1}^{ij}$ for $l = 0, \dots, N_p^i - 1$, then the filter can be designed by specifying $\bar{b} > 1$, $\lambda_{\max,t}^i$ and calculating $r_t = (\bar{b}\bar{a}_t)^{-1/(N_p^i-1)}$ from (5.72).*

5.5.4 Stability of Multi-Agent Team with Collision Avoidance

In this section, we will study the stability of the multi-agent team and the influence of collision avoidance on it. Extending stability results for individual agents under collision avoidance in the previous section, here we will establish a generalized small gain condition to prove stability of the interconnected system under collision avoidance.

Theorem 5.5.5 *For a team of agents A^i with dynamics (5.18), each with local ISpS Lyapunov function $\dot{V}_t^i(x_t^i, u_t^i, \tilde{w}_t^i)$ under Theorem 5.5.4, there exist $\alpha^i \in \mathcal{K}_\infty$ and $\rho^i \in \mathcal{K}_\infty$ such that $\alpha^i \triangleq (\mathcal{I} + \rho^i) \circ \alpha_2^i(|x_t^i|)$ and $\dot{V}_{t+1}^i(x_{t+1}^i, u_{t+1}^i, \tilde{w}_{t+1}^i) - \dot{V}_t^i(x_t^i, u_t^i, \tilde{w}_t^i) \leq \alpha^i(|x_t^i|)$ for $x_t^i \in \tilde{X}_t^i \sim \mathcal{B}^n(\tilde{c}^i)$. Let the nonlinear ISpS Lyapunov gain from A^i to $A^j \in G^i$ be denoted by the function $\gamma_{ij}(s) : \mathcal{R}_{\geq 0} \rightarrow \mathcal{R}_{\geq 0}$ and given by*

$$\gamma_{ij}(s) \triangleq \alpha_1^i \circ (\alpha^i)^{-1} \circ \sigma_1^i \circ (\alpha_1^j)^{-1}(s), \quad (5.79)$$

then the multi-agent team

i. the multi-agent team satisfies the following small gain condition for all $t \geq 0$

$$\dot{V}(x_t^i, u_t^i, \tilde{w}_t^i) > \max_{j \in G^i, j \neq i} \{\gamma_{ij}(\dot{V}(x_t^j, u_t^j, \tilde{w}_t^j))\} \quad (5.80)$$

ii. is ISpS stable.

Proof. Consider the nonlinear functions defined in 5.5.1. There exists a function $\hat{\rho}^i \in \mathcal{K}_\infty$, such that considering (5.78), the following holds for all $\hat{x}_t^i \in \tilde{X}_t^i \sim \mathcal{B}^n(\tilde{c}^i)$

$$\begin{aligned} \dot{V}(\hat{x}_{t+1}^i, u_{t+1}^i, \tilde{w}_{t+1}^i) - \dot{V}(\hat{x}_t^i, u_t^i, \tilde{w}_t^i) \\ \leq -\acute{\alpha}_2(|\hat{x}_t^i|) + \acute{\sigma}_1(|\tilde{w}_t^i|) + \acute{\sigma}_2(|\tilde{w}_{t+1}^i|) + \acute{c}^i \leq -\hat{\rho}^i \circ \acute{\alpha}_2^i(|\hat{x}_t^i|) \end{aligned} \quad (5.81)$$

This is true since Lyapunov function $\dot{V}^i(\cdot)$ has a negative gradient withing X_{MPC}^i as shown in Theorem 5.5.4, excluding the ball of radius \tilde{c}^i , as mentioned in Theorem 5.5.1. Hence, (5.81) will hold for the arbitrarily chosen nonlinear scaling function $\hat{\rho}^i \in \mathcal{K}_\infty$. The rest of the steps are similar to those in the proofs of Lemma 5.5.2 and Theorem 5.5.3, and therefore will not be repeated here. ■

This section completes the stability analysis of the multi-agent team under Algorithm. We have shown conditions for stability of the team both with and without collision avoidance active. We will now particularize the results for the specific task of formation control with collision avoidance and data compression with the comprehensive examples in Section 5.6. As a final ingredient, we will particularize the result for quadratic cost to design the terminal control law.

5.5.5 Terminal Region Optimization and Terminal Control Law Design

In many cases the cost functional in MPC is quadratic. As shown in Chapter 4, this form is amenable to efficient convex optimization and LMI techniques. Let

the cost functional (5.27) be quadratic, such as

$$J_t^i(\tilde{x}^i, u^i, \tilde{w}^i, N_c^i, N_p^i, k_f^i) = \left(\tilde{x}_{t,t+N_p}^i\right)^T Q_f^i \left(\tilde{x}_{t,t+N_p}^i\right) + \sum_{l=t}^{t+N_p^i-1} \left[\tilde{x}_l^{iT} Q^i \tilde{x}_l^i + u_l^{iT} R^i u_l^i + \sum_{j \in G^i} (\tilde{x}_l^i - \tilde{x}_l^j)^T S^{ij} (\tilde{x}_l^i - \tilde{x}_l^j) \right] \quad (5.82)$$

with positive definite matrices Q^i , R^i , S^i and Q_f^i . Comparing (5.82) with cost functional (5.10), it is easy to see that $h^i(\tilde{x}^i, u^i) = |\tilde{x}^i|_{Q^i} + |u^i|_{R^i}$, $q^i(\tilde{x}^i, \tilde{w}^i) = \sum_{j \in G^i} |\tilde{x}^i - \tilde{w}^j|_{S^{ij}}$ and $h_f^i(\tilde{x}_{t+N_p}^i) = |\tilde{x}_{t+N_p}^i|_{Q_f^i}$. The local transition and terminal costs have the usual meaning, but cooperative cost term is more involved. It basically allows synchronization of state of A^i with states of other agents in its neighborhood, by assigning different weights S^{ij} to them, based on desired priorities. It is clear that the most important aspect of determining the stability of the system (5.12) under RH control law (5.17) is the terminal inequality (5.49), based on which we will first state an important result about stabilizing general linearization of the nominal system. Let $A_v^i \triangleq \frac{\partial \tilde{f}^i}{\partial \tilde{x}^i} \Big|_{\tilde{x}^i = \tilde{x}_v^i, u^i = u_v^i, \tilde{w}^i = \tilde{w}_v^i}$ and $B_v^i \triangleq \frac{\partial \tilde{f}^i}{\partial u^i} \Big|_{\tilde{x}^i = \tilde{x}_v^i, u^i = u_v^i, \tilde{w}^i = \tilde{w}_v^i}$ be linearization about an arbitrary point in the terminal set X_f^i .

Lemma 5.5.3 (Stabilization of Arbitrary Points in X_f^i) *Under Assumption 5.3.2, let the cost functional be quadratic, as defined in (5.82). Let $\psi^i(\tilde{w}_l^i) = \sum_{j \in G^i} \tilde{x}_l^{iT} S^{ij} \tilde{x}_l^j$ and $\tilde{S}^i = M^i \max_j (\lambda_{S_{\max}^{ij}}) I_n$, such that $q(\tilde{x}^i, \tilde{w}^i) \leq \psi^i(|\tilde{w}^i|) + \tilde{x}^{iT} \tilde{S}^i \tilde{x}^i$, for $\tilde{x}^i \in X_f^i$ and allowable disturbances $\tilde{w}^i \in \tilde{W}_{t+l}^i$, $\forall l = N_C, \dots, N_P$. Then, there exists a terminal control law $u^i = K_v^i \tilde{x}^i$, for*

$\tilde{x}^i \in X_f^i$, and terminal constraint set X_f^i as defined in Claim 5.3.1, such that the closed loop general linearization $A_{CL_v}^i \triangleq A_v^i + B_v^i K_v$ of the nominal system (5.12) is locally stable. Let $\tilde{Q}^i \triangleq Q^i + K_v i^T R^i K_v - \tilde{S}^i$. Stability of the point $\tilde{x}^i = \tilde{x}_v^i, u^i = u_v^i, \tilde{w}^i = \tilde{w}_v^i$ is ensured with desired rate of convergence \hat{a}^i , if the following Lyapunov LMI holds

$$A_{CL_v}^{iT} Q_f^i A_{CL_v}^i - Q_f^i + \tilde{Q}^i \leq 0 \quad (5.83)$$

subject to:

$$Q^i + K_v i^T R^i K_v - \tilde{S}^i > \hat{a}^i I_n, \quad (5.84)$$

$$k_f^i(\tilde{x}^i) = K_v^i \tilde{x}^i \in U^i \quad (5.85)$$

and

$$\tilde{x}^i T Q_f^i \tilde{x}^i \leq a^i \quad (5.86)$$

Rate of convergence \hat{a}^i is obtained from (5.40).

Proof. For the cooperative cost component, we have from (5.82)

$$\begin{aligned} q^i(\tilde{x}^i, \tilde{w}^i) &= \sum_{j \in G^i} (\tilde{x}_l^i - \tilde{x}_l^j)^T S^{ij} (\tilde{x}_l^i - \tilde{x}_l^j) \leq \sum_{j \in G^i} \left(\tilde{x}_l^{iT} S^{ij} \tilde{x}_l^i + \tilde{x}_l^{jT} S^{ij} \tilde{x}_l^j \right) \\ &\leq M^i \max_j \left(\lambda_{S_{\max}^{ij}} \right) \tilde{x}_l^{iT} I_n \tilde{x}_l^i + \sum_{j \in G^i} \tilde{x}_l^{jT} S^{ij} \tilde{x}_l^j \quad (5.87) \end{aligned}$$

Now, let $\psi^i(\tilde{w}^i) = \sum_{j \in G^i} \tilde{x}_l^j{}^T S^{ij} \tilde{x}_l^j$ and $\tilde{S}^i = M^i \max_j (\lambda_{S_{\max}^{ij}}) I_n$. Then it is obvious that

$$q^i(\tilde{x}^i, \tilde{w}^i) \leq \psi^i(|\tilde{w}^i|) + \tilde{x}^{iT} \tilde{S}^i \tilde{x}^i \quad (5.88)$$

We know the nominal system (5.12) with nominal disturbance model (5.8) is stable if condition (5.49) holds in X_f^i . Rewriting (5.49) in terms of quadratic cost (5.10)

$$\begin{aligned} h_f^i(\tilde{f}^i(\tilde{x}^i, k_f^i(\tilde{x}^i))) - h_f^i(\tilde{x}^i) \\ \leq -\tilde{x}^{iT} \left(Q^i + K_v^{iT} R^i K_v^i \right) \tilde{x}^i - q^i(\tilde{x}^i, \tilde{w}^i) + \psi^i(|\tilde{w}^i|) \\ \leq -\tilde{x}^{iT} \left(Q^i + K_v^{iT} R^i K_v^i \right) \tilde{x}^i + q^i(\tilde{x}^i, \tilde{w}^i) - \psi^i(|\tilde{w}^i|) \end{aligned}$$

We were able to do the last step above, since $-q^i(\tilde{x}^i, \tilde{w}^i) + \psi^i(|\tilde{w}^i|) \leq 0$. Substitute (5.88) in the inequality above

$$\begin{aligned} \tilde{f}^i(\tilde{x}^i, k_f^i(\tilde{x}^i))^T Q_f^i \tilde{f}^i(\tilde{x}^i, k_f^i(\tilde{x}^i)) - \tilde{x}^{iT} Q_f^i \tilde{x}^i \\ \leq -\tilde{x}^{iT} \left(Q^i + K_v^{iT} R^i K_v^i - \tilde{S}^i \right) \tilde{x}^i \quad (5.89) \end{aligned}$$

The rest of the steps are similar to the proof of Lemma 4.3.2, and therefore not repeated here. █

Remark 5.5.1 *We have completed the stability analysis of multi-agent formation control task. However, some comments are necessary.*

- I. *The convex OCP for maximizing the terminal constraint set is the same as OCP 4.3.1. Therefore, Algorithm 3 can be used with obvious changes in*

notation.

II. The requirement that $Q^i + K_v^{i^T} R^i K_v^i - \tilde{S}^i > 0$ limits the maximum weight that can be assigned in the cooperative cost to neighbors. It is obvious that $Q^i \approx \tilde{S}^i$ will result in very large control gain K^i , but since control is constrained, the OCP 4.3.1 may be rendered infeasible. Therefore, in general $Q^i \gg \tilde{S}^i$, which means each agent should place more emphasis on its local control objective more than cooperative goals.

III. We will show how to specify the “designer function” $\bar{\alpha}^i$ and $\acute{\alpha}^i$ in Section 5.5.3. One possible way to design the function $\bar{\alpha}^i$ is by choosing

$$\bar{\rho}^i(s) = \bar{k}^i s, \quad \bar{k}^i > 0 \quad (5.90)$$

for suitable $\bar{k}^i \in \mathbb{R}_{>0}$, such that (5.63) is satisfied. As we showed in Example 3.3.1, we can derive explicit analytic forms of Lipschitz constants and other bounds in the development above. Therefore, we can show that

$$i. \quad \alpha_1^i(|\tilde{x}^i|) = \alpha_2^i(|\tilde{x}^i|) = \lambda_{Q_{\min}^i} |\tilde{x}^i|^2$$

$$ii. \quad \alpha_{1f}^i(|\tilde{x}^i|) = \lambda_{Q_{f,\min}^i} |\tilde{x}^i|^2$$

$$iii. \quad \alpha_{2f}^i(|\tilde{x}^i|) = \lambda_{Q_{f,\max}^i} |\tilde{x}^i|^2$$

$$iv. \quad L_{hx}^i = \lambda_{Q_{\max}^i} |\tilde{x}^i|_{\max}$$

$$v. \quad L_{hu}^i = \lambda_{R_{\max}^i} |u^i|_{\max}$$

$$vi. \quad L_{qx}^i = |\tilde{x}^i|_{\max} \sum_{j \in G^i} \lambda_{S_{\max}^{ij}} = M^i \max_j \left(\lambda_{S_{\max}^{ij}} \right) |\tilde{x}^i|_{\max} \text{ from (5.87), where}$$

M^i is the size of the neighborhood of A^i .

- vii. From (5.41), $x^i T Q_f^i x^i \leq a^i$ for $\tilde{x}^i \in X_f^i$, therefore $|\tilde{x}^i| \leq \sqrt{a^i / \lambda_{Q_f^i, \max}}$, $\forall \tilde{x}^i \in X_f^i$. Therefore, $L_{hf}^i = \sqrt{a^i \lambda_{Q_f^i, \max}}$.
- viii. $L_{kf}^i = \lambda_{k_{f \max}^i} \sqrt{a^i / \lambda_{Q_f^i, \max}}$, where $\lambda_{k_{f \max}^i}$ is the maximum eigenvalue of $K^{iT} K^i$, if the terminal control is given by $k_f^i(\tilde{x}^i) = K^{iT} \tilde{x}^i$.

From the definitions in Lemma 5.5.1 and those derived above, we have

$$\begin{aligned} \sigma_1^i(s) &= \frac{L_{gw}^{i, N_p^i-1} - 1}{L_{gw}^i - 1} L_{qw}^i L_{gw}^i s, & \alpha_1^{j-1}(s) &= \left(\frac{s}{\lambda_{\min Q^j}} \right)^{\frac{1}{2}}, \\ \alpha_1^{i-1}(s) &= \left(\frac{s}{\lambda_{\min Q^i}} \right)^{\frac{1}{2}}, & \bar{\alpha}^{i-1}(s) &= \alpha_2^{i-1} \left(\frac{1}{\bar{k}^i + 1} s \right), & \alpha_1^i \circ \alpha_1^{i-1} &= \mathcal{I} \end{aligned}$$

such that (5.61) can be evaluated as

$$\bar{\gamma}_{ij}(s) \triangleq \frac{1}{\bar{k}^i + 1} \frac{L_{gw}^{i, N_p^i-1} - 1}{L_{gw}^i - 1} L_{qw}^i L_{gw}^i \left(\frac{s}{\lambda_{\min Q^j}} \right)^{\frac{1}{2}} \quad (5.91)$$

It is obvious that it is always possible to verify (5.62) by choosing a sufficiently large value of $\bar{k}^i > 0$. In other words for the case with collision avoidance inactive, as long as the agents are locally ISpS, the team will also be ISpS provided there is at least one spanning tree in the team.

IV. We can similarly derive the nonlinear gain (5.80) in the collision avoidance multi-agent case by definitions in Section 5.2.2. choosing

$$\hat{\rho}^i(s) = \hat{k}^i s, \quad \hat{k}^i > 0 \quad (5.92)$$

for suitable $\acute{k}^i \in \mathbb{R}_{\geq 1}$, such that (5.81) is satisfied. Therefore, from (5.80)

$$\acute{\gamma}_{ij}(s) = \frac{1}{(\acute{k}^i + 1)} \frac{(1 + \bar{\phi}^i) L_{qw}^i (L_{gw}^i N_p^{i-1} - 1)}{\underline{\kappa}^j} \frac{1}{L_{gw}^i - 1} \left(\frac{s}{(1 + \underline{\phi}^j) \lambda_{\min Q^j}} \right)^{\frac{1}{2}} \quad (5.93)$$

It is also obvious that it is always possible to verify (5.80) by choosing a sufficiently large value of $\acute{k}^i \in \mathbb{R}_{>0}$. In other words, as long as the agents are locally ISpS, the team under collision avoidance will also be ISpS provided there is at least one spanning tree in the team.

5.6 Illustrative Examples

The theoretical tools developed in this section will now be particularized for a numerical example. This will allow us to provide concise numerical values for the expressions derived in this chapter and motivate the reader about applicability of the algorithms proposed. We validate the theoretical results and algorithm introduced in this paper by means of simulations. First, a fleet of autonomous vehicles with strongly connected network topology is considered and then the same simulation is repeated for a simply (weakly) connected network.

We consider a fleet of autonomous underwater vehicles (AUVs) moving in the horizontal plane, with the following continuous-time models:

$$\begin{aligned} m^i \ddot{x}^i &= -\mu_1^i \dot{x}^i + (u_R^i + u_L^i) \cos \theta^i \\ m^i \ddot{y}^i &= -\mu_1^i \dot{y}^i + (u_R^i + u_L^i) \sin \theta^i \end{aligned}$$

$$I_{\theta}^i \ddot{\theta}^i = -\mu_1^i \dot{\theta}^i + (u_R^i + u_L^i) r_1 \quad (5.94)$$

where $m^i = 0.75$, $I_{\theta}^i = 0.00316$, $\mu_1^i = 0.15$, $\mu_2^i = 0.005$ and $r_1^i = 8.9$ are the dimensionless vehicle mass, inertia, linear and rotational damping coefficients, and the vehicle radius respectively. For simplicity, the dynamics is considered to be the same for all agents, and the parameters are specified in [59]. The state vector is $z^i \triangleq [x^i, y^i, \theta^i, \dot{x}^i, \dot{y}^i, \dot{\theta}^i]^T$, consisting of horizontal (x) and vertical distance (y), horizontal (\dot{x}) and vertical (\dot{y}) speeds, heading (θ) and rotational speed $\dot{\theta}$. Control vector consists right (u_R) and left (u_L) force inputs. The model (5.94) is discretized at $T = 0.1s$ (assumed to be the same for all vehicles). The inputs are constrained to $0 \leq u_{R,L}^i \leq 6$, and the maximum turn rate is constrained to $-57\dot{\theta} \leq 57$. The communication delay is bounded by $0.1s = T \leq \Delta_{ij} \leq 6T = 0.6s$. It is assumed that Δ_{ij} is uniformly distributed: $\Delta_{ij} = \mathcal{U}(\mathcal{T}, \mathcal{T})$, and that $\Delta_{ij} \neq \Delta_{ji}$.

The distributed cost function at each agent (leader is A^1) is

$$J_t^i = \sum_{l=t}^{t+N_p^i-1} \left((\tilde{z}_l^i - g_l^i)^T Q^i (\tilde{z}_l^i - g_l^i) + u_l^{iT} R^i u_l^I + \sum_{j \in G^i} (\tilde{z}_l^i - \tilde{z}_l^j + a^{ij})^T S^{ij} (\tilde{z}_l^i - \tilde{z}_l^j + a^{ij}) \right) + \left(\tilde{z}_{t+N_p^i}^i - g_l^i \right)^T Q_f^i \left(\tilde{z}_{t+N_p^i}^i - g_l^i \right) + \sum_{j \in G^i} \frac{\bar{\lambda} R_{\min}^i \mathbf{1}_{(R_{\min}^j - d_k^{ij}) > 0, \forall t \leq k \leq (t+N_p^i)}}{\sum_{k=t}^{t+N_p^i} \lambda(d_k^{ij}) d_k^{ij}} \quad (5.95)$$

Goal g_k^i is the way-point (WP) for leader and for followers it is the leader's planned trajectory, i.e. $g^i = \tilde{w}_l^1, \forall i \neq 1$. Alignment vectors a^{ij} define the formation geometry such that adjacent agents occupy designated positions in a given formation

geometry with the team's consensus speed and heading. The weighting matrices are specified as

$$Q^i = \begin{bmatrix} 0.1 & 0 & 0 & 0 & 0 & 0 \\ 0 & 0.1 & 0 & 0 & 0 & 0 \\ 0 & 0 & 1 & 0 & 0 & 0 \\ 0 & 0 & 0 & 0.1 & 0 & 0 \\ 0 & 0 & 0 & 0 & 0.1 & 0 \\ 0 & 0 & 0 & 0 & 0 & 1 \end{bmatrix}, \quad R^i = \begin{bmatrix} 0.01 & 0 \\ 0 & 0.01 \end{bmatrix}, \quad (5.96)$$

which means more emphasis is placed on heading consensus than the displacement from the ideal position in the formation. The spatial filter is designed with filter constant $\lambda = 0.95$. In the simulations, the only source of uncertainty considered is the neural network compression errors in trajectory approximation.

Example 5.6.1 (Strongly Connected Team) Let us first consider the case of a strongly connected team of three AUVs ($N=3$), whose network topology is shown in Fig. 5.5. Each agent can communicate with each other in both directions. Therefore, $M^i = 2$ for all agents and $G^1 = \{A^2, A^3\}$, $G^2 = \{A^1, A^3\}$ and $G^3 = \{A^1, A^2\}$. In this simulation, the three vehicles are requested to maintain a triangular formation, with three vehicles at vertices of an equilateral triangle, initially oriented at 45° from the horizontal, at a distance of 15 units from each other. A minimum distance of $R_{\min} = 5$ units should also be maintained to avoid collision. The cooperation weights are assigned as $S^{ij} = 0.25 \times Q^i$.

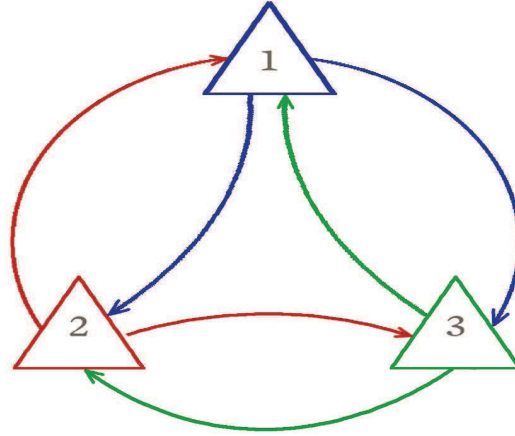


Figure 5.5: Network topology of strongly connected team. Notice two way communication between all vehicles

Fig. 5.6 shows trajectory of the fleet with initial positions marked by circles and markers showing position and orientation of agents are plotted for every 10 samples. Turning tight corners, such as right angle turns when transitioning between waypoints, is a difficult task for constrained individual systems, but more so when operating in a fleet while avoiding collisions. Synchronization of states is achieved quickly, shown in Fig. 5.7, without violation of constraints on states and inputs (Fig. 5.10). The effect of delay is manifest in lag in synchronization, while temporary divergence is due to collision avoidance.

As can be observed from Fig. 5.8, the collision avoidance system starts repelling the agents before they come too close. The distributed cost (5.27) is normalized with its maximum value. Initially, leader's (Agent 1) cost decreases monotonously, but suffers a discontinuous increase as the waypoint changes. However, for the other two agents, the decrease in cost function is not smooth, indicating onset of collision avoidance to discourage potential collision courses. However,

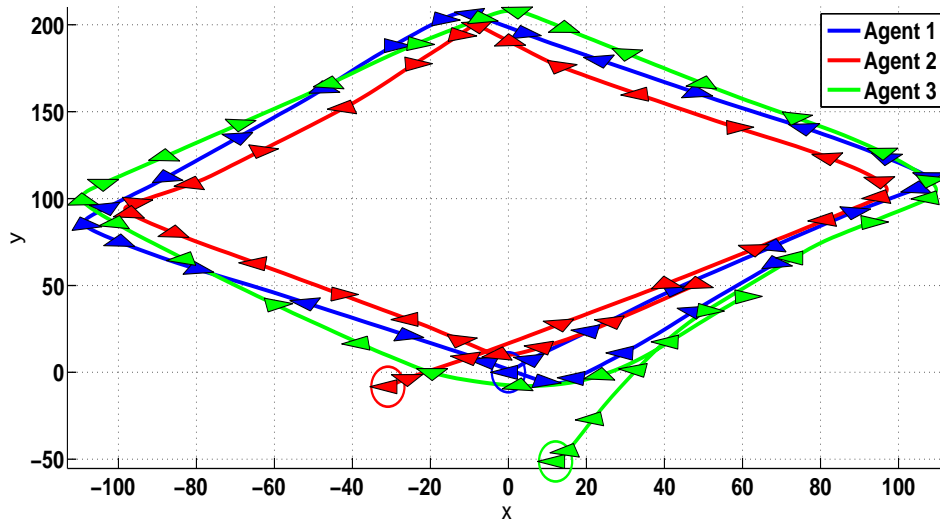


Figure 5.6: Trajectory of fleet of three AUVs connected in a strongly connected network.

when the leader transitions to the next waypoint at about 5 seconds, the sharp turn causes an oscillation in its cost in order to find a collision free trajectory. Distance between Agent 1 and Agent 3 reaches its lowest value at this point due to delay in communication, but they are successfully pushed away from each other. Despite the relatively large random delays (Fig. 5.9), the proposed algorithm was able to perform well.

Example 5.6.2 (Weakly Connected Team) In this simulation, five vehicles ($N = 5$) are requested to maintain a V-formation, with three vehicles positioned in the same manner as in Fig.5.5. Two more vehicles are added at vertices of an equilateral triangle having the leader (Agent 1) at its apex and Agents 4 and 5 at a distance of 30 units from the leader at the port and starboard sides of Agent 1, respectively. Agents 1,2 and 3 agents have two-way communication with each other, thus forming a strongly connected subgraph. However, Agents 4

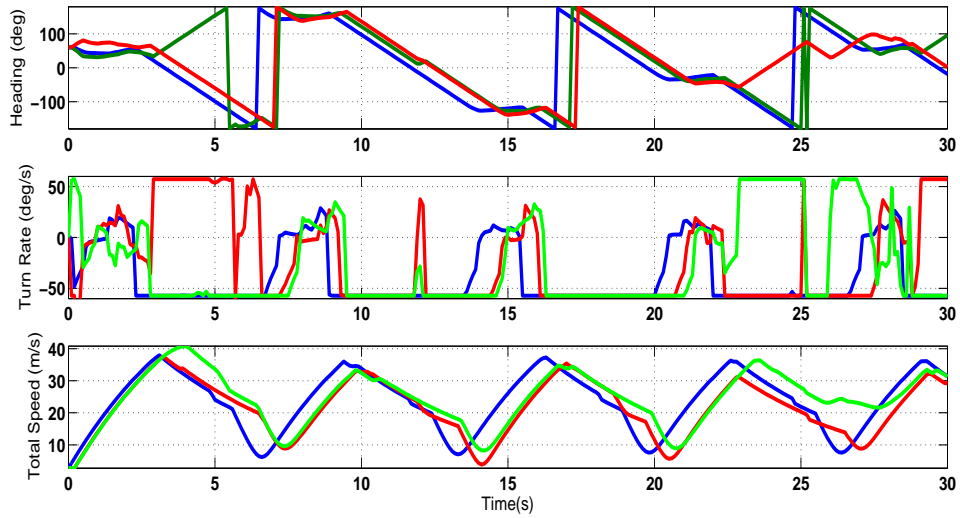


Figure 5.7: States of Agents connected in a Strongly Connected Network. Agent 1 (blue), Agent 2 (red) and Agent 3 (green). Top to bottom: Heading, Turn rate and Velocity.

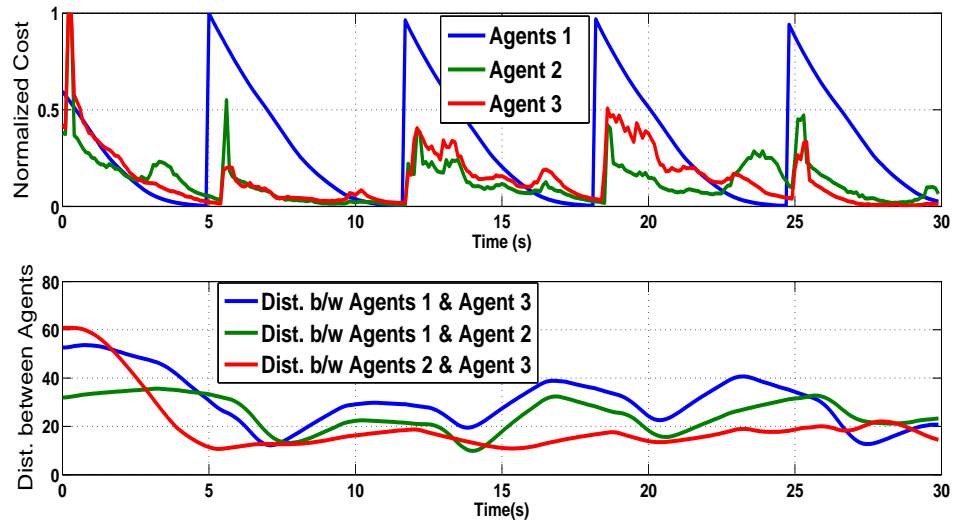


Figure 5.8: Normalized cost of each vehicle (top) and Inter-Agent Distances (bottom) for Fleet in a Strongly Connected Network. Notice the spikes in cost when collision avoidance is active, and that the minimum separation of 5 units is not violated.

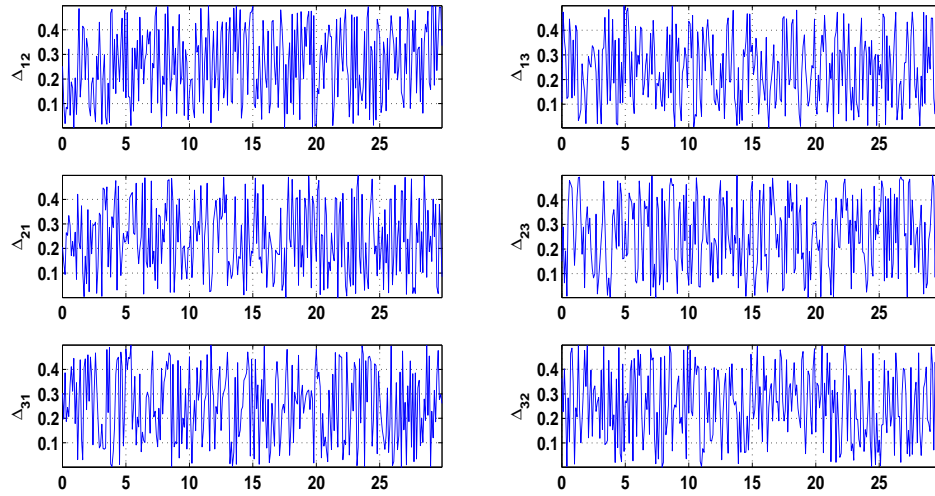


Figure 5.9: Propagation delays in strongly connected team. Notice that the delay in one direction of communication is not the same as the opposite direction of communication between the same agents.

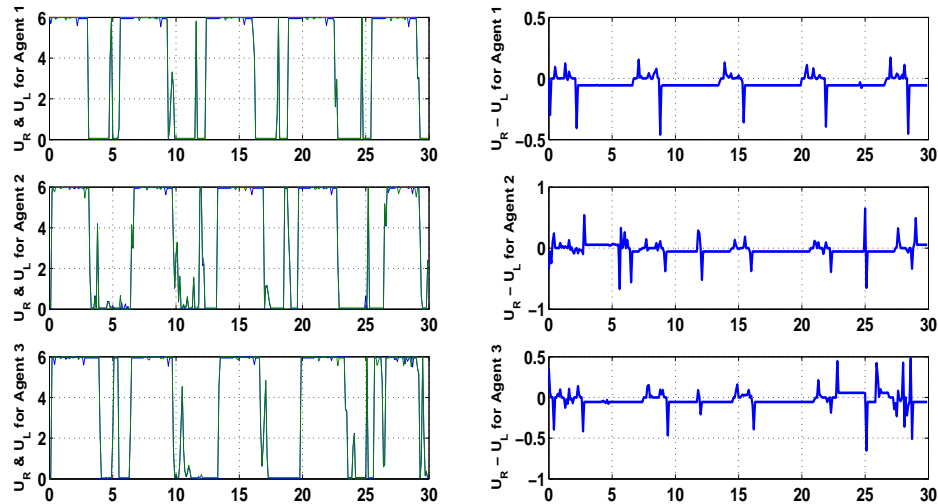


Figure 5.10: Control evolution in strongly connected team. U_R is shown in blue and U_L is shown in green.

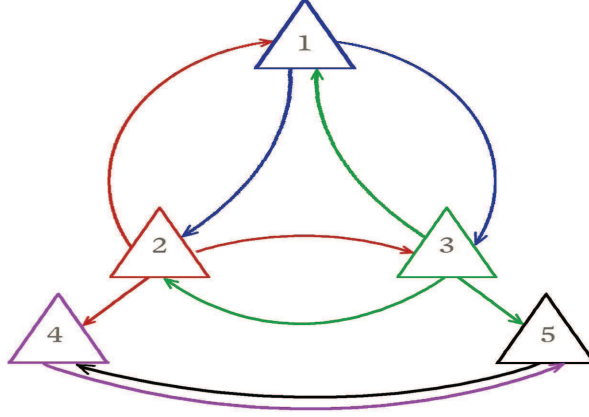


Figure 5.11: Network topology of weakly connected team. Notice only one-way communication for A^4 and A^5 .

and 5 have an undirected link with each other and directed link from Agents 2 and 3, respectively. Therefore, the overall network is a weakly connected mixed graph. Moreover, there exists a spanning tree with Agent 1 as the root node, see Fig.5.11. Rest of the simulation parameters are the same as in Example 5.6.1, except $S^{ij}=0.25 Q^i$ (for $i \neq 1$) and $S^{1j}=0.2 S^{ij}$. Therefore, $M^1 = 2$ for all agents and $G^1 = \{A^2, A^3\}$, $G^2 = \{A^1, A^3\}$, $G^3 = \{A^1, A^2\}$, $G^4 = \{A^2, A^5\}$ and $G^5 = \{A^3, A^4\}$. Fig. 5.12 shows trajectory of the weakly connected fleet. Only the first two waypoints are shown in the interest of clarity. Turning tight corners, such as right angle turns when transitioning between waypoints, is especially difficult agents on the inside of the turn, such as Agents 2 and 4. Hence, collision among these agents is more possible. It should be noted that Agents 4 and 5 receive information about change in formation configuration from the leader, Agent 1, with extra delay due to multiple hops, i.e. $\Delta_{14} = \Delta_{12} + \Delta_{24}$ and $\Delta_{15} = \Delta_{13} + \Delta_{35}$. Thus, effectively $\bar{\Delta}_4 = \bar{\Delta}_5 = 2\bar{\Delta}$. However, as seen in Fig. 5.14, any collision

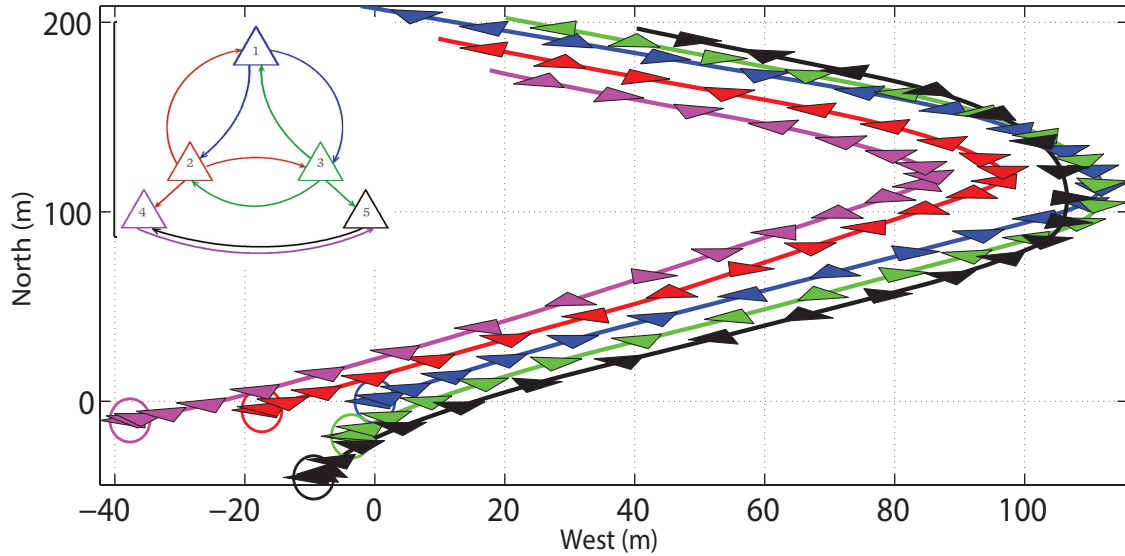


Figure 5.12: Trajectory of fleet of 5 AUVs connected in a weakly connected network, in a V-formation.

is successfully avoided throughout the trajectory. Synchronization of states is achieved effectively, shown in Fig. 5.13, without any violation of constraints on states and inputs (not shown here). It is evident that the proposed algorithm performs well in both weakly connected and strongly connected networks. The small gain condition (5.80) is obeyed by the team, as shown in Fig 5.16 for the first waypoint of Agent 1.

5.7 Conclusion

We presented distributed NMPC framework for formation control of constrained agents robust to uncertainty due to data compression and propagation delays. Collision avoidance is ensured by means of spatially filtered potential field. Rigorous proofs are provided ensuring practical stability regardless of network topology.

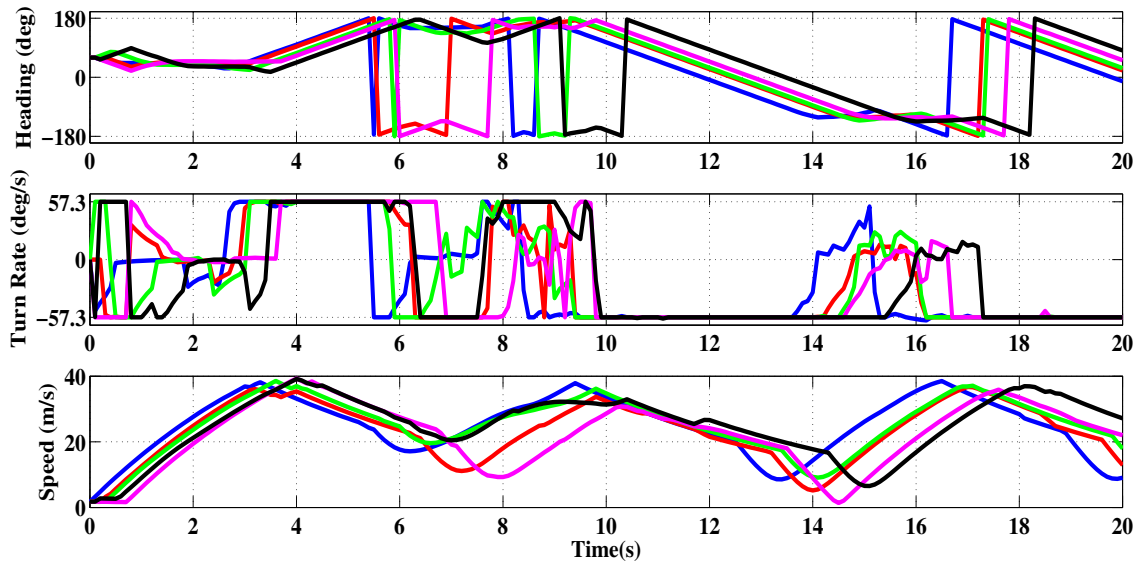


Figure 5.13: States of Agents connected in a Weakly Connected Network. Agent 1 (blue), Agent 2 (red), Agent 3 (green), Agent 4 (purple) and Agent 5 (black). Top to bottom: Heading, Turn rate and Velocity.

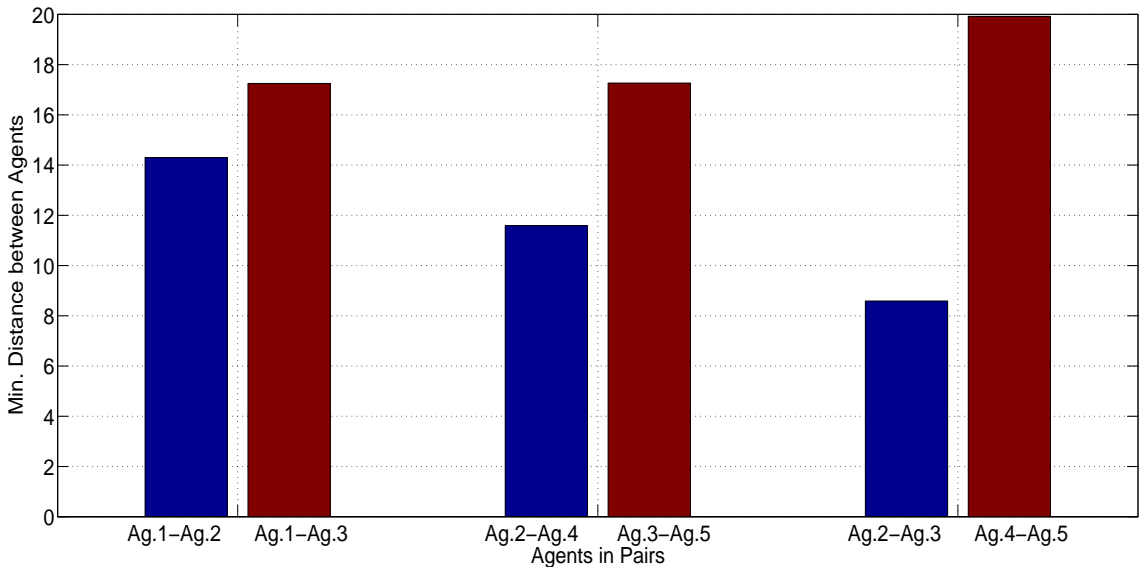


Figure 5.14: Inter-vehicle distances in weakly connected fleet example.

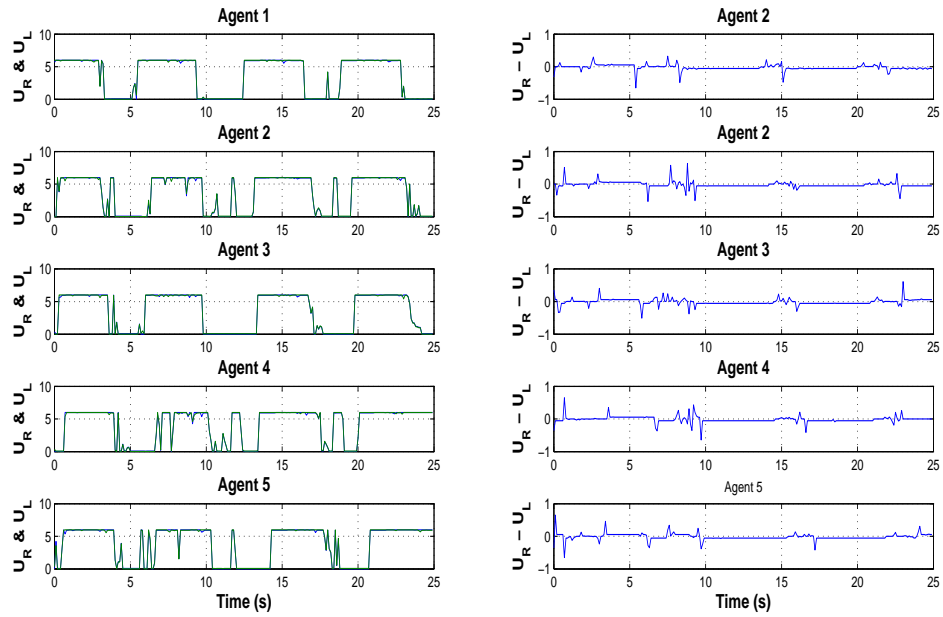


Figure 5.15: Control evolution in in weakly connected team. U_R is shown in blue and U_L is shown in green.

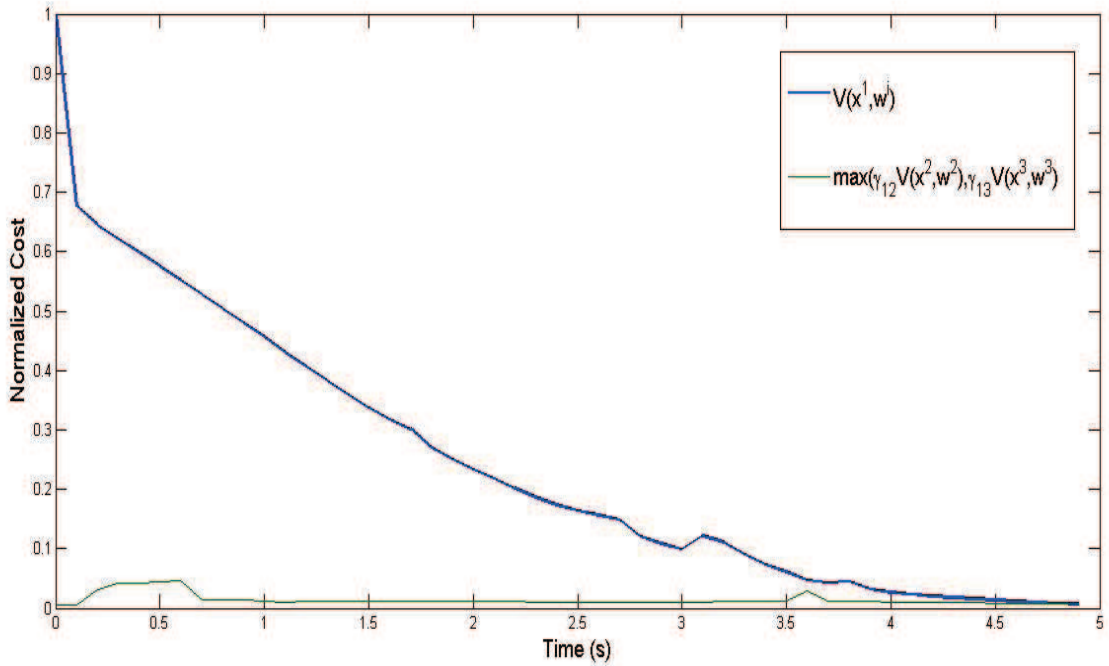


Figure 5.16: Small gain condition (5.80) for Agent 1 in weakly connected team. Value of design function parameter $\hat{k}^1 = 5000$.

Simulations illustrate good performance of the proposed scheme in both strongly- and weakly-connected networks. Future research directions include the need to cater for model uncertainty, disturbances and fault tolerance.

CHAPTER 6

CONCLUSION AND FUTURE WORK

6.1 Epilogue

This chapter summarizes the contributions of this thesis to the existing scientific body of work on distributed and robust nonlinear model predictive control. It also points out possible future extensions of this research. Due to “natural” affinity of all human engineered solutions to converge to optimum solutions provided in nature, there is a great emphasis in current research to mimic biological multi-agent and distributed control architectures. Formation “flight” is one of these tasks modeled after similar behavior of birds, ants, fish etc. to move in geometric formations, with non-obvious benefits for the entire team. Formation control was the focus of this thesis, where we found the avenue to contribute with original and need research due to gaps in existing scientific literature in this regard. An online

optimal control technique for distributed implementation called Model Predictive Control was chosen as the breadboard for designing a generalized robust control design framework, catering for an unprecedented array of sources of uncertainty. A number of theorems, lemmas, postulates and corollaries form the basis on which eight different algorithms are formulated for implementation of numerical recipes backed by solid theoretical results.

6.2 Thesis Contributions

In preceding sections, we were able to provide original results and solutions for the thesis problem statement in Section 1.3. We will summarize each of them below.

6.2.1 Robustness to Simultaneous Multiple Sources of Uncertainty

Existing literature mostly considers either modeling uncertainty with perfect measurements [85] or measurement noise with perfect model [68]. The proposed approach provides a unified framework for dealing with many types of uncertainties, along with the inclusion of a non-additive disturbance with uncertain dynamics and unknown input, data compression errors and propagation delays. A number of sources of uncertainty are taken into account to provide robustness to the algorithms developed. In existing literature, usually only measurement / estimation errors or model mismatch are taken into account. We consider the simultaneous presence of six sources of uncertainty

- i. error in estimating current state,
- ii. error in estimating current external input (disturbance or external information),
- iii. error in predicting future system state due to model mismatch,
- iv. error in predicting future external input due to disturbance model mismatch (disturbance model is another uncertain dynamic system with unknown input),
- v. error in approximating trajectory due to data compression, and
- vi. error in approximating the last segments (tail) of the compressed trajectory due to propagation delays.

We provide detailed feasibility and stability analysis to closed form analytic expressions relating the growth of uncertainty along the prediction horizon, and its effect on recursive feasibility and robust stability. We provide explicit bounds on growth of prediction uncertainty along the horizon in both single and multi-agent case. Based on these results, the nominal constraints are restricted for robust satisfaction of original constraints by the perturbed systems with Algorithms 2 and 8. These results are provided in Sections 3.2.5 and 5.3. New bounds on prediction error growth along the prediction horizon have been derived (Lemma 3.2.1) based on the bounds on components of the combined uncertainty. In addition, constraint tightening for robust satisfaction of original constraints in the presence of this combination of uncertainties (Theorem 3.2.1) is also a new development.

6.2.2 Results in Input-to-State Practical Stability

Input-to-state stability (ISS) framework in existing literature is extended with Theorem 3.2.2 to cater for the combination of uncertainties mentioned above. New generalized input to state practical stability (ISpS) and generalized small gain conditions are derived for the centralized (Section 3.2.7) and distributed (Section 5.5) controllers. Analytical results proving ISpS and generalized small gain conditions are presented. Theorems 2.5.2, 3.2.2, 3.2.3, 5.5.1 and 5.5.2 provide extensive insights into the conditions of practical stability. It is shown that the presence of uncertainty means asymptotic (ISS) stability cannot be achieved and one can only achieve ultimate boundedness (ISpS), even if there is only one source of uncertainty. The insights gained help choose various designer parameters in controller implementation.

6.2.3 Results on Recursive Stability and Allowable Uncertainty

Recursive feasibility is ensured by the newly developed Theorems 3.1 which relates it to the size of the one-step controllable set to the terminal region. One-step controllable set and robust output feasible set are determined based on min-max optimization (Algorithms 5 and 6) rather than the existing set based approaches [78]. This is an iterative approach based on min-max optimization to find the maximum initial feasibility set for the worst case realization of uncertainties. Due to the non-convex nature of this optimization, it is susceptible to local minima

and hence we also provide a methodology for selecting the correct initial iterates. This is the most computationally expensive algorithm, but since it is implemented offline, computational time is not an issue.

6.2.4 Terminal Region Maximization and Terminal Control Optimization

Size of the terminal constraint set is often taken as a measure of the output feasible set of MPC algorithms. Therefore, there is an overriding interest in maximizing this region. However, this is not a straightforward task as the states and controls are constrained. We develop a terminal constraint region maximization approach (Theorem 4.3.1 and Algorithm 3) based on PLDIs and LMIs, which makes it very easy to use existing efficient convex optimization techniques. An improvement is also suggested warm started with a novel approach (Algorithm 4) involving algebraic Riccati equations. Since very efficient algorithms for solving Riccati equations exist, this is achieved with a very low computational load.

6.2.5 Data Compression and Trajectory Reconstruction

We propose a practically stable (ultimately bounded) formulation of the distributed nonlinear model predictive controller (DNMPC), in which agents communicate compressed information to each other with propagation delays and collision avoidance is guaranteed, despite the presence of these delays and uncertainties. Data compression (Section 5.2.1) using neural networks approach is used ensuring

a considerable reduction of the data packet size (as much as 75 %). Moreover, the approach allows the agents to be sampled locally at different rates as well as to have different dynamics, constraints and prediction horizons, while being robust to propagation delays and uncertainty in neighbors' trajectories. Moreover, a method to estimate the tail of the received trajectory lost due to delays is provided in Section 5.2.1, where we also find the effect this has on growth of uncertainty in prediction.

6.2.6 Collision Avoidance

Collision avoidance algorithms existing in literature are based on additive potential fields which penalize current states of the system. We propose a novel spatial filter (Section 5.2.2), ensure that the smallest separation between two agents in the future horizon gets the highest weight. On the other hand, taking a simple average or a time-based forgetting factor [59], results in poor performance in collision avoidance, as trajectories which enter very late in safety zone have a small repelling potential, and hence not prevented from very early on. Such strategy results in agents getting very close before they start repelling each other to avoid collision, causing a loss of tracking performance. However, with the proposed approach, trajectories are immediately penalized upon falling within the safety zone and are obviously avoided in the NMPC optimal control selection process. Conditions for stability of this approach are shown in Section 5.5 in terms of Theorem 5.5.4.

6.2.7 Stability of Different Network Topologies

Unlike [59] and existing literature, the stability results of Section 5.5 are not limited to strongly connected networks. It is shown even a weakly connected network topology for multiple agents can be designed for fleet-wide stability and recursive feasibility. We prove generalized small gain conditions (5.62) and (5.80), which proves stability for all network topologies with at least one spanning tree. The result is general, not limited by the number of subsystems and the way in which subsystem gains are distributed is arbitrary. We prove that it is easy to ensure fleet stability by designing simple nonlinear functions. Simulations are provided for both strongly connected and weakly connected fleet network topologies, which prove the validity of theoretical development.

6.3 Future Recommendations

From our survey of the literature and during the course of the research, we found a number of avenues amenable to extensive academic and scientific inquiry. We believe the research in observer/estimator based distributed NMPC is still relatively untouched. There is a need to provide nonlinear separation principles for distributed NMPC and observer design. Also, cooperative and opportunistic estimation is another area where our results can be readily extended. We also recommend exploring competitive tasks, such as predator-prey games and pursuit-evasion tasks. Collaborative adaptive filtering and model free predictive control (we have carried out some preliminary work in these directions with recurrent

neural networks and collaborative LMS filters for predator-prey games).

6.4 Concluding Remarks

Current body of published work revealed a lack of generalized theoretical framework for robust distributed nonlinear model predictive control catering for various sources of uncertainties occurring simultaneously. We developed several algorithms for robust and distributed nonlinear model predictive control for a team of vehicles in the presence of uncertainties and propagation delays. Due to limited bandwidth allocable to each communication channel in a multi-vehicle team, we propose an algorithm to compress trajectory information before sending it over the network. Due to communication and computational delays, the trailing part of propagated trajectories is lost, for which another method for reconstruction of trajectory tail is provided. Newly derived bounds on prediction error growth allows us to place tighter constraints on nominal state evolution in order to satisfy constraints on the actual system. Finally, methods for maximizing size of the terminal constraint set, optimizing the terminal control law, computing recursive feasibility conditions and determining the feasible set of the NMPC optimal control problem are presented. This thesis also bridged the gap between theory and adhoc practicality of existing most existing algorithms by developing a rigorously proven framework for the robustness, feasibility and stability of robust and distributed NMPC. The new framework caters to simultaneous presence of six sources of uncertainty consisting of errors in estimation, modeling, prediction,

data compression and loss of information due to delay. We hope this work will provide an important step toward scientific discovery in distributed robust and optimal multi-agent control.

REFERENCES

- [1] I. Al-Jazari, *The Book of Knowledge of Ingenious Mechanical Devices*. Dordrecht, Holland: D. Reidel Publishing Company, 1974.
- [2] T. Arai *et al.*, “Advances in Multi-Robot Systems,” *IEEE Trans. Robot. Autom.*, vol. 18, no. 5, pp. 655–661, Oct. 2002.
- [3] Y. Jia and W. Zhang, “Distributed Adaptive Flocking of Robotic Fish System with a Leader of Bounded Unknown Input,” *Int. J. of Control Autom. Syst.*, vol. 12, no. 5, pp. 1049–1058, Oct. 2014.
- [4] S.-Y. Tu and A. H. Syed, “Tracking Behavior of Mobile Adaptive Networks,” in *44th Asilomar Conf. on Signals, Syst. Comput.*, Pacific Grove, CA, 7-10 Nov. 2010, pp. 698–702.
- [5] —, “Cooperative Prey Herding based on Diffusion Adaptation,” in *IEEE Int. Conf. Acoust., Speech, Signal Process.*, Prague, Czech Republic, 22-27 May 2011, pp. 3752–3755.

- [6] C. Yu and R. Nagpal, “Biologically-Inspired Control for Multi-Agent Self-Adaptive Tasks,” in *24th AAAI Conf. Artificial Intell.*, Atlanta, GA, 12-25 Jul. 2010, pp. 1–6.
- [7] T. Balch and R. Arkin, “Behavior-based Formation Control for Multi-Robot Teams,” *IEEE Trans. Robot. Autom.*, vol. 14, no. 6, pp. 926–939, Dec 1998.
- [8] C. Yu and R. Nagpal, “A Self-adaptive Framework for Modular Robots in a Dynamic Environment: Theory and Applications,” *Int. J. Robot. Research*, vol. 30, no. 8, pp. 1015–1036, Jul. 2011.
- [9] B. Sinopoli *et al.*, “Distributed Control Applications within Sensor Networks,” *Proc. IEEE*, vol. 91, no. 8, pp. 1235–1246, Aug. 2003.
- [10] K. Hungerford *et al.*, “Distributed, Complete, Multi-Robot Coverage of Initially Unknown Environments using Repartitioning,” in *Int. Conf. Auton. Agents and Multi-Agent Syst.*, Paris, France, 5-9 May 2014, pp. 1453–1454.
- [11] J. Redding *et al.*, “Collaborative Mission Planning, Autonomy and Control Technology (CoMPACT) for Unmanned Surface Vehicles,” in *AIAA Guidance, Navig. Control Conf.*, Chicago, IL, 10-13 Aug. 2009, pp. 1–23.
- [12] S. Moon *et al.*, *Handbook of Unmanned Aerial Vehicles*. Netherlands: Springer, 2014, ch. Cooperative Task Assignment and Path Planning for Multiple UAVs, pp. 1547–1576.

- [13] L. Felicetti and G. Palmerini, "Evaluation of Control Strategies for Spacecraft Electrostatic Formation Keeping," in *IEEE Aerosp. Conf.*, Big Sky, MT, 1-8 Mar. 2014, pp. 1–9.
- [14] R. Turner *et al.*, "Distributed context-based organization and reorganization of multi-auv systems," *J. Unmanned Syst. Tech.*, vol. 2, no. 1, pp. 1164–1167, Mar. 2014.
- [15] M. Langerwisch *et al.*, "Heterogeneous Teams of Unmanned Ground and Aerial Robots for Reconnaissance and Surveillance - A Field Experiment," in *Int. Symp. Safety, Security and Rescue Robot.*, Linköping, Sweden, 21-26 Oct. 2013, pp. 1–6.
- [16] L. Humphrey *et al.*, "Formal Specification and Synthesis of Mission Plans for Unmanned Aerial Vehicles," in *AAAI Spring Symposium Series*, Palo Alto, CA, 24-26 Mar. 2014, pp. 116–121.
- [17] Y. Ying, "Cooperative Task Assignment of Multiple UCAVs based on MAS and CNP," in *IEEE Int. Conf. Granular Comput.*, Beijing, China, 13-15 Dec. 2013, pp. 391–395.
- [18] S. Yu and T. Ura, "A System of Multi-AUV Interlinked With a Smart Cable For Autonomous Inspection of Underwater Structures," *Int. J. Offshore and Polar Eng.*, vol. 14, no. 4, pp. 265–273, Dec. 2004.
- [19] S. El-Ferik, B. Siddiqui, R. B. Mansour, and F. Al-Sunni, "Dual Submarine Leak Detection System," U.S. Patent 8 499 617, Aug 6, 2013.

- [20] J. de Hoog *et al.*, “Role-based Autonomous Multi-Robot Exploration,” in *Future Comput., Service Comput., Cogn., Adaptive, Content, Patterns (COMPUTATIONWORLD)*, Athens, Greece, 15-20 Nov. 2009, pp. 482–487.
- [21] G. Cubber *et al.*, “Search and Rescue Robots Developed by the European ICARUS Project,” in *IARP Workshop on Robotics for Risky Environment and Extreme Robotics*, St. Petersburg, Russia, 1-3 Oct. 2013, pp. 1–6.
- [22] W. Ren and Y. Cao, *Distributed Coordination of Multi-agent Networks*. London, UK: Springer, 2011.
- [23] F. Kendoul, “Survey of Advances in Guidance, Navigation, and Control of Unmanned Rotorcraft Systems of Unmanned Rotorcraft Systems,” *J. Field Robot.*, vol. 29, no. 2, pp. 315–378, Mar.-Apr. 2012.
- [24] X. Xiang *et al.*, “Coordinated Control for Multi-AUV Systems based on Hybrid Automata,” in *IEEE Int. Conf. Robot. Biomimetics*, Sanya, China, 15-18 Dec. 2007, pp. 2121–2126.
- [25] J. Farrell, *Aided Navigation: GPS with High Rate Sensors*, W. Rinaldi, Ed. New York, NY: McGraw-Hill, 2008.
- [26] N. Kottege, “Underwater Acoustic Localisation in the context of Autonomous Submersibles,” Ph.D. Dissertation, Australian National University, 2011.

- [27] W. B. Dunbar *et al.*, “Nonlinear and Cooperative Control of Multiple Hovercraft with Input Constraints,” in *European Control Conf.*, Cambridge, UK, 1-4 Sep. 2003, pp. 1–6.
- [28] A. Das and F. L. Lewis, “Synchronization of Unknown Nonlinear Networked Systems via Cooperative Adaptive Control,” in *8th IEEE Int. Conf. Control Autom.*, Xiamen, China, 9-11 Jun. 2010, pp. 2048–2055.
- [29] W. Zhang *et al.*, “Adaptive Backstepping-based Synchronization of Uncertain Networked Lagrangian Systems,” in *Amer. Control Conf.*, San Francisco, CA, 29 Jun.-1 Jul. 2011, pp. 1057–1062.
- [30] A. R. Mehrabian *et al.*, “Distributed H_∞ Optimal Control of Networked Uncertain Nonlinear Euler-Lagrange Systems with Switching Communication Network Topologies,” in *50th IEEE Conf. Decision Control*, Orlando, FL, 12-15 Dec. 2011, pp. 1379–1386.
- [31] S. Zelinski *et al.*, “Optimization-based Formation Reconfiguration Planning For Autonomous Vehicles,” in *IEEE Int. Conf. Robotics Autom.*, Taipei, Taiwan, 14-19 Dec. 2003, pp. 3758–3763.
- [32] W. Li and C. Cassandras, “A Cooperative Receding Horizon Controller for Multivehicle Uncertain Environments,” *IEEE Trans. Autom. Control*, vol. 51, no. 2, pp. 242–257, Feb. 2006.

- [33] W. B. Dunbar, “Model Predictive Control: Extension to Coordinated Multi-vehicle Formations and Real-time Implementation,” California Inst. Tech., Pasadena, CA, Tech. Rep. CDS TR 01-016, 2001.
- [34] W. Dunbar and R. Murray, “Model Predictive Control of Coordinated Multi-vehicle Formations,” in *41st IEEE Conf. Decision Control*, vol. 4, Atlanta, GA, 10-13 Dec. 2002, pp. 4631–4636.
- [35] W. B. Dunbar and R. M. Murray, “Distributed Receding Horizon Control for Multi-Vehicle Formation Stabilization,” *Automatica*, vol. 42, no. 4, pp. 549–558, Apr. 2006.
- [36] W. Dunbar *et al.*, “Distributed Receding Horizon Control of Vehicle Platoons: Stability and String Stability,” *IEEE Trans. Autom. Control*, vol. 57, no. 3, pp. 620–633, Mar. 2012.
- [37] M. A. Müller *et al.*, “A General Distributed MPC Framework for Cooperative Control,” in *Proc. 18th IFAC World Congr.*, Milano, Italy, 28 Aug.-2 Sep. 2011, pp. 7987–7992.
- [38] D. Mayne *et al.*, “Constrained Model Predictive Control: Stability and Optimality,” *Automatica*, vol. 36, no. 6, pp. 789–814, Jun. 2000.
- [39] M. A. Müller *et al.*, “Cooperative Control of Dynamically Decoupled Systems via Distributed Model Predictive Control,” *Int. J. Robust Nonlin. Control*, vol. 22, no. 12, pp. 1376–1397, Aug. 2012.

- [40] L. Grüne and J. Pannek, *Nonlinear Model Predictive Control, Theory and Algorithms*. London, UK: Springer, 2011.
- [41] T. Jahn and J. Pannek, “Stability of Constrained Adaptive Model Predictive Control Algorithms,” in *18th IFAC World Congr.*, vol. 18, Milano, Italy, 28 Aug.-2 Sep. 2011, pp. 9272–9277.
- [42] L. Grüne and K. Worthmann, *Distributed Decision Making and Control*. Springer-Verlag, 2012, ch. A Distributed Nonlinear Model Predictive Control Scheme without Stabilizing Terminal Constraints, pp. 259 – 285.
- [43] J. Pannek, “Parallelizing a State Exchange Strategy for Noncooperative Distributed Nonlinear Model Predictive Control,” *Syst. Control Lett.*, vol. 62, no. 1, pp. 29–36, Jan. 2013.
- [44] R. Saber *et al.*, “Cooperative Control of Multi-Vehicle Systems Using Cost Graphs and Optimization,” in *Amer. Control Conf.*, Denver, CO, 4-6 Jun. 2003, pp. 2217–2222.
- [45] D. Shim *et al.*, “Decentralized Reflective Model Predictive Control of Multiple Flying Robots in Dynamic Environment,” in *42nd IEEE Conf. Decision Control*, vol. 4, Maui, HI, 9-12 Dec. 2003, pp. 3621–3626.
- [46] K. Wesselowski and R. Fierro, “A Dual-Mode Model Predictive Controller for Robot Formations,” in *42nd IEEE Conf. Decision Control*, Maui, HI, 9-12 Dec. 2003, pp. 3615–3620.

- [47] H. Fukushima *et al.*, “Distributed Model Predictive Control for Multi-Vehicle Formation with Collision Avoidance Constraints,” in *44th IEEE Conf. Decision Control*, Seville, Spain, 12-15 Dec. 2005, pp. 5480–5485.
- [48] Y. Yoon *et al.*, “Communication in Distributed Model Predictive Collision Avoidance,” in *Conf. Robot Commun. Coordination*, Athens, Greece, 15-17 Oct. 2007, pp. 1–4.
- [49] J. J. Arrieta-Camacho, L. T. Biegler, and D. Subramanian, *Assessment and Future Directions of Nonlinear Model Predictive Control*. Springer, 2007, ch. Trajectory Control of Multiple Aircraft: An NMPC Approach, pp. 629–639.
- [50] Z. Chao *et al.*, “UAV Formation Flight Based on Nonlinear Model Predictive Control,” *Math. Problems Eng.*, vol. 2012, no. 1, pp. 1–15, 2012.
- [51] M. Saska, “Trajectory Planning and Optimal Control for Formations of Autonomous Robots,” Ph.D. Dissertation, University of Würzburg, 2009.
- [52] T. Schouwenaars *et al.*, “Decentralized Cooperative Trajectory Planning of Multiple Aircraft with Hard Safety Guarantees,” in *AIAA Guidance, Navigation Control Conf.*, Providence, RI, 16-18 Aug. 2004, pp. 1–14.
- [53] S. Longhi *et al.*, “Cooperative control of underwater glider fleets by fault tolerant decentralized MPC,” in *17th IFAC World Congr.*, Seoul, Korea, 6-11 Jul. 2008, pp. 16 021–16 026.

- [54] A. Fonti *et al.*, “Cooperative and decentralized navigation of autonomous underwater gliders using predictive control,” in *18th IFAC World Congr.*, Milano, Italy, 28 Aug.-2 Sep. 2011, pp. 12 813–12 818.
- [55] H. A. Izadi *et al.*, “Fault Tolerant Model Predictive Control of Quad-Rotor Helicopters with Actuator Fault Estimation,” in *18th IFAC World Cong.*, vol. 18, Milano, Italy, 28 Aug.-2 Sep. 2011, pp. 6343–6348.
- [56] D. Simon, *Optimal State Estimation Kalman, H_∞ and Nonlinear Approaches*. Hoboken, NJ: John Wiley & Sons, 2006.
- [57] C. Leung *et al.*, “Planning Under Uncertainty using Model Predictive Control for Information Gathering,” *Robot. Auton. Syst.*, vol. 54, no. 11, pp. 898–910, Nov. 2006.
- [58] E. Franco *et al.*, “Cooperative Control of Distributed Agents with Nonlinear Dynamics and Delayed Information Exchange: A Stabilizing Receding-Horizon Approach,” in *44th IEEE Conf. Decision Control*, Seville, Spain, 12-15 Dec. 2005, pp. 2206–2211.
- [59] —, “Cooperative Constrained Control of Distributed Agents with Nonlinear Dynamics and Delayed Information Exchange: A stabilizing Receding Horizon Approach,” *IEEE Trans. Autom. Control*, vol. 53, no. 1, pp. 324–338, Feb. 2008.

- [60] L. Magni *et al.*, “Regional Input-to-State Stability for Nonlinear Model Predictive Control,” *IEEE Trans. Autom. Control*, vol. 51, no. 9, pp. 1548–1553, Sep. 2006.
- [61] J. Shin and H. J. Kim, “Nonlinear Model Predictive Formation Flight,” *IEEE Trans. Syst., Man, Cybern. A, Syst., Humans*, vol. 39, no. 5, pp. 1116–1126, Sep. 2009.
- [62] H. A. Izadi *et al.*, “Decentralized Receding Horizon Control of Multiple Vehicles subject to Communication Failure,” in *Amer. Control Conf.*, St. Lois, MO, 10-12 Jun. 2009, pp. 3531–3536.
- [63] —, “Decentralized Receding Horizon Control for Cooperative Multiple Vehicles Subject to Communication Delay,” *AIAA J. Guidance, Control, Dynamics*, vol. 32, no. 6, pp. 1959–1965, Nov.-Dec. 2009.
- [64] —, “Decentralized Receding Horizon Control with Communication Bandwidth Allocation for Multiple Vehicle Systems,” *Optim. Control Appl. and Methods*, vol. 33, no. 1, pp. 1–22, Jan.-Feb. 2012.
- [65] W. Ren and R. Beard, *Distributed Consensus in Multi vehicle Cooperative Control Theory and Applications*. London, UK: Springer, 2008.
- [66] P. Christofides *et al.*, *Networked and Distributed Predictive Control: Methods and Nonlinear Process Network Applications*. London, UK: Springer, 2011.

- [67] —, “Distributed Model Predictive Control: A Tutorial Review,” *Computer Chemical Eng.*, vol. 51, no. 1, pp. 21–41, Apr. 2013.
- [68] R. Huang *et al.*, “Robust Stability of Nonlinear Model Predictive Control based on Extended Kalman Filter,” *J. Process Control*, vol. 22, no. 1, pp. 82–89, Jan. 2012.
- [69] F. Arrichiello *et al.*, “Opportunistic Localization of Underwater Robots using Drifters and Boats,” in *IEEE International Conf. Robotics Autom.*, Saint Paul, MN, 14-18 May 2012, pp. 5307–5314.
- [70] E. Sontag, “Smooth Stabilization implies Coprime Factorization,” *IEEE Trans. Autom. Control*, vol. 34, no. 4, pp. 435–443, Apr 1989.
- [71] E. Sontag and Y. Wang, “New Characterizations of Input-to-State Stability,” *IEEE Trans. Autom. Control*, vol. 41, no. 9, pp. 1283–1294, Sep. 1996.
- [72] Y. Lin *et al.*, “A Smooth Converse Lyapunov Theorem for Robust Stability,” *SIAM J. Control Optim.*, vol. 34, no. 1, pp. 124–160, Jan. 1996.
- [73] S. El-Ferik, B. A. Siddiqui, and F. L. Lewis, “Distributed Nonlinear MPC Formation Control with Limited Bandwidth,” in *Amer. Control Conf.*, Washington, DC, 17-19 Jun. 2013, pp. 6388–6393.
- [74] H. Zhang and P. Dower, “Computation of Tight Integral Input-to-State Stability Bounds for Nonlinear Systems,” *Syst. Control Lett.*, vol. 62, no. 4, pp. 355–365, Apr 2013.

- [75] H. K. Khalil, *Nonlinear Systems*, 3rd ed. NY: Prentice-Hall, 2002.
- [76] S. Sastry, *Nonlinear Systems: Analysis, Stability, and Control*, J. Marsden *et al.*, Eds. NY: Springer-Verlag, 1999.
- [77] J. Sarangapani, *Neural Network Control of Nonlinear Discrete-Time Systems*. Boca Raton, FL: CRC Press, 2006.
- [78] E. Kerrigan, “Robust Constrained Satisfaction: Invariant Sets and Predictive Control,” Ph.D. Thesis, University of Cambridge, Cambridge, UK, Nov. 2000.
- [79] D. Limon *et al.*, “Input to State Stability of Min-Max MPC Controllers for Nonlinear Systems with Bounded Uncertainties,” *Automatica*, vol. 42, no. 5, pp. 797–803, May 2006.
- [80] L. Gruyitch *et al.*, *Stability Domains*, ser. Nonlinear Systems in Aviation, Aerospace, Aeronautics and Astronautics. Boca Raton, FL: CRC Press, 2003.
- [81] D. Limon *et al.*, *Nonlinear Model Predictive Control: Towards New Challenging Applications*. Berlin, Germany: Springer, 2009, ch. Input-to-State Stability: A Unifying Framework for Robust Model Predictive Control, pp. 1–26.
- [82] Z. Jiang and Y. Wang, “Input-to-State Stability for Discrete-Time Nonlinear Systems,” *Automatica*, vol. 37, no. 6, pp. 857–869, Jun. 2001.

- [83] C. Garcia *et al.*, “Model Predictive Control: Theory and Practice - A Survey,” *Automatica*, vol. 25, no. 3, pp. 335–348, May 1989.
- [84] S. El-Ferik, B. A. Siddiqui, and F. Lewis, “Constraint Tightened Robust Nonlinear Predictive Control with Uncertain Disturbance Model,” *Automatica*, Dec. 2014, submitted, under review.
- [85] G. Pin and T. Parisini, “Networked Predictive Control of Uncertain Constrained Nonlinear Systems: Recursive Feasibility and Input-to-State Stability Analysis,” *IEEE Trans. Autom. Control*, vol. 51, no. 1, pp. 72–87, Jan 2011.
- [86] L. Wang, *Model Predictive Control System Design and Implementation using Matlab*. London, UK: Springer-Verlag, 2009.
- [87] R. Soeterboek, *Predictive Control - A Unified Approach*. Upper Saddle River, NJ: Prentice-Hall, Inc., 1992.
- [88] J. Maciejowski, *Predictive Control with Constraints*. London, UK: Prentice-Hall, Inc., 2002.
- [89] —, “Reconfigurable Control Using Constrained Optimization,” in *European Control Conf.*, Brussels, Belgium, 1-4 Jul. 1997, pp. 107–130.
- [90] S. Yu *et al.*, “Nonlinear Model Predictive Control for Path Following Problems,” *Int. J. Robust Nonlin. Control*, 2014.

- [91] L. Chisci *et al.*, “Systems with Persistent Disturbances: Predictive Control with Restricted Constraints,” *Automatica*, vol. 37, no. 7, pp. 1019–1028, Jul. 2001.
- [92] G. Grimm *et al.*, “Examples when the Nonlinear Model Predictive Control is Nonrobust,” *Automatica*, vol. 40, no. 10, pp. 1729–1738, Oct. 2004.
- [93] H. Li and Y. Shi, “Distributed Model Predictive Control of Constrained Nonlinear Systems with Communication Delays,” *Syst. Control Lett.*, vol. 62, no. 10, pp. 819–826, Oct. 2013.
- [94] D. Marruedo *et al.*, “Input-to-State Stable MPC for Constrained Discrete-Time Nonlinear Systems with Bounded additive Uncertainties,” in *Proc. 41st IEEE Conf. Decision Control*, vol. 4, Las Vegas, NV, USA, 10-13 Dec. 2002, pp. 4619–4624.
- [95] G. Pin *et al.*, “Robust Model Predictive Control of Nonlinear Systems With Bounded and State-Dependent Uncertainties,” *IEEE Trans. Autom. Control*, vol. 54, no. 7, pp. 1681–1687, Jul. 2009.
- [96] D. Mayne, “Control of Constrained Dynamic Systems,” *Eur. J. Control*, vol. 7, no. 2-3, pp. 87–99, 2001.
- [97] B. Roset *et al.*, “Design of Stabilizing Output Feedback Nonlinear Model Predictive Controllers with an Application to DC-DC Converters,” in *European Control Conf.*, Kos, Greece, 2-5 Jul. 2007, pp. 2999–3004.

- [98] S. Boyd and L. Vandenberghe, *Convex Optimization*. New York, NY, USA: Cambridge University Press, 2004.
- [99] S. Boyd *et al.*, *Linear Matrix Inequalities in System and Control Theory*, ser. Studies in Applied Mathematics. Philadelphia, PA, USA: SIAM, Jun. 1994, vol. 15.
- [100] S. Yu *et al.*, *Nonlinear Model Predictive Control*, ser. Lecture Notes in Control and Information Sciences. Berlin, Germany: Springer Berlin Heidelberg, 2009, vol. 384, ch. Enlarging the Terminal Region of NMPC with Parameter-Dependent Terminal Control Law, pp. 69–78.
- [101] K. Toh *et al.*, “SDPT3 A Matlab Software Package for Semidefinite Programming,” *Optim. Methods Software*, vol. 11, no. 1-4, pp. 545–581, 1999.
- [102] K. Fujisawa *et al.*, “Exploiting Sparsity in Primal-Dual Interior-Point Method for Semidefinite Programming,” *Mathematical Programming*, vol. 79, no. 1-3, p. 235253, Oct. 1997.
- [103] F. Lewis *et al.*, *Optimal Control*, 3rd ed. New York, NY: John Wiley & Sons, 2012.
- [104] I. Polik and T. Terlaky, “A survey of the S-Lemma,” *SIAM Review*, vol. 49, no. 3, pp. 371–418, 2007.
- [105] C. Wang *et al.*, “Solving Log-Determinant Optimization Problems by a Newton-CG Primal Proximal Point Algorithm,” *SIAM J. Optimization*, vol. 20, no. 6, pp. 2994–3013, Aug. 2010.

- [106] M. Kočvara and M. Stingl, “PENNON - a Code for Convex Nonlinear and Semidefnite Programming,” *Opt. Methods and Software*, vol. 18, no. 3, pp. 317–333, 2003.
- [107] J. Löfberg, “YALMIP : A Toolbox for Modeling and Optimization in MATLAB,” in *Proceedings of the CACSD Conference*, Taipei, Taiwan, 2004. [Online]. Available: <http://users.isy.liu.se/johanl/yalmip>
- [108] M. Vašak *et al.*, “Efficient Computation of the One-Step Robust Sets for Piecewise Affine Systems with Polytopic Additive Uncertainties,” in *European Control Conf.*, Kos, Greece, 2-5 Jul. 2007, pp. 1430–1435.
- [109] H. Lin *et al.*, “Optimal Persistent Disturbance Attenuation Control for Linear Hybrid Systems,” *Nonlinear Analysis Theory, Methods and Applications*, vol. 65, no. 6, pp. 1231–1250, Sep. 2006.
- [110] G. Pin, “Robust Nonlinear Receding Horizon Control with Constraint Tightening,” Ph.D. Dissertation, University of Trieste, Trieste, Italy, Apr. 2009.
- [111] M. Branch and A. Grace, *Optimization Toolbox User’s Guide*, The Math Works, Inc., 24 Prime Park Way, Natick, MA 01760-1500, 2002.
- [112] P. Falcone *et al.*, “Predictive Active Steering Control for Autonomous Vehicle Systems,” *IEEE Trans. Con*, vol. 15, no. 3, pp. 566–580, May 2007.
- [113] M. Jamshidi, *Large-Scale Systems: Modeling, Control and Fuzzy Logic*, ser. Prentice Hall Series on Environmental and Intelligent Manufacturing Systems. Upper Saddle River, NJ: Prentice Hall, 1996, vol. 8.

- [114] M. Mahmoud, *Decentralized Control and Filtering in Interconnected Dynamical Systems*. New York, NY: CRC Press, 2010.
- [115] D. Srinivasagupta *et al.*, “Time-stamped Model Predictive Control: An Algorithm for Control of Processes with Random Delays,” *Comput. Chem. Eng.*, vol. 28, no. 8, pp. 1337–1346, Jul. 2004.
- [116] D. Raimondo, “Nonlinear Model Predictive Control: Stability, Robustness and Applications,” Ph.D. Dissertation, University of Pavia, Pavia PV, Italy, Jan. 2009.
- [117] E. Fiorelli *et al.*, “Adaptive Sampling using Feedback Control of an Autonomous Underwater Glider Fleet,” in *13th Symp. Unmanned Untethered Submersible Tech.*, Durham, NH, 26-28 Aug. 2003, pp. 1–16.
- [118] S. Dashkovskiy *et al.*, “Small Gain Theorems for Large Scale Systems and Construction of ISS Lyapunov Functions,” *SIAM J. Control Optim.*, vol. 48, no. 6, pp. 4089–4118, May 2010.
- [119] I. Karafyllis and Z. Jiang, *Stability and Stabilization of Nonlinear Systems*. London: Springer, 2011.

Vitae

Name: Bilal Ahmed Siddiqui
Nationality: Pakistani
Date of Birth: 5th October, 1980
Email Address: *airbilal@{kfupm.edu.sa, gmail.com}*
Permanent Address: House No. 8, Phase II, Malir Cantt.,
Karachi, Sindh, Pakistan

Education

BE Mechanical Engineering (2004) NED University of Engineering and
Technology, Karachi, Pakistan
MS Aerospace Engineering (2010) King Fahd University of Petroleum and
Minerals, Dhahran, Saudi Arabia
PhD Systems Engineering (2014) King Fahd University of Petroleum and
Minerals, Dhahran, Saudi Arabia

Selected Publications

1. S. El-Ferik, B. A. Siddiqui, and F. L. Lewis, Distributed Nonlinear MPC Formation Control with Limited Bandwidth, in American Control Conference, Washington, DC, 17-19 Jun. 2013, pp. 63886393. [73]. [Adjudged as the best presentation in the session].
2. S. El-Ferik, B. Siddiqui, R. B. Mansour, and F. Al-Sunni, Dual Submarine Leak Detection System, U.S. Patent 8 499 617, Aug 6, 2013. [19]. [Awarded

4th prize in innovation track and 5th Students' Conference organized by Ministry of Higher Education (MoHE) at Mecca, April 2013].

3. S. El-Ferik, B. A. Siddiqui, and F. L. Lewis, Distributed Nonlinear MPC of Multi-Agent Systems with Data Compression and Random Delays, IEEE Transactions on Automatic Control, Oct. 2014, accepted for publication.
4. S. El-Ferik, B. A. Siddiqui, and F. Lewis, Constraint Tightened Robust Non-linear Predictive Control with Uncertain Disturbance Model, Automatica, Dec. 2014, submitted, under review. [84]
5. S. El-Ferik and B. A. Siddiqui, "Algorithms and System for Collaborative Multi-agent Robust Predictive Control with Data Compression", submitted to US Patent Office, December 2014.
6. S. El-Ferik and B. A. Siddiqui, "Method for Determining Robust Constraints and Optimum Parameters for Nonlinear Predictive Control", submitted to US Patent Office, December 2014